# NUCLEAR PHYSICS

MONTHLY JOURNAL DEVOTED TO THE EXPERIMENTAL AND THEORETICAL STUDY OF ATOMIC NUCLEI, NUCLEAR FIELDS AND THE FUNDAMENTAL ASPECTS OF COSMIC RADIATION

EDITOR: L. ROSENFELD · COPENHAGEN

VOLUME IX/2

NORTH-HOLLAND PUBLISHING COMPANY-AMSTERDAM

1.E.1:
2.L

*Nuclear Physics* **9** (1958/59) 181—197; © *North-Holland Publishing Co., Amsterdam*
Not to be reproduced by photoprint or microfilm without written permission from the publisher

# GAMMA-RAYS FROM INELASTIC NEUTRON SCATTERING IN $Na^{23}$

JOAN M. FREEMAN and J. H. MONTAGUE

*Atomic Energy Research Establishment, Harwell, Didcot, Berks.*

Received 17 September 1958

**Abstract:** Gamma-rays following inelastic neutron scattering in $Na^{23}$ have been measured with neutron bombarding energies up to 3.7 MeV, and the modes of decay of the first six excited states have been investigated. Transitions to the ground state and to the first excited state at 0.44 MeV have been observed with a ring geometry arrangement, and the cascade transitions have been confirmed by $\gamma$-$\gamma$ coincidence measurements. Where possible, estimates were made of the ratio of the intensities of emission from a particular level to the ground state and to the first excited state. The following gamma-rays were observed (an asterisk indicates a transition to the first excited state): 0.438 MeV from the first excited state; 2.088 and 1.643* MeV from the second excited state (intensity ratio 0.19); 2.386 and 1.954* MeV from the third excited state (intensity ratio 3.0); 2.635 MeV from the fourth and 2.27* MeV from the fifth excited state; 2.979 and 2.56* MeV from the sixth excited state (intensity ratio of the order unity). Cross section curves for excitation of the levels at 0.44, 2.08 and 2.39 MeV have also been measured.

## 1. Introduction

Since the successful interpretations of the level and decay schemes of $Al^{25}$ and $F^{19}$ in terms of the collective model [1,2]), interest has been directed towards the possibility of interpreting the $Na^{23}$ level scheme in a similar fashion. This latter case is not so simple, since it appears necessary to consider the interactions between levels in three different K-bands. Preliminary calculations along these lines for the $Na^{23}$ levels have been made in this laboratory and are being published elsewhere [3]). The present experiments were undertaken to obtain more information about the decay scheme for $Na^{23}$.

The data available on $Na^{23}$ when these investigations were begun are summarized by Endt and Braams [4]). The positions of the levels up to 4.8 MeV are well established from the work of Buechner and Sperduto [5]) on the magnetic analysis of inelastically scattered protons; those levels of interest in the present work are shown in fig. 1. The first excited state at 440 keV has been produced in a variety of reactions and its spin is fairly definitely $\frac{5}{2}^+$ [4]). The 2.08 MeV level is known, from $Ne^{23}$ decay and (p, p'$\gamma$) work, to decay mainly to the 440 keV level with emission of a 1.64 MeV gamma-ray. In previous studies of the gamma-rays following inelastic neutron scattering,

the cross section for production of 440 keV radiation has been measured by Hausman *et al.*[6]) for neutron energies up to 800 keV; Wolf [7]), with 2.5 MeV neutrons, has observed gamma-rays with energies 0.45, 1.69 and 2.2 MeV; Morgan [8]), using 0.80 and also 5.1 MeV neutrons, has found 0.150, 0.439, 0.610, 1.63, 2.07 and 3.01 MeV gamma-rays. Recently Lind *et al.*[9]) have reported briefly the observation of 0.44, 1.60, 2.05, 2.34 and 2.70 MeV gamma-rays at a number of neutron bombarding energies.

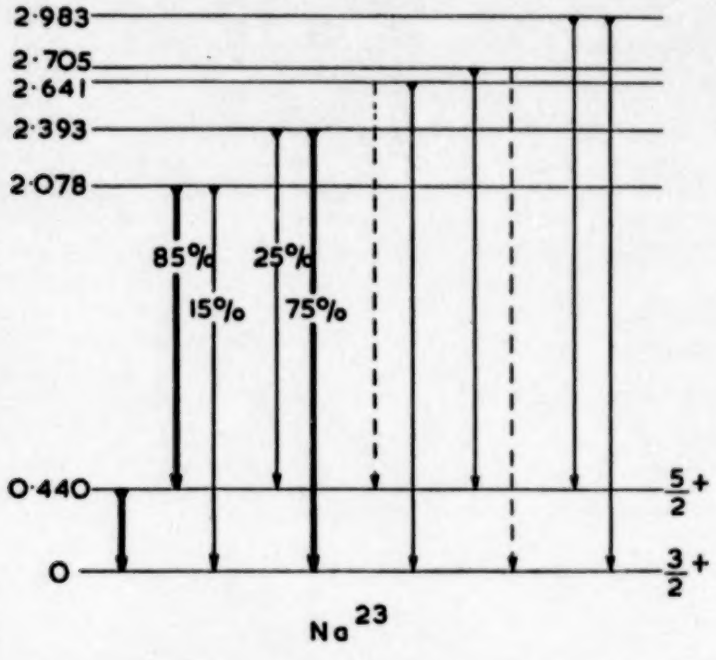


Fig. 1. Level scheme for $Na^{23}$. The level energies shown here were taken from ref.[5]). The gamma-ray transitions shown by the full lines are those observed in the present work. The transitions shown by broken lines have not definitely been seen.

In the work to be described here gamma-rays from the $Na^{23}(n, n'\gamma)Na^{23}$ reaction were examined as a function of neutron energy up to 3.7 MeV, which allowed the first six levels to be excited and studied. Cascade transitions to the first excited state at 440 keV were also examined separately by a coincidence technique. The results of these observations are given in fig. 1. Where branching ratios could be estimated quantitatively these are indicated. The transitions marked by broken lines were not definitely observed and may be weak or absent. The energies shown on this level scheme are those which were determined from the magnetic analysis work [5]). These values are slightly more accurate than the ones obtained from the present gamma-ray energy measurements; however, the two sets of values are in good agreement as will be seen from the summary given in table 1 (section 3).

For gamma-ray investigations inelastic neutron scattering had some advantages over inelastic proton scattering as a method of excitation. In the

first place, because the neutrons had no Coulomb barrier to overcome, this method allowed each $Na^{23}$ level to be studied in turn, a little above the threshold for its excitation, without confusion due to gamma-rays from higher levels. In the second place the proton-induced reaction is complicated by the competing $Na^{23}(p, \alpha\ \gamma)Ne^{20}$ reaction which gives very intense 1.63 MeV gamma-radiation from the first excited state of $Ne^{20}$, and makes analysis of the $Na^{23}$ gamma-rays more difficult.

## 2. Experimental Method

### 2.1. APPARATUS

The gamma-rays following the $Na^{23}(n, n')$ reaction were studied primarily with the ring-geometry apparatus shown in fig. 2. Neutrons were obtained from the bombardment of a zirconium-tritide target with protons from the Harwell 5 MeV electrostatic generator. The initial experiments were carried out with the target about 1 m from the analyzing magnet in a thick-walled

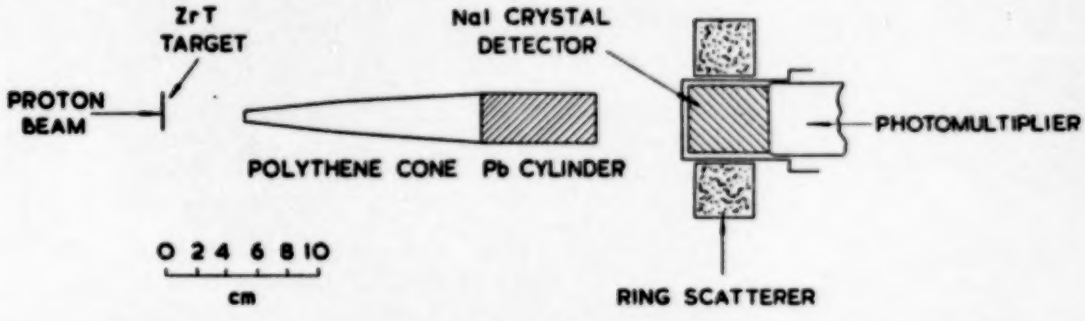


Fig. 2. Ring geometry arrangement used for observing the gamma-rays following inelastic neutron scattering.

room, of dimensions 12 m by 7 m by 3.5 m, part of which had a light floor over a cellar 3 m deep. Later the proton beam was focussed, by means of electrostatic lenses, at a distance of 12 m from the analyzing magnet, in such a way that the tritium target could be located 3 m from the ground in a large thin-walled area. This latter arrangement was found to give a very worthwhile reduction in the background neutron flux compared with the earlier arrangement.

The scattering sample was a ring of sodium metal, of inside diameter 5.5 cm, outside diameter 13 cm and thickness 3.7 cm, encased in a thin stainless steel can; in some of the experiments a ring of sodium peroxide powder in a brass container was used. The ring was placed with its axis in the direction of the proton beam and its centre 37 cm from the neutron source, so that it received neutrons emitted at a mean angle of 7° with respect to the proton beam direction. For most of the experiments the total energy spread of the neutrons reaching the ring was about 50 keV, being

determined almost entirely by the ZrT target thickness. Gamma-rays from the scattering ring were detected with a NaI (Tl) crystal, 4.5 cm in diameter and 5 cm long, situated at the centre of the ring and in optical contact with the photocathode of an E.M.I. photomultiplier. The crystal was shielded from the neutron source by a cone consisting of 16 cm of polythene backed by 8 cm of lead; the cone was truncated and slightly tapered to allow for small departures from alignment of the target spot.

### 2.2. NEUTRON FLUX MEASUREMENTS

The neutron flux was monitored continuously during the experiments by means of a $BF_3$ long counter set up 2 m from the source in a direction making an angle of 40° with the proton beam direction. For the determination of the absolute neutron flux at the scattering sample this monitor counter was compared with a second long counter which had been absolutely calibrated [10]). The latter was set up to receive neutrons emitted in the 0° direction, after removal of the scattering and detecting apparatus and the shield, and the ratio of the counting rate in this detector to the rate in the monitor counter was measured as a function of neutron energy. The small correction for the ratio of the neutron flux in the forward direction to that at 7° (the mean angle of acceptance by the scattering ring) was obtained from published data on differential cross sections for the T(p, n) reaction [11]).

### 2.3. GAMMA-RAY SPECTRA AND BACKGROUND MEASUREMENTS

Gamma-ray pulses from the sodium-iodide detector were amplified and recorded on a hundred channel pulse-height analyzer. Appreciable contributions to the spectra arose from background effects, due mainly to neutrons being scattered from the sample and the associated apparatus into the NaI crystal and producing gamma-rays by inelastic scattering there. The background was determined at each neutron bombarding energy by replacing the sodium sample with one of carbon, selected because carbon has no excited states below 4.4 MeV. The carbon was enclosed in a container similar to that used for the sodium, and its mass was chosen to produce about the same amount of elastic neutron scattering as did the sodium ring. The criteria adopted to ensure that the carbon scatterer was giving closely the correct background spectrum were (i) that, at a neutron energy just below the 2.17 MeV threshold for excitation of the 1.64 MeV gamma-ray from sodium, the spectra obtained with the sodium and carbon rings were the same in the gamma-ray energy range 1 to 2 MeV, for the same number of neutron monitor counts, and (ii) that, at each neutron energy, the correct peak-to-valley ratio was obtained for the highest observed sodium gamma-ray peak, after subtraction of the carbon background. A typical pair of spectra obtained at a neutron energy of 2.88 MeV for the sodium and carbon rings is

shown in fig. 3; the spectra have been normalized to the same number of neutron monitor counts and have been corrected for the dead-time of the pulse-height analyzer; the pulse-height scale has been converted to the equivalent gamma-ray energy scale by means of the detector calibrations to be discussed below. The difference spectrum obtained by subtracting these two curves is given in fig. 4c.

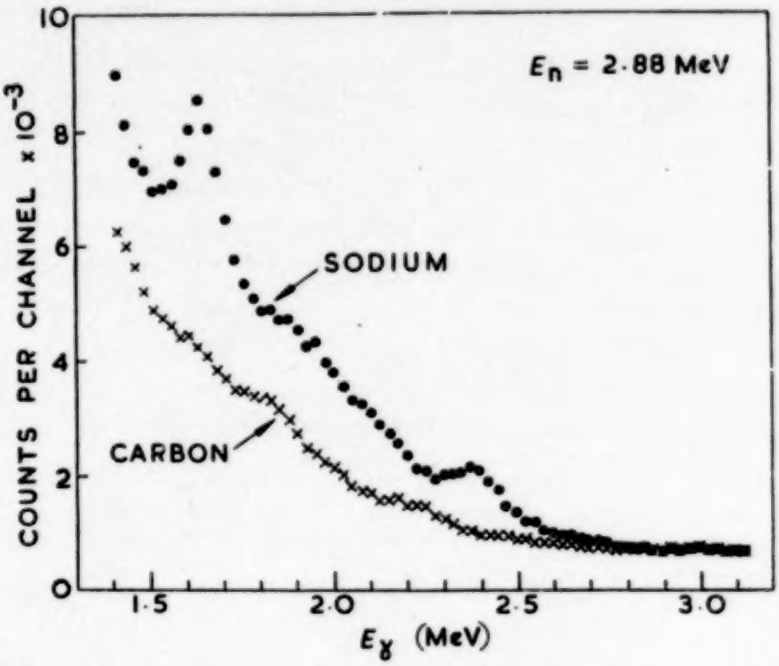


Fig. 3. Gamma-ray spectra obtained in a NaI crystal with a sodium ring (circles), and with a carbon ring (crosses), in the apparatus of fig. 2, for the same number of bombarding neutrons (energy 2.88 MeV).

## 2.4. DETECTOR CALIBRATION

*Energy calibration* of the detector was carried out by placing small gamma-ray sources alongside the crystal, in approximately the same position as was normally occupied by the scattering sample, and determining the positions in the pulse-height spectra of the full-energy peaks corresponding to the various gamma-rays. Such calibrations were carried out frequently between runs and were required to remain constant to 1 % or better during a run. The following calibration sources were used: $Au^{198}$(0.412 MeV), $Be^{7}$(0.478 MeV), $Na^{22}$(0.511 and 1.277 MeV), $Ce^{144}$(1.48 and 2.18 MeV), RdTh(2.615 MeV), and $Na^{24}$(1.368 and 2.754 MeV).

*Spectral "shapes"* for monoenergetic gamma-rays from some of the sources just mentioned were obtained in a similar way. These were required for analysis of the sodium spectra observed in the energy range 1.55 to 3 MeV. For each gamma-ray energy the pulse-height spectrum from a NaI crystal is complex, showing in addition to the full energy peak (usually referred to as

the photopeak) a Compton distribution and also, for harder gamma-rays, peaks due to pair production with loss of one or both annihilation gamma-rays. Moreover the spectral shape is dependent on the location of the source with respect to the crystal, and on self-absorption effects. Thus in the present experiments, when several sodium levels were being excited, the observed spectrum was quite complicated and the only peak that could be interpreted unambiguously was the photopeak of the highest energy gamma-ray present. In order to investigate the lower energy gamma-rays the spectrum corresponding to radiation of this highest energy was subtracted from the total spectrum, after normalization to the number of counts in the observed photopeak. This "peeling off" procedure could then be repeated for the next highest energy gamma-ray, and so on. When standard spectral shapes were required for energies lying between the values available from the radioactive sources, interpolations between the measured shapes were used.

*The absolute detector efficiency* had to be obtained as a function of gamma-ray energy in order that the yields of the various gamma-rays could be calculated. The most convenient quantity to measure was the photopeak efficiency $\varepsilon$, defined as the ratio of the counting rate in the photopeak to the corresponding source strength in the scattering sample. This was obviously dependent on the shape of the scatterer and on the relative positions of the scatterer and detector; it was thus desirable to make calibration sources of the same shape as the scattering sample. It was also necessary to allow for self-absorption in the scatterer and calibrating sources [12]).

The absolute photopeak efficiency for the detector was determined at gamma-ray energies of 1.368 and 2.753 MeV with the aid of a calibrated $Na^{24}$ source. The latter was enclosed in an aluminium can which was in the form of a 34° sector of a ring of the same dimensions as the scatterer, and was placed against the crystal in the same position as the scatterer. The source consisted of part of a sample of sodium bicarbonate which had been irradiated in the neutron flux of the Harwell BEPO reactor; the specific activity of the sodium bicarbonate was measured by absolute counting of the remainder of the sample in a standardized $4\pi$ beta-ray counter. The error in the absolute measurements was about $\pm 5$ per cent, due mainly to uncertainties in the calibration of the $Na^{24}$ source. It should be noted that the relative error in the efficiencies for the two gamma-ray energies was only about $\pm 2$ per cent.

Day[12]) has determined photopeak efficiencies for a similar experimental arrangement at several gamma-ray energies between 0.4 and 2.8 MeV. He found that, within 2 per cent, $\varepsilon$ varied with $E_\gamma$ according to a simple power law above 0.5 MeV. It was therefore felt justifiable to assume that in the present case $\varepsilon$ was given by

$$\varepsilon = AE_\gamma^{\,B} \qquad (1)$$

where $A = 6.14 \times 10^{-3} \pm 5$ per cent and $B = 1.09 \pm 2$ per cent, as determined

from the two $Na^{24}$ calibration points. It did not seem desirable to extrapolate the relationship (1) too far toward low energies, particularly as Day's results had shown departures from a power law below 0.5 MeV. It was possible to measure the relative efficiencies for gamma-rays of 0.511 and 1.28 MeV with a $Na^{22}$ source placed beside the crystal in the mean position of the scatterer. By normalizing the 1.28 MeV point to the curve (1) the absolute efficiency at 0.511 MeV was determined; this was found to be 9 % higher than that given by equation (1). Below 0.511 MeV it was possible to estimate the shape of the curve by adapting to the present geometry the results of Maeder *et al.*[13]) for the ratio of the counts in the photopeak to the total number of counts in the gamma-ray spectrum. From these ratios the relative photopeak efficiencies were obtained by multiplying by the calculated intrinsic detection efficiency of the NaI crystal, and these were normalized to the point at 0.511 MeV to give absolute photopeak efficiencies. It was found, on a log-log plot, that the slope of the calculated curve thus obtained was within 2 % of that of the line joining the two $Na^{22}$ points.

The only gamma-ray energy below 1.6 MeV that is of interest in the present experiments is at 0.44 MeV, corresponding to the transition from the first excited state to the ground state of $Na^{23}$. The absolute photopeak efficiency adopted for this gamma-ray energy was $(3.28 \pm 0.3) \times 10^{-2}$.

## 3. Experimental Results

For neutron energies below 2 MeV the sodium minus carbon difference spectra showed only the 440 keV gamma-ray from the first excited state of $Na^{23}$. The excitation function for this radiation was followed from the threshold up to 1.4 MeV (see section 5). No evidence was found for the 610 keV level reported by Morgan [8]). A gamma-ray peak at about 620 keV was observed in both sodium and carbon runs; its height was about 7 % of the height of the 440 keV peak at a neutron energy of 1.2 MeV. It was attributed to the effect of inelastic neutron scattering in the iodine of the crystal detector (a level in iodine at about 630 keV is known). By subtraction of the sodium and carbon runs this peak was eliminated. Allowing for statistical errors, and for the relative efficiency of the NaI crystal for 440 and 610 keV gamma-rays, an upper limit of 3 per cent was calculated for the possible intensity of 610 keV compared with 440 keV gamma-radiation from the sodium sample, at neutron energies between 1.0 and 1.2 MeV.

The transitions from the second and higher excited states of sodium were studied by taking pulse height spectra at a series of neutron energies beginning just below the 2.17 MeV threshold for the 2.08 MeV level. Some typical examples are given in fig. 4; these spectra have had carbon backgrounds subtracted from them. The arrows indicate the expected positions of

photopeaks corresponding to possible gamma-ray transitions. These spectra show clearly the appearance of gamma-ray transitions from successively higher levels as the neutron bombarding energy, $E_n$, is increased. In curve a, taken at a neutron energy of 2.26 MeV, only the two transitions from the second excited state at 2.08 MeV are seen; the prominent lower peak corresponds to the 1.64 MeV transition to the first excited state and the upper peak to the ground state transition. At a neutron energy of 2.68 MeV (curve b) the gamma-rays from the 2.39 MeV state, at energies 1.95 and 2.39 MeV, have become visible and by $E_n = 2.88$ MeV (curve c) they are well resolved. Curve d, for $E_n = 3.03$ MeV, shows evidence for transitions from one or both of the close pair of levels at 2.64 and 2.71 MeV; the peak at 2.64 MeV may contain contributions from both ground-state gamma-rays since these would not be resolved. The transitions to the first excited state probably account for the filling-in of the spectrum between the 2.08 and 2.39 MeV peaks; further evidence for these transitions is found from the coincidence studies discussed in section 4. The remaining two spectra, taken at neutron energies of 3.20 and 3.67 MeV, show the ground state transition from the 2.98 MeV level. The first excited state transition from this level is not resolved here, but is observed in the coincidence studies.

The energies of the observed gamma-rays were estimated from spectra such as those shown in fig. 4; the best values thus obtained are listed in table 1, which includes the results of coincidence measurements to be discussed in section 4. For the 2.08 and 2.39 MeV levels estimates were made of the intensity ratio $I_G/I_{0.44}$ where $I_G$ and $I_{0.44}$ are the intensities of the transitions to the ground state and to the 0.44 MeV first excited state respectively.

TABLE 1

Gamma-Ray transitions in $Na^{23}$

| Level energy according to Buechner and Sperduto [5]) (MeV) | Observed $E_\gamma$(MeV) | | Intensity ratio $I_G/I_{0.44}$ |
|---|---|---|---|
| | to ground state | to 0.44 MeV state | |
| 0.440 | 0.438±0.005 | | |
| 2.078 | 2.088±0.015 | 1.643±0.008 | 0.19±0.04 |
| 2.393 | 2.386±0.010 | 1.954±0.015 | 3.0 ±0.6 |
| 2.641 | 2.635±0.015 | | |
| 2.705 | | 2.27 ±0.02 | |
| 2.983 | 2.979±0.015 | 2.56 ±0.02 | ≈1 |

These estimates are also given in table 1. Concerning these measurements the following points should be noted:

(i) The measurement of the relative intensities of transitions from a particular level was made at a neutron energy which did not allow appreciable excitation of any higher level. In this way the complexity of the spec-

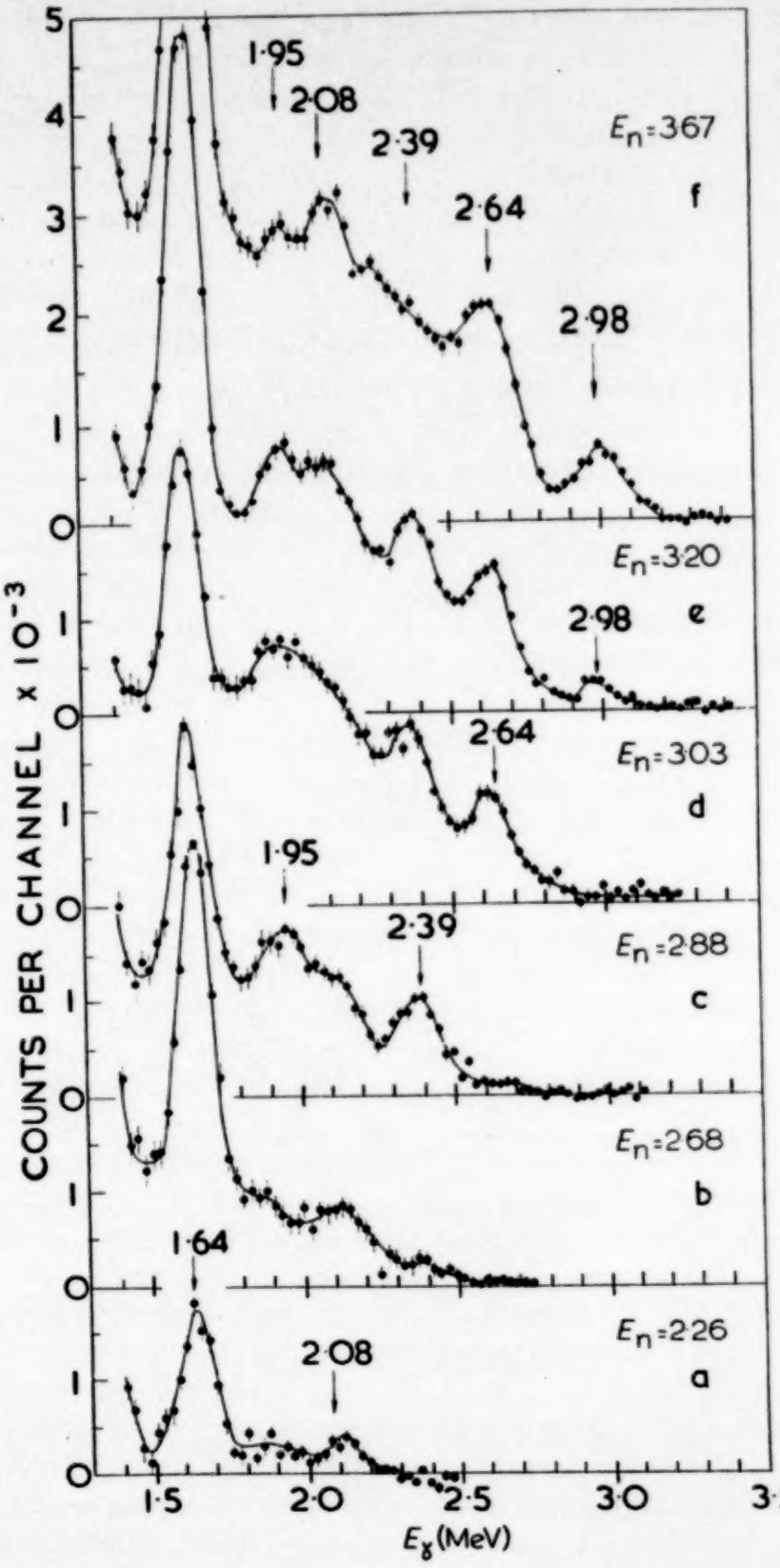


Fig. 4. Typical gamma-ray spectra from $Na^{23}$ for the neutron bombarding energies shown; the carbon backgrounds have been subtracted. These spectra were all taken for about the same number of incident neutrons. The arrows show the expected positions of gamma-ray photopeaks.

trum was kept to a minimum and the highest energy peak observed was the photopeak for the ground state transition from the level of interest.

(ii) For determination of the energy and yield of gamma-rays to the first excited state, the spectral shapes of the ground-state gamma-ray and of any gamma-rays of intermediate energy had first to be subtracted from the pulse-height spectrum. For example, for studying the decay characteristics of the 2.39 MeV level, a spectrum similar to fig. 4, curve c, was used, and the intensity of the 1.95 MeV transition was determined after subtraction of appropriately normalized shapes for the 2.39 and 2.08 MeV gamma-rays.

(iii) In considering transitions from a particular level, a correction had to be made for the fact that some of the counts in the ground-state photopeak were due to the simultaneous detection of a gamma-ray to the first excited state and the cascading 0.44 MeV radiation from the first excited state to the ground state. The percentage of this "add-up" contribution depended on the geometry and on the efficiency of detection of the second gamma-ray. It was particularly important for the 2.08 MeV level for which the ground-state transition was rather weak. The amount of "add-up" was estimated with the aid of a $Na^{22}$ source which gives two 0.511 MeV annihilation gamma-rays in coincidence with each 1.28 MeV gamma-ray. After correction for the difference in photopeak efficiency for 0.44 and 0.51 MeV gamma-rays, it was found that, in the $Na^{23}$ case, the add-up peak would amount to 5 per cent of the photopeak yield of the transition to the first excited state.

With reference to the pair of levels at 2.64 and 2.71 MeV, the best value for the energy corresponding to the photopeak of the unresolved ground-state transitions was 2.635 MeV. This implied that most of the transitions were from the lower level. However, it was not possible from this result to rule out 2.71 MeV transitions of comparable intensity, since the complex response of a NaI crystal leads to a bias in favour of the lower energy contribution to a photopeak made up of two unresolved components. In order to investigate this point further the NaI crystal was replaced with a plastic scintillator of similar dimensions. A typical spectrum, taken at the same neutron energy as the NaI spectrum of fig. 4d (3.03 MeV) is given on a log plot as curve A in fig. 5. The various photopeaks of the NaI run are here replaced by Compton edges; the arrows show the positions at which the intensities of the Compton distributions for the various gamma-rays would be expected to fall to ten per cent of their values at the Compton peaks. To the highest energy Compton edge in curve A has been fitted the spectrum of a 2.64 MeV gamma-ray (curve B). The difference spectrum is shown by the crosses (curve C); it can be seen that the highest energy portion of this curve can be well fitted by the spectral shape of a 2.39 MeV gamma-ray (curve D), which is the next-highest energy gamma-ray expected. If curve A had been fitted with a 2.71 MeV spectrum instead of the 2.64 MeV shape of curve B, it

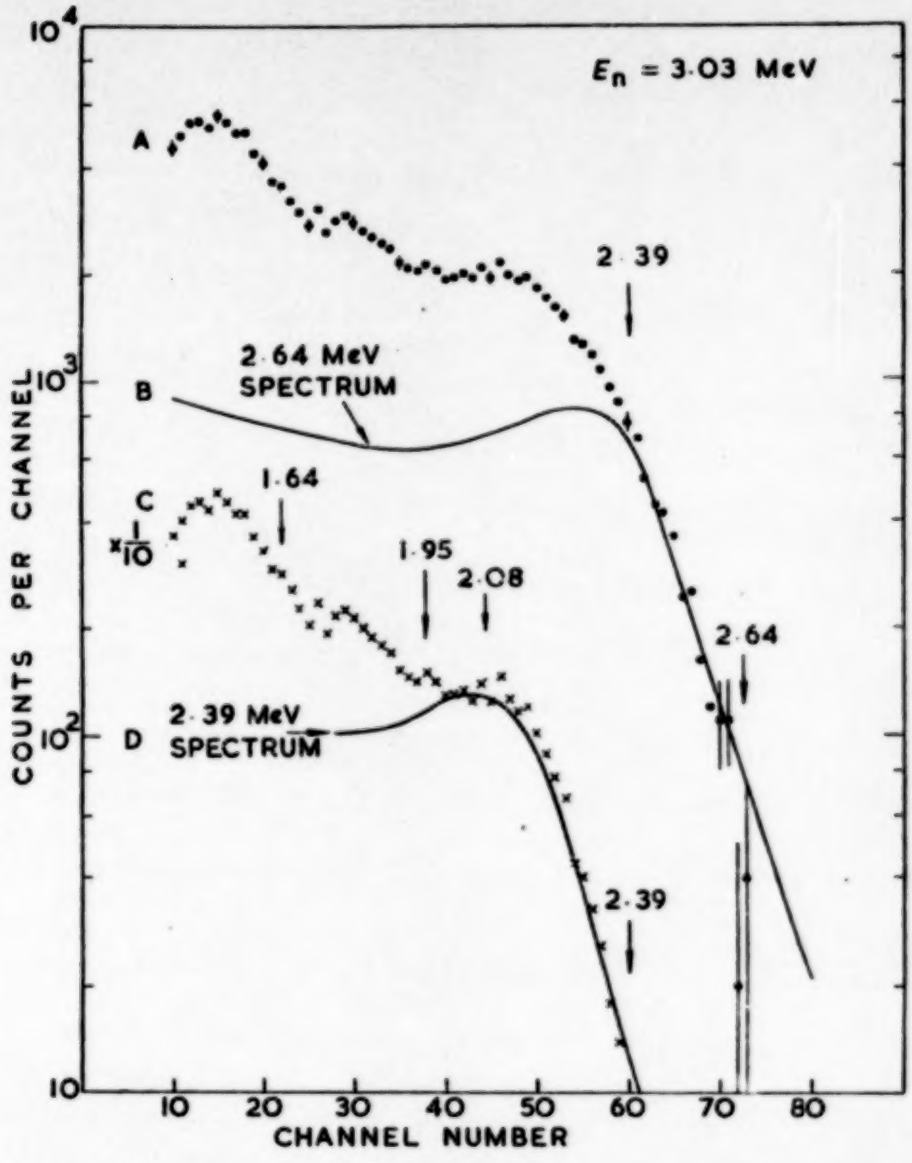


Fig. 5. Spectrum of gamma-rays from $Na^{23}$ obtained with a plastic scintillator in the ring geometry apparatus of fig. 2. Curve A: the Compton spectrum after subtraction of the background obtained with a carbon ring. Curve B: the spectrum of a 2.64 MeV gamma-ray, fitted to curve A. Curve C: the difference spectrum (×1/10). Curve D: the spectrum of a 2.39 MeV gamma-ray fitted to curve C.

would not have been possible to fit the residual peak and Compton edge with a 2.39 MeV spectrum (particularly if allowance were made for the presence of some 2.27 MeV radiation). The data are therefore consistent with there being no 2.71 MeV gamma-ray; considering the statistical errors and the uncertainties in the energy calibration, we conclude that the 2.71 MeV component cannot be more than 25 per cent of the 2.64 MeV component at this neutron energy.

Apart from the specific application just discussed, it can be seen from fig. 5 that organic scintillation spectra can be generally useful for supplementing the information derived from sodium iodide spectra.

## 4. Coincidence Measurements

For studying those gamma-rays which cascaded through the first excited state of $Na^{23}$ at 440 keV, the apparatus shown in fig. 6 was used. The sodium sample was a cylinder of metallic sodium, 6 cm in diameter and 2.5 cm thick, enclosed in a thin-walled stainless steel can. This was placed 32 cm from the ZrT target so that it received neutrons emitted in the forward direction. On opposite sides of the scatterer were two 4.5 cm diameter NaI crystals, of

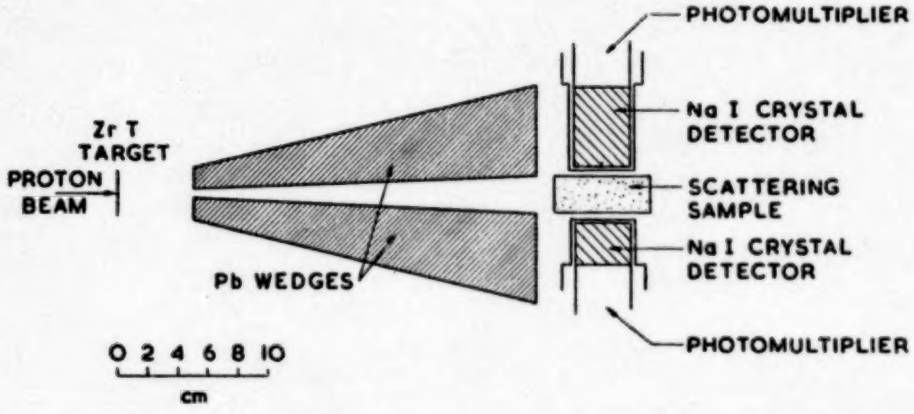


Fig. 6. Apparatus for measuring the gamma-ray spectrum in coincidence with 440 keV radiation from the first excited state of $Na^{23}$.

thickness 2.5 and 5.0 cm respectively, each attached to its own photomultiplier. The crystals were shielded from the direct neutrons by a pair of lead wedges. The pulses from the smaller crystal were fed into a single-channel pulse-height analyzer which was adjusted to select only those pulses corresponding to the peak of the 440 keV spectrum. These were then fed into one channel of a coincidence circuit, the other side of which received pulses from the larger NaI crystal. The pulses entering the coincidence circuit had a rise-time of about 0.1 $\mu$s allowing a resolving time of 0.2 $\mu$s to be used. The pulses from the larger crystal were also fed through a slower amplifier and a suitable delay to a hundred-channel kicksorter; a gate in the latter was operated by the coincidence circuit so that only those gamma-ray pulses were analysed which were in coincidence with the 440 keV radiation. In these experiments the random coincidence rate was only about ten per cent of the genuine rate, but an appreciable background contribution to the latter arose from double scattering events of various kinds in the two crystals. This amounted to almost half the total genuine coincidence rate, but could be

allowed for by obtaining a similar coincidence spectrum, for the same number of neutron monitor counts, with a carbon scatterer substituted for the sodium sample. The carbon runs gave monotonically decreasing curves and the smoothed average of these at each neutron energy was used for subtraction from the sodium spectrum.

Coincidence measurements were made at two neutron bombarding energies, 2.95 and 3.47 MeV. The results are shown in fig. 7. The arrows indicate the expected positions for cascade gamma-rays from $Na^{23}$ levels. At the lower neutron energy only the 2.08 and 2.39 MeV levels are appreciably excited; the curve gives good evidence for the 1.95 MeV cascade from the 2.39 MeV level as well as the prominent 1.64 MeV peak due to the 2.08 MeV level decay. At the higher neutron bombarding energy a peak close to 2.54 MeV indicates cascade transitions from the 2.98 MeV level to the 440 keV first excited state.

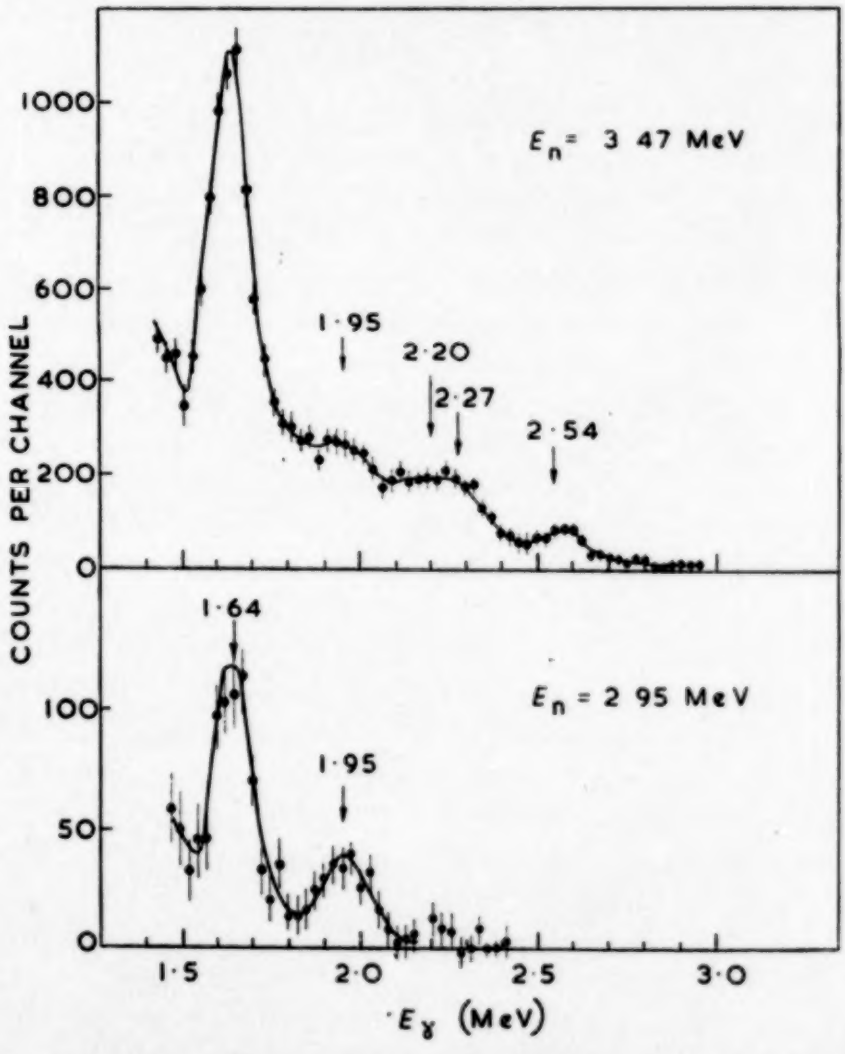


Fig. 7. Gamma-ray spectra in coincidence with 440 keV gamma-rays, obtained at the neutron bombarding energies shown. The arrows show the positions expected for the photopeaks of possible cascade gamma-rays from $Na^{23}$ levels.

From the intensities relative to the 1.64 MeV gamma-ray of this peak and of the 2.98 MeV peak observed in the ring geometry experiments at approximately the same neutron energy, one concludes that the 2.98 MeV level decays to the ground and first excited states with about equal probability. After subtraction of the 2.54 MeV spectral shape from the upper coincidence spectrum of fig. 7, there remains a peak, the position of which would correspond to 2.27 MeV radiation arising from cascade decay of the 2.71 MeV level. Arrows on the curve indicate the positions expected for this peak and for a 2.20 MeV gamma-ray which would correspond to cascades from the slightly lower 2.64 MeV level. It is not certain from this measurement whether the lower-energy cascade is present; the 2.27 MeV transition appears to be definite and the stronger of the two. The results taken in conjunction with the corresponding ring geometry measurements imply that the 2.71 MeV level decays mainly, perhaps almost entirely, by cascade to the 440 keV state and that the 2.64 MeV level decays more strongly by a ground-state transition.

## 5. Cross Section Measurements

Measurements of the excitation cross sections as a function of neutron energy were made for the $Na^{23}$ levels at 0.44 MeV, 2.08 MeV and 2.39 MeV, and are plotted in fig. 8a and 8b. The measurements were of two kinds:

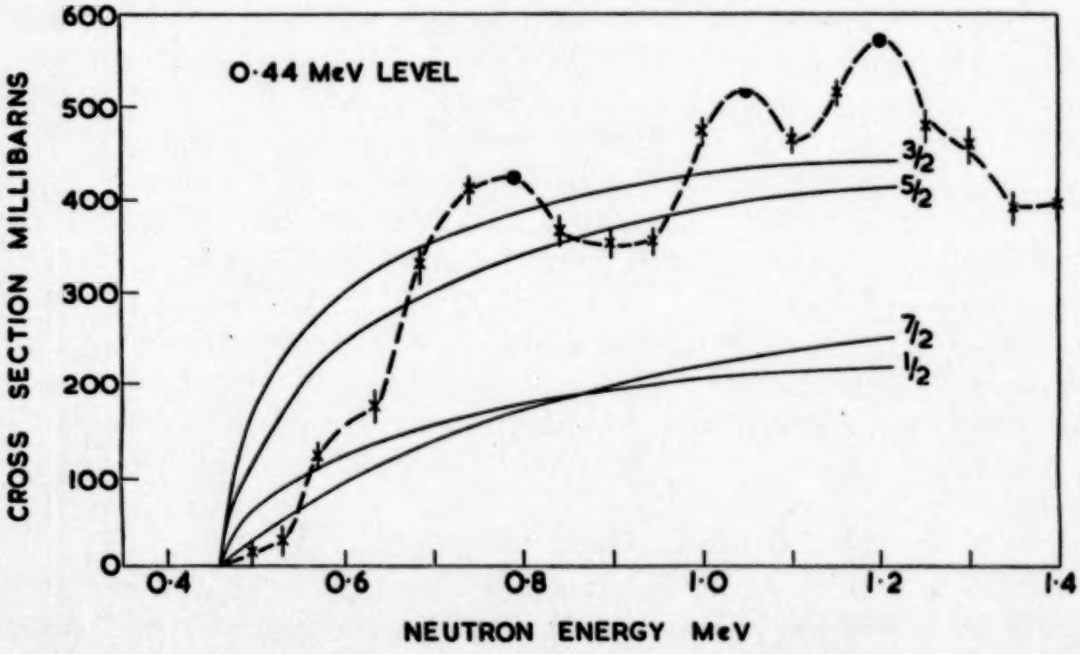


Fig. 8a. Cross section for excitation of the 440 keV level in $Na^{23}$ by inelastic neutron scattering (neutron energy spread 50 keV). Circles represent absolute measurements and crosses relative measurements. Errors in absolute magnitude are about $\pm 20$ per cent. The full curves show calculations based on the Hauser-Feshbach theory for a black nucleus for different values of the spin of the 440 keV level (ground state assumed $\frac{3}{2}$).

(i) Gamma-ray yields were determined from pulse height spectra similar to those shown in fig. 4 by integrating the number of counts in the photopeak of the principal gamma-ray from the level in question, after the contributions from gamma-rays of higher energy had been subtracted. In the case of the 2.08 and 2.39 MeV levels, the measured gamma-ray branching ratios were used to obtain the total emission from each level. Absolute cross sections were then calculated from the crystal calibration (with corrections for self-

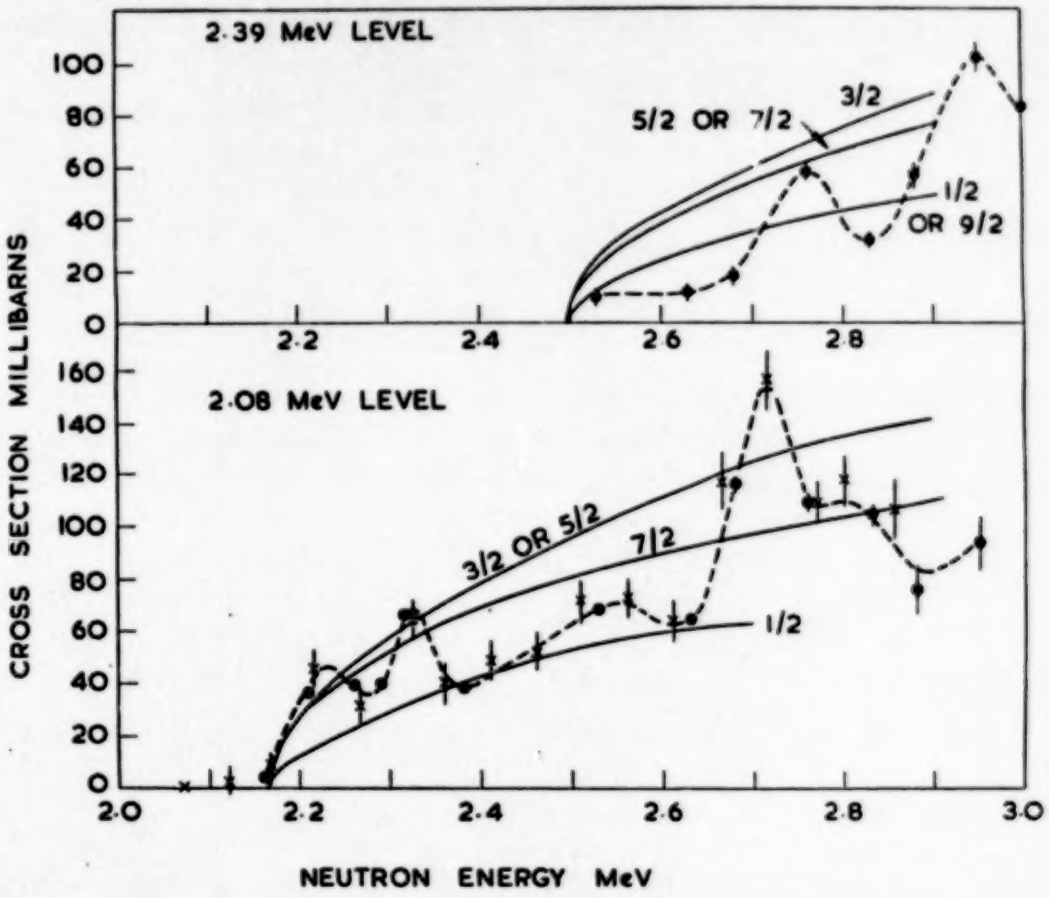


Fig. 8b. Cross sections for excitation of the 2.08 and 2.39 MeV levels in $Na^{23}$. The points have the same significance as in fig. 8a. The full curves show the trends predicted by the Hauser-Feshbach theory, assuming $\frac{1}{2}$ for the spin of the 440 keV level.

absorption), the measured neutron flux, and the mass of the sample. They were estimated over $4\pi$ with the assumption that the observed radiation, which was accepted at angles between about 45° and 150° with respect to the bombarding neutrons, represented closely enough the average over the full angular range. The absolute cross sections are shown in the figures by solid points. The accuracy is about $\pm 20$ per cent; contributions to the total standard deviation arise from uncertainties in the number of photopeak counts, the effective crystal efficiency, the neutron flux and the geometry.

(ii) Relative cross sections were also measured for the 0.44 and 2.08 MeV levels by setting a single-channel pulse-height analyzer to accept pulses lying in a narrow band at the energy of the photopeak of the appropriate gamma-ray (0.44 and 1.64 MeV respectively). The relative yield at each neutron energy was found by taking the difference between the channel counts per incident neutron when the sodium scatterer was present and when the carbon scatterer was present. These relative points were normalized to the absolute measurements, and are shown in the figures as crosses. The normalization constants required to fit different parts of each curve varied slightly; the maximum variation was 10 per cent.

The smooth curves shown in figs. 8a and 8b are absolute excitation cross sections calculated on the basis of the theory of Hauser and Feshbach [14]) for several possible values of the spins of the excited states. A black nucleus has been assumed, with a radius of $4.1 \times 10^{-13}$ cm.

## 6. Discussion

The pronounced resonance structure in the experimental cross section curves of figs. 8a and 8b implies that there are comparatively few levels in the compound nucleus. Thus a comparison with the Hauser-Feshbach theory would not be expected to be valid since this theory assumes a statistical distribution of levels in the compound state. The slow rise from threshold for excitation of the 440 keV level suggests an absence in this energy region of compound states with spins such that s-wave neutron emission is possible. This fact seems to be borne out by analyses of neutron total cross section resonances in the range $E_n = 300$ to 550 keV [4]); these all appear to have spins 0 or 1 and would therefore require $l > 0$ for neutron emission to the $\frac{5}{2}$ level at 440 keV. It is somewhat surprising therefore that at higher neutron energies the cross section curve for excitation of the 440 keV state is, on the average, consistent in absolute magnitude with the statistical curve for a spin $\frac{5}{2}$. There is a similar general consistency in the case of the 2.08 and 2.39 MeV levels when plausible spin assignments are made (see below).

The cross section curves for the 2.08 and 2.39 MeV levels, which were investigated simultaneously, indicate distinctly different resonances in the two cases. Since the angle of acceptance of the gamma-rays was quite large, no marked angular distribution effects would be expected. The results therefore imply that those compound nucleus levels which favour inelastic neutron emission to the one level do not in general favour emission to the other. The spins of the 2.08 and 2.39 MeV levels must therefore differ, very likely by more than one unit (assuming positive parities for both states). Since the 2.08 MeV state decays preferentially to the $\frac{5}{2}$ (440 keV) state, whereas the 2.39 MeV state prefers a transition to the $\frac{3}{2}$ ground state, it seems probable

that the 2.08 MeV level has the higher spin value ($\geqq \frac{5}{2}$) and the 2.39 MeV level has the lower spin value ($\frac{1}{2}$ or $\frac{3}{2}$). Thus the assignments $\frac{7}{2}$ and $\frac{1}{2}$ respectively for these two levels, as suggested from the collective model considerations [3]), appear to be quite consistent with the experimental observations.

Of the next highest set of three levels, the 2.64 and 2.98 MeV levels must have spins $\leqq \frac{7}{2}$ since the ground state transitions are in evidence. The 2.71 MeV level may have a higher spin, since it appears to decay predominantly to the first excited state.

The authors would like to thank Dr. R. C. Hanna for his very helpful collaboration in the early stages of the experiment; Dr. A. T. G. Ferguson for his assistance in measuring the neutron flux; Dr. R. A. Allen, Mr. B. Slade and Mr. R. L. Otlet for the irradiation and calibration of the $Na^{24}$ source; and Mr. J. E. Hailstone for carrying out the computations for the theoretical cross section curves with the aid of the Hollerith 555 Calculator. The active interest of Dr. E. B. Paul throughout the work is gratefully acknowledged, as is also the efficient running of the electrostatic generator by Mr. F. D. Pilling, Mr. W. E. Sparrow and the accelerator staff.

## References

1) A. E. Litherland, E. B. Paul, G. A. Bartholomew and H. E. Gove, Phys. Rev. **102** (1956) 208
2) E. B. Paul, Phil. Mag. **2** (1957) 311
3) E. B. Paul and J. H. Montague, Nuclear Physics **8** (1958) 61
4) P. M. Endt and C. M. Braams, Revs. Mod. Phys. **29** (1957) 683
5) W. W. Buechner and A. Sperduto, Phys. Rev. **106** (1957) 1008
6) H. Hausman, J. E. Monahan, F. P. Mooring and S. Raboy, Bull. Amer. Phys. Soc. **1** (1956) 56
7) E. A. Wolf, Phil. Mag. **1** (1956) 102
8) I. L. Morgan, Phys. Rev. **103** (1956) 1031
9) D. A. Lind, R. B. Day and R. M. Kloepper, Bull. Amer. Phys. Soc. **2** (1957) 309
10) W. D. Allen and A. T. G. Ferguson, Proc. Phys. Soc. A **70** (1957) 639
11) J. L. Fowler and J. E. Brolley, Revs. Mod. Phys. **28** (1956) 103
12) R. B. Day, Phys. Rev. **102** (1956) 767
13) D. Maeder, R. Müller and V. Wintersteiger, Helv. Physica Acta **27** (1954) 3
14) W. Hauser and H. Feshbach, Phys. Rev. **87** (1952) 366

2.A.1 *Nuclear Physics* 9 (1958/59) 198—204: © *North-Holland Publishing Co., Amsterdam*
Not to be reproduced by photoprint or microfilm without written permission from the publisher

# NEUTRON RESONANCE PARAMETERS OF TANTALUM FROM 20 TO 100 eV

F. W. K. FIRK

*Atomic Energy Research Establishment, Harwell, Didcot, Berks.*

Received 20 September 1958

**Abstract:** Values of the peak total cross section ($\sigma_0$) and the total width ($\Gamma$) for thirteen resonances in Ta between 20 and 100 eV have been determined using the Harwell 15 MeV linear accelerator and time-of-flight spectrometer. The radiation widths ($\Gamma\gamma$) have been obtained assuming the spin weighting factor $g = \frac{1}{2}$. Refinements in the methods of analysis of transmission data have enabled the parameters to be determined. These methods include a general "area" analysis which includes the effect of interference between resonance and potential scattering [1]).

## 1. Introduction

Previous measurements of resonance parameters of Ta in the energy region 20 to 100 eV [2,3]) have been made to determine values of $g\Gamma_n$ and $\bar{\Gamma}_n^0/D$ where $\Gamma_n$ is the neutron width, $\bar{\Gamma}_n^0$ is the average reduced neutron width and $D$ the level spacing per spin state. The work described was carried out to determine $\sigma_0$ and $\Gamma$ and hence $\Gamma_\gamma$ using the relations

$$g\Gamma_n = \sigma_0\Gamma/4\pi\lambda\!\!\!^{-}_R{}^2 \qquad (1)$$

and

$$\Gamma_\gamma = \Gamma - \Gamma_n \qquad (2)$$

where $\lambda\!\!\!^{-}_R$ is the normalised de Broglie wavelength of the neutron at the resonance energy $E_R$ and the spin weighting factor, $g$, is given by

$$g = (2J+1)/2(2I+1)$$

where $I$ is the spin of the target nucleus in the ground state and $J = I \pm \frac{1}{2}$. A value of $g = \frac{1}{2}$ was used to determine $\Gamma_\gamma$. (For Ta the possible values of $g$ are $\frac{7}{16}$ or $\frac{9}{16}$.)

## 2. Experimental Procedure

An evacuated 31.8 m flight path and 100 timing channels each of 1 $\mu$sec duration were used with the Harwell 15 MeV linear accelerator. The neutron pulse width was $< 1$ $\mu$sec [4]), and the pulse repetition frequency 400 p.p.s. The resolution was 0.032 $\mu\text{sec} \cdot \text{m}^{-1}$. The detector consisted of a can of $B^{10}$ surrounded by five NaI(Tl) crystals and photo-tubes connected in parallel. These were set to detect the 480 keV $\gamma$-rays obtained from neutron capture in the $B^{10}$ [5]).

Transmission measurements were made with five different sample thicknesses of Ta. The diameter of the neutron beam at the sample holder was 3". The background was continuously monitored using a gate which opened for 100 $\mu$sec at the end of each machine cycle [4]).

## 3. Analysis of the experimental data

The basis for obtaining $\sigma_0$ and $\Gamma$ was the standard many-sample area technique [6,7]). The method due to Hughes [7]) enables corrections for finite sample thickness and Doppler effect to be carried out simultaneously. This method yields $\sigma_0$ as a function of $\Gamma$. Four different areas were measured for strong resonances at 23.9 and 39.0 eV and the best values of $\sigma_0$ and $\Gamma$ obtained from the intersection of the $(\sigma_0, \Gamma)$ curves. The results of a typical many-sample area analysis are given for the 23.9 eV resonance in fig. 3. This technique was used (with fewer samples) for resonances at 20.2, 35.0, 35.8, 62.9, 76.8, 82.7, 84.7 and 98.8 eV. The "observed" transmissions for two different sample thicknesses, $n = 0.01908 \times 10^{24}$ and $n = 0.00152 \times 10^{24}$ atoms/cm$^2$ are shown in fig. 1 and 2 respectively.

There are two main difficulties associated with the standard area method of analysis; both apply to the cases where $n\sigma_0 \gg 1$.

Firstly, the basic level by which the observed transmissions must be divided before the area is calculated is often difficult to determine. The basic level ($T_c$) is the transmission due to potential scattering toegether with contributions from the wings of nearby resonances. This means that the parameters of all major resonances must be initially determined by selecting the most reasonable basic level obtained from the experimental points. Contributions from these resonances can then be calculated over any energy region where they are of importance. The contribution of nearby resonances (ignoring resonance-resonance interference) to the cross section at an energy $E_R$ is given by

$$\sum_{s \neq R} \frac{\sigma_{0s} \Gamma_s^2}{4(E-E_s)^2} + \sum_{s \neq R} \frac{k_s a \sigma_{0s} \Gamma_s}{(E-E_s)} = \sum \sigma_{\text{wings}} \qquad (3)$$

where the summation over s refers to resonances of energy $E_s$, $k_s$ is the wave number of a neutron of energy $E_s$ and $a$ is the potential scattering length.

The basic level is then

$$T_c = \exp\left(-4\pi n a^2 - n \sum \sigma_{\text{wings}}\right)$$

where $n$ is the number of atoms/cm$^2$ of sample.

The value of $\sum \sigma_{\text{wings}}$ was calculated in the region of the 23.9 and 39.0 eV resonances. Successive approximations finally gave the values of $T_c$ in the regions of the 23.9 and 39.0 eV resonances to $\approx$ 1 %.

The second difficulty of the standard area analysis is due to the omission

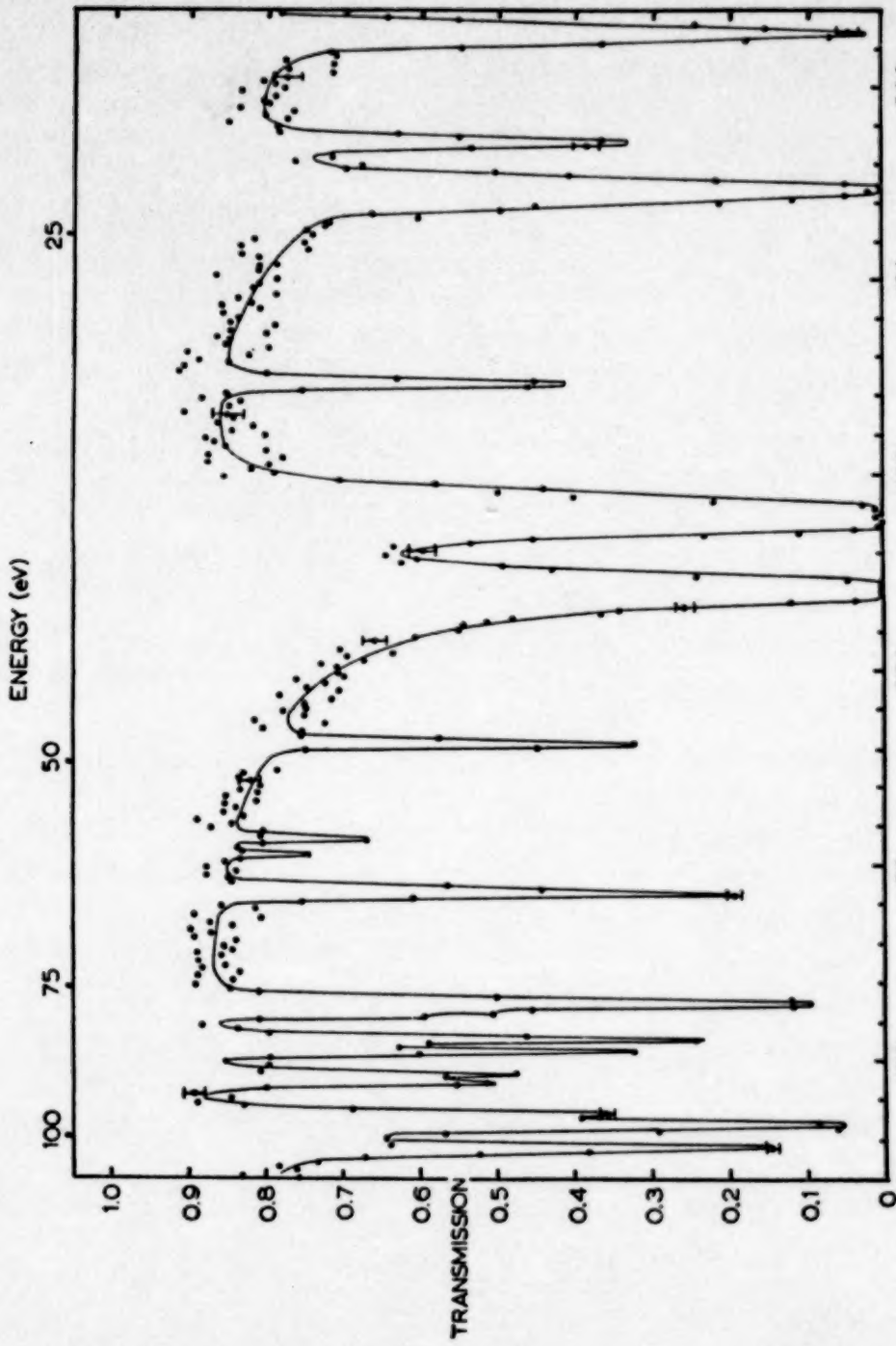


Fig. 1. The observed transmission of Ta as a function of the time-of-flight $n = 0.01908 \times 10^{24}$ atoms/cm$^2$.

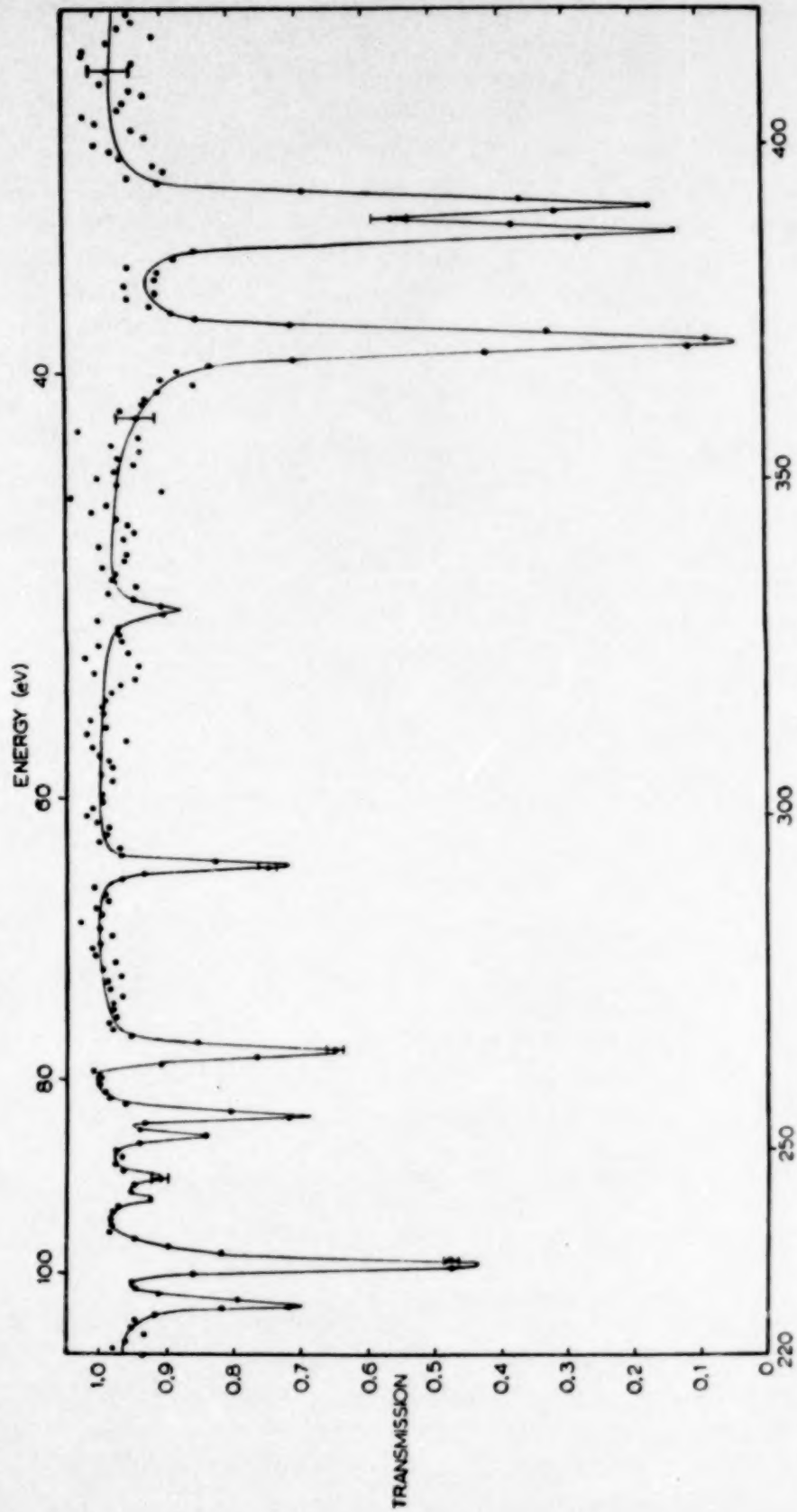


Fig. 2. The observed transmission of Ta as a function of the time-of-flight $n = 0.00152 \times 10^{24}$ atoms/cm$^2$.

from the expression for the total cross section of the interference term

$$\frac{2ka\sigma_0 x}{1+x^2} \text{ where } x = \frac{2}{\Gamma}(E-E_R).$$

For resonances with large values of $\Gamma_n$ the interference between resonance and potential scattering may be appreciable even at low neutron bombarding energies. Lynn [1]) has produced a general method of area analysis which includes the effects of interference and this method has been used in ana-

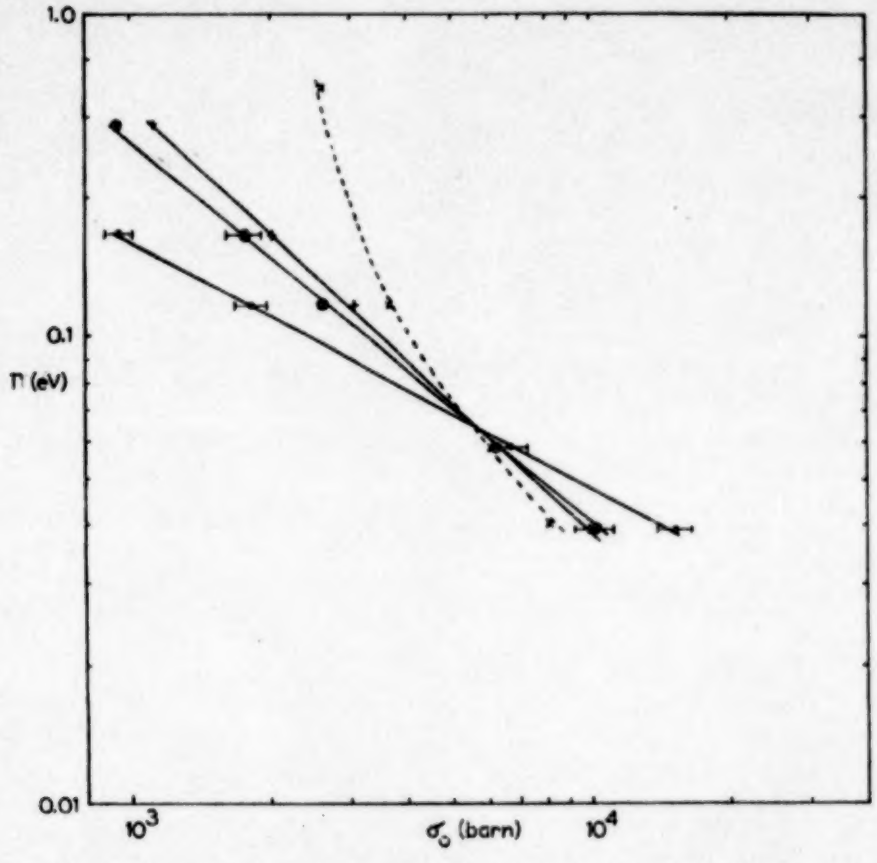


Fig. 3 An analysis of the 23.9 eV resonance in Ta. A plot of log $\Gamma$ versus log $\sigma_0$.
• • • Area measurement $n = 0.00054 \times 10^{24}$ atoms/cm².
○○○ Area measurement $n = 0.00076 \times 10^{24}$ atoms/cm².
+++ Area measurement $n = 0.000304 \times 10^{24}$ atoms/cm².
××× Minimum transmission $n = 0.000304 \times 10^{24}$ atoms/cm².

lysing the 39.0 and 98.8 eV resonances. A small correction was also made to the thickest sample area of the 23.9 eV resonance.

For weak resonances ($\sigma_0\Gamma^2 < 1$, say) it is difficult to obtain $\sigma_0$ and $\Gamma$ from area methods alone unless a large amount of experimental time is available for improving the statistical accuracy of the results. In these cases the "minimum transmission" method of Lynn and Rae [8]) is useful.

TABLE 1

Neutron resonance parameters of tantalum

| 1<br>Resonance energy (eV) | 2<br>Sample thickness (atoms/cm$^2$ $\times 10^{24}$) | 3<br>Observed area (eV) | 4<br>$\sigma_0\Gamma^2$ (b · eV$^2$) | 5<br>$\sigma_0$ (b) | 6<br>$\Gamma$ (meV) | 7<br>$g\Gamma_n$ (meV) | 8<br>$\Gamma_\gamma$ (meV) |
|---|---|---|---|---|---|---|---|
| 20.2±0.2 | 0.00954<br>0.01908 | 0.463±0.014<br>0.620±0.019 | 4.7 ± 0.3 | 1300±300 | 60±11 | 0.60±0.06 | 59±11 |
| 22.7±0.2 | 0.00954<br>0.01908 | 0.127±0.010<br>0.215±0.016 | 0.5 ± 0.1 | 200±70 | 51±20 | 0.90±0.02 | 51±20 |
| 23.9 | 0.000304<br>0.00076<br>0.00954<br>0.01908 | 0.142±0.010<br>0.279±0.011<br>0.915±0.027<br>1.190±0.048 | 23.1 ± 1.3 | 5800±800 | 63± 8 | 3.8 ±0.3 | 55±8 |
| 29.9 | 0.01908 | 0.210±0.010 | 0.56± 0.1 | 150±70 | 60±20 | 0.10±0.05 | 60±20 |
| 35.0 | 0.000304<br>0.00152 | 0.198±0.017<br>0.539±0.019 | 36 ± 3 | 7300±2000 | 70±14 | 5.8 ±0.6 | 58±14 |
| 35.8 | 0.000304<br>0.00152 | 0.215±0.018<br>0.592±0.020 | 44 ± 4 | 7600±2000 | 76±14 | 7.9 ±0.8 | 60±14 |
| 39.0±0.3 | 0.000304<br>0.00152<br>0.01908 | 0.476±0.024<br>1.015±0.030<br>3.23 ±0.10 | 174 ±10 | 16700±2500 | 102±10 | 25.4 ±3 | 51±13 |
| 49.0 | 0.00954<br>0.01908 | 0.299±0.015<br>0.464±0.019 | 1.6 ± 0.2 | 500±200 | 56±14 | 0.53±0.05 | 55±15 |
| 57.3 | 0.01908 | 0.158±0.013 | 0.3 ± 0.1 | | | | |
| 58.8 | | | | | | | |
| 62.9±0.5 | 0.00152<br>0.01908 | 0.251±0.018<br>0.970±0.030 | 9.7 ± 0.7 | 1800±400 | 73±20 | 3.2 ±0.6 | 67±20 |
| 76.8 | 0.00152<br>0.01908 | 0.45 ±0.04<br>1.29 ±0.10 | 20 ± 3 | 5000±1000 | 60±15 | 8 ±2 | 44±20 |
| 78.3 | | | | | | | |
| 78.9 | | | | | | | |
| 82.7 | 0.00152<br>0.01908 | 0.37 ±0.04<br>1.2 ±0.10 | 15 ± 2.5 | 3000±800 | 72±20 | 6.8 ±1 | 58±22 |
| 84.7 | 0.01908 | 0.78 ±0.07 | 4.4 ± 0.7 | 1050±200 | 65±18 | 2.2 ±0.4 | 61±20 |
| 88.9 | | | | | | | |
| 90.7 | | | | | | | |
| 96.7 | | | | | | | |
| 98.8±1 | 0.00152<br>0.01908 | 1.28 ±0.05<br>3.88 ±0.19 | 260 ±25 | 9000±2000 | 170±30 | 58 ±8 | 54±32 |

This method requires a knowledge of the shape of the resolution function of the spectrometer. For the Harwell spectrometer used in these measurements the shape of the resolution function is found to be approximately Gaussian of full width $R = 0.8$ $\mu$sec at $e^{-\frac{1}{4}}$ of its maximum [4]). The results of this technique yield a set of values of $\sigma_0$ as a function of $\Gamma$ which may then be used in conjunction with the $(\sigma_0, \Gamma)$ curve from one area measurement. This method was used for the resonances at 22.7, 29.9 and 49.0 eV and also used as a check for the 23.9 eV resonance. The analysis of the 23.9 eV resonance shown in fig. 3 includes a "minimum transmission" measurement.

## 4. Results

The resonance parameters obtained for thirteen Ta resonances between 20 eV and 100 eV are listed in table 1. Resonances at 57.3, 58.8, 78.3, 78.9, 88.9, 90.7 and 96.7 eV were observed but were not sufficiently well resolved to be analysed. The observed areas are given in column 3 of table 1. These areas include wing corrections (dependent upon the final parameters) but do not include corrections for Doppler broadening and finite sample thickness.

The errors in $\Gamma_\gamma$ do not include the error introduced by assuming $g = \frac{1}{2}$.

The average reduced neutron width for the thirteen resonances measured is $\Gamma_n^0 = 2.4 \pm 0.9$ meV. The level spacing per spin state is $D = 8 \pm 2$ eV giving $\Gamma_n^0/D = (3.0 \pm 1.3) \times 10^{-4}$.

Together with measurements of neutron scattering and capture gamma ray yields obtained using the Harwell 15 MeV accelerator these results give values of $J$ and $\Gamma_\gamma$ for resonances at 23.9 and 39.0 eV. The combined data for Ta obtained by the Harwell accelerator group are reported in the following paper of Evans, Kinsey, Waters and Williams.

The author is indebted to Mr. M. C. Moxon for his assistance during the experiment and computation. He is grateful to Mr. J. E. Lynn for his advice on the analysis of the data and for the use of his new area technique before publication. Finally, he wishes to thank Dr. B. B. Kinsey under whom the work was carried out, for his continued interest and encouragement.

## References

1) J. E. Lynn, Nuclear Physics **7** (1958) 599
2) R. G. Fluharty, F. B. Simpson and O. D. Simpson, Phys. Rev. **103** (1956) 1778
3) I. A. Radkevitch, V. V. Vladimirsky and V. V. Sokolovsky, J. Nuclear Energy **5** (1957) 92
4) J. E. Lynn, F. W. K. Firk and M. C. Moxon, Nuclear Physcis **5** (1958) 603
5) E. R. Rae and E. M. Bowey, Proc. Phys. Soc. A **56** (1953) 1073
6) E. Melkonian, W. W. Havens, Jr. and L. J. Rainwater, Phys. Rev. **92** (1953) 102
7) D. J. Hughes, J. Nuclear Energy **1** (1955) 237
8) J. E. Lynn and E. R. Rae, J. Nuclear Energy **4** (1957) 418

2.A.1 *Nuclear Physics* 9 (1958/59) 205—217; © *North-Holland Publishing Co., Amsterdam*
Not to be reproduced by photoprint or microfilm without written permission form the publisher

# RADIATION WIDTHS OF NEUTRON RESONANCES IN Ta

J. E. EVANS, B. B. KINSEY, J. R. WATERS and G. H. WILLIAMS
*Atomic Energy Research Establishment, Harwell, Didcot, Berks*

Received 20 September 1958

**Abstract:** The radiation widths of 12 neutron resonances in Ta have been determined from a combination of transmission, resonance scattering, and capture measurements. The spins of the compound states corresponding to two of these resonances were found; both were of spin 4. In addition an unresolved pair near 35 eV, are probably both spin 4. The radiation widths of those with spin 4 were close to a mean value of 63 meV.

## 1. Introduction

A considerable amount of data on the radiation widths of neutron resonances [1]) has been accumulated. This refers mainly to the lowest energy resonances; in any one nucleus (with the exception of Ag[2])) there is little or no information on the radiation widths of resonances other than that with the lowest energy. As Firk has shown in the preceding paper [8]), approximate results for radiation widths can be obtained from transmission measurements alone. Such measurements, however, unsupported by other data, are insufficiently accurate to reveal detail of immediate interest, viz., the spread of the radiation widths about their mean value for a particular isotope, and the dependence (if any) of the mean value on the spin. The results previously obtained for Ag [2]) showed that the radiation widths for different resonances differed little from their mean value, and that the mean values for the two Ag isotopes differed, surprisingly enough, by less than the error of measurement. The present work was started in the hope of obtaining more information of the spin dependence of radiation widths; in this paper we report a determination of the radiation widths of resonances in tantalum using the Harwell linear accelerator. We have combined the results of measurements of resonance scattering and capture $\gamma$-rays with transmission data: those of Firk [8]), and where relevant, those of Harvey *et al.* [3]) and of Fluharty *et al.* [4]).

## 2. Method

A method of combining transmission, resonance scattering, and resonance capture data has been described by Rae [5]). Each experimental result can be represented by a plot of the neutron width against the total width. The form

of the relationship between these two quantities and their numerical values depend on the type of experiment.

A transmission measurement consists of the determination of the area of the dip in the curve of neutron transmission against time of flight. Evaluation of such measurements can be made most conveniently with the aid of curves given by Hughes [6]), who has plotted the area ($A$) under the transmission curve (normalised to eliminate potential scattering), divided by the Doppler width $\Delta$, as a function of $n\sigma_0\Gamma/\Delta$, for different values of $\Gamma/\Delta$. Here $n$ is the number of atoms/cm$^2$ of the target surface; $\Gamma$ is the total width $\Gamma = \Gamma_n + \Gamma_\gamma$; and $\sigma_0$ is the peak resonance cross section for $\Delta = 0$, viz., $\sigma_0 = 4\pi\lambda^2 g\Gamma_n/\Gamma$, in which $g$ is the statistical weight factor, $g = \frac{1}{2}[1 \pm 1/(2I+1)]$ for a nucleus with spin $I$. Using Hughes' curves, determination of $A/\Delta$ gives a relationship in the form

$$g\Gamma_n\Gamma^p = \text{constant} = T$$

where the power $p$ to which $\Gamma$ is raised lies between 0 and 1.

The experimental methods employed to determine resonance scattering and capture have been described elsewhere [2]). In short, resonance scattering is measured with a neutron detector ($BF_3$ counters), resonance capture with a $\gamma$-ray detector (NaI crystals) †. The area under the scattering or capture curve was measured for a number of targets of different thicknesses. Neglecting self-screening effects, the areas for very thin foils are proportional to their thickness; when suitably calibrated, the quantities $S = g\Gamma_n^2/\Gamma$ for resonance scattering and $C = g\Gamma_n(1-\Gamma_n/\Gamma)$ for resonance capture can be derived from them. For thicker foils, the area obtained, divided by the thickness, decreases with increasing thickness owing to the effects of absorption. For each foil the observed areas can be corrected for absorption by choosing an approximate value for $\sigma_0\Gamma$ from the transmission data, and obtaining the appropriate correction from Hughes' curves. The corrected values of $S$ and $C$, when plotted against the thickness of the foil fall on a straight line (provided the thickness is not excessive ($n\sigma_0 \gtrsim 1$)), usually parallel to the axis of thickness (see fig. 1). The values obtained by linear extrapolation of these corrected results to zero thickness gives the final values of $S$ and $C$.

If precise enough, the various experimental quantities, $T$, $S$, and $C$, give rise to curves in the $\Gamma_n$, $\Gamma$ plane which would pass through the same point for one value of the statistical factor, $g$, but not for the other. In practice these curves are never concurrent; it is not possible therefore to determine the value of $g$ unambiguously, but only the relative probabilities of the two

† It was found that the X-ray burst from the 15 MeV linear accelerator at the start of the cycle caused overloading of the capture detector amplifier. The result of this was a change in amplifier gain at short delay times, detected by noting the variation in height of the pulses from a $Cs^{137}$ source when measured at different delay times. The overloading was removed by pulsing off the photomultipliers during the period of the X-ray burst.

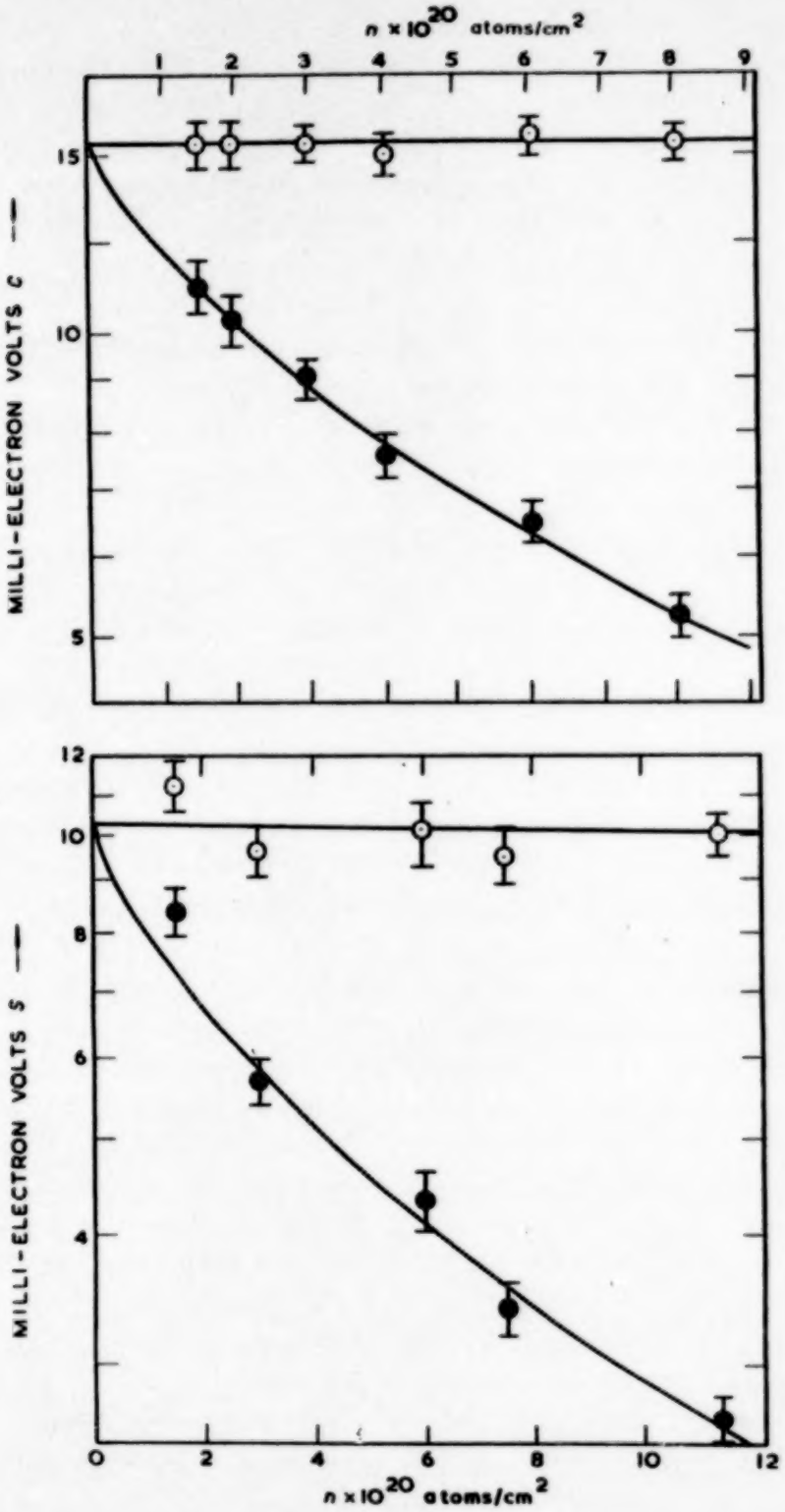


Fig. 1. Capture and scattering measurements for the 39 eV resonance. Full circles: experimental results; open circles: experimental results corrected from Hughes curves [6]).

possible solutions. This was done by a root mean square method [2]) coded for machine calculation †. For Ta the distinction between the possible values of $g$ was more difficult to make than in the previous work on Ag (spin $\frac{1}{2}$), because the spin of Ta is $\frac{7}{2}$ and the two values of $g$, $\frac{7}{16}$ and $\frac{9}{16}$, differ rather little from one another. The more probable $g$ value is the one with the lower value of $\chi^2_{\min}$, the sum of the squares of the weighted deviations of the experimental values of $\Gamma_n$ from the mean; $\chi^2_{\min}$ is shown in column 8 of table 1.

As described elsewhere [5]) the areas obtained with the capture $\gamma$-ray detectors were calibrated in a separate measurement of a low energy resonance together with a determination of the neutron spectrum. With a low energy resonance a thick sample produces a flat-topped resonance peak when counting rates are plotted against flight time. The ordinate of this peak is the quantity we require, for it represents the $\gamma$-ray yield when practically every neutron incident on the foil is absorbed in it. For Ta, we used the 4.28 eV resonance, the calibration being performed by inserting a 0.020 in. Ta foil normal to the beam and parallel to the plane containing the counters. The thickness of this foil was sufficient to cause an appreciable absorption of tne measured $\gamma$-radiation. The effect (about 8 percent) was determined by finding the appropriate ordinate at resonance for a series of foils of different thickness (each thick enough to give a flat-topped resonance peak) and extrapolating the results to zero thickness. The neutron spectrum was measured by counting the 480 keV $\gamma$-rays from a thick plate of $B^{10}$ in the beam as a function of time of flight [5]). The shape of the neutron spectrum was in agreement with that obtained with the Pb calibration of the scattering measurements.

The calibration of the capture measurements involved two assumptions.

First, it was assumed that every neutron incident on the thick foil was absorbed. This is not strictly true. The fraction of neutrons scattered out of the Ta sample at the 4.28 eV resonance was measured in the scattering apparatus with a resolution similar to that of the capture experiment at the same energy. For Ta foils 0.002 and 0.004 in. thick, the fraction was found to be 1.4 and 0.95 percent respectively. For 0.004 in. foils over 99 percent of the neutrons in the centre of the resonance are removed from the beam. Thus for 0.020 in. foils, almost all the neutrons are removed and the extra thickness will certainly cause further capture events. It was reasonable, therefore, to assume that the effect of scattered neutrons on the capture calibration was no more than 1 percent and could therefore be ignored.

Second, it was assumed that the efficiency of detection of $\gamma$-rays from different resonances is the same for each or, in effect, that the energy spectra

† We are indebted to Mr. J. E. Lynn and Dr. E. R. Rae for suggesting this method and for arranging the coding.

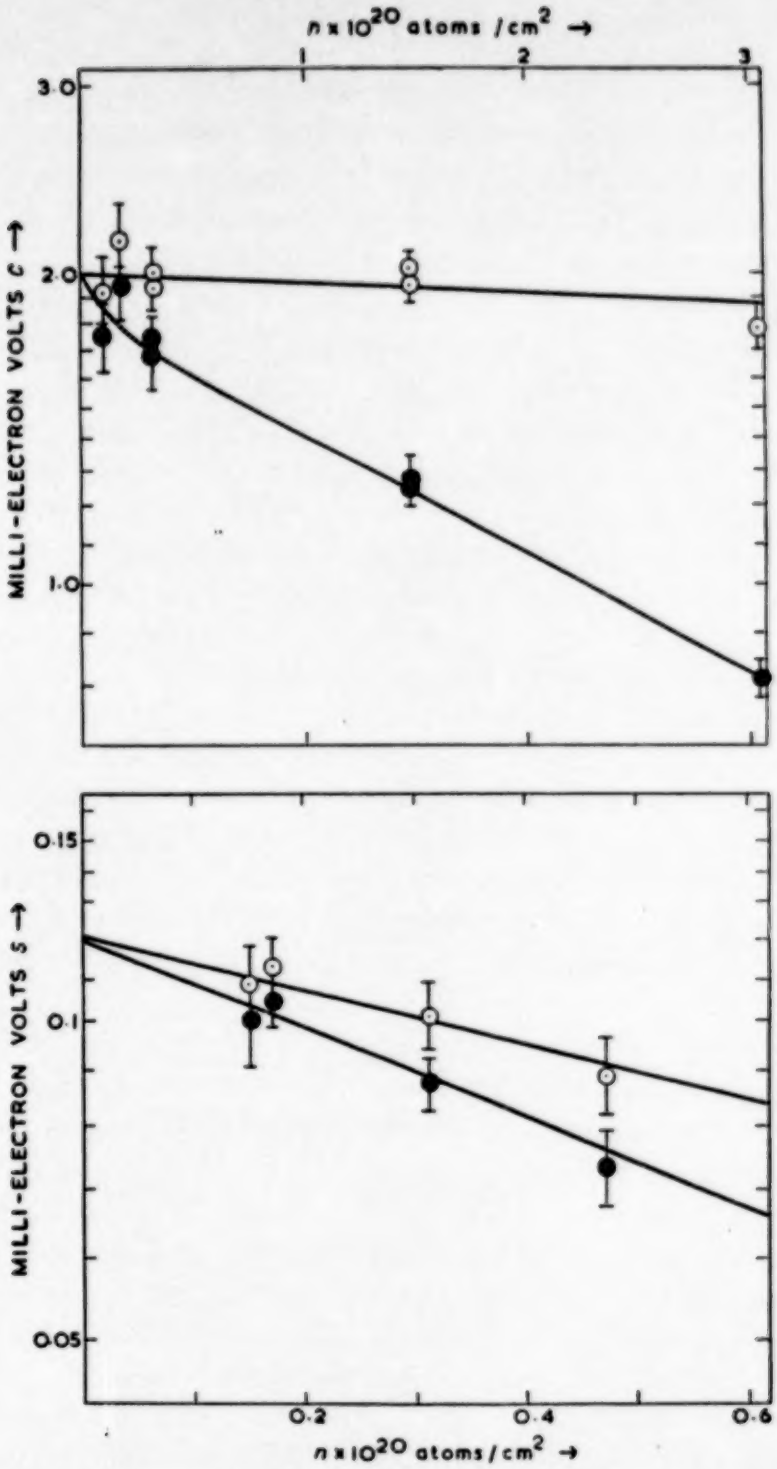


Fig. 2. Capture and scattering measurements for the 4.28 eV resonance.

of the capture radiation for different resonances are similar. The validity of this assumption has been discussed before [5]); it has been studied experimentally by Rae [5]) who determined the relative average efficiencies of detection of capture $\gamma$-rays at different resonances by measurement of the ratio of the

coincident to single counting rates in two NaI crystals mounted near a Ta target. To an accuracy of 5 to 10 percent no difference was found.

The scattering areas, which were calibrated by scattering from a sample of spectroscopically pure Pb, present no similar theoretical difficulties. The method of correcting the experimental scattering areas for absorption as described above is really inadequate, for, as explained in an earlier paper [2]), the neutrons scattered by low energy resonances have a high probability of being recaptured as they leave the foil. The method of correcting for self-absorption described above, in which this effect is ignored, although inadequate, does give an approximately linear plot when the corrected areas are plotted against the thickness (figs. 1 and 2). The intercept obtained by extrapolating this straight line to zero thickness should give the required result. For higher energy resonances, the absorption of the scattered neutrons becomes insignificant because their energies are shifted outside the resonance region. In the present apparatus, the mean scattering angle is 90°, and the corresponding ratio of the energy shift to the half width of the resonance is $4E/A\Gamma$ where $E$ is the resonance energy and $A$ is the atomic weight. For the Ta resonances, $\Gamma$ is 0.1 eV or less, and it is clear that the shift is sufficient to move the energy of the scattered neutron outside the resonance region for neutrons of 10 eV or more. This is shown by the horizontal line through the corrected values of $S$ for the 39 eV resonance, for which the corrections are sufficient. For the 4.28 eV resonance the energy shift is not enough to take the energies of the scattered neutrons out of the resonance region; the corrections are insufficient and the line forming the corrected points slopes downwards (see fig. 2).

Since the resonance scattering is proportional to the square of the neutron width, measurements with the present apparatus are limited to strong resonances. The scattering measurements, however, are essential for the determination of the spin.

## 3. Results

The results of the scattering and capture measurements are listed in columns 2 and 3 of table 1. They were calculated on the basis of the resonance energies obtained by Firk (column 1). The figures in brackets are standard deviations expressed as percentages. These take into account the consistency of the several measurement values of $S$ and $C$ when extrapolating to zero thickness and also the fluctuations in the number of counts observed. Column 4 contains the number of transmission measurements used in the least squares solution of the problem, the initial referring to the group responsible for the measurement; column 5 contains the spin corresponding to the most probable solution, and columns 6 and 7 refer to the final results for the radiation and neutron widths respectively. Where scattering measure-

TABLE 1

Parameters for Ta resonances

| $E_R$ (eV) | $S$ (meV) | $C$ (meV) | Transmission data | $J$ | $\Gamma_\gamma$ (meV) | $\Gamma_n$ (meV) | $\chi^2_{min}$ |
|---|---|---|---|---|---|---|---|
| 4.28 | 0.12 (8) | 1.96 (5) | 3E | — | 67.0±2.8 [c]) | 4.4 ±0.1 [c]) | 12.1 [c]) |
| | | | | | 62.1±2.6 [d]) | 3.6 ±0.1 [d]) | 14.4 [d]) |
| 10.4 | 0.105 (10) | 1.98 (6) | 2H | 4 | 65 ±6 | 3.6 ±0.1 | 1.0 [d]) |
| | | | | | | | 3.7 [c]) |
| 13.95 | Not detected | 0.495 (8) | 3H; 2Fl | — | 52 ±2.6 [c]) | 1.30±0.04 [c]) | |
| | | | | | 52 ±2.6 [d]) | 1.01±0.03 [d]) | |
| 20.2 | Not detected | 0.50 (7) | 4H; 2F; 2Fl | — | 70 ±6 [c]) | 1.22±0.06 [c]) | |
| | | | | | 70 ±6 [d]) | 0.95±0.04 [d]) | |
| 22.7 | Not detected | 0.16 (50) | | | | | |
| 23.9 | 0.30 (10) | 3.06 (7) | 4H; 3F; 4Fl | — | 63.7±3.4 [c]) | 7.2 ±0.2 [c]) | 19.3 [c]) |
| | | | | | 59.8±3.2 [d]) | 5.8 ±0.2 [d]) | 19.8 [d]) |
| 29.9 | Not detected | Too small to measure | | | | | |
| 35.0 | 2.5 (12) [b]) | 13.3 (4) [b]) | 2F; 1Fl | 4 [a]) | 63 ±6 | 12.3 ±0.4 | |
| 35.8 | | | 2F; 1Fl | 4 [a]) | 71 ±7 | 14.7 ±0.5 | |
| 39.0 | 10.2 (7) | 15.4 (4) | 4H; 3F | 4 | 64.3±3.3 | 44.3 ±0.9 | 4.2 [d]) |
| | | | | | | | 17.4 [c]) |
| 49.0 | Not detected | Too small to measure | | | | | |
| 57.3 | Not detected | Too small to measure | | | | | |
| 58.8 | Not detected | Too small to measure | | | | | |
| 62.9 | Not detected | 2.22 (8) | 2F; 2H; 1Fl | | 59 ±7 [c]) | 7.0 ±0.4 [c]) | |
| | | | | | 62 ±7 [d]) | 5.4 ±0.3 [d]) | |
| 76.8 | Not detected | 8.4 (10) | | | | | |
| 78.3 | Not detected | | | | | | |
| 78.9 | Not detected | | | | | | |
| 82.7 | Not detected | 7.5 (10) | | | | | |
| 84.7 | Not detected | | | | | | |
| 88.9 | Not detected | 3.25 (7) | | | | | |
| 90.7 | Not detected | | | | | | |
| 96.7 | Not detected | Not resolved | | | | | |
| 98.8 | 34 (6) [b]) | 17.6 (8) | | | | | |

[a]) Solution corresponding to case (a) (see text); [b]) sum of areas for unresolved pair; [c]) for $J = 3$; [d]) for $J = 4$.

$S$ is the result of the resonance scattering measurement, $S = g\Gamma_n^2/\Gamma$; $C$ is the result of resonance capture measurements, $C = g\Gamma_n(1-\Gamma_n/\Gamma)$. Percentage error is given in parentheses; $J$ is the spin determined by combining these measurements with transmission data. The numbers here refer to the numbers of measurements made by various groups: E: present work; F: Firk [8]); H: Harvey *et al.* [3]); Fl: Fluharty *et al.* [4]).

ments were not feasible, the two possible solutions for the resonance parameters differ very little, and the results included in the table are mean values. Some of the items in this table deserve special comment.

### 3.1. THE 4.28 eV RESONANCE

The scattering and capture measurements for this resonance are shown in fig. 2. The peak total cross section ($\sigma_0$) of this resonance is large and metallic foils of Ta with thicknesses of 0.001 in. and above are all relatively thick in terms of the product $n\sigma_0$. Thin samples were made by depositing the oxide ($Ta_2O_5$) on to 0.001 in. Al foils by sedimentation from water. The slopes of the corrected results shown in fig. 2 should be noted. The curve for the capture results is flat as we should expect; that for the scattering results falls off for increasing thickness because the correction takes no account of the absorption of the neutron after scattering. Because no accurate measurements of the transmission areas for this resonance have been quoted, we have made transmission measurements for this resonance with the results given in table 2. The Rae diagram for this resonance is given in fig 3. The values of $\chi^2_{min}$ show that the measurements are not accurate enough to determine $J$.

TABLE 2

Transmission data for the 4.28 eV resonance
(statistical percentage errors are given in parentheses)

| Area in eV | Number of atoms/cm² |
|---|---|
| 0.181 (5) | $0.147 \times 10^{21}$ |
| 0.402 (3) | 0.606 |
| 0.612 (3) | 1.46 |

The 4.28 eV resonance is of special interest in that other workers have also attempted to measure its parameters. The latest is that of Wood [7]) who studied this resonance with a crystal spectrometer and determined the resonance parameters by a study of the shape of the spectrum of both the transmitted and scattered neutrons, allowing for instrumental resolution and Doppler width. His work appears to favour $J = 4$. His figure for $\sigma_0\Gamma^2$ ($72 \pm 5$ b · eV²) is in good agreement with our transmission data (see fig. 3); so also are the neutron widths; but his result for the total width ($53 \pm 5$ meV) ($J = 4$) is significantly lower than ours (66 meV) ($J = 4$). Fig. 3 illustrates the difficulty in obtaining precise results from measurements of this kind; the diagram appears to favour $J = 4$, but it must be remembered that the standard errors are not shown. The values of $\chi^2_{min}$ are a better indication since they include these standard errors.

Fig. 3 shows an interesting feature of this resonance in common with that of other resonances in which the neutron width is much lower than the radiation width, e.g., the 10.4 and the 23.9 eV resonances. The radiation width is determined, in the main, by the intersection of the transmission curves with the scattering curve, and the capture area curve, being flat in the vicinity of the intersection, makes the most probable value of the radiation width rather insensitive to the measured value of the capture area. For weak resonances, then, the capture areas, within the limits of the validity of the calibration, determine the spin, rather than the radiation width.

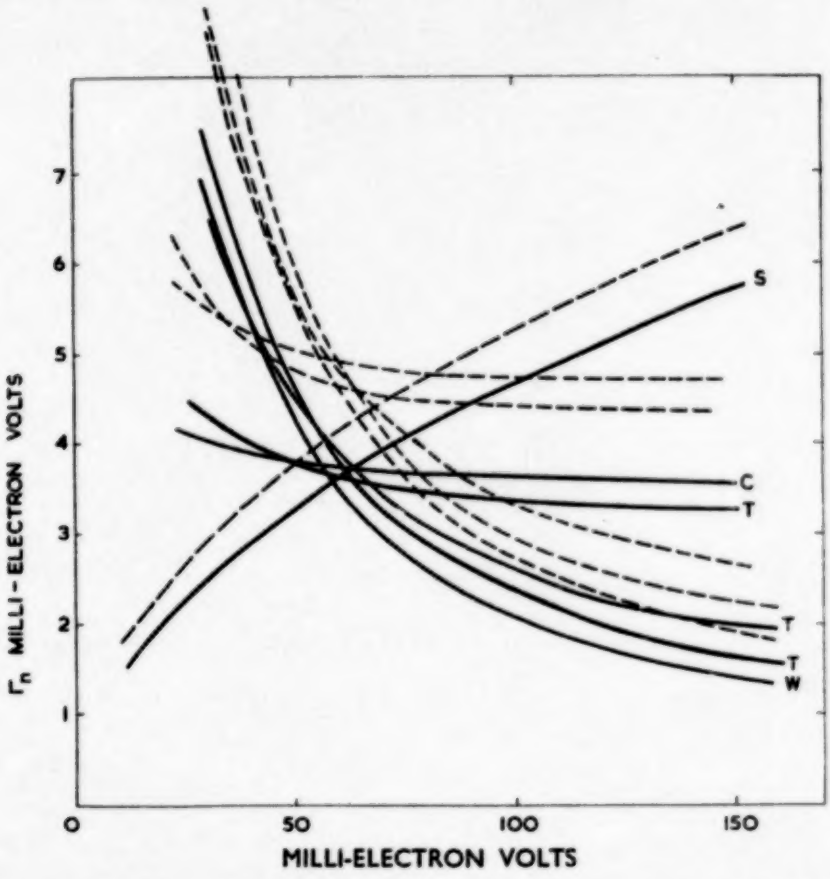


Fig. 3. Rae diagram for measurements on the 4.28 eV resonance. Full lines, spin 4 ($g = {}^{9}/_{16}$); broken lines, spin 3 ($g = {}^{7}/_{16}$). *S* and *C* are the scattering and capture results. The transmission measurements (*T*) are those quoted in table 2. *W* represents Wood's figures [7]) for $\sigma_0\Gamma^2$.

### 3.2. THE 35.0 AND 35.8 eV RESONANCES

These resonances were not resolved in the scattering measurements and only partially separated from the peak due to the 39 eV resonance. The capture measurements, some of which were made at 11 m with a short neutron pulse and 0.5$\mu$sec timing channels, partially resolved them. An attempt was made to resolve these resonances with the scattering apparatus by shortening the length of the counters (see ref.[2])) and using narrower

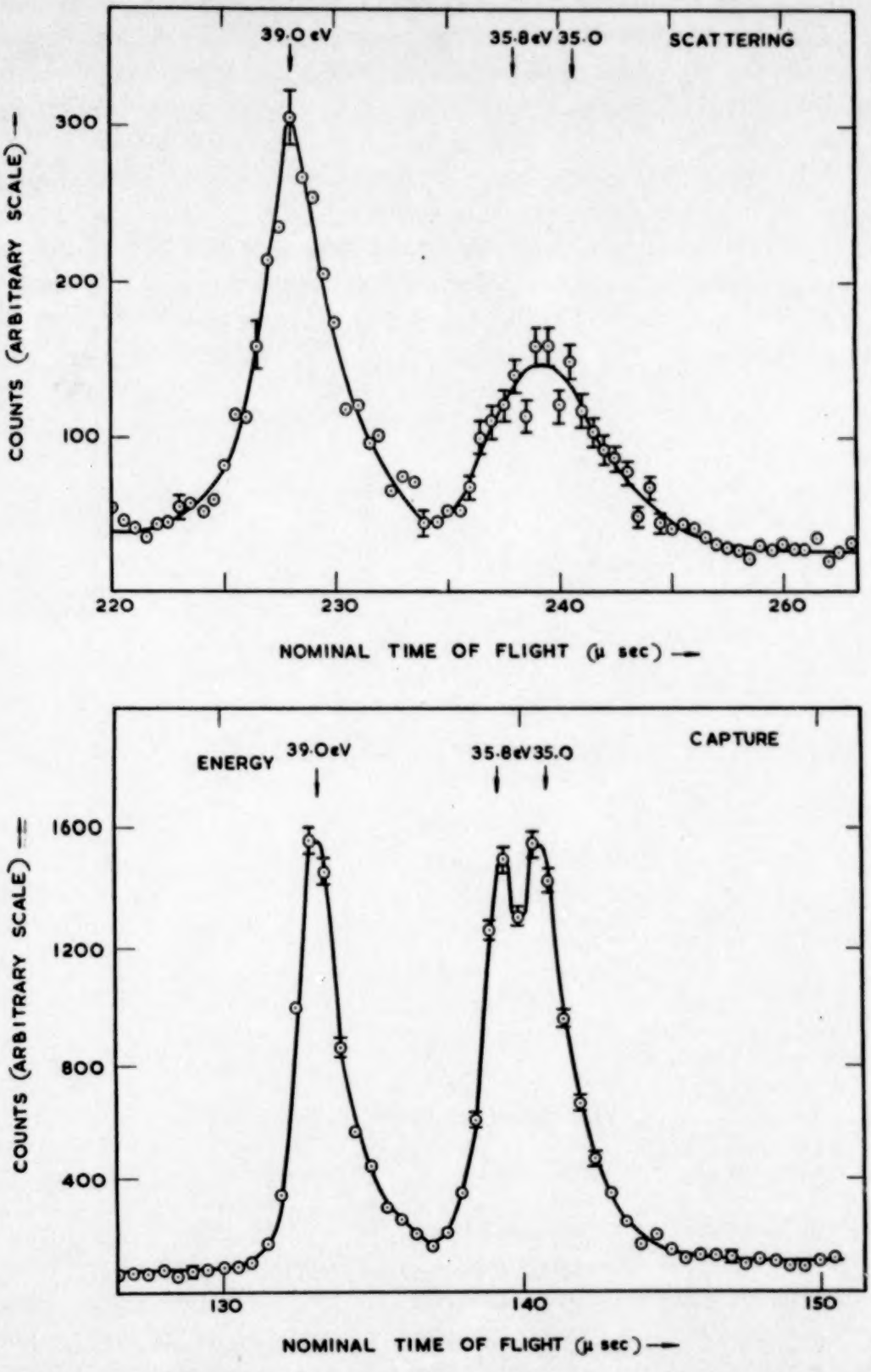


Fig. 4. Counting rate curves for the 39, 35.0 and 35.8 eV resonances.

channels. The results are shown in fig. 4; they are insufficient to determine the parameters of these resonances completely, but when the separate transmission areas are considered it is possible to eliminate certain spin assignments.

The transmission data of Firk and of Fluharty *et al.* show consistently that the transmission areas for the 35.8 eV resonance are about 10 percent greater than for the 35.0 eV resonance. If we assume that this effect is real, (and the statistics of individual measurements do not prove it conclusively), it must reflect a difference in 10 percent between the products $g\Gamma_n$. There are four cases to consider: (a) either both resonances correspond to spin 4; (b) that at 35.8 has spin 4, the other spin 3; or (c) vice-versa; or (d) both states have spin 3. With these criteria we may deduce the ratios of the neutron widths, and hence the appropriate division of the total observed scattering and capture areas between the two resonances. The solution of the eight sets of equations definitely favours (a) for which both resonances correspond to spin 4. If this interpretation is correct interference between the two resonances should be observable, but it would require very high resolution to see it; this effect would tend to decrease the values of the transmission and scattering areas and an upward adjustment of these quantities would improve the concurrence in the Rae diagram. Construction of theoretical curves to represent the two components of the unresolved group, for each of the four cases mentioned above, leads, in each instance, to widths in agreement with those found, but without making it possible to decide between them.

### 3.3. THE 39 eV RESONANCE

This is interesting in that the neutron and radiation widths are nearly equal giving concurrence in the Rae diagram near the apex of the parabola representating the capture measurements (fig. 5).

### 3.4. THE RESONANCES FROM 76 TO 85 eV

Most of the resonances in this range could not be resolved (fig. 6) with the present capture apparatus, and the results listed in table 1 refer to the corrected values for the sums of the areas extrapolated to zero thickness.

### 3.5. THE 99 eV RESONANCE

Recent measurements by Firk[9]) have shown that there are two resonances at this energy, very close together. The resonance at 96 eV could not be resolved from the 99 eV resonances when studied by the capture detector. Although weak, the former will have a rather large effect on the measurement of the capture area of the other two; however, its influence on the scattering area is negligible. According to Firk[9]), the transmission areas for a target

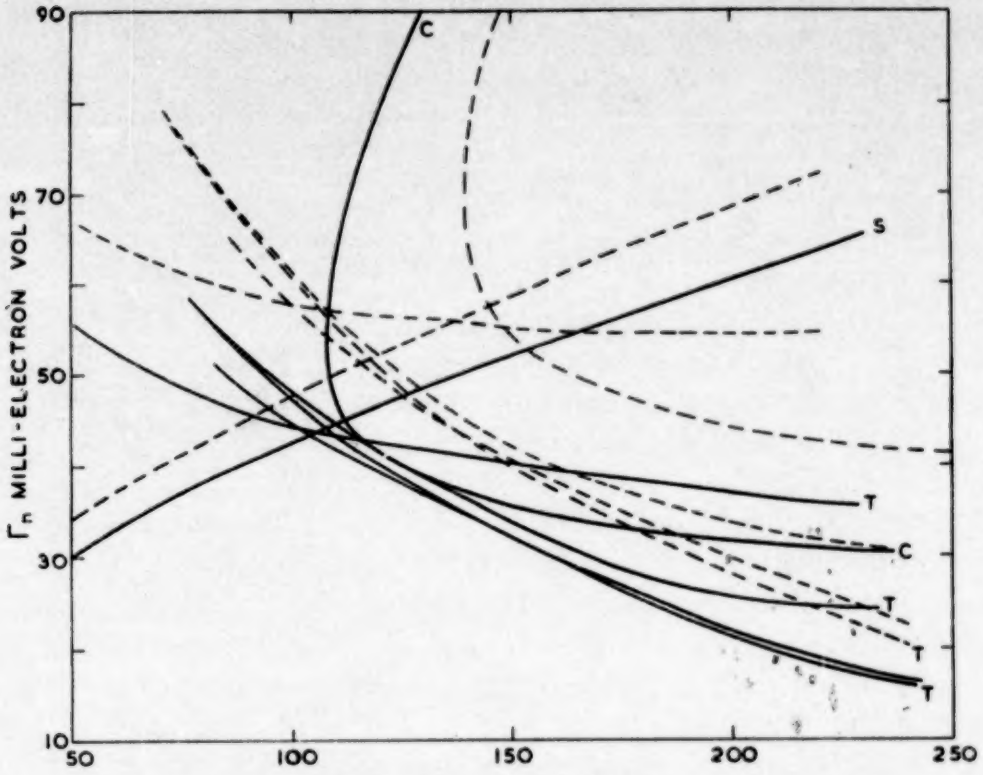


Fig. 5. Rae diagram for the 39 eV resonance. Only Firk's transmission measurements ($T$) are shown in this diagram. Full lines, spin 4 ($g = {}^{9}/_{18}$); broken lines, spin 3 ($g = {}^{7}/_{18}$). $S$ and $C$ are the scattering and capture results.

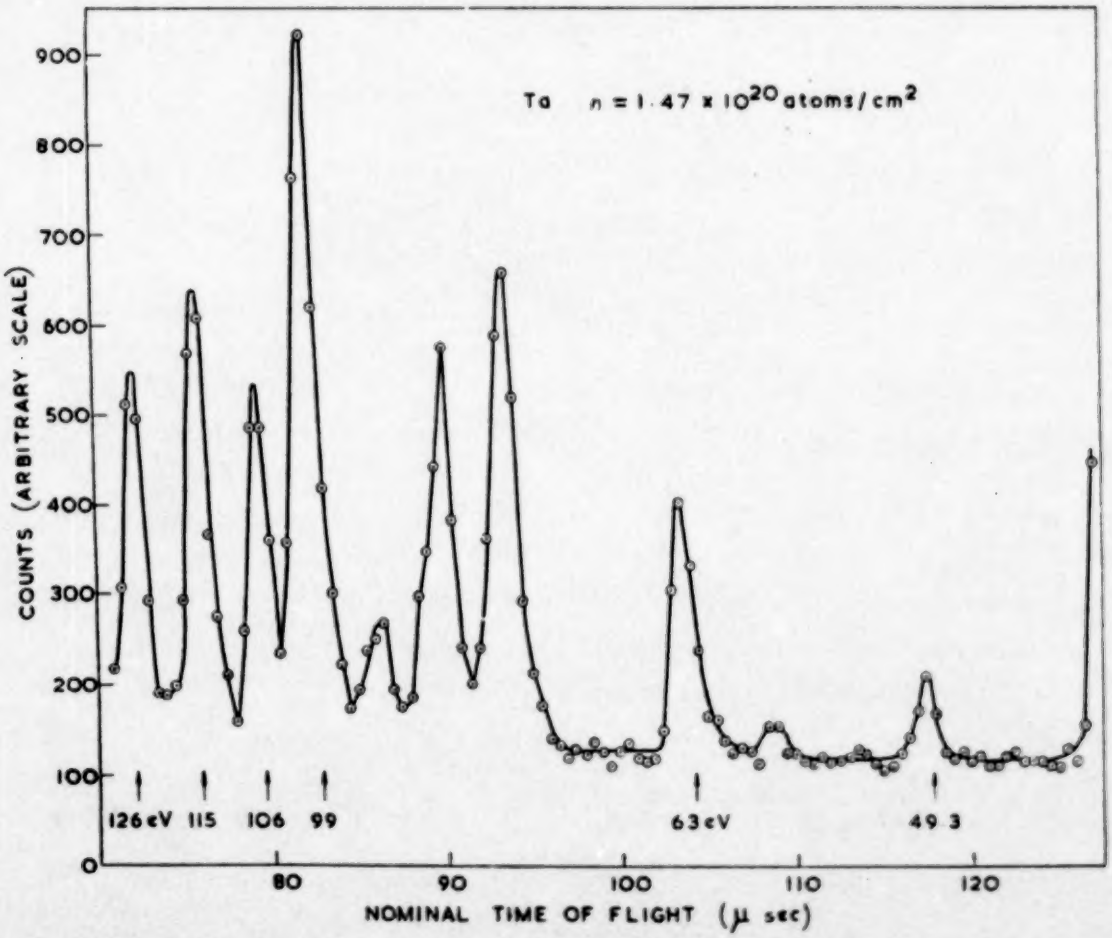


Fig. 6. Capture $\gamma$-ray counting rates for higher energy resonances.

thickness corresponding to $n = 9.54 \times 10^{21}$ atoms/cm$^2$ were 0.6 and 2.65 eV for the 96 and 99 eV resonance respectively. Knowing approximately the neutron and radiation widths in the latter resonance, we deduced that the ratios of the capture areas should be approximately 0.14 regardless of the spins. The capture area for the two resonances at 99 eV in table 1 was reduced by this amount and the entry in table 1 gives this corrected value.

## 4. Conclusions

The present measurements are too scanty to make possible definite conclusions about the spin dependence of radiation widths. Two resonances almost certainly have spin 4, two others probably; the radiation widths of these four have a mean value of 65 meV and differ very little from it. Of the remaining five, four agree within their errors with a width of 65 meV, and one has a lower radiation width of $52 \pm 2$ meV. This difference is probably real but its significance is not clear.

We are indebted to Dr. E. R. Rae and Mr. J. E. Lynn for discussions during the course of this work and for much valuable advice and criticism; to Mr. Frank Allen for preparation of thin foils of $Ta_2O_5$; and to the computing group for the least squares calculations.

## References

1) D. J. Hughes and J. A. Harvey, Nature **173** (1954) 942; J. S. Levin and D. J. Hughes, Phys. Rev. **101** (1956) 1328
2) E. R. Rae, E. R. Collins, B. B. Kinsey, J. E. Lynn and E. R. Wiblin, Nuclear Physics **5** (1957) 89
3) J. A. Harvey, D. J. Hughes, R. S. Carter and V. E. Pilcher, Phys. Rev. **99** (1955) 10
4) R. G. Fluharty, F. B. Simpson and O. D. Simpson, Phys. Rev. **103** (1956) 1778
5) E. R. Rae, Proc. Int. Conf. Peaceful Uses of Atomic Energy **4** (1955) 10; see also J. E. Lynn and E. R. Rae, J. Nuc. Energy **4** (1957) 418
6) D. J. Hughes, J. Nuc. Energy **1** (1955) 237
7) R. E. Wood, Phys. Rev. **104** (1956) 1425
8) F. W. K. Firk, Nuclear Physics **9** (1958/59) 198
9) F. W. K. Firk, to be published

1.D.1 *Nuclear Physics* 9 (1958/59) 218—224; © *North-Holland Publishing Co., Amsterdam*
Not to be reproduced by photoprint or microfilm without written permission from the publisher

# EVALUATION OF SLATER INTEGRALS WITH HARMONIC OSCILLATOR WAVE FUNCTIONS

KENNETH W. FORD †
*University of California, Los Alamos Scientific Laboratory*
*Los Alamos, New Mexico* ††

and

E. J. KONOPINSKI
*Indiana University, Bloomington, Indiana* †††

Received 16 August 1958

**Abstract:** Formulas are given which make the evaluation of the expansion coefficients needed in the Talmi method of nuclear spectroscopy simpler than heretofore. For the case of a gaussian two-body potential, a formula is given which makes possible the direct evaluation of Slater integrals without recourse to the Talmi expansion.

## 1. Introduction

Talmi [1]) pointed out the advantage in nuclear spectroscopy calculations of the use of harmonic oscillator wave functions. In particular, he showed that the Slater double integral could be expanded as a finite series of single integrals. Moreover, in Talmi's method, the two-body potential itself is used directly, its Legendre polynomial expansion not being required.

Several authors have considered the expansion coefficients needed for application of the Talmi method. Some coefficients were given numerically by Talmi [1]). An explicit formula for the coefficients as a multiple sum was given by Kronheimer [2]). A similar formula from which the coefficients can be derived was given by Tauber and Wu [3]). A numerical table of the Talmi expansion coefficients was prepared by Kennedy [4]), and a more extensive similar table by True [5]). Thieberger [6]) has given simplified methods for calculating the coefficients in certain cases.

In this note we present formulas which make possible the evaluation of the Talmi coefficients more easily than heretofore. For the special case of a gaussian two-body potential, we also present a formula for the direct evaluation of Slater integrals which makes the Talmi expansion unnecessary.

† Present address: Physics Dept., Brandeis University, Waltham 54, Massachusetts.
†† Supported in part by the U.S. Atomic Energy Commission.
††† Supported in part by the National Science Foundation.

## 2. The Talmi Coefficients

We do not consider here the angular factors which enter into the evaluation of the matrix elements of two-body potentials, since they have been treated thoroughly by Racah [7]). The radial factors, which are the Slater integrals, can be expressed (for harmonic oscillator wave functions) in terms of the double integrals

$$f_k(m,m') = \frac{1}{2k+1}\int\int x_1^m x_2^{m'} v_k(bx_1, bx_2) \exp(-x_1^2-x_2^2)x_1^2 dx_1 x_2^2 dx_2. \quad (1)$$

For nodeless wave functions, the Slater integral is proportional to one such integral $f_k$; otherwise it is proportional to a sum of such integrals. In eq. (1), $k$, $m$, and $m'$ are all odd or all even integers, and $k$ is less than or equal to the smaller of $m$ and $m'$; $x_1 = r_1/b$, $x_2 = r_2/b$; $b$ is the length constant appearing in the wave functions, $\psi \propto \exp(-\frac{1}{2}r^2/b^2)$; and $v_k(r_1, r_2)$ is defined by

$$v_k(r_1, r_2) = \tfrac{1}{2}(2k+1)\int V(|\mathbf{r}_1-\mathbf{r}_2|)P_k(\cos\theta_{12})d(\cos\theta_{12}), \quad (2)$$

where $V$ is the two-body potential, and $P_k$ is a Legendre polynomial.

The Talmi expansion is the expression of the double integral (1) in terms of the single integrals

$$J_{2\sigma} = \int_0^\infty x^{2\sigma} \exp(-\tfrac{1}{2}x^2)V(bx)x^2 dx. \quad (3)$$

(Our normalization of this Talmi integral differs from that in ref.[1]), therefore we have changed the notation from $I$ to $J$.) In an earlier publication [8]) the expansion was written, following Kennedy's notation [4]), as

$$f_k(m, m') = (\tfrac{1}{2}\pi)^{\frac{1}{2}} \sum_\sigma C_k^{2\sigma}(m, m')J_{2\sigma}, \quad (4)$$

where $\sigma$ takes on integer values from 0 to $\bar{m} \equiv \frac{1}{2}(m+m')$. We prefer now to write the expansion in a slightly different way in order to exhibit more clearly the symmetry properties of the expansion coefficients:

$$f_k(m, m') = (\tfrac{1}{2}\pi)^{\frac{1}{2}} 2^{-2\bar{m}-3} \sum_\sigma (2\bar{m}-2\sigma+1)!!\, T_k^{2\sigma}(m, m')J_{2\sigma}, \quad (5)$$

where, as above, $\bar{m}$ is the average of $m$ and $m'$, $\bar{m} = \frac{1}{2}(m+m')$, and the double factorial notation is used, $(2n+1)!! = 1 \cdot 3 \cdot 5 \cdots (2n+1)$. For notational convenience later on, we also introduce a symbol for the "double binomial coefficient",

$$\left\{ \begin{matrix} r \\ s \end{matrix} \right\} = \frac{(r+1)!!}{(s+1)!!(r-s+1)!!}, \quad (6)$$

where $r$ and $s$ are integers. Note that it shares with the ordinary binomial coefficient the properties $\left\{ \begin{matrix} r \\ 0 \end{matrix} \right\} = \left\{ \begin{matrix} r \\ r \end{matrix} \right\} = 1$, and $\left\{ \begin{matrix} r \\ s \end{matrix} \right\} = \left\{ \begin{matrix} r \\ r-s \end{matrix} \right\}$. We shall refer to the $T_k^{2\sigma}(m, m')$ defined by (5) as Talmi coefficients or $T$-coefficients.

The $C$-coefficients are integers; the $T$-coefficients are rational numbers. Both have the symmetry property expressed by

$$T_k^{2\sigma}(m, m') = T_k^{2\sigma}(m', m). \tag{7}$$

Hence we restrict consideration to $m' \leqq m$. In addition, the $T$-coefficients have the symmetry property

$$T_k^{2\sigma}(m, m') = (-1)^k T_k^{2\bar{m}-2\sigma}(m, m'), \tag{8}$$

and the end-point values

$$T_k^{0}(m, m') = 1, \quad T_k^{2\bar{m}}(m, m') = (-1)^k. \tag{9}$$

The $T$-coefficients are given by the formula †

$$T_k^{2\sigma}(m, m') = \begin{Bmatrix} 2\bar{m} \\ 2\sigma \end{Bmatrix} \sum_p \sum_q \frac{(-1)^p(-4)^q}{\binom{\bar{m}+\frac{1}{2}}{q}} \binom{\frac{1}{2}(m-k)}{q} \binom{\frac{1}{2}(m'-k)}{q} \binom{k}{p} \binom{\bar{m}-k-2q}{\sigma-q-p}. \tag{10}$$

The summation indices $p$ and $q$ run over all values allowed by the binomial coefficients.

It does not appear to be possible to write a general formula for the $T$-coefficients which is simpler than a double sum. However, other double sum formulas than (10) may be found. For example,

$$T_k^{2\sigma}(m, m') = \begin{Bmatrix} 2\bar{m} \\ 2\sigma \end{Bmatrix} (-1)^\sigma \sum_p \sum_q \cdot \frac{(-1)^p(-4)^q}{\binom{\bar{m}+\frac{1}{2}}{q}} \binom{\frac{1}{2}(m'-k)}{q} \binom{\frac{1}{2}(m'+k)+\frac{1}{2}}{q} \binom{\frac{1}{2}(m-m')}{p} \binom{m'-2q}{\sigma-p-q}. \tag{11}$$

Various special cases may be cited. When $k$ takes on its minimum value, 0, (10) reduces to a single sum

$$T_0^{2\sigma}(m, m') = \begin{Bmatrix} 2\bar{m} \\ 2\sigma \end{Bmatrix} \sum_q \frac{(-4)^q}{\binom{\bar{m}+\frac{1}{2}}{q}} \binom{\frac{1}{2}m}{q} \binom{\frac{1}{2}m'}{q} \binom{\bar{m}-2q}{\sigma-q}. \tag{12}$$

When $k$ takes on its maximum value, $m'$, (10) reduces to a single sum:

$$T_{m'}^{2\sigma}(m, m') = \begin{Bmatrix} 2\bar{m} \\ 2\sigma \end{Bmatrix} \sum_p (-1)^p \binom{m'}{p} \binom{\frac{1}{2}(m-m')}{\sigma-p}. \tag{13}$$

When $m = m'$, (11) becomes a single sum:

$$T_k^{2\sigma}(m, m) = \begin{Bmatrix} 2m \\ 2\sigma \end{Bmatrix} (-1)^\sigma \sum_q \frac{(-4)^q}{\binom{m+\frac{1}{2}}{q}} \binom{\frac{1}{2}(m-k)}{q} \binom{\frac{1}{2}(m+k)+\frac{1}{2}}{q} \binom{m-2q}{\sigma-q}. \tag{14}$$

† Some mathematical details are contained in section 3 and in the Appendix.

Except for the normalization here included, this formula is equivalent to eq. (8) of ref.[6]). Finally, single terms result when $\sigma = \sigma_{\min} = 0$ or $\sigma = \sigma_{\max} = \bar{m}$ (given by eq. (9)), when $k = m' = 0$,

$$T_0^{2\sigma}(m, 0) = \begin{Bmatrix} m \\ 2\sigma \end{Bmatrix} \binom{\frac{1}{2}m}{\sigma}, \tag{15}$$

or when $k = m' = m$,

$$T_m^{2\sigma}(m, m) = \begin{Bmatrix} 2m \\ 2\sigma \end{Bmatrix} (-1)^\sigma \binom{m}{\sigma}. \tag{16}$$

This last special case is also pointed out by Thieberger [6]).

In practice, generation of the $T$-coefficients from a recursion relation is much easier than direct evaluation of the above formulas. We have obtained the following recursion relation which seems well-suited for generating a table of $T$-coefficients:

$$T_k^{2\sigma}(m, m') = -\frac{k-1}{k} T_{k-2}^{2\sigma}(m, m') + \frac{2k-1}{k} [T_{k-1}^{2\sigma}(m-1, m'-1) - T_{k-1}^{2\sigma-2}(m-1, m'-1)]. \tag{17}$$

This relation is most readily proved from the quadruple sum formula for the $T_k^{2\sigma}(m, m')$ given by eq. (A4). For the special case $k = 1$, (17) becomes,

$$T_1^{2\sigma}(m, m') = T_0^{2\sigma}(m-1, m'-1) - T_0^{2\sigma-2}(m-1, m'-1). \tag{18}$$

Thus if one knows the coefficients for $k = 0$, (18) may be used to find the $k = 1$ coefficients, then (17) used to find the coefficients for $k = 2, 3, \cdots$ successively. To expedite this procedure, we present in table 1 values of the $T$-coefficients for $k = 0$ and for $m$ and $m' = 0, 2, \cdots, 10$ †. Correct answers are obtained from eqs. (17) and (18) if zero is substituted for any non-existent coefficient on the right. For example, from eq. (18),

$$T_1^0(m, m') = T_0^0(m-1, m'-1) - T_0^{-2}(m-1, m'-1) = 1-0 = 1;$$

or

$$T_1^2(1, 1) = T_0^2(0, 0) - T_0^0(0, 0) = 0-1 = -1.$$

Finally, we present two sum rules which provide useful checks on a table of $T$-coefficients. The first is

$$\sum_\sigma T_k^{2\sigma}(m, m') = \begin{cases} (-1)^{\frac{1}{2}k} \dfrac{(k-1)!!}{(k)!!} 2^{2\bar{m}} \dfrac{(\frac{1}{2}m)!(\frac{1}{2}m')!}{(\bar{m}+1)!}, & \text{for } k \text{ even,} \\ 0, & \text{for } k \text{ odd.} \end{cases} \tag{19}$$

The vanishing of the sum for odd $k$ follows at once from (8). (Note that for

† The entries in this table have been evaluated from eq. (12) on an automatic computer. They have been checked against the independently evaluated coefficients of True [5]), and have been checked with the sum rules (19) and (20).

odd $k$ and even $\bar{m}$, (8) implies $T_k^{\bar{m}}(m, m') = 0$.) The result for even $k$ is readily derived from eq. (A4). In (19), define $(-1)!! = (0)!! = 1$. The second sum rule is

$$\sum_\sigma \left[ T_k^{2\sigma}(m, m') \Big/ \begin{Bmatrix} 2\bar{m} \\ 2\sigma \end{Bmatrix} \right] = \left[ 2^{\bar{m}} \Big/ \begin{Bmatrix} 2\bar{m} \\ m \end{Bmatrix} \right] \delta_{k0}, \tag{20}$$

which follows readily from (10). The non-vanishing sum for $k = 0$ also follows from considering the long range limit, $V =$ constant.

TABLE 1

Coefficients $T_0^{2\sigma}(m, m')$

| $m$ | $m'$ | $\sigma$ | | | | | | | |
|---|---|---|---|---|---|---|---|---|---|
| | | 0 | 1 | 2 | 3 | 4 | 5 | 6 | 7 |
| 0 | 0 | 1 | | | | | | | |
| 2 | 0 | 1 | 1 | | | | | | |
| | 2 | 1 | 2/3 | 1 | | | | | |
| 4 | 0 | 1 | 10/3 | 1 | | | | | |
| | 2 | 1 | 5/3 | 5/3 | 1 | | | | |
| | 4 | 1 | 4/3 | 58/5!! | 4/3 | 1 | | | |
| 6 | 0 | 1 | 21/3 | 21/3 | 1 | | | | |
| | 2 | 1 | 12/3 | 42/5!! | 12/3 | 1 | | | |
| | 4 | 1 | 7/3 | 78/5!! | 78/5!! | 7/3 | 1 | | |
| | 6 | 1 | 6/3 | 129/5!! | 636/7!! | 129/5!! | 6/3 | 1 | |
| 8 | 0 | 1 | 36/3 | 378/5!! | 36/3 | 1 | | | |
| | 2 | 1 | 23/3 | 126/5!! | 126/5!! | 23/3 | 1 | | |
| | 4 | 1 | 14/3 | 97/5!! | 1 548/7!! | 97/5!! | 14/3 | 1 | |
| | 6 | 1 | 9/3 | 159/5!! | 1 539/7!! | 1 539/7!! | 159/5!! | 9/3 | 1 |
| | 8 | 1 | 8/3 | 228/5!! | 1 704/7!! | 31 974/9!! | 1704/7!! | 228/5!! | 8/3 |
| 10 | 0 | 1 | 55/3 | 990/5!! | 990/5!! | 55/3 | 1 | | |
| | 2 | 1 | 38/3 | 385/5!! | 1 980/7!! | 385/5!! | 38/3 | 1 | |
| | 4 | 1 | 25/3 | 175/5!! | 2 915/7!! | 2 915/7!! | 175/5!! | 25/3 | 1 |
| | 6 | 1 | 16/3 | 180/5!! | 3 600/7!! | 23 430/9!! | 3600/7!! | 180/5!! | 16/3 |
| | 8 | 1 | 11/3 | 268/5!! | 3 300/7!! | 47 310/9!! | 47310/9!! | 3 300/7!! | 268/5!! |
| | 10 | 1 | 10/3 | 355/5!! | 3 560/7!! | 88 050/9!! | 708060/11!! | 88 050/9!! | 3 560/7!! |

## 3. Gaussian Two-Body Potential

The Slater integral $f_k(m, m')$, eq. (1), may be evaluated directly without recourse to the Talmi expansion for the delta function potential, for the infinite range potential, and for various other special forms of the two-body potential (e.g. $V \approx r^{2n}$ [6]). In this section we show that for the gaussian potential, which is of practical interest for shell-model calculations, the integral $f_k(m, m')$ may also be evaluated directly.

Let

$$V = V_0 \exp(-r^2/r_0^2) = V_0 \exp(-\beta x^2), \tag{21}$$

where $\beta = b^2/r_0^2$, with $b$ and $x$ defined below eq. (1). Setting $x^2 = x_1^2 + x_2^2 - 2x_1x_2u$, and inserting (2) into (1), we have

$$I_k(m,m') = \tfrac{1}{2}V_0 \int dx_1 x_1^{m+2} e^{-(1+\beta)x_1^2} \int dx_2 x_2^{m'+2} e^{-(1+\beta)x_2^2} \int du P_k(u) e^{2\beta x_1 x_2 u}, \quad (22)$$

where $u = \cos\theta_{12}$. The last integral, over $u$, is equal to $i^{k+\frac{1}{2}}(\pi/\beta x_1 x_2)^{\frac{1}{2}} J_{k+\frac{1}{2}}(-2i\beta x_1 x_2)$. The next integral, over $x_2$,

$$\int J_{k+\frac{1}{2}}(-2i\beta x_1 x_2) e^{-(1+\beta)x_2^2} x_2^{m'+\frac{1}{2}} dx_2, \quad (23)$$

is closely related to the Weber-Sonine integral [9]),

$$W(a, \nu, p^2) = \int_0^\infty J_\nu(at) e^{-p^2t^2} t^{\nu+1} dt = a^\nu (2p^2)^{-\nu-1} \exp(-a^2/4p^2). \quad (24)$$

Form $(\partial/\partial p^2)^\alpha W(a, \nu, p^2)$, then set $\alpha = \frac{1}{2}(m'-k)$, $a = -2i\beta x_1$, $\nu = k+\frac{1}{2}$, and $p^2 = 1+\beta$, to obtain an integral proportional to (23). The last integral, over $x_1$, is an elementary form for each of the terms resulting from the differentiation. The final result is

$$I_k(m, m') = \pi V_0 2^{-\frac{1}{2}(m+k)-4}(m+k+1)!!\,[\tfrac{1}{2}(m'-k)]! \times \sum_p (-1)^p \binom{\frac{1}{2}(m-k)}{p} \binom{\bar{m}+\frac{1}{2}-p}{\frac{1}{2}(m'-k)-p} \frac{\beta^k (1+\beta)^{\bar{m}-k-2p}}{(1+2\beta)^{\bar{m}+\frac{1}{2}-p}}. \quad (25)$$

This sum may be converted to a hypergeometric function, and an equivalent formula which demonstrates the $m$, $m'$ symmetry more obviously is

$$I_k(m, m') = \pi V_0 \frac{(2\bar{m}+1)!!}{2^{\bar{m}+4}} \frac{\beta^k (1+\beta)^{\bar{m}-k}}{(1+2\beta)^{\bar{m}+\frac{1}{2}}} \cdot F\left(-\tfrac{1}{2}(m-k), -\tfrac{1}{2}(m'-k); -\bar{m}-\tfrac{1}{2}; \frac{1+2\beta}{(1+\beta)^2}\right), \quad (26)$$

in the notation of ref.[10]).

For the gaussian potential the Talmi integrals are

$$J_{2\sigma} = V_0(\tfrac{1}{2}\pi)^{\frac{1}{2}}(2\sigma+1)!!(1+2\beta)^{-\frac{1}{2}-\sigma}. \quad (27)$$

The right side of (26) may be expanded as $(1+2\beta)^{-\frac{1}{2}}$ multiplied by a power series in $(1+2\beta)^{-1}$. Comparing this expansion with (5) and with (27), one obtains at once the general formula (10) for the $T$-coefficients.

We are indebted to Dr. W. True for some helpful comments and for making available to us his numerical table of $C$-coefficients.

## Appendix

The method of derivation of eq. (10) is described below eq. (26). Eq. (11) is derived in the same way after first applying to the hypergeometric function in (26) the following Kummer transformation [10]):

$$F(a, b; c; z) = (1-z)^{-b} F(c-a, b; c; z/(z-1)). \quad (A1)$$

A much more cumbersome formula for the $T_k^{2\sigma}(m, m')$, but one which is convenient for derivation of the recursion relations (17) and (18) and the sum rule (19), may be found in the following way. Transform from $\mathbf{x}_1, \mathbf{x}_2$, with $\mathbf{x}_1 \cdot \mathbf{x}_2 = x_1 x_2 u$, to the centre of mass and relative coordinates, $\mathbf{X} = \frac{1}{2}(\mathbf{x}_1 + \mathbf{x}_2)$ and $\mathbf{x} = \mathbf{x}_2 - \mathbf{x}_1$, with $\mathbf{x} \cdot \mathbf{X} = xX\beta$, to obtain [1])

$$f_k(m, m') = \tfrac{1}{2} \iiint [x_1^m x_2^{m'} P_k(u)] V(bx) \exp(-2X^2 - \tfrac{1}{2}x^2) x^2 \mathrm{d}x X^2 \mathrm{d}X \mathrm{d}\beta, \quad \text{(A2)}$$

where the quantity in square brackets is understood to be expressed in terms of $x$, $X$, $\beta$. Write

$$\begin{aligned} x_1 &= (X^2 + \tfrac{1}{4}x^2 - xX\beta)^{\frac{1}{2}}, \\ x_2 &= (X^2 + \tfrac{1}{4}x^2 + xX\beta)^{\frac{1}{2}}, \\ P_k(u) &= \sum_\gamma b_\gamma^{\,k} u^\gamma, \\ u &= (X^2 - \tfrac{1}{4}x^2)/x_1 x_2. \end{aligned} \quad \text{(A3)}$$

The integrals in (A2) are then done in the order $\beta$, $X$, $x$, and comparison of the result with (5) leads to the formula

$$T_k^{2\sigma}(m, m') = \sum_\gamma \sum_p \sum_q \sum_r b_\gamma^{\,k} (-1)^{p+r} \binom{\mu}{p} \frac{2^{\mu-p-1}}{\mu'+p+1} \binom{2\mu'+2p+2}{2q+1} \binom{\gamma}{r} \binom{\mu-p}{\sigma-q-r}, \quad \text{(A4)}$$

where $\mu \equiv \frac{1}{2}(m-\gamma)$, $\mu' \equiv \frac{1}{2}(m'-\gamma)$, and

$$b_\gamma^{\,k} = (-1)^{\frac{1}{2}(k-\gamma)} 2^\gamma \begin{Bmatrix} k+\gamma-2 \\ k-\gamma-1 \end{Bmatrix}, \quad \text{(A5)}$$

using definition (6). The index $\gamma$ is only odd (even) if $k$ is odd (even).

## References


1) I. Talmi, Helv. Phys. Acta **25** (1952) 185
2) E. H. Kronheimer, Phys. Rev. **90** (1953) 1003
3) G. E. Tauber and T. Y. Wu, Phys. Rev. **94** (1954) 1307
4) J. M. Kennedy (Chalk River), unpublished
5) W. W. True (Princeton University), unpublished
6) R. Thieberger, Nuclear Physics **2** (1956/57) 533
7) G. Racah, Phys. Rev. **62** (1942) 438
8) W. W. True and K. W. Ford, Phys. Rev. **109** (1958) 1675
9) W. Magnus and F. Oberhettinger, Formulas and Theorems for the Special Functions of Mathematical Physics (Chelsea, New York, 1949) p. 35
10) A. Erdélyi *et al.*, Higher Transcendental Functions (McGraw-Hill, New York, 1953) Vol. I, Ch. II

2.E:2.L *Nuclear Physics* 9 (1958/59) 225—236; © *North-Holland Publishing Co., Amsterdam*
Not to be reproduced by photoprint or microfilm without written permission from the publisher

# TIME DEPENDENT THEORY OF SCATTERING OF NUCLEONS BY NUCLEI

F. COESTER and H. KÜMMEL †

*Department of Physics, State University of Iowa, Iowa City, Iowa* ††

Received 7 July 1958

**Abstract:** The optical model for the scattering of nucleons by nuclei is derived from the general time dependent scattering theory. The exclusion principle is taken into account without approximations. A suitably defined single particle wave function is shown to satisfy a "Schrödinger equation" with a non-hermitian "optical potential" defined by an integral equation in terms of the two body interaction. Solutions of this integral equation are not discussed. Thus the derivation of the model as such is separated from the approximations needed for its application to concrete problems. If the exclusion principle is taken into account the wave functions of the optical model are probability amplitudes only asymptotically for $t \to \pm \infty$. This asymptotic property is sufficient for the calculation of $S$-matrix elements and cross sections.

## 1. Introduction

The scattering of nucleons by large nuclei is in some respects analogous to the scattering of light in matter. This analogy suggests the description of the nucleon-nucleus interaction by an index of refraction or a complex single particle potential. Such a model was first proposed by Fernbach, Serber and Taylor [1]) to interpret high energy scattering and applied by Feshbach, Porter and Weisskopf [2]) to explain the low energy scattering experiments of Barschall [3]). The model has become well known as the "optical model". The success of the model raises several questions: Can this model be derived from the Schrödinger equation for the many particle system? What is the relation between the single particle wave function of the optical model and the complete scattering state? What approximations are involved? These questions have been investigated by several authors [4–7]) from the standpoint of the general time independent scattering theory. The main aim of that work is to derive an expression of the optical potential in terms of nucleon-nucleon scattering operators.

The analogy outlined above implies that the scattered particle is treated as distinct and distinguishable from the nucleons in the target. In this case our

† Fulbright grantee on leave of absence from Freie Universität Berlin, West-Berlin, Germany.

†† This work was supported in part by the U.S. Atomic Energy Commission.

questions have an easy answer along the following lines: The wave function of the optical model is obtained from the full scattering state by taking its projection into the subspace spanned by all states of the form $\varphi_0\chi$ where $\varphi_0$ is the groundstate of the target and $\chi$ is any single particle state. The single particle wave function resulting from this projection is the wave function of the optical model. By definition it gives the probability for finding the scattered particle in a specified region of space and the target in the ground state. Its norm is not constant in time. To derive the optical model we must eliminate from the Schrödinger equation all components of the scattering state which are not in this subspace and obtain a "Schrödinger equation" for the optical model wave function alone. In sec. 2 we shall carry out this elimination starting from the general time dependent scattering theory [8]). The potential in the resulting equation is an integral operator with respect to the time. This operator can be replaced by a time independent operator depending on the average energy of the incoming wave packet provided the energy distribution of that wave packet is sufficiently narrow. It is important not to confuse the coherent energy distribution of individual nucleons with the energy spread in the beam. The latter is immaterial at this point, the former is essentially determined by the geometry of the accelerator and is always so narrow that the approximation just mentioned should be excellent.

The results obtained in sec. 2 are equivalent to those obtained earlier from the time independent theory [4]). The time dependent theory merely provides a better insight into the physical meaning of the model. The main purpose of sec. 2, however, is to provide the background for a derivation which takes the indistinguishability of the target nucleons and the scattered nucleons into account. Both the definitions of the optical model wave function and the reduction of the Schrödinger equation must be substantially modified (sec. 3). The optical model wave function which we shall define in sec. 3 is a probability amplitude only asymptotically for $t \to \pm\infty$ but not for finite times. The asymptotic properties are sufficient for the calculation of cross sections. The equation for the optical potential differs from that of sec. 2 by characteristic exchange terms.

For the sake of simplicity we neglect the recoil of the target nucleus. However, this assumption is not essential and our entire development can easily be modified to include recoil effects. Simple rules which accomplish this modification are given in appendix A.

## 2. Scattering without Exchange

In this section we treat the scattering of a particle s by a nucleus of mass number $A$. The Hamiltonian of the system is

$$H = H_N + T_s + U \tag{1}$$

where $H_N$ is the Hamiltonian of the target nucleus, $T_a$ is the kinetic energy of the scattered particle and $U$ is the interaction of the scattered particle with the target. $\Psi(t)$ is the state of the whole system satisfying

$$i\frac{\partial}{\partial t}\Psi = H\Psi \tag{2}$$

and the initial condition

$$\lim_{t\to-\infty} ||\Psi(t)-\phi_a(t)|| = 0 \tag{3}$$

where $||\Psi||$ denotes the norm of $\Psi$. The initial state $\phi_a(t)$ is given by

$$\phi_a(t) = e^{-i(H_N+T_a)t}\varphi_0\chi_a \tag{4}$$

where $\varphi_0$ is the initial state of the target:

$$H_N\varphi_0 = E_0\varphi_0, \quad ||\varphi_0|| = 1. \tag{5}$$

$\chi_a$ is the initial wave packet of the scattered particle moving with an average momentum $k_a$ and average energy $E_a-E_0$; one takes $||\chi_a|| = 1$. The $S$-matrix is given by [8])

$$(f|S|a) = \lim_{t\to+\infty}(\phi_f(t), \Psi(t)) \tag{6}$$

where

$$\phi_f(t) = e^{-i(H_N+T_a)t}\varphi_f\chi_f \tag{7}$$

is the final state. For elastic scattering $\varphi_f = \varphi_0$.

Let $\Lambda_0$ be the projection operator into the space spanned by all states of the form $\varphi_0\chi$ where $\chi$ is any single particle wave function and define

$$\begin{aligned}\Psi_0(t) &\equiv \Lambda_0\Psi(t),\\ \Psi'(t) &\equiv (1-\Lambda_0)\Psi(t).\end{aligned} \tag{8}$$

From (3) follows $\lim_{t\to-\infty}||\Psi'(t)|| = 0$. Eq. (2) may be written in the form

$$i\frac{\partial\Psi_0(t)}{\partial t} = (H_N+T_a)\Psi_0+\Lambda_0U(\Psi_0+\Psi'), \tag{9}$$

$$i\frac{\partial\Psi'}{\partial t} = (H_N+T_a)\Psi'+(1-\Lambda_0)U(\Psi_0+\Psi'). \tag{10}$$

In order to eliminate $\Psi'$ from (9) we integrate (10) using the retarded Green's function $S(t-t')$ defined by

$$\begin{aligned}\left(i\frac{\partial}{\partial t}-H_N-T_a\right)S(t-t') &= \delta(t-t'),\\ S(t-t') &= 0 \quad \text{for} \quad t<t'.\end{aligned} \tag{11}$$

$S(t-t')$ may be represented by the Fourier integral

$$S(t-t') = \lim_{\varepsilon \to +0} \frac{1}{2\pi} \int_{-\infty}^{+\infty} d\omega \, \frac{e^{-i\omega(t-t')}}{\omega - H_N - T_s + i\varepsilon}. \tag{12}$$

From (10) follows

$$\Psi'(t) = \int dt' \, S(t-t')(1-\Lambda_0) U(\Psi_0(t') + \Psi'(t')) \tag{13}$$

and hence

$$U(\Psi_0(t) + \Psi'(t)) = U\Psi_0(t) + \int dt' \, US(t-t')(1-\Lambda_0) U(\Psi'(t') + \Psi_0(t')). \tag{14}$$

If we define an operator $V^s(t-t')$ by the equation

$$V^s(t-t') = U\Lambda_0 \delta(t-t') + \int dt'' \, S(t-t'')(1-\Lambda_0) V^s(t''-t')\Lambda_0 \tag{15}$$

we can solve (14) by putting

$$U(\Psi_0(t) + \Psi'(t)) = \int dt' \, V^s(t-t')\Psi_0(t'). \tag{16}$$

Inserting (16) into (9) we have an equation for $\Psi_0(t)$ only,

$$i \frac{\partial \Psi_0(t)}{\partial t} = (H_N + T_s)\Psi_0(t) + \int dt' \, \Lambda_0 V^s(t-t')\Psi_0(t'). \tag{17}$$

This integro-differential equation reduces to a differential equation if $V^s(t-t')$ can be represented by a Fourier integral

$$V^s(t-t') = \frac{1}{2\pi} \int_{-\infty}^{+\infty} dE \, e^{-iE(t-t')} V^s(E) \tag{18}$$

and if the energy distribution of the wave packet $\Psi_0$ is sufficiently narrow for $V^s(E)$ to be practically constant over this distribution. In that case we have from (15) and (17)

$$V^s(E)\Lambda_0 = U\Lambda_0 + U \frac{1}{E - H_N - T_s + i\varepsilon} (1-\Lambda_0) V^s(E) \quad (\varepsilon \to +0), \tag{19}$$

and

$$i \frac{\partial \Psi_0(t)}{\partial t} = (H_N + T_s + \Lambda_0 V^s(E_a))\Psi_0. \tag{20}$$

Finally we define the wave function $\psi_0$ of the optical model by

$$\psi_0(t) = (\varphi_0, \Psi_0(t)) \tag{21}$$

and the optical potential $\mathscr{V}$ by

$$\mathscr{V}(E_a) = (\varphi_0, V^s(E_a)\varphi_0). \tag{22}$$

From (20) we have the following equation for $\psi_0$:

$$i \frac{\partial \psi_0}{\partial t} = (E_0 + T_s + \mathscr{V}(E_a))\psi_0. \tag{23}$$

From (6) follows for the elastic scattering $S$-matrix elements

$$(\mathrm{f}|S|\mathrm{a}) = \lim_{t\to+\infty} (\chi_\mathrm{f}\,,\, \mathrm{e}^{i(E_0+T_\mathrm{s})t}\psi_0(t)). \tag{24}$$

The connection with the time independent theory is now easily established by defining a wave matrix $\Omega^{(+)}(E)$ by

$$(\mathrm{f}|\Omega^{(+)}|\mathrm{a}) = \frac{1}{2\pi}\int_{-\infty}^{+\infty} \mathrm{d}t\, \mathrm{e}^{iEt}(\chi_\mathrm{f}\,,\, \psi_0(t)). \tag{25}$$

From (23), (24) and (25) follow the familiar formulas of the time independent scattering theory,

$$(\mathrm{f}|\Omega^{(+)}(E)|\mathrm{a}) = \delta_\mathrm{fa} + \left(\mathrm{f}\left|\frac{1}{E-E_0-T_\mathrm{s}+i\varepsilon}\,\mathscr{V}(E_\mathrm{a})\Omega^{(+)}(E)\right|\mathrm{a}\right) \quad (\varepsilon\to+0), \tag{26}$$

and

$$(\mathrm{f}|S|\mathrm{a}) = \delta_\mathrm{fa} - i(\mathrm{f}|\mathscr{V}(E_\mathrm{a})\Omega^{(+)}(E_\mathrm{f})|\mathrm{a}). \tag{27}$$

$S$-matrix elements for inelastic scattering may be obtained along the same lines as follows: Let

$$\psi_n(t) \equiv (\varphi_n\,,\, \Psi(t)) \tag{28}$$

where $\varphi_n$ is an excited state of the target and define

$$\mathscr{V}_n(E_\mathrm{a}) = (\varphi_n\,,\, V^\mathrm{s}(E_\mathrm{a})\varphi_0). \tag{29}$$

For inelastic scattering we have then

$$(\mathrm{f}|S|\mathrm{a}) = \lim_{t\to\infty} (\chi_\mathrm{f}\,,\, \mathrm{e}^{i(E_n+T_\mathrm{s})t}\psi_n(t)), \tag{30}$$

where $\psi_n(t)$ satisfies according to (10) and (15) the equation

$$i\frac{\partial\psi_n}{\partial t} = (E_n+T_\mathrm{s})\psi_n + \mathscr{V}_n(E_\mathrm{a})\psi_0(t). \tag{31}$$

From (30) we have in analogy to (27)

$$(\mathrm{f}|S|\mathrm{a}) = -i(\mathrm{f}|\mathscr{V}_n(E_\mathrm{a})\Omega^{(+)}(E_\mathrm{f})|\mathrm{a}). \tag{32}$$

Cross sections are obtained from the $S$-matrix in the usual manner †.

## 3. Exchange Effects

Our derivation of the optical model in the previous section depended in an essential manner on the projection operator $\Lambda_0$ for the definition of the wave function and on the separation of the Hamiltonian into a "free Hamiltonian" and the scattering interaction $U$. If the scattered particle is a nucleon indistinguishable from the nucleons in the target we do not have a projection operator $\Lambda_0$ and the Hamiltonian cannot be separated into a "free Hamiltonian" and a scattering interaction.

† See for instance ref.[4]) and ref.[8]) Sec. 12.

In order to satisfy the exclusion principle throughout it is advantageous to work in an occupation number representation. This is, of course, merely a matter of convenience. The entire development could be written somewhat more lengthily in terms of configuration space wave functions. In fact the transition between the two representations can be carried out at any stage according to the relations

$$\psi(x_0 x_1 \ldots x_A) = \frac{1}{\sqrt{(A+1)!}} (\boldsymbol{\phi}_0, \mathbf{a}(x_0)\mathbf{a}(x_1) \ldots \mathbf{a}(x_A \boldsymbol{\Psi})), \tag{33}$$

$$\boldsymbol{\psi} = \frac{1}{\sqrt{(A+1)!}} \int dx_0 \ldots \int dx_A \, \psi(x_0 \ldots x_A)\mathbf{a}^+(x_A) \ldots \mathbf{a}^+(x_0)\boldsymbol{\phi}_0, \tag{34}$$

where $\mathbf{a}(x)$ and $\mathbf{a}^+(x)$ are respectively annihilation and creation operators satisfying

$$\{\mathbf{a}(x), \mathbf{a}^+(x')\} = \delta(x-x'), \tag{35}$$

and $\boldsymbol{\phi}_0$ is the vacuum state. Black type symbols denote state vectors and operators in the occupation number representation. We ignore spin variables in order not to overburden the notation. They could, of course, be introduced at any level of our development.

The Hamiltonian $H$ of the complete system is

$$H = -\int dx \mathbf{a}^+(x) \frac{\nabla^2}{2m} \mathbf{a}(x) + \tfrac{1}{2} \int dx \int dx' \mathbf{a}^+(x)\mathbf{a}^+(x')V(x-x')\mathbf{a}(x)\mathbf{a}(x'). \tag{36}$$

The scattering state $\boldsymbol{\Psi}(t)$ satisfies the time dependent Schrödinger equation and the initial condition

$$\lim_{t \to -\infty} ||\boldsymbol{\Psi}(t) - \boldsymbol{\phi}_a(t)|| = 0. \tag{37}$$

The initial state $\boldsymbol{\phi}_a(t)$ is given by

$$\begin{aligned} \boldsymbol{\phi}_a(t) = \frac{1}{\sqrt{A!}} e^{-iE_a t} \int dx_1 \ldots \int dx_A \int dx \, \varphi_0(x_1 \ldots x_A)\chi_a(x, t) \\ \times \mathbf{a}^+(x_A) \ldots \mathbf{a}^+(x_1)\mathbf{a}^+(x)\boldsymbol{\phi}_0. \end{aligned} \tag{38}$$

$\varphi_0$ is again the initial state of the target nucleus. $\chi_a(x, t)$ is a free wave packet satisfying

$$i \frac{\partial \chi_a}{\partial t} = -\frac{\nabla^2}{2m} \chi_a. \tag{39}$$

By definition $||\varphi_0|| = ||\chi_a|| = 1$. In general when the wave packet overlaps with the target the norm of $\boldsymbol{\phi}_a(t)$ is not unity and is not constant in time. The norm $||\boldsymbol{\phi}_a||$ is unity if $\chi_a$ and $\varphi_0$ do not overlap. More precisely the condition is

$$\int dx \int dx' \chi_a^*(x', t)\chi_a(x, t) \int dx_2 \ldots \int dx_A \varphi_0^*(x x_2 \ldots x_A)\varphi_0(x' x_2 \ldots x_A) = 0. \tag{40}$$

According to theorem 2 of appendix B this condition is always satisfied in the limit $t \to \pm \infty$. We have thus

$$\lim_{t \to \pm \infty} ||\boldsymbol{\phi}_a(t)|| = 1. \tag{41}$$

We define the wave function of the optical model by

$$\psi_0(x, t) = (\boldsymbol{\phi}_0, \mathbf{a}(x)\mathbf{A}_0\boldsymbol{\Psi}(t)) \tag{42}$$

where

$$\mathbf{A}_0 = \frac{1}{\sqrt{A!}} \int dx_1 \ldots \int dx_A \varphi_0^*(x_1 \ldots x_A)\mathbf{a}(x_1) \ldots \mathbf{a}(x_A). \tag{43}$$

In order to extract an equation for $\psi_0$ from the time dependent Schrödinger equation for $\boldsymbol{\Psi}$ we introduce a set of operators $\mathbf{A}_n$ defined by

$$\mathbf{A}_n = \frac{1}{\sqrt{A!}} \int dx_1 \int dx_2 \ldots \int dx_A \varphi_n^*(x_1 \ldots x_A)\mathbf{a}(x_1) \ldots \mathbf{a}(x_A) \tag{44}$$

and the corresponding wave functions

$$\psi_n(x, t) = (\boldsymbol{\phi}_0, \mathbf{a}(x)\mathbf{A}_n\boldsymbol{\Psi}(t)). \tag{45}$$

The $\varphi_n$ represent a complete orthonormal set of states which are either stationary or approximately stationary states to any desired degree of accuracy †. In the continuous spectrum they are wave packets with very narrow energy distribution. From the completeness of the $\varphi_n$ follows

$$\sum_{n=0}^{\infty} \mathbf{A}_n^+ \mathbf{A}_n \mathbf{a}(x)\boldsymbol{\Psi}(t) = \mathbf{a}(x)\boldsymbol{\Psi}(t). \tag{46}$$

Multiplying the Schrödinger equation for $\boldsymbol{\Psi}(t)$ by $\mathbf{a}(x)\mathbf{A}_n$ one obtains with (44), (35) and (46) after some straightforward manipulations the following coupled set of equations for the $\psi_n(x, t)$††:

$$i \frac{\partial \psi_n}{\partial t} = \left(E_n - \frac{\nabla^2}{2m}\right) \psi_n + \sum_{m=0}^{\infty} \int dx' (x|U_{nm}|x')\psi_m(x', t) \tag{47}$$

where

$$\begin{aligned}(x|U_{nm}|x') = \frac{A}{A+1} \Big[ &\int dy V(x-y)\rho_{nm}(y)\delta(x-x') - V(x-x')(x|\rho_{nm}|x') \\ &- (A-1) \int dy V(x-y)(xy|\rho_{nm}|yx') \Big],\end{aligned} \tag{48}$$

$$(xy|\rho_{nm}|x'y') \equiv \int dx_3 \ldots \int dx_A \varphi_m(xyx_3 \ldots x_A)\varphi_n^*(x'y'x_3 \ldots x_A), \tag{49}$$

† Such states are usually realized by placing the system in a large box.

†† Recent work by Newton [9]) on inelastic scattering and nuclear reactions is based on a time independent form of eq. (47).

$$(x|\rho_{nm}|x') \equiv \int dy\,(xy|\rho_{nm}|yx'), \tag{50}$$

$$\rho_{nm}(y) \equiv (y|\rho_{nm}|y). \tag{51}$$

In general, if the two body interaction is non-local and spin dependent, we must replace the second term of (36) by

$$\tfrac{1}{4}\int dq_1 \int dq_2 \int dq_3 \int dq_4 (q_1 q_2|V|q_3 q_4)\mathbf{a}^+(q_1)\mathbf{a}^+(q_2)\mathbf{a}(q_3)\mathbf{a}(q_4). \tag{36a}$$

$q$ denotes both space and spin variables. The integrations include the summation over the spin indices. $V$ is antisymmetric in both pairs of variables. The general result for $U_{nm}$ is then

$$\begin{aligned}(q|U_{nm}|q') = \frac{A}{A+1}\int d\bar{q} \int d\bar{q}' \Big[ &(q\bar{q}|V|\bar{q}'q')(\bar{q}'|\rho_{nm}|\bar{q}) \\ &- \frac{A-1}{2}\int dq''(q\bar{q}|V|\bar{q}'q'')(q''\bar{q}'|\rho_{nm}|\bar{q}q')\Big]\end{aligned} \tag{48a}$$

instead of (48).

The initial condition for $\psi_n(x,t)$ follows from (37):

$$\lim_{t\to-\infty} ||\psi_n - \delta_{n0}\chi_{\mathbf{a}}|| = 0. \tag{52}$$

We can prove (52) by remarking that

$$\lim_{t\to-\infty} ||\mathbf{A}_n \Psi(t) - \mathbf{A}_n \boldsymbol{\phi}_{\mathbf{a}}(t)|| = 0 \tag{53}$$

follows from (37) since $\mathbf{A}_n$ is a bounded operator. Furthermore

$$\lim_{t\to-\infty} ||(\boldsymbol{\phi}_0, \mathbf{a}(x)\mathbf{A}_n \boldsymbol{\phi}_{\mathbf{a}}(t)) - \delta_{n0}\chi_{\mathbf{a}}(x,t)|| = 0 \tag{54}$$

since

$$\lim_{t\to-\infty} \Big\| \int dx'(x|\rho_{n0}|x')\chi_{\mathbf{a}}(x',t)\Big\| = 0 \tag{55}$$

according to theorem 2 of appendix B. (52) follows directly from (53) and (54).

We can now eliminate $\psi_m$ from (47) by essentially the same steps we employed in sec. 2. The Green function $S_n(t-t')$ satisfies the equation

$$\begin{aligned}\left(i\frac{\partial}{\partial t} - E_n - \frac{p^2}{2m}\right) S_n(t-t') &= \delta(t-t'), \\ S_n(t-t') &= 0 \quad \text{if} \quad t < t'.\end{aligned} \tag{56}$$

From (47) follows

$$\sum_{m=0}^{\infty} U_{nm}\psi_m(t) = U_{n0}\psi_0(t) + \sum_{m=0}^{\infty}\sum_{m'=1}^{\infty}\int dt' U_{nm'}S_{m'}(t-t')U_{m'm}\psi_m(t'). \tag{57}$$

Defining $V_n^{\mathbf{a}}(t-t')$ by the equation

$$V_n^s(t-t') = U_{n0}\delta(t-t') + \int dt'' \sum_{m'=1}^{\infty} U_{nm'} S_{m'}(t-t'') V_{m'}^s(t''-t') \qquad (58)$$

we have

$$\sum_{m=0}^{\infty} U_{nm}\psi_m(t) = \int dt' V_n^s(t-t')\psi_0(t'). \qquad (59)$$

The optical potential $\mathscr{V}(E)$ is given by

$$\mathscr{V}(E) = V_0^s(E) \qquad (60)$$

and for inelastic scattering

$$\mathscr{V}_n(E) = V_n^s(E) \qquad (61)$$

where $V_n^s(E)$ is again the Fourier transform of $V_n^s(t-t')$ and satisfies the equation

$$V_n^s(E) = U_{n0} + \sum_{m=1}^{\infty} U_{nm} \frac{1}{E-E_m-T_s+i\varepsilon} V_m^s(E). \qquad (62)$$

With our new optical potential we have again eqs. (23) and (31). Eqs. (60), (62) and (48) give in second order perturbation theory the result obtained by Verlet [10]).

The $S$-matrix element $(f|S|a)$ is defined by

$$(f|S|a) = \lim_{t\to+\infty} \frac{(\boldsymbol{\phi}_{nt}(t), \boldsymbol{\Psi}(t))}{||\boldsymbol{\phi}_{nt}(t)||} \qquad (63)$$

where

$$\boldsymbol{\phi}_{nt}(t) = \frac{1}{\sqrt{A!}} \int dx \int dx_1 \ldots \int dx_A \, \chi_t(x,t) e^{-iE_n t} \varphi_n(x_1 \ldots x_A) \mathbf{a}^+(x_A) \ldots \mathbf{a}^+(x_1) \boldsymbol{\phi}_0. \qquad (64)$$

The asymptotic normalization

$$\lim_{t\to\pm\infty} ||\boldsymbol{\phi}_{nt}(t)|| = 0 \qquad (65)$$

can be proved in exactly the same manner as (41).

$\chi(x,t)$ is a normalized wave packet satisfying (39). According to the definition of $\psi_n$ we have

$$(\boldsymbol{\phi}_{nt}(t), \boldsymbol{\Psi}(t)) = (\chi_t(t), e^{iE_n t}\psi_n(t)). \qquad (66)$$

From (63), (65) and (66) follows

$$(f|S|a) = \lim_{t\to+\infty} (\chi_t(t), e^{iE_n t}\psi_n(t)) \qquad (67)$$

which is formally identical with (24) and (30) for $n = 0$ and $n \neq 0$ respectively.

We conclude that the exclusion principle does not affect the validity of the optical model as such. Its effects enter into our results only through the exchange terms in (48).

*Added in proof*: This conclusion implies that solutions of eq. (62) exist †. An explicit formal solution of the analogous eq. (19) is well known:

$$V^{S}(E) = U\Lambda_0 + U(1-\Lambda_0)\frac{1}{E-H_N-T_S-U+i\varepsilon}(1-\Lambda_0)U\Lambda_0. \qquad (68)$$

The existence of the right hand side of (68) is guaranteed at least for $\varepsilon > 0$ by general theorems. In order to find a similar solution for (62) we write (62) in an operator form. Consider a formal Hilbert space the elements of which are the functions $f(n, x)$ and the scalar product is

$$(f, g) = \sum_{n=0}^{\infty} \int dx f^*(n, x) g(n, x). \qquad (69)$$

The operators $U$, $H_N$ and $T_S$ operating in this space are then defined by

$$Uf(n, x) = \sum_m \int dx' (x|U_{nm}|x') f(m, x'), \qquad (70)$$

$$H_N f(n, x) = E_n f(n, x), \qquad (71)$$

$$T_S f(n, x) = -\frac{\nabla^2}{2m} f(n, x). \qquad (72)$$

The projection operator $\Lambda_0$ is defined by

$$\Lambda_0 f(n, x) = \delta_{n0} f(0, x) \qquad (73)$$

In terms of these operators we may replace (62) by (19) and obtain again the formal solution (68).

This formal development also brings out more clearly the fact that the scattering of neutrons by nuclei is identical to that of distinguishable particles provided the scattering interaction $U$ is given by (48).

## Appendix A

It is easy to modify our formulae in such a manner that the recoil of the target nucleus is properly described. The stationary states $\varphi_n$ must be replaced by almost stationary wave packets $\varphi_{np}$ where $p$ is the average momentum of such a wave packet. $\varphi_{np}$ satisfies the relation

$$H_N \varphi_{np} = \left(E_n + \frac{P^2}{2mA}\right) \varphi_{np} \qquad (A1)$$

where $P$ is the operator of the total momentum of the target nucleus: $(\varphi_{np}, P\varphi_{np}) = p$; $\|\varphi_{np}\| = 1$. The optical potential is then a "two body potential" depending in a momentum representation on both the momentum of the scattered particle and the momentum of the target nucleus.

† We are indebted to Dr. R. Haag for raising this question.

## Appendix B

In this appendix we prove two mathematical theorems about the asymptotic behaviour of wave packets.

*Theorem 1*:

$$\lim_{t\to\pm\infty}\int \mathrm{d}x f^*(x)\chi(x,t) = 0 \tag{B1}$$

if $f(x)$ is any quadratically integrable function and $\chi(x,t)$ is a quadratically integrable solution of the free Schrödinger equation

$$\left(i\frac{\partial}{\partial t} + \frac{\nabla^2}{2m}\right)\chi(x,t) = 0. \tag{B2}$$

Proof: Let $f(k)$ and $\chi(k)$ be respectively the Fourier transforms of $f(x)$ and $\chi(x,0)$. We have then

$$\int \mathrm{d}x f^*(x)\chi(x,t) = \int \mathrm{d}k f^*(k)\chi(k)\mathrm{e}^{-i\omega(k)t}, \quad \omega = \frac{k^2}{2m}. \tag{B3}$$

The right hand side of (B2) vanishes for $t \to \pm\infty$ according to the Riemann-Lebesgue theorem †. Since

$$\int \mathrm{d}k|f^*(k)\chi(k)| \leqq \left(\int \mathrm{d}k|f(k)|^2 \int \mathrm{d}k'|\chi(k')|^2\right)^{\frac{1}{2}} < \infty \tag{B4}$$

by Schwarz' inequality the conditions for the applicability of this theorem are satisfied.

*Theorem 2*:

$$\lim_{t\to\pm\infty}\int \mathrm{d}x \int \mathrm{d}x' F(x,x')\chi(x',t)\chi^*(x,t) = 0 \tag{B5}$$

if $F(x,x')$ is a quadratically integrable function of $x$ and $x'$.

Proof: Let $F(k,k')$ be the Fourier transform of $F(x,x')$. We have then

$$\int \mathrm{d}x \int \mathrm{d}x' F(x,x')\chi(x',t)\chi^*(x,t) = \int \mathrm{d}k \int \mathrm{d}k' \chi^*(k)F(k,k')\chi(k')\mathrm{e}^{i(\omega(k)-\omega(k'))t}. \tag{B6}$$

According to the Riemann-Lebesgue theorem † the right hand side of (B6) vanishes for $t \to \pm\infty$. In order to apply the Riemann-Lebesgue theorem we must make sure that the integrand in (B6) is absolutely integrable. By Schwarz' inequality

$$\begin{aligned}&\int \mathrm{d}k \int \mathrm{d}k'|\chi^*(k)F(k,k')\chi(k')| \\ &\qquad \leqq \left(\int \mathrm{d}k|\chi(k)|^2 \int \mathrm{d}k' \left|\int \mathrm{d}k'' F(k',k'')\chi(k'')\right|^2\right)^{\frac{1}{2}} < \infty.\end{aligned} \tag{B7}$$

The quadratic integrability of $\int \mathrm{d}k'' F(k',k'')\chi(k'')$ follows from the quadratic integrability of $F$.

† See for instance ref. [11]), p. 12.

## References

1) Fernbach, Serber and Taylor, Phys. Rev. **75** (1949) 1352
2) Feshbach, Porter and Weisskopf, Phys. Rev. **96** (1954) 448
3) H. H. Barschall, Phys. Rev. **86** (1952) 431
4) N. C. Francis and K. M. Watson, Phys. Rev. **92** (1953) 291
5) Brueckner, Eden and Francis, Phys. Rev. **100** (1955) 891
6) K. M. Watson, Phys. Rev. **105** (1957) 1388
7) H. Rollnik, Z. Naturf. **13a** (1958) 59
8) H. Ekstein, Phys. Rev. **101** (1956) 880
9) R. G. Newton, Ann. of Phys. **4** (1958) 29
10) L. Verlet, Nuovo Cimento **7** (1958) 821
11) E. C. Titchmarsh, Introduction to the Theory of Fourier Integrals (Oxford, 1937)

2.1 *Nuclear Physics* 9 (1958/58) 237—241; © *North-Holland Publishing Co., Amsterdam*
Not to be reproduced by photoprint or microfilm without written permission from the publisher

# ELECTRIC POLARIZABILITY OF ATOMIC NUCLEI

A. M. BALDIN

*P. N. Lebedev Physical Institute,* USSR *Academy of Sciences, Moscow*

Received 28 June 1957

**Abstract:** A quantitative estimate is given of the effects depending on the existence of a tensor (spin-dependent) part in the electric polarizability of nuclei.

It has been pointed out in ref. [1]) that part of the polarizability of atomic nuclei may be of a tensor nature (depend on the spin) and that in this connection a study of photonuclear reactions on polarized nuclei should be of great interest. The purpose of the present note is to give a quantitative estimate of the orders of magnitude of the effects which may possibly be observed as a consequence of this property of atomic nuclei.

The mean value of the electric dipole polarizability tensor of an arbitrary system of electric charges is defined by the well known formula

$$\langle a|\hat{\alpha}_{\mu\nu}|a\rangle = \sum_n \frac{1}{E_n - E_a} \{\langle a|\hat{d}_\mu|n\rangle\langle n|\hat{d}_\nu|a\rangle + \langle a|\hat{d}_\nu|n\rangle\langle n|\hat{d}_\mu|a\rangle\}; \tag{1}$$

$|a\rangle$ and $|n\rangle$ are the wave functions of the ground and intermediate states of the system, $\hat{\alpha}_{\mu\nu}$ is the operator of the electric dipole polarizability tensor of the system, and $\hat{d}_\mu$ is the operator of the $\mu^{\text{th}}$ dipole moment projection of the system.

Neglecting the spin one finds that after simple transformations formula (1) goes over into the well known Kramers-Heisenberg formula which relates the mean value of the polarizability with the cross section for all the processes involving absorption of a photon by the system:

$$\alpha = \frac{1}{2\pi^2}\int_0^\infty \frac{\sigma}{\omega^2}\,\mathrm{d}\omega. \tag{2}$$

We now take into account the dependence on the spin of the system and select from the set of quantum numbers those numbers which are explicitly quantum numbers of the spin projections $|a\rangle \equiv |a_0, m\rangle$. The most general form of the dependence of operator $\hat{\alpha}_{\mu\nu}$ on the spin of the system follows from symmetry of the tensor $\langle a|\hat{\alpha}_{\mu\nu}|a\rangle$:

$\langle a|\hat{\alpha}_{\mu\nu}|a\rangle$:

$$\langle a|\hat{\alpha}_{\mu\nu}|a\rangle = \langle a_0|\hat{\alpha}^{\mathrm{T}}|a_0\rangle \frac{1}{j(j+1)} \left\langle m' \left| \frac{\hat{J}_\mu \hat{J}_\nu + \hat{J}_\nu \hat{J}_\mu}{2} - \tfrac{1}{3}\hat{J}^2 \delta_{\mu\nu} \right| m \right\rangle + \langle a_0|\hat{\alpha}|a_0\rangle \delta_{m'm} \delta_{\mu\nu}; \tag{3}$$

$J_\mu$ is the spin projection operator of the system.

The first term has been written in such a way that the sum of the diagonal elements of this tensor vanish. From the following it will be clear why this is convenient.

In a static electric field the polarizability property of a nucleus can thus be described by two parameters which, for brevity, we denote by

$$\alpha^{\mathrm{T}} = \langle a_0|\hat{\alpha}^{\mathrm{T}}|a_0\rangle, \quad \alpha = \langle a_0|\hat{\alpha}|a_0\rangle.$$

For the measurement of the quantities $\alpha^{\mathrm{T}}$ and $\alpha$ a study of photonuclear reactions on oriented nuclei should be performed.

Let $\rho_{m'm}$ be the density matrix describing the spin state of the oriented nuclei. We shall find the mean values of the diagonal terms of the polarizability tensor operator.

Multiplying eq. (1) for $\mu = \nu$ by $\rho_{m'm}$, summing over $m'$ and $m$ and using (3) we obtain, after simple transformations, a generalization of the Kramers-Heisenberg formulae

$$\alpha_{\mathrm{T}} \left[ \frac{J_\mu^2}{j(j+1)} - \tfrac{1}{3} \right] + \alpha = \frac{1}{2\pi^2} \int \frac{\bar{\sigma}}{\omega^2} \, \mathrm{d}\omega. \tag{4}$$

Here $J_\mu^2$ is the mean value of the square of the spin vector projection on the direction of the electric field. $\bar{\sigma}$ is the cross section for inelastic processes in oriented nuclei induced by polarized photons. It can be seen from formula (4) that if $\alpha_{\mathrm{T}}$ is not zero $\int(\bar{\sigma}/\omega^2)\mathrm{d}\omega$ depends on the relative orientation of the spin vector and the electric field.

A case which can more easily be obtained experimentally is that of $\gamma$ quanta which are not polarized. Then

$$\alpha_{\mathrm{T}} \left\{ \tfrac{1}{6} - \tfrac{1}{2} \frac{J_\kappa^2}{j(j+1)} \right\} + \alpha = \frac{1}{2\pi^2} \int \frac{\bar{\sigma}_{\mathrm{av}}}{\omega^2} \, \mathrm{d}\omega; \tag{5}$$

$J_\kappa$ is the spin projection on the photon wave vector, $\bar{\sigma}_{\mathrm{av}}$ is the cross section for an unpolarized photon beam.

If the nuclei are not oriented the contribution from $\alpha_{\mathrm{T}}$ vanishes and

$$\alpha = \frac{1}{2\pi^2} \int \frac{\bar{\sigma}_{\mathrm{av}}}{\omega^2} \, \mathrm{d}\omega = \frac{1}{2\pi^2} \sigma_{-2}^0. \tag{6}$$

The notation employed here is the usual one; $\sigma_{-2} = \int(\sigma/\omega^2)\mathrm{d}\omega$.

Consider the limiting cases of formulas (4) and (5). Assume that the nuclei are completely oriented and that

1) the photon electric field vector is parallel to the spin vector:

$$\frac{1}{2\pi^2}\sigma^{\mathrm{P}}_{-2} = \alpha + \Delta \tag{7}$$

where

$$\Delta = \alpha_{\mathrm{T}}\frac{2j-1}{3(j+1)};$$

or

2) the photons are not polarized and the spin vector is perpendicular to the photon wave vector:

$$\frac{1}{2\pi^2}\sigma^{\perp}_{-2} = \alpha + \tfrac{1}{4}\Delta; \tag{8}$$

or

3) the photons are not polarized and the spin vector is parallel to the photon wave vector:

$$\frac{1}{2\pi^2}\sigma^{\parallel}_{-2} = \alpha - \tfrac{1}{2}\Delta. \tag{9}$$

Since the cross section $\sigma(\omega)$ is a function with a relatively sharp maximum, the position of the latter is usually characterized by the quantity

$$\omega_{\mathrm{M}} = \left[\frac{\sigma}{\sigma_{-2}}\right]^{\frac{1}{2}}.$$

As can be seen from (6), (7), (8) and (9) the position of this maximum depends on the orientation of the nuclear spin with respect to the wave vector of the photon. The magnitude of the shift of the maximum is related in a simple fashion to the tensor part of the polarizability $\alpha_{\mathrm{T}}$.

For non-polarized photons the largest shift of the maximum can be expressed by

$$\frac{\omega^{\parallel}_{\mathrm{M}} - \omega^{\perp}_{\mathrm{M}}}{\omega_{\mathrm{M}}} \approx \frac{3}{8}\frac{\Delta}{\alpha}.$$

The magnitude of the maximal shift is twice as large if polarized photons are employed.

In order to obtain a quantitative estimate of the shift some kind of model for the tensor polarizability must be used. A model of this type is contained in the nuclear dipole vibrations model [2]) as extended by Okamoto [3]) and Danos [4]) to non-spherical nuclei †. It should be emphasized that this model is not valid for light nuclei whereas the foregoing considerations are independent of the model employed.

† The author's attention was drawn to this circumstance by D. Wilkinson and J. Levinger.

In the aforementioned model the polarizability expression has the form $\alpha_{\mu\nu} = \int \rho' x_\mu x_\nu \mathrm{dv}$ where $\rho'$ is a constant. The integral is taken over the volume of the nucleus. It can be written in the form

$$\left\{\int \rho'(x_\mu x_\nu - \tfrac{1}{3}\delta_{\mu\nu} r^2)\mathrm{dv} + \tfrac{1}{3}\delta_{\mu\nu}\int \rho' r^2 \mathrm{dv}\right\}.$$

The first term refers to tensor polarizability and the second to scalar. The first term, moreover, is proportional to the quadrupole moment of the nucleus. If the shape of the nucleus is expressed by

$$R = R_0[1 + \sum_{\lambda\mu} \gamma_{\lambda\mu} Y_{\lambda\mu}(\vartheta\varphi)]$$

then $\alpha_{\mu\nu}$ can be written as

$$\alpha_{\mu\nu} = \rho' \frac{R_0^5}{15} 4\pi \left[Q_{\mu\nu} \frac{5}{3ZR_0^2} + \delta_{\mu\nu}\right]$$

where $Q_{\mu\nu}$ is the quadrupole moment tensor and $Z$ is the atomic number of the nucleus.

Comparing this expression with the mean value $\langle a_0, m = j|\alpha_{\mu\nu}|a_0, m = j\rangle$ we obtain the following expression for the shift of the maximum:

$$\tfrac{3}{8} \frac{5}{3R_0^2 Z} Q$$

where $Q$ is the spectroscopic quadrupole moment of the nucleus.

For $Co^{59}$ this quantity equals $\approx 0.05$, i.e., the shift of the giant resonance will be of the order of one megavolt. This effect is evidently large enough to be measured. An experiment of this type would seem to be very desirable as it may not only prove the existence of the tensor part of the polarizability of the atomic nuclei but also permit one to estimate its magnitude.

The author is thankful to Professor R. E. Peierls and Dr. J. Levinger for discussion of the results presented above.

*Note added in the proof*: Let us consider two independent computations of the shift of the maximum which are more exact than those presented above.

1) Performing an analysis similar to that presented above for the sum rule $\int (\sigma/\omega)\mathrm{d}\omega = 4\pi^2\langle a|d_z^2|a\rangle$ with the tensor $\hat{d}_\mu \hat{d}_\nu$ instead of $\hat{\alpha}_{\mu\nu}$ one obtains

$$\sigma_{-1}^{\perp} - \sigma_{-1}^{\parallel} = \pi^2 e^2 Q \quad \text{or} \quad \frac{\omega^{\parallel} - \omega^{\perp}}{\omega} = \pi^2 e^2 \frac{Q}{\sigma_{-1}^0}.$$

Here we have neglected correlations in the positions of the nucleons: $\langle r_i r_j\rangle_{i\neq j} = 0$. For the photodisintegration of the deuteron these equations are exact.

2) Let us introduce an "intrinsic" polarizability $\alpha_T^{(i)}$ and correspondingly an "intrinsic" second moment of the cross section $\sigma_{-2}^{(i)}$. This can be done in complete analogy with the "intrinsic" quadrupole moments of nuclei. The additional width $\Delta\Gamma$ of the giant resonance [3,4]) can be related to the difference between the maximum and minimum values of $\sigma_{-2}^{(i)}$, and, according to the sum rule, also to $\alpha_T^{(i)}$. Using the relation between $\alpha_T^{(i)}$ and $\alpha_T$ one gets

$$\omega^{\parallel}-\omega^{\perp}=\tfrac{1}{2}\,\frac{j(2j-1)}{(j+1)(2j+3)}\,\Delta\Gamma.$$

No particular polarizability model has been used here. All these estimations yield the same order of magnitude for $\omega^{\parallel}-\omega^{\perp}$.

## References

1) A. M. Baldin, Report at the All-Union Conference on Low and Medium Energy Nuclear Reactions (Moscow, 1957)
2) A. B. Migdal, JETP **15** (1945) 81; H. D. Jensen and Steinwedel, Z. Naturforsch. **5** (1950) 413
3) K. Okamoto, Progr. Theor. Phys. **15** (1956) 75
4) M. Danos, Bull. Am. Phys. Soc. **1** (1956) 35

8.C *Nuclear Physics* 9 (1958/58) 242—254; © *North-Holland Publishing Co., Amsterdam*
Not to be reproduced by photoprint or microfilm without written permission from the publisher

# ON QUANTUM THEORIES WITH INDEFINITE METRIC

R. ASCOLI

*Istituto di Fisica dell'Università, Torino*

*Istituto Naz. Fisica Nucleare, Sez. Torino*

and

E. MINARDI

*Società Nazionale Cogne, Aosta*

*Istituto Naz. Fisica Nucleare, Sez. Torino*

Received 30 June 1958

**Abstract:** We show that any probabilistically interpretable quantum theory using a Hilbert space of indefinite metric is equivalent to a quantum theory using a Hilbert space of positive definite metric. However, in general a formally local theory is transformed in this way into a theory that is no longer local: the formally local quantities cannot be measured. We give general criteria which permit to decide whether a theory may be probabilistically interpreted or not. When applied to the scattering of two $\theta$ on one N particle in the Lee model, these criteria lead to the result that the probabilistic interpretation is possible not only in the case of the dipole ghost, but also in the case of the complex conjugate energy eigenvalues of the interacting V particle. We also conclude that in both cases, however, the probabilistic interpretation of more complicated scattering problems is only possible provided that new discrete energy eigenstates of negative norm do not appear.

## 1. Introduction

In the last few years it was shown that an inconsistent quantum field theory, such as the Lee Model without form factor, may be transformed into a consistent theory when an indefinite metric in Hilbert space is introduced [1, 2]). However, the theory so obtained has in general no physical meaning, because the probabilities of some processes may be negative, if probability is defined in such a way that it is conserved. It would be very satisfactory if such a situation would occur in the case of processes referring to very small space time regions, but not for scattering processes.

It is therefore interesting that W. Heisenberg has recently shown [2]) that negative probabilities do not occur at least in a scattering process referring to the Lee Model. The proof of Heisenberg concerns the case of a particular choice of the parameters entering into the Lee Model, so that a coincidence occurs between the two roots of the equation giving the eigenvalues of the energy of an interacting V particle (dipole ghost case).

On the contrary it was shown by Källén and Pauli [1]) that it is not possible to have always positive probabilities in scattering processes if the same equation has two non-coincident real roots.

The work of Heisenberg has raised many interesting problems: we limit ourselves here mainly to the problems connected with the possibility of defining probabilities in scattering experiments (such a possibility is a necessary but not a sufficient condition for the physical acceptability of a theory).

Firstly, it is not clear whether it is essential to choose the case of the dipole ghost. Indeed, besides the cases studied by Källén and Pauli and by Heisenberg there is a third possibility in the Lee Model, namely the occurrence of two complex roots in the energy eigenvalue equation for a V particle, and this possibility till now had not been studied.

Secondly, even in the case studied by Heisenberg the problem was not solved whether a probabilistic interpretation is possible even in scattering processes other than the scattering of two $\theta$ on one N particle.

Thirdly, it is not clear whether the successful result obtained by Heisenberg is connected with some peculiar feature of the Lee Model, or whether analogous results could also be obtained in the case of less unphysical quantum field theories.

In this work we examine from a general point of view the fundamental principles of any physically meaningful quantum theory using a Hilbert space with indefinite metric. We arrive at theorems which lead to some general conclusions about the structure of these theories. These theorems also give general criteria to decide whether it is possible to define scattering probabilities in a given theory. In particular they permit to answer the questions raised above.

For these purposes we must first discuss the general principles of quantum physics without making any assumption about the metric of the Hilbert space.

## 2. Mathematical Remarks about Products of Vectors and Operators in a Hilbert Space of Arbitrary Metric

There is in the literature some uncertainty in the notation of products of vectors and operators when an indefinite metric is used. We shall use whenever possible the abstract notation introduced by Dirac in his famous book [3]). This possibility is based on the fact that the whole mathematical work of Dirac up to § 8 (p. 28) does not make use of formula (8), p. 21,

$$\langle A|A\rangle \neq 0 \text{ except when } |A\rangle = 0, \qquad \text{(I)}$$

so that no assumption about the metric is made. So all the formal rules of calculation which do not make reference to representations may be postulated quite independently of the metric.

In particular the conjugate $\alpha^+$ of any operator $\alpha$ is defined in such a way.

As an application of these remarks the following theorem may be proved in the usual way:

*Theorem 0.* Let a transformation $S$ in the Hilbert space have the properties of conserving linear relations and norms for all the vectors. Then this transformation satisfies

$$S^+S = 1 \tag{I}$$

and conversely.

The proof is found in Dirac's book [3]), §§ 25, 26, 27, because formula (I) is not used in these sections.

## 3. The Physical Interpretation of Vectors and Operators at one Instant of Time

### 3.1. PHYSICAL STATES

Let us consider a theory in which a Hilbert space $h$ of indefinite metric is used. The first problem is to know whether it is possible to give any vector of $h$ a physical interpretation analogous to the one which is usual in ordinary quantum physics.

To discuss this question, we shall assume all the postulates of a more physical nature which form the basis of quantum mechanics, but we shall not introduce the usual postulate that the norm of every vector is positive.

We first introduce the following definition:

*Definition 1.* We call physical state a situation in which there exists at least one set of measurements the result of which individuates it completely.

Then we assume the following postulates concerning physical states:

*Postulate 1.* All the properties of any physical state are derivable from the knowledge of a direction in a Hilbert space $h$.

Any vector having such a direction is said to correspond to the state, or even it is itself called the state.

*Postulate 2* (*Superposability Principle*). Any direction in the plane containing two physical states is a physical state, with one possible exception in each plane †.

From postulates 1 and 2 it follows that the physical states form a Hilbert space $h_I$, with the possible exception of a subspace of it††.

As has been said no postulate about the metric of this Hilbert space is assumed.

*Postulate 3.* If the system is in the physical state $A$, a definite probability $W_{BA}$ exists of observing the physical state $B$, independently of the measurements used to individuate the state $B$.

† Such an exception is introduced to allow the consideration of a semidefinite metric: it arises in the case of the direction of vectors of norm zero.

†† The exception arises in the case of a semidefinite metric, for the subspace of the vectors of norm zero.

*Postulate 4.* Let a physical state $|A\rangle$ be decomposed into a sum of physical states $|\phi_i\rangle : |A\rangle = \sum_i |\phi_i\rangle$. Let the observation of any one of the states $\phi_i$ exclude the observation of another state $\phi_j$, i.e. let $W_{\phi_i\phi_j} = 0$ for $i \neq j$. Then the sum of the probabilities for observing the states $\phi_i$ when the system is in the state $A$ is $1 : \sum_i W_{\phi_i A} = 1$.

From postulates 1 and 3 it follows that $W_{BA}$ can only be a function of the quantity $\frac{|\langle B|A\rangle|^2}{\langle B|B\rangle\langle A|A\rangle}$. This function must be chosen in such a way that postulate 4 is satisfied. It may be shown that the following theorem holds:

*Theorem 1.* The only expression for $W_{BA}$ satisfying postulates 1 and 4 is

$$W_{BA} = \frac{|\langle B|A\rangle|^2}{\langle B|B\rangle\langle A|A\rangle} \tag{2}$$

where the formal rules of calculation may also be used when the denominator is zero.

We do not report here the proof of this theorem†. However, it is immediately seen that the expression (2) satisfies postulate 4 quite independently of the metric. Indeed, from $W_{\phi_i\phi_j} = 0$ follows $\langle\phi_i|\phi_j\rangle = 0$ and then we have

$$\sum_i W_{\phi_i A} = \sum_i \frac{|\langle\phi_i|\phi_i\rangle|^2}{\langle\phi_i|\phi_i\rangle\langle A|A\rangle} = \frac{\sum_i \langle\phi_i|\phi_i\rangle}{\langle A|A\rangle} = \frac{\langle A|A\rangle}{\langle A|A\rangle} = 1.$$

From theorem 1 follows

*Theorem 2.* A necessary and sufficient condition that $W_{BA}$ be never negative is that the Hilbert space $h_1$ of the physical states has not an indefinite metric.

As a consequence of theorem 2 we have the result that in a probabilistically interpretable theory using a Hilbert space of indefinite metric there are certainly vectors which do not correspond to physical states.

Thus the Hilbert space $h_1$ of the physical states is a subspace of definite or semidefinite metric of the total Hilbert space $h$††.

Now we assume the following postulate:

*Postulate 5.* A physical state $A$ is entirely characterized by the knowledge of the probability $W_{BA}$ of observing any other physical state $B$.

Let the Hilbert space $h_1$ of the physical states have semidefinite metric. Now we show that all its vectors of zero norm are vectors which do not correspond to physical states as a consequence of postulate 5. Indeed any vector of norm zero of a Hilbert space of semidefinite metric has a zero scalar product with any other vector, as the zero vector. Now, owing to postulate 1 the zero vector does not correspond to any physical state,

† The proof, which has been given by one of us (R.A.), will possibly be published elsewhere.

†† The possibility of a Hilbert space $h_1$ of semidefinite metric is based on the exception introduced in the formulation of postulate 2. (See footnote † p. 244.)

because it does not individuate a direction; then owing to postulate 5, no vector of zero norm can correspond to a physical state.

*Theorem 3.* All the physical states of any system may be described by the vectors of a Hilbert space $h'_I$ of positive definite metric.

Indeed, let us consider two vectors, the difference of which is a vector of norm zero. Then, owing to postulate 5, they correspond to the same physical state, because they have the same scalar product with any vector. Let us consider a subspace $h'_I$ of $h_I$ of definite metric, having the highest possible dimension †. Then we see that any physical state is represented by a vector of the subspace $h'_I$. In fact any vector $|A\rangle$ of $h_I$ is the sum of a vector $|A'\rangle$ of $h'_I$ and a vector of norm zero; hence the vector $|A'\rangle$ represents the same physical state as the vector $|A\rangle$. So we have proved that the physical states may always be represented by directions in a space of positive definite or negative definite metric. Now we remark that, owing to (2), a reversal of the sign of the norm of all the vectors does not modify any probability. Hence we conclude from postulate 5 that the physical states may always be represented by the vectors of a Hilbert space of positive definite metric, so that the theorem 3 is proved.

We remark that the vector $|A'\rangle$ is obtained from the vector $|A\rangle$ through a projection operation $P$:

$$|A'\rangle = P|A\rangle. \tag{3}$$

Now the operation $P$ conserves any scalar product, thus, owing to theorem 0, one has

$$P^+P = 1. \tag{4}$$

From theorem 3 and postulate 1 we conclude that the results of any theory using a Hilbert space of indefinite metric may be obtained from the knowledge of the directions of the vectors in a Hilbert space of positive definite metric. Thus any theory using indefinite metric is equivalent to a theory using positive definite metric. However, this theory has different properties from the original one. The fundamental difference arises when operators are taken into consideration. This is done in the next subsection. Some consequences will be discussed in § 5.

### 3.2. OBSERVABLE QUANTITIES.

Let us suppose that the theory may be probabilistically interpreted. In this case we have defined the subspace $h_I$ of definite or semidefinite metric, and its subspace $h'_I$ of definite metric.

Then the remaining concepts of quantum physics may be introduced in the usual way in the Hilbert space $h'_I$.

We limit ourselves to the concepts which will be used in this work.

† The passage from the space $h_I$ to the space $h'_I$ is defined in a more abstract and general way by J. Von Neumann [4]) and it is called process of necessary identification in $h_I$.

*Definition 2.* We call observable any quantity which may be measured in all the physical states.

Through this definition, definition 1 and the previous postulates we derive, as usual, the theorem:

*Theorem 4.* To any observable $\alpha$ a linear operator $\alpha'_I$ in the space $h'_I$ corresponds in such a way that, if the system is in an eigenstate of this operator, a measurement of the observable gives certainly the corresponding eigenvalue.

Moreover, we deduce that there is a complete system of eigenvectors of $\alpha'_I$ in the space $h'_I$; the eigenvectors belonging to different eigenvalues are orthogonal; the operator corresponding to a real observable is a hermitian operator in the space $h'_I$; conversely, for any hermitian operator in $h'_I$ there is a corresponding set of compatible real observables.

Let us now introduce operators in the total Hilbert space $h$.

An important character of any theory using a Hilbert space $h$ of indefinite metric is that in general no observable corresponds to an operator, even if it is selfconjugate: this is a fundamental difference from the usual theories. More exactly we have the theorem:

*Theorem 5.* A necessary and sufficient condition that an operator in $h$ correspond to a set of compatible real observables is that it act on the vectors of $h'_I$ as a hermitian operator in $h'_I$.

We observe that an operator in $h$ in general does not transform any vector of $h'_I$ into a vector of $h'_I$ and does not in general have eigenvectors belonging to $h'_I$. So it is convenient to introduce the following definition:

*Definition 3.* We say that a linear operator of the total Hilbert space $h$ is an observable operator $\alpha$ corresponding to the observable $\alpha$ if it acts on the vectors of the subspace $h'_I$ as the operator $\alpha'_I$, defined in theorem 4.

### 3.3. CHARACTERIZATION OF THE VECTORS REPRESENTING PHYSICAL STATES.

Let us examine how the condition that a vector correspond to a physical state may be formulated. A way which is always possible is to write some set of equations which the vector has to satisfy.

However, there is another very natural way. Let $\alpha$ be some set of observable operators. In general they will have, besides physically meaningful eigenvalues, also eigenvalues without physical meaning such as a complex energy. Then any superposition of eigenvectors containing also this last kind of eigenvectors will certainly not be a physical state.

Hence in some cases the physical states are entirely characterized by the condition that they must be a superposition of eigenstates belonging to physically meaningful eigenvalues of some set of observable operators.

More generally, the condition that a vector be a physical state may be that it satisfy a requirement of this kind, together with some set of equations.

## 4. Possibility of Defining Scattering Probabilities and Transition Probabilities

### 4.1. GENERAL THEOREMS.

Till now we have examined the situation at a given time.

Let us now suppose that we have some set of equations of motion. Let us use the Schrödinger picture.

We shall discuss under which conditions scattering probabilities may be defined.

For this purpose we must start from some measurement by which the state is determined at a certain time and ask for the probability of observing some state at another time; then we let the interval between the two times tend to infinity. We shall call the two times $-\infty$ and $+\infty$. Such a process has a meaning if the states $\phi(-\infty)$ at $t = -\infty$ and $\phi(+\infty)$ at $t = +\infty$ are both physical states, i.e. if both belong to the space $h_I$: if it happens that the state at $t = +\infty$ does not belong to $h_I$, whereas the state at $t = -\infty$ belonged to $h_I$, then the scattering probability cannot be defined because the state at $t = +\infty$ cannot be identified. Therefore, we have this theorem:

*Theorem 6.* A necessary and sufficient condition for the possibility of defining scattering probabilities in a theory with arbitrary metric is that the equations of motion be such that if the state at $t = -\infty$ is a physical state, also the state at $t = +\infty$ is a physical state.

If such a condition is satisfied, postulate 4 guarantees automatically the conservation of scattering probability.

Let us further assume that the equations of motion have the properties of conserving superposition relationships and norms in scattering problems for the physical states. Then a linear operator $S_I$ in the space $h_I$ exists, so that

$$|\phi(+\infty)\rangle = S_I|\phi(-\infty)\rangle \tag{5}$$

and it satisfies, owing to theorem 0,

$$S_I^+ S_I = 1. \tag{6}$$

Let us now use the operator $P$ (formula (3)) to project all the states of the Hilbert space $h_I$ on the subspace $h'_I$. Let $|\phi'(-\infty)\rangle$ be a vector of $h'_I$. Then

$$|\phi'(+\infty)\rangle = P|\phi(+\infty)\rangle = PS_I|\phi'(-\infty)\rangle = S'_I|\phi'(-\infty)\rangle \tag{7}$$

where

$$S'_I = PS_I. \tag{8}$$

Thus, a matrix $S'_I$ in the space $h'_I$ is defined and, owing to (4) and (6), it satisfies

$$S_I'^+ S'_I = S_I^+ P^+ PS_I = 1. \tag{9}$$

Now any physical state may be represented by a vector of $h'_I$. Therefore, we have the theorem:

*Theorem 7.* In any theory with arbitrary metric a necessary and sufficient condition for the possibility of defining scattering probabilities and of having a unitary $S$ matrix that operates on a space of definite metric is that the equations of motion transform a physical state at $t = -\infty$ into a physical state at $t = +\infty$ and conserve superposition relationships and norms of the physical states in scattering problems.

Let us now put the sufficient condition given by theorem 7 into a form which is useful for the application to particular theories.

We call supplementary condition for scattering problems an equation for the state at a given time, such that if it is satisfied at $t = -\infty$ it is also satisfied at $t = +\infty$. Let us further say that a set $\alpha$ of operators is conserved in scattering problems when any eigenvector of it at $t = -\infty$ is not modified at $t = +\infty$.

Then, using theorem 2 and the considerations of § 3.3 we obtain the theorem:

*Theorem 8.* Let $\alpha$ be a set of observable operators conserved in scattering problems. Let us suppose that the equations of motion conserve superposition relationships and norms for all the vectors in scattering problems. Then a sufficient condition for the possibility of defining scattering probabilities and a unitary $S$ matrix is that the eigenstates of the observable operators $\alpha$ which are allowed by any supplementary conditions for scattering problems and which belong to physically meaningful eigenvalues never have negative norm.

Let us now assume that the equations of motion conserve superposition relationships and norms for all the vectors not only in scattering problems, but also at any time. Such an assumption is equivalent to assuming that the state vector $|\phi(t)\rangle$ satisfies, at least formally, an equation of the type †

$$i\frac{\mathrm{d}|\phi(t)\rangle}{\mathrm{d}t} = H|\phi(t)\rangle \tag{10}$$

where $H^+ = H$.

In this case it is also possible to define at least formally an evolution operator $U(t)$, such that

$$|\phi(t)\rangle = U(t)|\phi(-\infty)\rangle. \tag{11}$$

Then we have, from the same arguments as those used to prove theorem 7:

*Theorem 9.* Let us add to the assumptions of theorem 8 the assumption that the equations of motion conserve superposition relationships and norms of all the vectors at any time. Then the state vector corresponds to a physical state at any time; it is possible to define the probability of observing any

† The proof is found for instance in Dirac's book [3]), § 27, since no assumption about the metric is made in that paragraph.

physical state at any time and it is also possible to define a unitary $S$ matrix and, at least formally, a unitary evolution operator $U(t)$.

### 4.2. APPLICATION TO FORMAL QUANTUM FIELD THEORIES

Let us further assume that the theory is a field theory from a formal point of view. Thus, we postulate that its solutions have asymptotical properties as $t$ tends to $\pm\infty$ analogous to those that are postulated for the solutions of any usual field theory. In particular any solution must always be a superposition of solutions of the following two kinds: 1) solutions representing formally at any instant of time a wave packet of one particle (however, we do not at present make any assumption about their norm and their time dependence so that they cannot in general be physically interpreted); 2) solutions representing asymptotically, as $t$ tends to $\pm\infty$, wave packets of the particles described by the first kind of solutions, the distance of the wave packets growing without bounds with $|t|$; the solutions of this second kind are said to represent formally states of scattering of formal one-particle states †. Further it is assumed that in any field theory the norm of any formal state of scattering is the product of the norms of the formal one-particle states that are scattered. (The last assumption is probably a consequence of the previous ones, as has been proved by Haag [5]) in the case of ordinary theories, but we do not investigate this question here.)

Then we find that in the case of formal quantum field theories, theorems 8 and 9 may be formulated considering, instead of all "the eigenstates of the observable operators $\alpha$", only "the one-particle eigenstates of the observable operators $\alpha$".

This conclusion is useful for application to particular quantum field theories.

## 5. Discussion and Conclusions

### 5.1. CONSIDERATIONS ABOUT THE STRUCTURE OF A PROBABILISTICALLY INTERPRETABLE QUANTUM THEORY WITH INDEFINITE METRIC

Although the theorems given here are easily proved, interesting consequences may be drawn from them. In particular they permit to arrive at some general conclusions about the structure of any probabilistically interpretable quantum theory using a Hilbert space with indefinite metric; moreover they permit to answer the questions posed at the beginning.

First, let us only suppose that it is possible to define scattering probabilities and a unitary $S$ matrix.

† It is difficult to put these requirements into a more satisfactory mathematical form using the work which has been done till now on this subject. Important contributions in this direction are those of R. Haag [5]).

Then from theorem 3 we conclude that every scattering probability may be deduced from the knowledge of a linear and unitary transformation in a Hilbert space $h'_1$ of definite metric. This means that the vectors that do not belong to such a space $h'_1$ may be in principle eliminated from the theory.

The interesting question is whether a formulation in which such vectors are eliminated is simpler or not.

Before discussing this question let us also consider the more interesting case of a probabilistically interpretable theory in which the equations of motion conserve at any time superposition relationships and norms for all the vectors.

In this case, owing to theorem 9, it is possible to ask for the probability of observing any physical state at any time, if the state vector at a certain time is given. We therefore conclude, using theorem 3, that every possible experimental result at any time may be deduced from the knowledge of a vector of a Hilbert space of definite metric $h'_1$. Thus the theory may be formulated as the description of the motion of a vector in the Hilbert space $h'_1$, as any usual quantum theory. Therefore, in this case also the vectors which do not belong to $h'_1$ may be eliminated from the theory.

Let us discuss what is the possible advantage of a formulation using a Hilbert space of indefinite metric. The fundamental feature of such a formulation is that in general an operator is not an observable operator and accordingly does not correspond to any quantity which may be measured (see section 3.2).

In particular we have the following result:

Let us call formally local quantum theory a theory in which some operators are introduced, which refer to points of space-time.

Then any probabilistically interpretable formally local quantum theory using a Hilbert space of indefinite metric is equivalent to a quantum theory with positive definite metric, which is not, however, in general a local quantum theory.

Indeed, every physical state must be characterized by the values of some complete set of commuting observable operators. Owing to the general assumption that it is possible to define scattering problems, it must be possible to choose a set containing the total energy and the total momentum.

This set will certainly not contain local operators, because they do not commute with the total momentum, owing to the postulates that are satisfied by this quantity.

Thus, the requirement that scattering problems may be defined does not imply that it is possible to construct also a set of observable operators containing local quantities.

Therefore, the local operators are not in general observable operators.

From the formal point of view this means that in general they do not

define operators in the space $h'_I$. As a consequence of this fact, if the theory is formulated as a quantum theory in the space of definite metric $h'_I$, in general it no longer contains local operators.

Let in particular the theory be a formally local quantum field theory if it is formulated in the Hilbert space with indefinite metric $h$. Then we see that in general it is not even a quantum field theory if it is formulated in the Hilbert space $h'_I$ of definite metric, because field operators are in general no longer defined in this space †.

We therefore conclude that the formulation in the Hilbert space $h'_I$ is in general more complicated.

From the point of view of the physical interpretation, the fact that a local operator is not in general an observable operator, means that a local operator does not in general correspond to any quantity which may be measured. Therefore, a formally local theory with indefinite metric constitutes in general a non-local theory in a sense that is directly connected with the physical reality.

Such a situation certainly occurs in the field theories with indefinite metric hitherto proposed. Indeed, their field operators, when applied to vectors of $h'_I$, do not in general lead to vectors of $h'_I$; therefore, owing to theorem 5, such field operators cannot be observable operators. Then the corresponding fields cannot be measured.

### 5.2. APPLICATION TO PARTICULAR QUANTUM FIELD THEORIES.

Theorem 9 contains as a particular case Heisenberg's statement that scattering probabilities and a unitary $S$ matrix may be defined in a formally Hamiltonian quantum theory in which only energy eigenvectors of positive or zero norm occur. This is the situation in the problem of the scattering of two $\theta$ particles on one N particle (subspace $(N+2\theta, V+\theta)$) in the Lee Model, in the case of the dipole ghost. The theorem given here has the advantage of making no reference to any particular model.

Another particular consequence of theorem 9 is that scattering probabili-

† The treatment of quantum electrodynamics given by Gupta and Bleuler provides a particular case in which field operators are defined even when the theory is formulated in a Hilbert space of definite metric. It is natural to ask whether it is possible in general to construct observable operators which are linear combinations of field operators referring to different space-time points. For this purpose the weight function defining the linear combination ought to be chosen in such a way that a complete system of eigenvectors of the resulting operator should belong to $h'_I$. (See theorem 5.) In general this is possible when the power of the dimension of the space of the weight functions is not smaller than the power of the dimension of the space $h'_I$. Now the space of the weight functions is separable, whereas the space $h'_I$ is not separable in the case of a quantum field theory. Therefore in this case it is not possible in general to construct observable operators depending linearly on the field operators. The possibility, however, occurs when particular problems are taken into consideration, such as a one particle problem or a particular scattering problem, because then the space of the physical states considered is separable.

ties and a unitary $S$-matrix may be defined in a formally Hamiltonian quantum theory in which all the energy eigenvectors belonging to real eigenvalues have positive norm. Such a situation occurs in the same subspace (N$+2\theta$, V$+\theta$) of the Lee Model in the case of the two complex conjugate energy eigenvalues of the interacting V particle.

We conclude, therefore, that the cases of the dipole ghost and of the complex energy eigenvalues are equivalent from the point of view of the possibility of defining scattering probabilities and a unitary $S$-matrix: there is such a possibility in both cases, provided that all other energy eigenvectors have positive norm, as is certainly true in the Lee Model for the scattering states of two $\theta$ on one N particle.

On the contrary, let us consider the same problem of the Lee Model in the case in which two energy eigenstates of the V particle of opposite norm occur. Then from theorem 7 it follows that scattering probabilities cannot be defined in the problem of the scattering of one N with two $\theta$ particles, unless some circumstance would prevent transitions to states of one $\theta$ particle and one V particle of negative norm. This is the conclusion of Källén and Pauli. More exactly, also in this case $S^+S = 1$, owing to (9), but the probability of a transition to a state of one $\theta$ and one V particle of negative norm becomes negative, if it is different from zero. Hence the theory cannot be interpreted, whenever the probability of this transition is different from zero. And in the case of the Lee Model there is no reason for such a probability to be zero.

Let us now consider again the Lee Model in the cases of the dipole ghost or of the complex energy eigenvalues of the interacting V particle. Then the application of theorem 7 shows that the occurrence of such circumstances in the subspace (N$+\theta$, V) does not guarantee in any way the possibility of defining scattering probabilities in problems of the Lee Model differing from the scattering of one N with two $\theta$ particles: in general this is not possible if an energy eigenvalue of negative norm occurs in some subspace. If, for instance, discrete energy eigenstates with negative norm would occur in the subspace (N$+2\theta$, V$+\theta$), the scattering probabilities could not be defined in the problem of the scattering of three $\theta$ on one N particle †. Even in this respect the occurrence of a dipole ghost or of complex energy eigenvalues of the V particle are equivalent from the point of view of the possibility of defining scattering probabilities ††.

Finally, theorem 9 immediately guarantees that in quantum electrodynamics treated by the method of Gupta and Bleuler transition prob-

† *Note added in proof*: Meanwhile, it has been proved by W. Heisenberg (summer 1957) that discrete energy eigenstates do not occur in the subspace (N$+2\theta$, V$+\theta$) of the Lee Model.

†† The reason why the theorems of § 4 permit to solve these problems in a simple way is that questions concerning non-physical vectors are disregarded. A study of problems of the Lee Model with more that one N or V particle will be published later.

abilities and a unitary $S$ matrix may be defined. In this theory a negative norm is introduced for the free photons belonging to the fourth component $A_4$ of the vector potential $A_\mu$. However, the supplementary condition permits only those states of the system of the free photons belonging to $A_2$ and $A_4$ which have norm zero, with the exception of the vacuum, which has positive norm. Therefore, no permitted energy eigenvectors of negative norm occur, and accordingly transition probabilities may always be defined.

5.3. FINAL REMARKS.

We wish to point out that naturally the theorems given here do not prove that a consistent relativistic quantum field theory with indefinite metric may actually be constructed.

Moreover, we observe that, even if such a theory may be constructed, the requirement that it must be possible to define scattering probabilities is certainly not sufficient for the physical interpretation. Indeed, it must also be required that the probability of the result of any measurement referring to a sufficiently large space-time region must have a meaning †. Naturally the exact formulation of such a requirement meets with the known difficulty of defining small and large space-time regions in a relativistically invariant way. Indeed, a satisfactory definition must be formulated with respect to a reference frame connected with the particles that enter into the process taken into consideration, i.e. the definition must depend on the state of the system.

In the case of quantum theories with definite metric such a definition contradicts the concept of field operator, because every operator corresponds to a quantity which may be measured whatever the state of the system. Therefore, such a theory would not be a field theory.

The situation is more favourable in the case of a quantum theory with indefinite metric, because here an operator does not in general correspond to a quantity which may be measured; therefore, in this case field operators may be introduced without contradicting a non local requirement depending on the state of the system.

† We do not exclude the possibility that with respect to such a requirement the cases of the dipole ghost and of the complex energy eigenvalues behave differently.

## References

1) G. Källén and W. Pauli, Mat. Fys. Medd. Dan. Vid. Selsk. **30** (1955) no. 7
2) W. Heisenberg, Nuclear Physics **4** (1957) 532
3) P. A. M. Dirac, The principles of quantum mechanics (Cambridge, 1957)
4) J. Von Neumann, Functional operators, Vol. II (Princeton, 1950)
5) R. Haag, Mat. Fys. Medd. Dan. Vid. Selsk. **29** (1955) no. 12; communication at the International Conference on mathematical problems of the quantum theory of fields (Lille, June 1957)

7.A *Nuclear Physics* 9 (1958/59) 255—266; © *North-Holland Publishing Co., Amsterdam*
Not to be reproduced by photoprint or microfilm without written permission from the publisher

# THE INVERSION PROBLEM IN WAVE MECHANICS AND DISPERSION RELATIONS

MARIO VERDE
*Istituto di Fisica dell'Università, Torino*
*Istituto Naz. Fisica Nucleare, Sez. Torino*

Received 3 September 1958

**Abstract:** The analytical properties of the eigensolutions of a wave equation as function of the energy, considered as a complex variable, serve to give a new derivation of the so called Gel'fand and Levitan integral equation which determines the interaction when the spectral function is known. This method allows an immediate extension to the Dirac and Klein-Gordon wave equations. It gives a natural generalization of dispersion relations for finite distances.

## 1. Introduction

The problem of finding the interaction which belongs to a given spectrum (bound and continuum eigenstates) is still of great interest in nuclear physics. The recent very valuable effort in the measurements of differential cross-sections for elastic scattering of electrons by heavy nuclei, can be mentioned as an important example in which there exists the need of providing the shape of a charge distribution from the knowledge of experimental diffraction curves.

This problem has been actually attacked numerically by successive trials with assigned shape and by adjusting the parameters associated with it.

Yet this direct procedure, despite its practical usefulness in the single cases, is unsatisfactory from a theoretical point of view. A true theory of these and related phenomena should provide the means of exact statements about the charge distribution from the scattering data. This is equivalent to saying that one should solve the inversion problem and find the functional dependence of the interaction from the eigenstates.

The mathematical aspect of this problem has made a definite progress after Gel'fand and Levitan [1]) have shown how the knowledge of the interaction is reduced to the solution of an integral equation whose kernel is simply connected to the entire spectrum of the total hamiltonian and to the eigenstates of the hamiltonian free of interaction.

This was shown for the case of a one-dimensional Schroedinger equation of motion and static potential [2]).

In order to cover also motions occurring at high velocity it is interesting

to extend the Gel'fand and Levitan method to the one-dimensional Dirac and Klein-Gordon type of equation of motion.

The most important point remains, however, a possible generalization to the three-dimensional wave-equation. An even more ambitious program should include the many-body case.

With these purposes in mind we have looked for a clue to the existence of a Gel'fand and Levitan type of equation and found that this lies in the analytical properties of the eigenwaves $\Phi(E, x)$ as functions of the energy $E$ regarded as a complex variable.

There is a simple connection between the regular and singular solutions of a wave equation, which is similar to the familiar integral relation between the real and imaginary part of the scattering amplitude. The analytical behaviour of the appropriate eigenwaves as functions of $E$ used for the derivation of dispersion relations when $x$ is infinite, continues to be valid for every $x$, and this circumstance allows us to obtain an integral equation, which leads, through the continuity equation, to the Gel'fand and Levitan operator.

In this paper we wish to show how this is obtained for one particle moving in an external field with fixed angular momentum and parity.

We hope that a generalization to the more interesting cases mentioned before, for which dispersion relations are already known [3]) can be obtained following a similar approach.

Marchenko [4]) has presented more recently a modified version of the Gel'fand and Levitan equation. Our treatment has its counterpart for this interesting extension.

We have preferred to follow the concise way of obtaining results familiar in theoretical physics, without entering in details of mathematical rigour, which would heavily burden the entire subject without adding anything new to its scope. In this connection, what is needed is to exercise care in avoiding to manipulate expressions which are mathematically meaningless.

We treat in sect. 2 the Schroedinger wave equation, which is the simplest, and extend the same method to the Dirac and Klein-Gordon cases in the following sections 3 and 4.

## 2. The Schroedinger Wave Equation

We consider the eigenstates $\Phi(E, x)$, $\Phi_0(E, x)$ of a particle moving in an external field $V(x)$ or $V_0(x)$ with a given momentum $l$. The normalization of the $\phi$'s is chosen by imposing boundary conditions at a single point, let us say $x = 0$, independent of $E$:

$$\Phi(E, x),\ \Phi_0(E, x) \propto x^{l+1} \quad \text{for} \quad x = 0.$$

This ensures, for regular potentials $V(x)$, $V_0(x)$, that the $\Phi$'s are integral functions of $E$, and this holds for every $x$ in the radial interval $(0, \infty)$ [1]). Besides we have to deal also with the outgoing wave $f(p, x)$ normalized to a unit amplitude for large $x$:

$$f(p, x) \sim e^{ipx} \quad \text{when } x \text{ is large;}$$

$$f(p, x) \approx f(p)x^{-l}/(2l+1) \quad \text{for } x = 0, \quad \text{and} \quad p^2 = E.$$

$f(p, x)$ and $f(p)$ are regular analytical functions of $p$ for $\operatorname{Im} p > 0$.

As is well known [2]), the zero's of $f(p)$, on the positive imaginary axis, furnish all the bound states. We can therefore assert that

$$\frac{1}{2i\pi}\int_C \frac{2q\mathrm{d}q}{q^2-p^2}\left\{\frac{f(q, x)}{f(q)}\Phi_0(q^2, x) - \frac{f_0(q, x)}{f_0(q)}\Phi(q^2, x)\right\} = 0 \qquad (1)$$

if the path of integration C is chosen, as illustrated in fig. 1, so that the singularities on the real axis $\pm p$ and all those coming from the zero's of $f(p)$ and $f_0(p)$ are avoided.

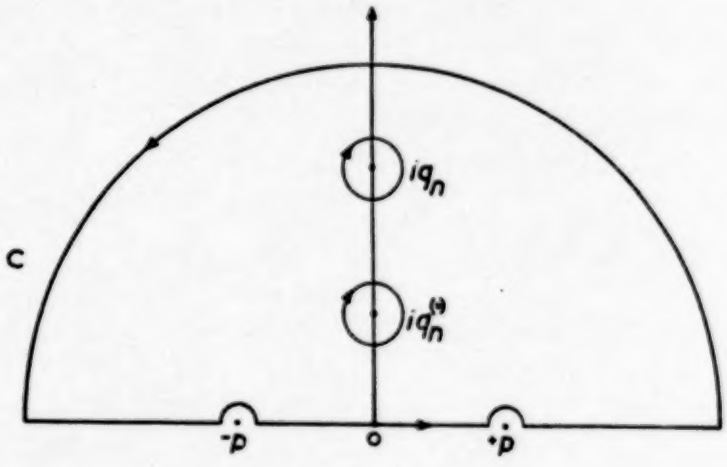


Fig. 1

Since the function

$$F(q, x) = \frac{f(q, x)}{f(q)}\Phi_0(q^2, x) - \frac{f_0(q, x)}{f_0(q)}\Phi(q^2, x) \sim O(1/q^2) \qquad (1')$$

when $q$ is large and $\operatorname{Im} q \geqq 0$, the path of integration can be enlarged to infinity, no contribution coming from the semicircle. If we now introduce the singular eigenstates

$$\phi^{(s)}(q^2, x) = \tfrac{1}{2}\left\{\frac{f(q, x)}{f)q)} + \frac{f(-q, x)}{f(-q)}\right\},$$

eq. (1) becomes

$$\phi^{(s)}(E,x)\Phi_0(E,x)-\phi_0^{(s)}(E,x)\Phi(E,x)$$
$$=\frac{1}{2i\pi}\,\mathrm{P.V.}\int_{-\infty}^{+\infty}\frac{q\mathrm{d}q}{q^2-p^2}F(q,x)-\sum_n\frac{2iq_n}{E_n-p^2}\frac{f(iq_n,x)}{\dot f(iq_n)}\Phi_0(E_n,x) \qquad (2)$$
$$+\sum_n\frac{2iq_n^{(0)}}{E_n^{(0)}-p^2}\frac{f_0(iq_n^{(0)},x)}{\dot f_0(iq_n^{(0)})}\Phi(E_n\varphi^{(0)},x);$$

$\dot f(iq_n)$ is a short notation for the derivative of $f(q)$ with respect to $q$ at the point $iq_n$.

It is now easy to derive from the continuity equation that

$$\frac{\Phi(E_n,x)}{N\{\Phi_n\}}=-2iq_n\frac{f(iq_n,x)}{\dot f(iq_n)},$$

where $N\{\Phi_n\}$ indicates the norm of the bound state $\Phi(E_n,x)$. With the further notation

$$\frac{\mathrm{d}\rho}{\mathrm{d}q}=\frac{2q^2}{\pi}\frac{1}{f(q)f(-q)} \qquad \text{for real values of } q$$

and

$$\frac{\mathrm{d}\rho}{\mathrm{d}E}=\sum_n\frac{\delta(E-E_n)}{N\{\Phi_n\}} \qquad \text{for negative values of } E$$

and analogous definitions for $\mathrm{d}\rho_0(\delta(E-E_n)$ being the familiar Dirac delta function) eq. (2) reads

$$\phi^{(s)}(E,x)\Phi_0(E,x)-\phi_0^{(s)}(E,x)\Phi(E,x)$$
$$=\mathrm{P.V.}\int_{-\infty}^{+\infty}[\mathrm{d}\rho(E')-\mathrm{d}\rho_0(E')]\frac{\Phi(E',x)\Phi_0(E',x)}{E'-E}; \qquad (3)$$

the integral must be considered in the sense of Stieltjes because of the presence of the discrete spectrum when $E'$ is negative.

One can proceed in exactly the same way, putting in eq. (1) instead of the function $F(q,x)$ as defined by the eq. (1') the function

$$G(q,x)=\frac{f(q,x)}{\dot f(q)}\Phi'_0(q^2,x)-\frac{f'_0(q,x)}{\dot f_0(q)}\Phi(q^2,x),$$

where the dashes indicate derivative with respect to the radial variable $x$; $\Phi'_0(E,x)$ remains [5]) an integral function of $E$, and $f'_0(q,x)$ an analytical function of $q$ for Im $q>0$. Also,

$$\frac{1}{2i\pi}\int_C\frac{2q\mathrm{d}q}{q^2-p^2}G(q,x)=0$$

where C is again the path of integration of fig. 1. Since for large values of $q(\mathrm{Im}\,q\geqq 0)$ $G(q,x)\to 1$, there is this time a contribution coming from the semicircle

$$\frac{1}{2i\pi}\int \frac{2q\mathrm{d}q}{q^2-p^2} = 1.$$

In this case we get

$$\phi^{(s)}(E,x)\Phi'_0(E,x)-\phi_0^{(s)\prime}(E,x)\Phi(E,x) = 1+\mathrm{P.V.}\int_{-\infty}^{+\infty}[\mathrm{d}\rho(E')-\mathrm{d}\rho_0(E')]\frac{\Phi(E',x)\Phi'_0(E',x)}{E'-E}. \quad (4)$$

From eq. (3) and eq. (4) we may now eliminate $\phi^{(s)}(E,x)$. In this connection we remember that

$$\phi_0^{(s)}(E,x)\Phi'_0(E,x)-\phi_0^{(s)\prime}(E,x)\Phi_0(E,x) = 1$$

since

$$\Phi_0 \propto x^{l+1}, \quad \phi_0^{(s)} \approx x^{-l}/(2l+1) \quad \text{for} \quad x = 0.$$

Then,

$$\Phi(E,x) = \Phi_0(E,x) + \int_{-\infty}^{+\infty}\mathrm{d}(\rho-\rho_0)\frac{\Phi(E',x)}{E'-E}\{\Phi_0(E,x)\Phi'_0(E',x)-\Phi_0'(E,x)\Phi_0(E',x)\}.$$

From the continuity equation one further deduces

$$\Phi(E,x) = \Phi_0(E,x)+\int_{-\infty}^{+\infty}\mathrm{d}(\rho-\rho_0)\Phi(E',x)\int_0^x\Phi_0(E,t)\Phi_0(E',t)\mathrm{d}t. \quad (5)$$

Since the integral

$$\int_{-\infty}^{+\infty}\mathrm{d}(\rho-\rho_0)\Phi(E,x)\Phi_0(E,t) \equiv K(x,t)$$

exists for every $t \leqq x$, we conclude that eq. (5) can finally be put in the form of Gel'fand and Levitan's integral equation

$$\Phi(E,x) = \Phi_0(E,x)+\int_0^x K(x,t)\Phi_0(E,t)\mathrm{d}t. \quad (6)$$

It is from this integral equation that one proceeds in order to solve the inversion problem. Since this is already a settled matter we have not to enter into it. We have deduced again eq. (6) in order to illustrate in a simple case our method of derivation, which will form the basis for the extension of the inversion problem to the relativistic kinematics.

## 3. The Inversion Problem for a Dirac Equation

For partial waves of given angular momentum $j$ and parity, for a particle of spin $\frac{1}{2}$ moving in a potential of spherical symmetry, we have to consider the two-component wave equation

$$\left\{-i\sigma_2\frac{\partial}{\partial x}+m\sigma_3+\frac{j+\frac{1}{2}}{x}\sigma_1+V(x)\right\}\varphi(E,x) = E\varphi(E,x) \quad (7)$$

where the $\sigma_\kappa$'s are the two-dimensional spin matrices of Pauli, and the usual assumption of $\hbar = c = 1$ has been made. An equivalent form of eq. (7), more convenient for our kind of considerations, is obtained by a unitary transformation by means of the operator $U = \exp i\sigma_2 Q$ with

$$\frac{\mathrm{d}Q}{\mathrm{d}x} = V(x).$$

This form reads

$$\left(-i\sigma_2 \frac{\partial}{\partial x} + \Omega\right) \phi(E, x) = E\phi(E, x)$$

where

$$\Omega = \mathrm{e}^{i\sigma_2 Q} \left(m\sigma_3 + \frac{j+\frac{1}{2}}{x}\sigma_1\right) \mathrm{e}^{-i\sigma_2 Q}. \tag{8}$$

Besides we have to consider the motion in a different potential $V_0(x)$ which goes into $V(x)$ for large $x$. In the equation corresponding to eq. (8) an operator $\Omega^{(0)}$ will appear, defined by the same eq. (8) with $V_0(x)$ instead of $V$.

Choosing the regular solutions $\phi_\alpha(E, x)$ and $\phi_\alpha^{(0)}(E, x)$ which behave for $x = 0$ as $x^{j+\frac{1}{2}}$ for every value of $E$, we can again assert [5]) that these solutions are integral functions of $E$.

We must also introduce, in analogy to the Schroedinger case of sect. 2, the outgoing waves. Since the energy is a double valued function of the momentum: $E_p = \pm V(p^2+m^2)$, the outgoing waves $f_\alpha(p, E, x)$ become one-valued functions on a 2-sheet Riemann surface with cuts joining the branch point $+im$ to $+i\infty$, and $-im$ to $-i\infty$. $f_\alpha(p, E, x)$ can be chosen to have an asymptotic behaviour for large $x$ given by

$$f_\alpha(p, E, x) \sim \begin{pmatrix} \sqrt{E+m} \\ \dfrac{ip}{\sqrt{E+m}} \end{pmatrix} \mathrm{e}^{ipx}. \tag{9}$$

The regular eigenwaves are related to the $f_\alpha$'s as follows:

$$2ip\phi_\alpha(E, x) = f(-p, E)f_\alpha(p, E, x) - f(p, E)f_\alpha(-p, E, x)$$

with

$$f(p, E) = \lim_{x=0} (2j+1)x^{j-\frac{1}{2}} f_1(p, E, x).$$

Then

$$\frac{1}{2i\pi} \int_{\mathrm{C}} \frac{q\mathrm{d}q}{Eq(E_q - E_p)} \cdot F_{\alpha\beta}(q, E_q, x) = 0, \tag{10}$$

where

$$F_{\alpha\beta}(q, E_q, x) = \frac{f_\alpha(q, E_q, x)}{f(q, E_q)} \phi_\beta^{(0)}(E_q, x) - \frac{f_\beta^{(0)}(q, E_q, x)}{f^{(0)}(q, E_q)} \phi_\alpha(E_q, x).$$

This time, as shown in fig. 2, the path of integration C, in order to be closed, must, in the upper half-plane of $q$, go twice around the branch point $+im$. We have indicated by a dotted line the part of the path which lies on the

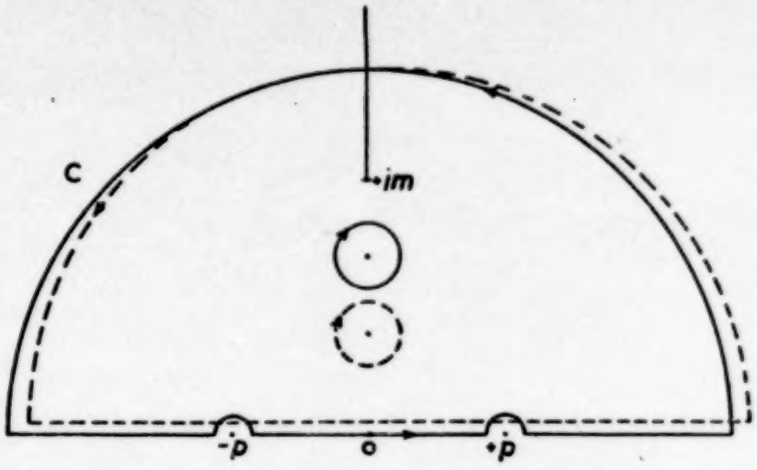


Fig. 2

sheet with $E_q < 0$ (for real $q$). Of course also here the zero's of $f(q, E_q)$ and $f^{(0)}(q, E_q)$ which are comprised in the segment 0, $im$ and on each of the two energy sheets, must be avoided as is shown in the same fig. 2. The points $\pm p$ may be chosen in correspondence to either of the two opposite energy values.

Since for large $q$ ($\mathrm{Im}\, q \geqq 0$)

$$F_{\alpha\beta}(q, E_q, x) \sim (i\sigma_2)_{\alpha\beta}$$

there is a finite contribution $(i\sigma_2)_{\alpha\beta}$ coming from the two semicircles when they are brought to infinity in the integral of eq. (10). One has now to introduce the singular eigenwaves similarly to the Schroedinger case, namely

$$\phi_\alpha^{(s)}(E, x) = \tfrac{1}{2}\left\{\frac{f_\alpha(p, E, x)}{f(p, E)} + \frac{f_\alpha(-p, E, x)}{f(-p, E)}\right\},$$

in order to write eq. (10) in the form

$$\begin{aligned}\phi_\alpha(E_p, x)\phi_\beta^{(0)(s)}(E_p, x) - \phi_\alpha^{(s)}(E_p, x)\phi_\beta^{(0)}(E_p, x) \\ = (-i\sigma_2)_{\alpha\beta} - \tfrac{1}{2}\mathrm{P.V.}\frac{1}{2i\pi}\int_{-\infty}^{+\infty}\frac{q\,dq}{E_q}\cdot\frac{F_{\alpha\beta}(q, E_q, x)}{E_q - E_p} \\ -\tfrac{1}{2}\mathrm{P.V.}\frac{1}{2i\pi}\int_{-\infty}^{+\infty}\frac{q\,dq}{E_q}\,\frac{F_{\alpha\beta}(q, -E_q, x)}{E_q + E_p} \\ -\sum_n \frac{iq_n}{E_n(E_n - E_p)}\,\frac{f_\alpha(iq_n, E_n, x)}{\dot{f}(iq_n, E_n)}\,\phi_\beta^{(0)}(E_n, x) \\ -\sum_n \frac{iq_n^{(0)}}{E_n^{(0)}(E_n^{(0)} - E_p)}\,\frac{f_\alpha^{(0)}(iq_n, E_n, x)}{\dot{f}^{(0)}(iq_n, E_n)}\,\phi_\alpha(E_n^{(0)}, x).\end{aligned} \tag{11}$$

The discrete summation includes all bound states for positive as well as negative values of the energy ($-m \leqq E_n \leqq m$). It is easy to deduce from the continuity equation (see below eq. (10)) that

$$\frac{\phi_\alpha(E_n, x)}{N\{\phi_n\}} = -i\frac{q_n}{E_n}\frac{f_\alpha(iq_n, E_n, x)}{\dot{f}(iq_n, E_n)}$$

where

$$N\{\phi_n\} = \sum_\alpha \int_0^\infty |\phi_\alpha(E_n, x)|^2 \mathrm{d}x$$

is the norm of the bound state $E_n$. Putting

$$\frac{\mathrm{d}\rho}{\mathrm{d}E} = \sum_n \frac{\delta(E-E_n)}{N\{\phi_n\}} \qquad \text{for} \quad -m \leqq E \leqq +m,$$

$$\frac{\mathrm{d}\rho}{\mathrm{d}p} = \frac{1}{\pi}\frac{p^2}{E}\frac{1}{f(p, E)f(-p, E)} \qquad \text{for } E \text{ outside the former interval,}$$

and with an analogous definition for the $\phi^{(0)}$'s eigenwaves, eq. (11) reads

$$\phi_\alpha(E_p, x)\phi_\beta^{(0),(s)}(E_p, x) - \phi_\alpha^{(s)}(E_p, x)\phi_\beta^{(0)}(E_p, x)$$
$$= (-i\sigma_2)_{\alpha\beta} + \mathrm{P.V.}\int_{-\infty}^{+\infty} [\mathrm{d}\rho(E_q) - \mathrm{d}\rho_0(E_q)]\frac{\phi_\alpha(E_q, x)\phi_\beta^{(0)}(E_q, x)}{E_p - E_q}.$$

From this, the singular solution $\phi^{(s)}$ is eliminated taking account of

$$\sum_\alpha \hat{\phi}_\alpha(E, x)\phi_\alpha(E, x) = 0, \quad \sum_\alpha \hat{\phi}_\alpha(E, x)\phi_\alpha^{(s)}(E, x) = 1,$$

where

$$\hat{\phi}_\alpha(E, x) = \sum_\beta (i\sigma_2)_{\alpha\beta}\phi_\beta(E, x)$$

in the adjoint of $\phi$.

Our equation finally becomes

$$\phi_\alpha(E, x)$$
$$= \phi_\alpha^{(0)}(E, x) + \sum_\beta \hat{\phi}_\beta^{(0)}(E, x)\,\mathrm{P.V.}\int_{-\infty}^{+\infty} \mathrm{d}(\rho - \rho^{(0)})\frac{\phi_\alpha(E', x)\phi_\beta^{(0)}(E', x)}{E - E'}. \quad (12)$$

For the continuity equation

$$\sum_\beta \hat{\phi}_\beta^{(0)}(E, x)\phi_\beta^{(0)}(E', x) = (E'-E)\int_0^x \sum_\beta \phi_\beta^{(0)}(E, y)\phi_\beta^{(0)}(E', y)\mathrm{d}y. \quad (13)$$

Therefore

$$\phi_\alpha(E, x) = \phi_\alpha^{(0)}(E, x) + \sum_\beta \int_0^x K_{\alpha\beta}(x, y)\phi_\beta^{(0)}(E, y)\mathrm{d}y \quad (14)$$

where

$$K_{\alpha\beta}(x, y) = \int_{-\infty}^{+\infty} \mathrm{d}(\rho^{(0)} - \rho)\phi_\alpha(E, x)\phi_\beta^{(0)}(E, y).$$

This kernel certainly exists for regular potentials and all $y \leqq x$; furthermore it is easy to deiive [6]) in several ways, e.g. from eq. (12), that

$$K_{\alpha\beta}(x, y) = \{(i\sigma_2)[\Omega-\Omega^{(0)}-(j+\tfrac{1}{2})(V-V_0)]\}_{\alpha\beta};$$

the $\Omega$'s are defined by eq. (8).

The possibility of having direct information on the potential if we know the values of $K_{\alpha\beta}(x, y)$ for $y = x$ is a consequence of the existence of an integral equation for $K_{\alpha\beta}(x, y)$ that can be easily deduced from eq. (14). Indeed, putting

$$K^{(0)}_{\alpha\beta}(x, y) = \int_{-\infty}^{+\infty} \mathrm{d}(\rho^{(0)}-\rho)\phi_\alpha{}^{(0)}(E, x)\phi_\beta{}^{(0)}(E, y),$$

which is a known quantity if the spectral function $\rho(E)$ is given, we derive from eq. (14), in complete analogy to the Schroedinger case,

$$K_{\alpha\beta}(x, y) = K^{(0)}_{\alpha\beta}(x, y)+\sum_\gamma \int_0^x K_{\alpha\gamma}(x, t)K^{(0)}_{\gamma,\beta}(t, y)\mathrm{d}t.$$

## 4. The Klein-Gordon Equation

There is nothing new for an analogous treatment of this case, we may therefore indicate briefly the essential points. One considers the eigenwaves $\phi(E, x)$ of the Klein-Gordon wave equation

$$\left\{(E-V)^2-m^2-\frac{l(l+1)}{x^2}+\frac{\partial^2}{\partial x^2}\right\}\phi(E, x) = 0$$

which are normalized so that for $x = 0$, $\phi(E, x)$ behave like $x^{l+1}$. Then $\phi(E, x)$ are integral functions of $E$. Besides, the outgoing waves $f(p, E, x)$ normalized so to have a unit amplitude for large $x$, are regular analytical on the upper half plane of $p$.

Putting

$$F(p, E_p, x) = \frac{f(p, E_p, x)}{f(p, E_p)}\phi^{(0)}(E_p, x)-\frac{f^{(0)}(p, E_p, x)}{f^{(0)}(p, E_p)}\phi(E_p, x),$$

$$G(p, E_p, x) = \frac{f(p, E_p, x)}{f(p, E_p)}\phi'^{(0)}(E_p, x)-\frac{f'^{(0)}(p, E_p, x)}{f^{(0)}(p, E_p)}\phi(E_p, x),$$

where the dashes indicate as before derivatives with respect to $x$ and

$$f(p, E_p) = \lim_{x=0}(2l+1)x^l f(p, E_p, x),$$

one has

$$\begin{aligned}\frac{1}{2i\pi}\int_C \frac{q\mathrm{d}q}{E_q}\frac{F(q, E_q, x)}{E_q-E_p} &= 0,\\ \frac{1}{2i\pi}\int_C \frac{q\mathrm{d}q}{E_q}\frac{G(q, E_q, x)}{E_q-E_p} &= 0,\end{aligned} \tag{15}$$

if C is chosen to be the same path of integration as in the Dirac case already discussed (see fig. 2). For large $q$, Im $q \geqq 0$,

$$F(q, E_q, x) \sim -\frac{1}{q}\sin\left(\frac{E_q}{q}\int_0^x (V-V_0)\mathrm{d}x'\right)$$

$$G(q, E_q, x) \sim \quad \cos\left(\frac{E_q}{q}\int_0^x (V-V_0)\mathrm{d}x'\right).$$

Therefore the semicircles in the integral of eq. (15) can be brought to infinity, no contribution coming from them in the first integral, but a finite value $\cos\int_0^x (V-V_0)\mathrm{d}x'$ in the second one. The two integrals become

$$\begin{aligned}
&\phi^{(0)}(E,x)\phi^{(s)}(E,x)-\phi^{(0),(s)}(E,x)\phi(E,x) \\
&\qquad = \mathrm{P.V.}\int_{-\infty}^{+\infty}\mathrm{d}(\rho-\rho^{(0)})\,\frac{\phi(E',x)\phi^{(0)}(E',x)}{E'-E} \\
&\phi'^{(0)}(E,x)\phi^{(s)}(E,x)-\phi'^{(0),(s)}(E,x)\phi(E,x) \\
&\qquad = \cos\int_0^x (V-V_0)\,\mathrm{d}x' + \mathrm{P.V.}\int_{-\infty}^{+\infty}\mathrm{d}(\rho-\rho^{(0)})\,\frac{\phi(E',x)\phi'^{(0)}(E',x)}{E'-E};
\end{aligned} \tag{16}$$

$\phi^{(s)}$ are the singular eigenwaves

$$\phi^{(s)}(E,x) = \tfrac{1}{2}\left\{\frac{f(p,E,x)}{f(p,E)} + \frac{f(-p,E,x)}{f(-p,E)}\right\}$$

which for $x = 0$ behave as $x^{-l}/(2l+1)$;

$$\frac{\mathrm{d}\rho}{\mathrm{d}p} = \frac{1}{\pi}\frac{p^2}{E}\frac{1}{f(p,E)f(-p,E)} \quad \text{for} \quad E \geqq +m \quad \text{or} \quad E \leqq -m,$$

$$\frac{\mathrm{d}\rho}{\mathrm{d}E} = \sum_n \frac{\delta(E-E_n)}{N\{\phi_n\}} \qquad \text{for} \quad -m < E < +m,$$

$N\{\phi_n\}$ being the norm of the bound state defined by

$$N\{\phi_n\} = 2\int_0^\infty (V-E_n)|\phi(E_n,x)|^2\mathrm{d}x.$$

This is an immediate consequence of the relation

$$\frac{\phi(E_n,x)}{N\{\phi_n\}} = -i\,\frac{q_n}{E_n}\,\frac{f(iq_n,E_n,x)}{\dot{f}(iq_n,E_n)}$$

which follows directly from the continuity equation.

It is now possible to eliminate the singular eigenwaves from eq. (16), remembering that

$$\phi^{(0),(s)}(E,x)\phi'^{(0)}(E,x)-\phi^{(0)}(E,x)\phi'^{(0),(s)}(E,x) = 1.$$

The final result reads †

† One of the eqs. (17) corresponding to $\alpha = 1$ has been presented for s-waves by E. Corinaldesi [7]). We wish to note that the approach used in our paper may also serve to obtain the Gel'fand and Levitan operator when a tensor force is present [8]).

$$\phi_\alpha(E,x)=\phi_\alpha^{(0)}(E,x)\cos\delta Q+\int_0^x K_{\alpha\beta}(x,y)\phi_\beta^{(0)}(E,y)\mathrm{d}y \qquad (17)$$

where

$$\delta Q=\int_0^x (V-V_0)\mathrm{d}x',\quad \phi_\alpha(E,x)\equiv\begin{pmatrix}\phi(E,x)\\ \dfrac{(E-V)}{m}\phi(E,x)\end{pmatrix}$$

$$K_{\alpha\beta}(x,y)=m\int_{-\infty}^{+\infty}\mathrm{d}(\rho^{(0)}-\rho)\phi_\alpha(E,x)\hat{\phi}_\beta^{(0)}(E,y)$$

and

$$\hat{\phi}_\alpha(E,x)=\sum_\beta(\sigma_1)_{\alpha\beta}\phi_\beta(E,x)$$

is the adjoint of $\phi$. Here use has been made of the continuity equation for $\phi^{(0)}$, which is

$$m(E-E')\sum_\alpha\int_0^x\hat{\phi}_\alpha^{(0)}(E',y)\phi_\alpha(E,y)\mathrm{d}y$$
$$=\phi^{(0)}(E,x)\phi'^{(0)}(E',x)-\phi^{(0)}(E',x)\phi'^{(0)}(E,x).$$

From eq. (17) it follows that

$$\bar{K}_{\alpha\beta}(x,y)=K_{\alpha\beta}^{(0)}(x,y)+\int_0^x\bar{K}_{\alpha\gamma}(x,t)K_{\gamma\beta}^{(0)}(t,y)\mathrm{d}t \qquad (18)$$

where the kernel

$$K_{\alpha\beta}^{(0)}(x,y)=m\int_{-\infty}^{+\infty}\mathrm{d}(\rho^{(0)}-\rho)\phi_\alpha^{(0)}(E,x)\hat{\phi}_\beta^{(0)}(E,y)$$

has to be considered as known once the spectral function $\rho(E)$ is given.

The potential $V(x)$ is related directly to the values of the kernels $\bar{K}_{\alpha\beta}(x,y)$ when $y=x$. It is indeed simple to derive from eq. (16) that for instance [6])

$$\frac{\bar{K}_{1,1}(x,x)}{\bar{K}_{1,2}(x,x)}=\frac{1}{m}\{\tfrac{1}{2}[V(x)-V_0(x)]+(l+\tfrac{1}{2})[V(0)-V_0(0)]\}.$$

We do not wish to discuss the actual solution of the Gel'fand and Levitan integral equation in practical cases. There is now an interesting suggestion for this made recently by T. Regge [8]), to whom we are glad to express our thanks for many discussions on these and related topics.

*Note added in proof:* We have received a manuscript by F. Prats and S. Toll (to be published in the Physical Review) in which the Gel'fand-Levitan operator corresponding to the Dirac wave-equation has been derived by a procedure analogous to that of Jost and Kohn [2]).

## References

1) I. M. Gel'fand and B. M. Levitan, Isvetia Akad. Nauk SSSR **15** (1951) 809; American Math. Soc. Translations **1** (1955) 253

2) R. Jost and W. Kohn, Mat. Fys. Medd. Dan. Vid. Selsk. **27** (1953) no. 9;
R. G. Newton and R. Jost, Nuovo Cimento **4** (1955) 590;
R. G. Newton, Phys. Rev. **100** (1955) 412;
I. Kay and H. E. Moses, Nuovo Cimento **3** (1956) 276

3) E. Corinaldesi, Nuclear Physics **2** (1957) 420
4) V. A. Marchenko, Doklady Akad. Nauk SSSR **104** (1955) 695
5) S. A. Coddington and N. Levinson, Theory of ordinary differential equations (McGraw-Hill Co., New York, 1955) Ch. I
6) Mario Verde, Nuovo Cimento **8** (1958) 560
7) E. Corinaldesi, Nuovo Cimento **11** (1954) 468
8) T. Regge, Nuovo Cimento (1958); V. De Alfaro, Nuovo Cimento, in course of publication

8.B *Nuclear Physics* 9 (1958/59) 267—272; © *North-Holland Publishing Co., Amsterdam*
Not to be reproduced by photoprint or microfilm without written permission from the publisher

# THE EFFECT OF A SCALAR MESON INTERACTION BETWEEN MUONS AND BARYONS

I. R. GATLAND
*Imperial College, London*

Received 3 September 1958

**Abstract:** The effect of a scalar meson interaction (as well as the usual photon interaction) in muon-nucleon scattering is evaluated in second order perturbation theory and is compared with the known properties of the muon. The existence of the new interaction is found to be compatible with the experimental results on the muon range and scattering and the nuclear photo-production of muon pairs if the meson mass is approximately three nucleon masses and the meson has medium strong interactions with baryons and muons.

## 1. Introduction

In a paper [1]) on elementary particles and their interactions Schwinger has proposed that a scalar meson ($\sigma$) be responsible for the baryon mass differences by interacting with the $\Xi$ particle. Also the $\sigma$ meson is supposed to interact with the muon to give it a large self-mass relative to the other leptons and to give a medium strong lepton-baryon interaction. The new meson has not been observed, but this is admissible if it has a fast decay, to 2 pions, say, if the $\sigma$ meson is scalar, or to 3 pions if pseudoscalar, as is possible if the $\sigma$ meson mass $\kappa > 2$ or 3 pion masses.

The existence of the $\sigma$ meson must also be compatible with the known properties of muons which are usually explained in terms of the photon interaction alone. In a recent paper [2]) Cowland has estimated the $\sigma$ mass and the strength of its coupling with muons such that the large $\mu$ self-mass is consistent with its observed anomalous magnetic moment. In the present paper the range, bremsstrahlung and scattering of muons, together with the nuclear photoproduction of muon-pairs, are investigated assuming the existence of a muon-baryon interaction through the $\sigma$ field. According to Cowland the $\sigma$-meson must be scalar, it has mass $\kappa \approx 3m$ (where $m$ is the nucleon mass) and the $\mu$-$\sigma$ coupling is of strength $g^2/4\pi \approx 2$. These figures will be used to illustrate the results obtained in the present paper.

## 2. Theory

The $\sigma$ meson will produce a $\mu$-N interaction through the $\mu$-$\sigma$ and $\sigma$-N interactions, of which the latter involves the $\sigma$-$\Xi$ coupling and at least 2

K-mesons. However, if the K-meson interactions are strong we may approximate to the $\sigma$-N interaction by a simple scalar interaction of strength $b^2/4\pi$, say.

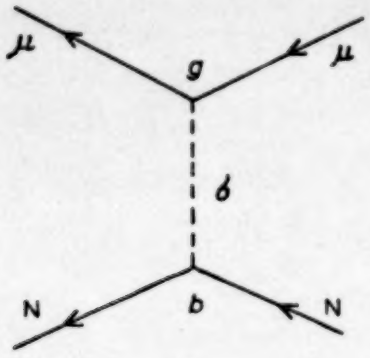


Fig. 1

The $\mu$-$\sigma$-N interaction is given to first order by the Feynman diagram in fig. 1. This is to be compared with the $\mu$-N interaction through the photon field ($\mu$-$\gamma$-N) which is the currently accepted theoretical basis for the muon properties. In general for muons and nucleons any internal photon line may be replaced by a $\sigma$-line in the Feynman diagrams as in the case of $\mu$-bremsstrahlung or the photoproduction of muon pairs. At low energies the $\mu$-$\gamma$-N interaction is only effective for protons. However, for interactions between muons and matter it may be assumed that protons and neutrons are present in about equal numbers and a factor $\frac{1}{2}$ included in the $\mu$-$\gamma$-N interaction. The scattering amplitude for the $\mu$-$\sigma$-N interaction may be calculated using fig. 1 and then the cross section found. After summing over the final spins and averaging over the initial spins the cross section is given by

$$\sigma_B = \int \frac{d^3p'\,d^3q'\,g^2b^2\delta(p+q-p'-q')[(p\cdot p')(q\cdot q')-\mu^2(p\cdot p')-m^2(q\cdot q')+m^2\mu^2]}{(4\pi)^2 p'_0 q'_0[(p\cdot q)^2-m^2\mu^2]^{\frac{1}{2}}(k^2+\kappa^2)^2} \qquad (1)$$

where

$p$ and $p'$ are the initial and final nucleon 4-momenta,
$q$ and $q'$ are the initial and final muon 4 momenta,
$m$ is the nucleon mass, $\mu$ the muon mass and $\kappa$ the $\sigma$ mass,
$k^2 = (p-p')^2 = (q'-q)^2$

and a space-like metric is used.

The $\delta$-function gives the following relations between the 4-momenta:

$$p\cdot q = p'\cdot q', \quad p\cdot q' = p'\cdot q, \quad p\cdot p'+m^2 = q\cdot q'+\mu^2.$$

Also, in the laboratory frame ($\mathbf{p} = 0$) put

$$p = (\mathbf{0}, m) \quad q = (\mathbf{q}, \varepsilon) \quad p' = (\mathbf{p}', E) \quad q' = (\mathbf{q}', \varepsilon');$$

then

$$k^2 = (p-p')^2 = p^2+p'^2-2p\cdot p' = -2m^2+2mE = 2m(E-m).$$

Specialising to the laboratory frame and integrating out the $\delta$-function gives the differential cross section for a final nucleon of energy $E$ as

$$\frac{\mathrm{d}\sigma_{\mathrm{B}}}{\mathrm{d}E} \approx \frac{\pi\alpha^2[(E-m)m+2\mu^2]E}{2q^2[(E-m)m+\frac{1}{2}\kappa^2]^2} \tag{2}$$

for $q > 3\mu$ where $q = \sqrt{(\varepsilon^2-\mu^2)} = |\mathbf{q}|$ and $\alpha = gb/4\pi$.
Also,

$$m \leqq E \leqq E_{\max},$$

where

$$E_{\max} = \frac{m(2\varepsilon^2+m^2+2\varepsilon m-\mu^2)}{2\varepsilon m+m^2+\mu^2}.$$

Integrating eq. (2) over $E$ from $m$ to $E_{\max}$ gives the total cross section.

The energy loss per collision is given by

$$\delta\varepsilon = \int_m^{E_{\max}} \frac{\mathrm{d}\sigma_{\mathrm{B}}}{\mathrm{d}E}(E-m)\mathrm{d}E \approx \frac{\pi\alpha^2}{4m} \quad \text{for} \quad \varepsilon \gg m. \tag{3}$$

At high energies the $\mu$-$\sigma$-N interaction governs the behaviour of the muons. However, at low energies the $\mu$-$\sigma$-N and $\mu$-$\gamma$-p interactions are comparable. The relative magnitude of the contributions from the $\sigma$ and photon interactions may be obtained by comparing the cross section given by fig. 1 for the $\sigma$ interaction and the lowest order diagram for the photon interaction (fig. 1 with $\sigma \to \gamma$, $g \to e$, $b \to e$). The coherent scattering which is of order $\mu/m$ is neglected and a factor $\frac{1}{2}$ is included in the $\mu$-$\gamma$-p interaction to approximate to the $\mu$-$\gamma$-N interaction. Suppose the incident muon is scattered through a small angle $\phi$; then, the ratio of the differential cross sections is

$$\frac{\mathrm{d}\sigma_{\mathrm{B}}}{\mathrm{d}\phi} \Big/ \frac{\mathrm{d}\sigma_{\gamma}}{\mathrm{d}\phi} \approx \frac{g^2b^2q^6\phi^6}{e^4\kappa^4[2\varepsilon^2-(\varepsilon+\frac{1}{2})(q^2\phi^2/m)+\frac{1}{2}(q^4\phi^4/m^2)]}$$

$$\approx \left(\frac{100\,\alpha\varepsilon^2\phi^3}{\kappa^2}\right)^2 \quad \text{for} \quad \varepsilon > 3\mu,\ \phi \ll 1,$$

if we take

$$e^2/4\pi \approx 1/100\sqrt{2}.$$

Now define $\phi_0$ as the value of $\phi$ such that $\mathrm{d}\sigma_{\mathrm{B}}/\mathrm{d}\phi = \mathrm{d}\sigma_{\gamma}/\mathrm{d}\phi$. Then

$$\phi_0 \approx \left(\frac{\kappa^2}{100\,\alpha\varepsilon^2}\right)^{\frac{1}{3}}. \tag{4}$$

## 3. Comparison with Experiment

The theoretical results obtained above may now be compared with the experimental results on the muon scattering cross section, range, etc.

The properties of muons have mainly been investigated by experiments with cosmic rays. In particular the muon appears to be the only particle which is not quickly absorbed by matter and hence can penetrate far underground. George [3]) has estimated theoretically the energy loss for an incident muon of energy $\varepsilon$ MeV passing through matter and gives the result that

$$\mathrm{d}\varepsilon/\mathrm{d}x = a+b\varepsilon+c \ln (\varepsilon/10^3)\ \mathrm{MeV}\cdot\mathrm{g}^{-1}\cdot\mathrm{cm}^2,$$

where

$a = 2.2\ \mathrm{MeV}\cdot\mathrm{g}^{-1}\cdot\mathrm{cm}^2$ is the energy loss due to ionisation,

$b = 5.1\times10^{-6}\ \mathrm{g}^{-1}\cdot\mathrm{cm}^2$ is due to bremsstrahlung, electron pair creation and star production,

$c = 0.1\ \mathrm{MeV}\cdot\mathrm{g}^{-1}\cdot\mathrm{cm}^2$ is due to Čerenkov radiation.

Using the general result for $\mathrm{d}\varepsilon/\mathrm{d}x$ and the muon energy spectrum at ground level, George calculated the muon intensity underground and found satisfactory agreement with the experimental results. Hence any further energy loss due to a $\mu$-$\sigma$-N interaction must be small compared with the total energy loss given above, i.e. less than $\frac{1}{2}$ MeV, say. The energy loss per collision for a high energy muon due to scattering on nucleons has been calculated in section 2 as

$$\delta\varepsilon = \pi\alpha^2/4m. \tag{3}$$

Since in general the scattering of a muon on a nucleus will be smaller (per nucleon) than on a free nucleon we may take the above expression as an upper limit for the energy loss. The number of nucleons per $\mathrm{g}\cdot\mathrm{cm}^{-2}$ of path is given by Avogadro's number $N_0 \approx 6\times10^{23}$. Hence the energy loss per $\mathrm{g}\cdot\mathrm{cm}^{-2}$ due to $\mu$-nucleus scattering at high energies is

$$\left(\frac{\mathrm{d}\varepsilon}{\mathrm{d}x}\right)_\sigma \leqq N_0\frac{\pi\alpha^2}{4m}\cdot 2\times10^{-11}\ \mathrm{MeV} \approx \frac{1}{5}\,\frac{g^2b^2}{(4\pi)^2}\,\mathrm{MeV}.$$

If $(\mathrm{d}\varepsilon/\mathrm{d}x)_\sigma \leqq \frac{1}{2}$ MeV, then $g^2b^2/(4\pi)^2 \leqq 2.5$. Thus the value given by Cowland for $g$ still allows a reasonable value for $b$, the strength of the $\sigma$-N coupling.

The scattering of muons in matter has been investigated by various groups, notably Amaldi *et al.*[4]), George and Trent [5]), Leontic and Wolfendale [6]) and more recently Lloyd and Wolfendale [7]). When compared with the theory of Coulomb scattering at a finite nucleus an anomalous contribution is apparent. This was first observed at large angles where the Coulomb scattering is negligible (see Amaldi [4])) but statistical analysis shows its presence at small angles also (see Leontic and Wolfendale [6])). Many attempts have been made to explain this by different nuclear models (see Rochester and Wolfendale [8])) but these have usually been found to be inadequate. For present purposes it is sufficient that an anomalous cross section exists. The

various estimates of its magnitude [6]) give figures of the order of $10^{-28}$ cm$^2$/nucleon for muons of energy $> 200$ MeV. The anomalous scattering is dominant for angles $\gtrsim 10°$. From section 2 the scattering cross section due to a $\mu$-$\sigma$-N interaction is given by eq. (2) integrated over $E$ from $m$ to $E_{max}$. To the lowest order the cross section varies linearly with $\alpha^2$ and its value is tabulated in table 1 for various values of the initial muon energy $\varepsilon$ and the $\sigma$-meson mass $\kappa$, assuming $\alpha^2 = 2$.

TABLE 1

Muon scattering cross-section

| $\kappa$ \ $\varepsilon$ | $\frac{1}{2}m$ | $\frac{1}{2}m$ | $m$ | $10m$ | $100\ m$ |
|---|---|---|---|---|---|
| $2m$ | 1.3 | 3 | 4 | 4 | 1.7 |
| $3m$ | 0.3 | 0.7 | 1.7 | 2.5 | 1.7 |
| $4m$ | 0.08 | 0.2 | 0.6 | 1.2 | 1.7 |

Cross-sections in units $10^{-28}$ cm$^2$.

From these figures it appears that the existence of a $\mu$-$\sigma$-N interaction is not only possible but that its scattering cross section is in reasonable agreement with the anomalous cross section observed. The angle at which the anomalous scattering becomes dominant is given by the muon scattering angle $\phi_0$ at which $d\sigma_B/d\phi = d\sigma_\gamma/d\phi$. This has been calculated in section 2 (see eq. (4)). Assuming $\kappa = 3m$ and $\alpha^2 = 2$ for $\varepsilon = m$ eq. (4) gives

$$\phi_0 = 25°.$$

Experimentally the anomalous scattering is observed at even smaller angles. However, the muon spectrum extends to much higher energies although the average energy at ground level is approximately 0.9 GeV $\approx 0.9\ m$.

A comparison of the scattering amplitudes through the $\sigma$ and photon fields may also be applied to muon bremsstrahlung and the photoproduction of muon pairs. Apart from the difference between the scalar meson and vector photon the lowest order Feynman diagrams with the $\sigma$ and photon intermediate fields differ by a factor

$$\frac{gb}{e^2}\,\frac{k^2}{k^2+\kappa^2} \approx \frac{gb}{e^2}\,\frac{k^2}{\kappa^2} \approx \frac{200\,k^2}{9m^2},$$

assuming $\alpha^2 = 2$ and $\kappa = 3m$. In the laboratory frame this gives $22(E-m)/m$.

The effect of the $\sigma$ field will be small compared with that of the photon field, provided that the main contribution to the process in question is from values of $k^2$ such that

$$k^2 \ll m^2/22 \quad \text{i.e.} \quad E-m \ll m/22 \approx 45\ \text{MeV}.$$

For pair production this is certainly true for incident photon energies up to 600 MeV. Masek and Panofsky [9]) working with bremsstrahlung from 575 MeV electrons find that

$$\frac{\sigma_{\text{exp}}}{\sigma_{\text{theo}}} = 1.93 \pm 0.68.$$

Thus the existence of a $\sigma$ interaction does not conflict with the experimental evidence on pair production but rather tends to explain the divergences from the theoretical figures as in the case of muon scattering.

## 4. Summary

Assuming that the $\sigma$ meson is scalar and that

$$\kappa \approx 3m, \quad g^2/4\pi \approx 2 \quad \text{and} \quad b^2/4\pi \approx 1,$$

the muon-nucleon scattering will not greatly reduce the muon range and in both muon pair production and muon nucleon scattering the $\sigma$-meson interaction accounts for the discrepancies between the experimental and theoretical results. On the other hand, in the case of scattering the theory may be modified, e.g. by the inclusion of pion interactions [10]), to explain the anomalous scattering, and for muon pair production the experimental evidence is not sufficient to require the introduction of a new interaction. However, the existence of the $\sigma$-meson is not incompatible with the present experimental results.

I wish to thank Professor A. Salam for suggesting and discussing the problem and Dr. P. T. Matthews for his helpful remarks; also Mr. W. S. Cowland for a preprint of his paper.

## References

1) J. Schwinger, Annals of Physics **2** (1957) 407
2) W. S. Cowland, Nuclear Physics **8** (1958) 397
3) E. P. George, Progress in Cosmic Ray Physics, Vol. I (North-Holland Publishing Co., Amsterdam, 1952) Ch. 7
4) E. Amaldi *et al.*, Phys. Rev. **81** (1951) 339
5) E. P. George and P. T. Trent, Proc. Phys. Soc. A **64** (1951) 1134
6) B. Leontic and A. W. Wolfendale, Phil. Mag. **44** (1953) 1101
7) J. L. Lloyd and A. W. Wolfendale, Proc. Phys. Soc. A **68** (1955) 1045
8) G. D. Rochester and A. W. Wolfendale, Phil. Mag. **45** (1954) 980
9) G. E. Masek and W. K. H. Panofsky, Phys. Rev. **101** (1956) 1094
10) G. N. Fowler, Nuclear Physics **3** (1957) 121

2.B:2.F *Nuclear Physics* **9** (1958/59) 273—286; © *North-Holland Publishing Co., Amsterdam*
Not to be reproduced by photoprint or microfilm without written permission from the publisher

# PROTON DISTRIBUTIONS FROM $S^{32}(n, p)P^{32}$

H. P. EUBANK, R. A. PECK, Jr. and F. L. HASSLER
*Department of Physics, Brown University, Providence, Rhode Island* †

Received 17 September 1958

**Abstract:** Energy spectra of protons from natural sulfur bombarded with 14 MeV neutrons are shown at 0°, 30°, 60°, and 90°, obtained with a CsI scintillation spectrometer in coincidence with two particle-defining proportional counters. The observed characteristics are those of direct interaction, and the total energy spectrum is well fitted by the level density formula of Newton. The energy discrimination interval being broad but fairly sharp at its extremes, energy groups are not resolved but angular distributions for successive spectral intervals show marked changes at certain energies. From these abrupt changes and the known resolution characteristics the strongest contributing levels in $P^{32}$ are located and assigned $l$ values. The levels so deduced match the strongest contributors to (d, p) and (n, $\gamma$) processes leading to $P^{32}$ and fit quantitatively the expected pattern of single particle transitions. Evidence is found of participation of protons from two initial states as expected, so that three final neutron levels account for five distribution components. All single particle excitations appear in the sequence expected except $2p_{\frac{1}{2}}$ (neutron), which seems to occur before $1f_{\frac{7}{2}}$. Integration of the spectra gives a mean "nuclear temperature" of 2.1 MeV and a cross section of $185 \pm 30$ mb for the first 9.5 MeV of residual excitation.

## 1. Introduction

The reaction $S^{32}(n, p)P^{32}$ ($Q = -0.93$ MeV) has an anomalously large cross section [1]) (0.25 barn) as determined by activation methods. Energy levels of the residual nucleus up to 7 MeV excitation have been accurately determined [2]) together with their neutron orbitals, and well correlated with neutron capture gamma transitions [3]) within $P^{32}$. The (d, p) transition to the $P^{32}$ ground state is a classic demonstration that the single particle orbital is a good quantum number [2,4]) as required by the shell model. It is of interest to examine the (n, p) reaction leading to $P^{32}$ to compare levels excited in this way with those from the (d, p) and (n, $\gamma$) processes, and to see whether shell model identifications can be extended beyond the ground state. Two tentative assignments have been advanced previously [2]).

## 2. Experimental

A narrow group of 14.1 MeV neutrons is produced by deuteron bombardment (175 keV) of tritiated zirconium film in a high frequency Cockcroft-

† Supported in part by the U.S. Atomic Energy Commission. A portion of the work was submitted (F.L.H.) in partial fulfilment of requirements for the Sc.M. degree at Brown University.

Walton accelerator [5]). Natural sulfur fused on a thick lead support formed a target layer of 31 mg/cm$^2$. Since the target was fixed relative to the detector in all measurements its non-uniformity is irrelevant to all relative measurements. Affixed to the front window of the counter array, the target was about 10 cm from the neutron source in all observations.

Protons pass through two gas proportional counters enroute to the 2.5 cm (diameter) $\times$2 mm CsI crystal which is the energy detector, known to exhibit linear energy response in the range 4—20 MeV. The gas counters employ gridded cathodes and share a common lead-lined gas chamber, closed opposite the nickel entrance window (diameter 1.4 cm) by a lucite disk to the outside of which the crystal is bonded. The crystal is 13 cm from the reaction target and the average maximum spread in reaction angle for a given counter orientation is $\pm$17°, including the maximum possible extension of the source of neutrons. The counter assembly is rotated about a vertical axis through the center of the target to study different reaction angles.

Detection circuitry is shown schematically in fig. 1. Pulses from the gas counters, their voltages set to preclude beta detection, are directed to a 0.25 $\mu$sec coincidence unit generating a 4 $\mu$sec gate pulse operating the 20 channel pulse height analyzer. The output of an RCA 6342 photomultiplier registering scintillations, when produced within the gate period of a gas counter coincidence, is displayed in the spectrum and added to the accumulated proton count. Before and after each observation the recoil proton group from a thin polyethylene sheet was observed at 0°, falling just below 40 volts and providing a reference for proton energy and neutron intensity. Each determination of a sulfur spectrum was accompanied by a similar one for a blank lead target, the latter smoothed and subtracted as background correction. Intensity normalization was to total accepted proton count checked by the polyethylene recoil group and by a fixed $BF_3$ "long counter".

A sharp proton group is rendered by the apparatus as a trapezoidal one with flat top width set by target thickness and essentially straight sides whose slope reflects the crystal resolution (14 % full width at half maximum by thin radiator observation, at 14 MeV). In fact, the sensibly flat portion varies more slowly with energy than does the target contribution alone since the crystal response peak deviates from triangularity with decreasing proton energy. Because the two contributing effects are energy dependent in opposite senses the width of the composite group, evaluated at half maximum intensity, varies only within $\pm$0.3 MeV over the first 8 MeV of proton spectrum while the target width alone ranges from 0.8 to 1.9 MeV. Thus the effective "energy window" has a large but nearly constant width and relatively sharp edges, the location of the true proton energy within this group being energy-dependent but known.

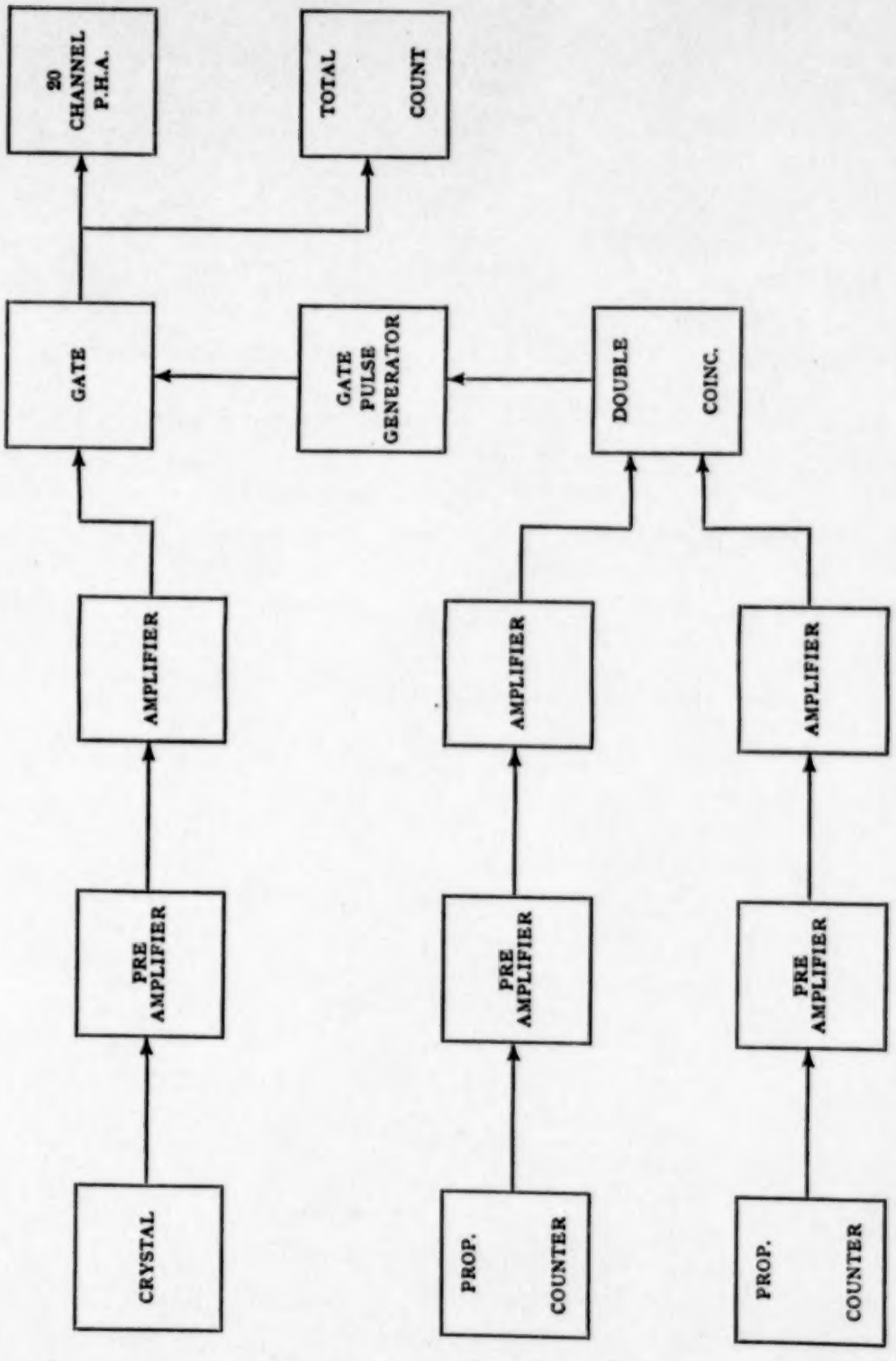


BLOCK DIAGRAM OF ELECTRONICS

Fig. 1. Detector circuitry.

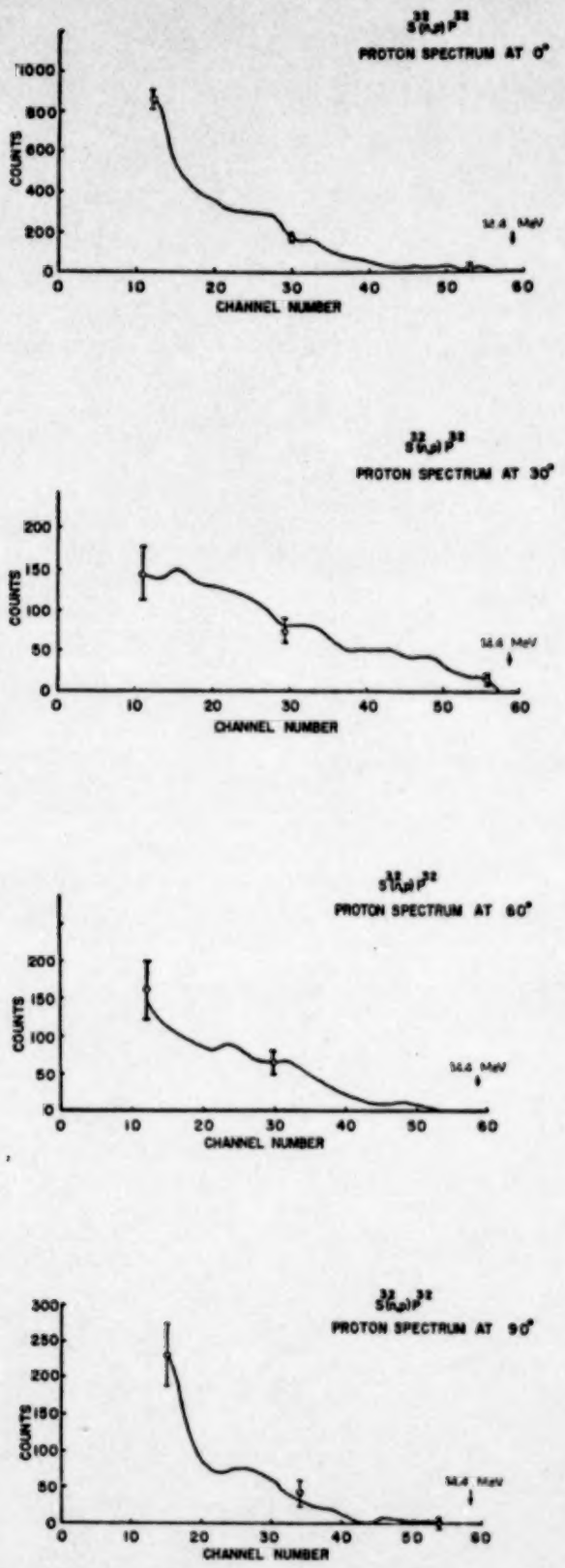


Fig. 2. Observed proton spectra after background removal.

## 3. Spectra

The energy spectra are displayed in fig. 2. Upon integration over energy and angle, assuming no appreciable yield past 90°, they yield a total cross section for residual excitations up to 9.5 MeV of 185±30 mb. This is lower than the activation values [1]) as anticipated, and of the latter supports the

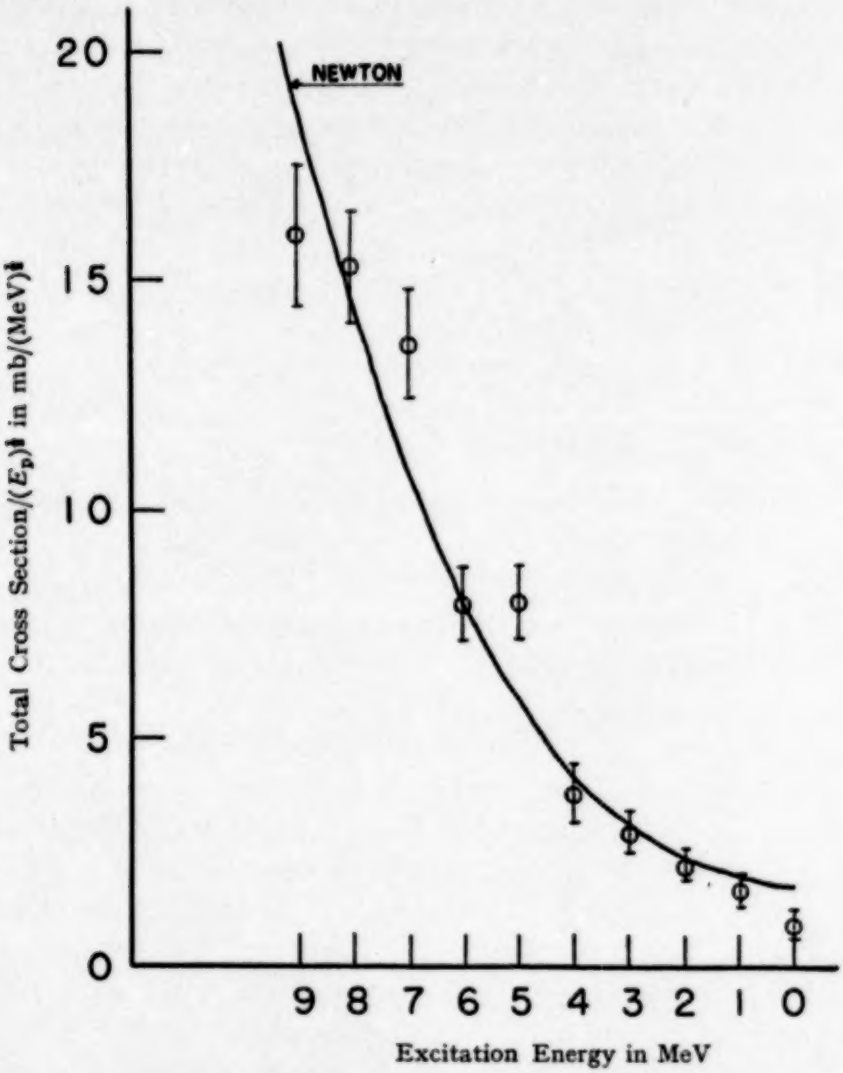


Fig. 3. Reaction spectrum after integration over angle and smoothing (summation over 1 MeV intervals). The proton wave number has been removed so that ordinates should be proportional to mean matrix element and level density. The curve is evaluated from ref. [8]).

lower and more recent value 254±10 mb. Of competing reactions which could be confused with (n, p) only the (n, α) is capable of contaminating the highest 8 MeV of the proton spectrum, and its yield should be depressed relative to that of (n, p) by the Coulomb barrier. The top of the proton

barrier falls at approximately 8.5 MeV on the excitation scale, slightly above the lowest proton energy shown in fig. 2.

The spectra were smoothed by collection over 1 MeV intervals and integrated over angles, to show the gross energy variation of total cross section. When plotted in the form [6]) appropriate to a compound nucleus process this variation gives a mean temperature parameter of 2.1 MeV but fails to fit either of the realistic level density formulae [7,8]) not containing adjustable factors. However, a good fit to the non-adjustable shell-dependent semi-empirical density function [8]) is obtained when the cross section is plotted directly (divided by the proton wave number). This correspondence is shown in fig. 3 and reinforces the presupposition that the reaction proceeds in the main otherwise than by compound nucleus formation. The conclusion is strengthened by the fact that most of the protons observed emerge above the Coulomb barrier, by the large magnitude of the cross section and by its concentration at angles in the forward hemisphere. An assumed symmetry about 90° would bring the measured cross section well above even the higher of the activation measurements.

## 4. Angular Distributions

Since the energy resolution precludes observation of distinct proton groups associated with individual levels, the spectra were arbitrarily summed over 1 MeV intervals for display of angular distributions (fig. 4). The relatively sharp edges of the energy "window" are manifested by abrupt changes in character of the distributions at certain energies and the large window width in the ranges of excitation over which the distributions remain unchanged, and which agree with the computed resolution width.

With only four points of an angular distribution it is still possible to assign $l$ values on the assumption of a surface interaction [9,10]) mechanism because of the large separation (about 20°) and width of the expected peaks. It is assumed that each distribution is represented by a linear combination of terms $j_l^2(Qr_0)$ with $l \leqq 3$ and $4.6\times10^{-13} \leqq r_0 \leqq 5.6\times10^{-13}$ cm. The lower radius is the classical $1.45\times10^{-13}\,A^{\frac{1}{3}}$ cm and is probably the best value for an (n, p) process [10]); the upper limit is the Gamow radius $(1.7+1.22\,A^{\frac{1}{3}})\times10^{-13}$ cm which fits the stripping data [2]) for $P^{31}$(d, p)$P^{32}$. For each angular distribution, the linear combination coefficients giving best fit to the four data points were determined by the least squares method, for every possible combination of terms $l = 0, 1, 2, 3$ (taken singly, in pairs, in trios, and all together). The adequacy of each set of coefficients was judged by the condition that the resulting linear combination of terms fit the observed data at each point within the latitude of error shown in fig. 4, a conservative condition since the errors include systematic factors several times the statistical probable errors. It is to be noted that even when four terms are

used a fit is not guaranteed since individual terms contribute to more than one data point and negative coefficients are not allowed.

The resulting $l$ assignments are given in table 1 and are unique except where alternatives are shown. It can be shown by quantitative argument that Coulomb and nuclear potential effects should not perturb the assignments [9,10,11]) and that changes of assumed radius, within the range specified, cannot affect assignments of $l = 0$ or 1. At worst, by raising the radius to equal the stripping value (an improbable value for the (n, p) process) it is possible to raise assignments of $l = 2,3$ to the next higher value. Contributions listed as "trace" are required by strict adherence to the error limits employed but would disappear from the minimal assignments if the error limit were increased by 50 %—100 %.

TABLE 1

Fewest $l$ terms which fit angular distributions

| $U$ (MeV) | major | minor | trace |
|---|---|---|---|
| 0 | 1 | | 2(0.06) |
| 1 | 1 | | 2(0.06) |
| 2 | 1 | | |
| 3 | 1 | {2(0.18)<br>3(0.13)} | |
| 4 | 1 | {2(0.28)<br>3(0.21)} | |
| 5 | 0 | 2(0.38) | 3(0.08) |
| 6 | 0 | 2(0.22) | |
| 7 | 0 | 2(0.19) | |
| 8 | 0 | 2(0.15) | |
| 9 | {0<br>1 | 1(0.13)<br>isotropic (0.18) | 2(0.05) |

First column identifies the centre of a 1 MeV wide interval of spectrum (excitation in $P^{32}$), and the rest $l$ terms required to fit the angular distribution of protons in the interval. More terms are possible, but fewer are not. Braces show alternatives in cases of ambiguity; other cases are unique. Parenthetic numbers are ratios of coefficient to that of major term, each term $(j_l^2)$ being normalized to unity at its peak before determination of coefficients.

Each block of $l$ values in table 1 can be attributed to a single sharp proton group whose true location in energy can be deduced from the known resolution characteristic of the system. The appearance of a term in the angular distribution at any one nominal excitation sets upper and lower limits on the true energy, the most stringent pair of limits for each block locating the level to within $\pm 0.8$ MeV or less. The five levels, two contributing only

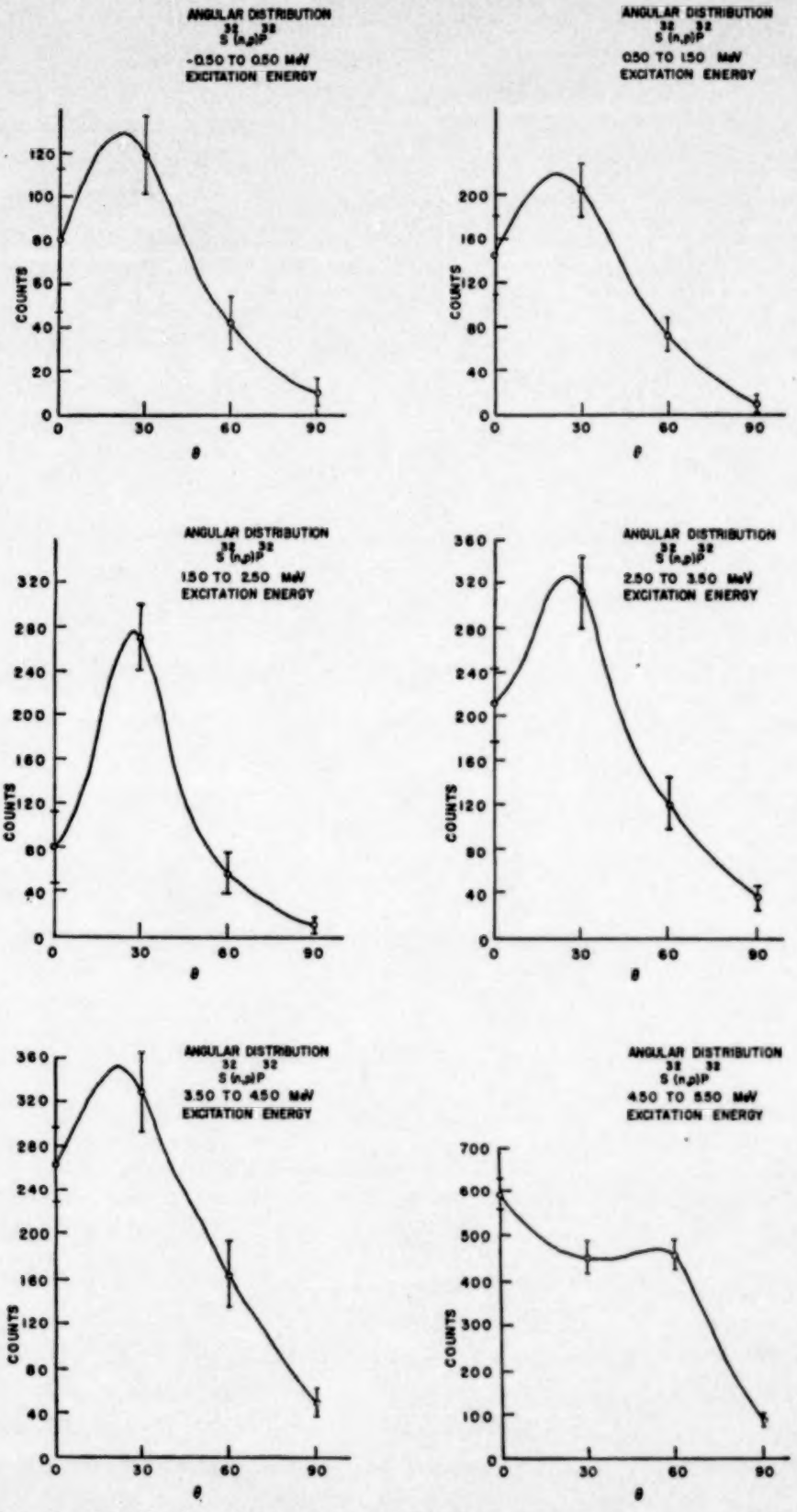


Fig. 4. Angular distributions for successive 1 MeV intervals of proton spectrum. Table 1 presents the *l* values deduced from these distributions.

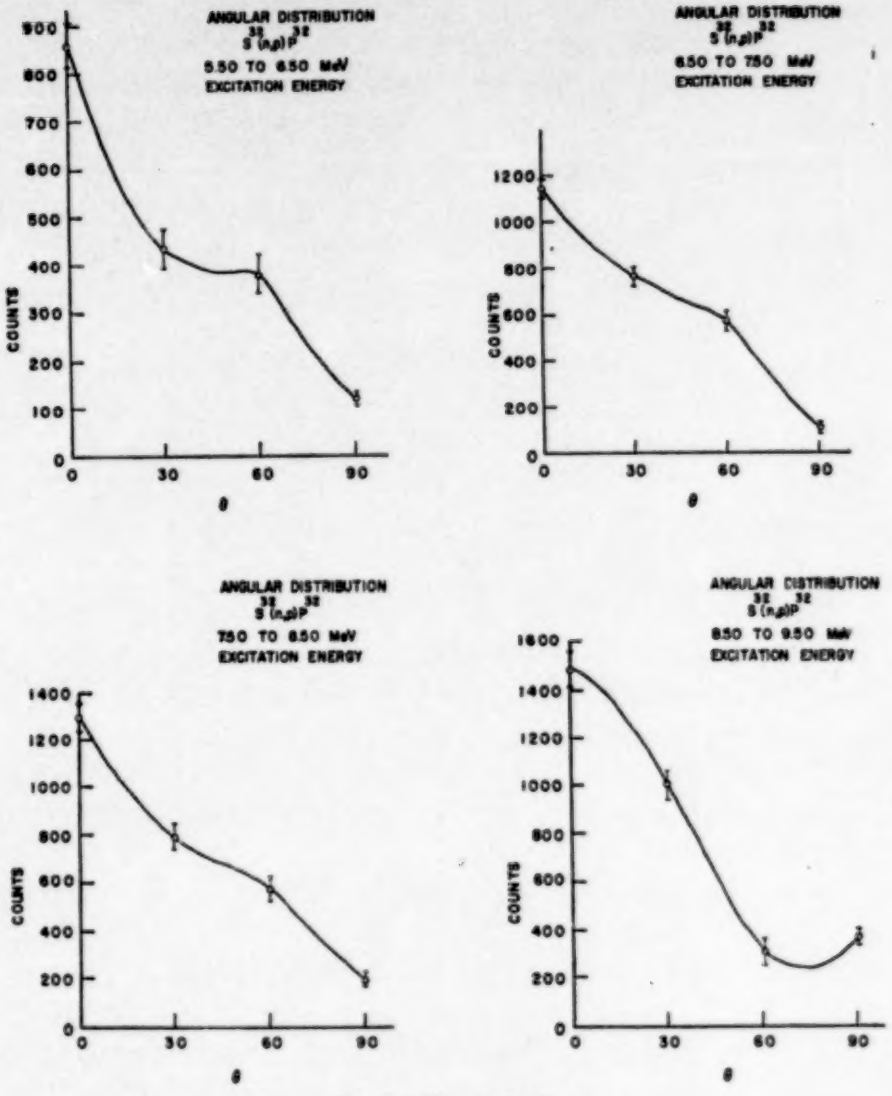


Fig. 4 (Continued)

TABLE 2

Simplest scheme of $P^{32}$ levels, with proposed assignments

| | This Paper | | | (d, p) | Single Particle Assignment | | |
|---|---|---|---|---|---|---|---|
| | $l$ | Intensity | $U$ (MeV) | $U$ (MeV) | $U$ (MeV) | Proton | Neutron |
| I | 2 | weak | 0.0±0.5 | 0.0 | 0.0 | $2s_{\frac{1}{2}}$ | $1d_{\frac{3}{2}}$ |
| II | 1 | strong | 2.5±0.8 | 3.3 | ? | $2s_{\frac{1}{2}}$ | $2p_{\frac{3}{2}}$ |
| III | 3 | weak | 4.6±0.8 | 5.1 | 5.4±0.5 | $2s_{\frac{1}{2}}$ | $1f_{\frac{7}{2}}$ |
| IV | 0+2 | strong | 7.6±0.6 | — | 7.3±0.2 | $1d_{\frac{3}{2}}$ | $1d_{\frac{3}{2}}$ |
| V | 1 | strong | 11.2±0.2 | — | 10.6±0.2 | $1d_{\frac{3}{2}}$ | $2p_{\frac{1}{2}}$ |

Smallest number of $P^{32}$ levels required to account for angular distributions (table 1), compared with levels [2]) from $P^{31}$(d, p) $P^{32}$ and proposed shell model transitions. Uncertainties in excitation (column 4): for I and V add uncertainty in effective energy "window width", to which the rest are insensitive.

"trace" intensities, which account sufficiently for all the distributions are identified in table 2. In cases of ambiguity in table 1 the alternatives have been chosen in each case which require the fewest $P^{32}$ levels for their explanation (lower line of table 1 in each case). Clearly the levels of table 2 are not the only set consistent with the observed distributions, but they do represent the simplest such set. Reconstitution of energy groups through the levels of table 2 and the known resolution pattern give good fits to the raw spectra.

## 5. Shell Model Assignments

The ground state of the target nucleus [12]) is 0+ with two protons in $2s_{\frac{1}{2}}$ and one in $1d_{\frac{3}{2}}$ outside the closed shell of eight protons. Both types of valence protons should contribute to the (n, p) process [9]); that the $S^{32}$(n, p) cross section is considerably larger than those of $Mg^{24}$ or $Si^{28}$ argues the same idea. Thus each final neutron level should produce two (n, p) groups separated in apparent excitation by the separation between $1d_{\frac{3}{2}}$ and $2s_{\frac{1}{2}}$ proton levels in $S^{32}$ ($7.3 \pm 0.2$ MeV; see appendix). Final neutron levels in order of increasing excitation should be [13]) $1d_{\frac{3}{2}}$, $1f_{\frac{7}{2}}$ and $2p_{\frac{3}{2}}$, separated respectively by magic numbers 20 and 28. The f level is estimated (appendix) to lie at $5.4 \pm 0.5$ MeV above the d, but no reliable estimate of the relative position of the p level has been made. Each neutron level should produce a close doublet of nuclear levels through $j$-$j$ coupling [14]) with the $2s_{\frac{1}{2}}$ proton in $P^{32}$.

The ground state transition is from $2s_{\frac{1}{2}}$ (proton) to $1d_{\frac{3}{2}}$ (neutron), the final state being a $j$-$j$ doublet 1+, 2+ so that $l = 0$ or 2, for both (n, p) and (d, p) processes, 0 being forbidden if $l$ is conserved. The (d, p) data show that the zero-excitation group is a close doublet [2]) and both (d, p) and (n, p) experiments show $l = 2$ unaccompanied by 0. The transition is strong in the (d, p) process, weak in the (n, $\gamma$) and (n, p). This level (I) is one of two weak ones in table 2, which are the only cases involving $\Delta l \geqq 2$; anomalous weakness of the reverse transition, in the beta decay of $P^{32}$, presumably reflects the large $l$ change [12]).

The final state for neutron level $2p_{\frac{3}{2}}$ is the doublet 1−, 2− allowing for the transition $l = 1$ or 3, and only 1 if $l$ is conserved. The (d, p) reaction shows a strong, close doublet with $l = 1$ at 3.3 MeV, in reasonable agreement with level II ($l = 1$, no 3). The 3.3 MeV level is the strongest contributor to (n, p), (d, p) and (n, $\gamma$) spectra. It is surprising that $2p_{\frac{3}{2}}$ should occur below $1f_{\frac{7}{2}}$ since the latter is known to occur first in ground state configurations [12]) of not much larger nuclei ($A^{39}$, $K^{40}$, $Ca^{41}$). However, the characteristics of neutron number 28 are not yet evaluated [15]), and a crossing of the f and p levels for a single excited neutron in $P^{32}$ is not improbable.

Neutron level $1f_{\frac{7}{2}}$ produces the $j$-$j$ doublet 3−, 4− for which, in both (d, p) and (n, p) reactions, $l = 3$ with or without $l$ conservation. In the (d, p) reaction [2]) only two groups are found with $l$ greater than 2, at excita-

tions 3.45 and 5.11 MeV. Their angular distributions are similar and suggest distorted $l = 3$ terms, each having intensity of the order expected for a single particle $l = 3$ transition. Configuration mixing in the $P^{31}$ ground state [16]) may account for one of the two (d, p) groups, in which case one would expect the group at the higher excitation to show the true position of the single neutron level relative to the $P^{32}$ ground state. This suggests for $1f_{\frac{7}{2}}$ (neutron) the 5.11 MeV level of the (d, p) spectrum, which shows evidence [2]) of a doublet nature and agrees with the calculated excitation of $1f_{\frac{7}{2}}$ ($5.4 \pm 0.5$ MeV; appendix). Of the (n, p) levels, III is in good agreement with both of these excitation values and shows the expected $l = 3$ without 1. The transition is weak in both (n, p) and (d, p) cases. One would not expect to observe strong gamma rays to or from an f level following slow neutron capture, and none are observed in association with the 5.11 MeV level, although the 3.45 MeV level shows a strong one [3]), arguing further against the assignment of $1f_{\frac{7}{2}}$ to that level.

None of the next six single neutron levels permits $l = 0$ in an (n, p) transition with a $2s_{\frac{1}{2}}$ proton, nor is any $l = 0$ group observed in the (d, p) spectrum above those already assigned. However, the transition $1d_{\frac{3}{2}}$ (proton) to $1d_{\frac{5}{2}}$ (neutron) for "level" IV is consistent with all of these circumstances. Allowed $l$ values for this transition are 0, 2, and 4, consistent with the 0 and 2 observed for IV and giving significance to the difference in $l$ between IV and I. The expected ratio [9]) of coefficients for $l = 2$ and 0 is $C^2_{22}(0,0;\ 0,\ 0)/C^2_{22}(2,\ 0;\ 0,\ 0)$ or 0.12 in the convention of table 1. Agreement with the observed ratios is reasonable since the least squares method underlying table 1 can emphasize particular terms. The excitation deduced ($7.6 \pm 0.6$ MeV) is in excellent agreement with the $7.3 \pm 0.2$ MeV (appendix) which separates $1d_{\frac{5}{2}}$ and $2s_{\frac{1}{2}}$ proton levels. The assignment of level IV would be readily checked by examination of the $P^{31}$ (d, p) $P^{32}$ spectrum above 7 MeV excitation, in which IV should have no counterpart. A similar test by the (n, $\gamma$) reaction is ruled out by the 0.5 MeV level in $P^{32}$, which gives the same gamma rays as would a 7.4 MeV level.

The next transition expected is from $1d_{\frac{5}{2}}$ (proton) to $2p_{\frac{1}{2}}$ (neutron), for which $l_{\min} = 1$ and the expected "excitation" is the sum of II and IV, or $10.6 \pm 0.2$ MeV using the best values. This transition gives a good account of V. A transition $1d_{\frac{5}{2}}$ (proton) to $1f_{\frac{7}{2}}$ neutron should appear at an excitation (sum of III and IV) outside the range of observation. It is possible that the next neutron level, $2p_{\frac{1}{2}}$ (proton from $2s_{\frac{1}{2}}$), is also involved around excitation 11 MeV, although it should be preceded by $1f_{\frac{5}{2}}$ (neutron) for which $l_{\min} = 3$.

The single particle assignments discussed are summarized in table 2. The spectral components discussed are not the only ones which can appear in the (n, p) reaction but are the strongest, as is to be anticipated for single particle transitions. The three which have counterparts in (d, p) and (n, $\gamma$)

reactions are there found to be doublets as expected, and only one (d, p) doublet is excluded from the scheme. Only one of the strong (n, p) components is expected to appear in the other processes, and that is identified with the strongest of the (d, p) and (n, $\gamma$) contributions. All expected single particle transitions appear in the expected sequence, excepting the apparently premature occurrence of the $2p_{\frac{1}{2}}$ neutron state, with $l$ values and energies in good agreement with predictions.

## Appendix

### SINGLE PARTICLE LEVEL SPACINGS

The position of any single nucleon level can be found for some core (mass number $A$) by the last nucleon binding energy in a nucleus $A+1$, corrected for pairing effects when appropriate. Such values can often be determined from experimental reaction energies with good accuracy, and the separation of adjacent levels can be referred to other cores with fair accuracy if the change in $A$ is not too great [17].

*Neutron levels.* The position of $1d_{\frac{3}{2}}$ for a $S^{32}$ core is given by the last neutron binding energy in $S^{33}$ and is $8.65\pm0.01$ MeV as determined independently by $Q$ values for $S^{32}$(d, p)$S^{33}$ and $S^{32}$(n, $\gamma$)$S^{33}$. The position of $1f_{\frac{7}{2}}$ for $S^{36}$ core is similarly given by the last neutron binding energy in $S^{37}$, found from mass data [18] to be $5.7\pm0.3$ MeV. Translation † of the latter to $A = 32$ yields $3.1\pm0.5$ MeV for the single neutron binding energy of $1f_{\frac{7}{2}}$ in $S^{32}$, locating the level at $5.5\pm0.5$ MeV above $1d_{\frac{3}{2}}$. Translation to core of $A = 31$ reduces the separation to $5.4\pm0.5$ MeV.

Although $2p_{\frac{1}{2}}$ is qualitatively located above $1f_{\frac{7}{2}}$ for masses as small as 40, quantitative information on its position is not forthcoming from binding energy data below $A = 53$. Translation of this information to $A = 32$ is worthless for so large a change in $A$. The problem is further complicated by the fact that in nuclei for which the level can be quantitatively located the corresponding proton states are partially occupied, introducing cross-pairing energies of unknown size, not operative in the lighter core of interest. Hence no quantitative estimate of the position of $2p_{\frac{1}{2}}$ is available for the $P^{31}$ core.

*Proton levels.* We require the separation between single proton levels $1d_{\frac{3}{2}}$ and $2s_{\frac{1}{2}}$ in a $P^{31}$ core, or more exactly the difference $D$ between the energy required to ionize a proton from $1d_{\frac{3}{2}}$ in $S^{32}$ and that required to ionize one from $2s_{\frac{1}{2}}$ in the same nucleus. An approximation to $D$ is obtained by subtracting the last proton binding energy in sulfur, proton configuration $(d_{\frac{3}{2}})^6(s_{\frac{1}{2}})^2$, from that in silicon, proton configuration $(d_{\frac{3}{2}})^6(s_{\frac{1}{2}})^0$, using the 16-neutron isotopes throughout. Pairing energies appear in the computation in the same senses as in the (n, p) processes, so need not be removed. Two

† Translation parameters (see refs. [17,20]): well depth 42.8 MeV, separation between diffuse-well and square-well positions 5.6 MeV for $1f_{\frac{7}{2}}$.

independent values for each of the necessary mass differences are provided by the reactions $Si^{29}(d, p)Si^{30}$, $Si^{29}(n, \gamma)Si^{30}$, $P^{31}(d, p)P^{32}$, $S^{32}(n, p)P^{32}$ and the beta decays of $Al^{29}$ and $P^{32}$. The resulting first approximation to $D$ is $4.80 \pm 0.13$ MeV.

In this calculation an error is introduced by the use of Al and Si masses to locate $1d_{\frac{1}{2}}$; ideally their roles should have been filled by proton configurations $(d_{\frac{1}{2}})^5(s_{\frac{1}{2}})^2$ and $(d_{\frac{1}{2}})^6(s_{\frac{1}{2}})^2$, still with 16 neutrons in each case. $D$ may be corrected for the omission of the pair of $s_{\frac{1}{2}}$ protons by addition of a Coulomb correction and a level shift correction. The latter should be well approximated by the shift in position of the $1d_{\frac{1}{2}}$ *proton* level due to the addition of a *neutron* pair in $2s_{\frac{1}{2}}$, i.e., by the mass combination $(Al^{29}-Si^{30})-(Al^{27}-Si^{28})$. The second of these differences was obtained in the foregoing calculation and the first is very well determined by three independent cycles of reaction data. The resulting level shift correction is $2.05 \pm 0.12$ MeV. The Coulomb term is computed directly, using for total Coulomb energy [19] $0.65\ Z^2\ A^{-\frac{1}{3}}$ MeV, and is $0.61 \pm 0.05$ MeV to be added to $D$. Hence the computed value for $D$ is $7.46 \pm 0.30$ MeV. A lower limit to the level shift correction is independently obtained, though less accurately, by determining the absolute position of $1d_{\frac{1}{2}}$ (proton) at $A = 27$ and translating it as though it were a neutron level. Since this fails to include cross-pairing effects which are automatically incorporated in the preceding calculation a smaller value is expected and found (1.6 MeV), but the general magnitude of the correction is confirmed.

The spacing $D$ may be independently estimated from the semi-empirical level positions of Ross *et al.*[19]. These are given only for a few nuclei and the appropriate translation device for proton levels is not clear. However, two reasonable guesses as to appropriate translation give consistent results.
(1) The separation can be read directly for $K^{39}$ and $Au^{127}$ as 4.36 and 1.28 MeV respectively. It is a reasonable supposition that this spacing is a unique function of $Z$ and $A$ and an empirical fact that the product $DZ^2A^{-1}$ is the same for these widely disparate nuclei (41.0 for Au, 40.4 for K). If the same value $(40.7 \pm 0.3)$ is assumed to hold for the core of interest, the resulting spacing is $5.60 \pm 0.04$ MeV. (2) The spacing can be read in the case of $K^{39}$ both for protons (4.36 MeV) and for neutrons (6.45 MeV). The neutron level spacing can legitimately be translated [17] from $A = 39$ to $A = 31$, yielding for the lighter core 8.01 MeV. Assuming that the ratio of proton level spacing is the same at $A = 31$ as at $A = 39$, one obtains 5.47 MeV as a second estimate of the proton spacing in a mass 31 core. From the two determinations we may conclude that the intrinsic spacing of the $1d_{\frac{1}{2}}$ and $2s_{\frac{1}{2}}$ proton levels in the $P^{31}$ core is $5.51 \pm 0.10$ MeV.

To the raw spacing of the preceding paragraph must be added the difference in the energies required to break a proton pairing bond in $1d_{\frac{1}{2}}$ and in $2s_{\frac{1}{2}}$. This difference should be positive [15], insensitive to $A$ and the same for

neutrons and protons. Hence a sufficient estimate of the correction is its neutron analogue, given by the mass combination $(Mg^{25}-Mg^{24})+(Mg^{26}-Mg^{27})+(Mg^{25}-Mg^{26})+(Mg^{28}-Mg^{27})$; it is necessary to use isotopes of even $Z$ to avoid cross-pairing complications and the requisite data cycles are incomplete for the 12-neutron isotopes of Si or S. Each of the mass differences can be obtained by at least two independent reaction cycles from the following data: (d, p) on $Mg^{24}$, $Mg^{25}$, $Mg^{26}$, and $Al^{27}$; (n, $\gamma$) on $Mg^{24}$ and $Al^{27}$; ($\gamma$, n) on $Mg^{25}$ and $Al^{27}$; $Al^{27}(\gamma, p)$; $Mg^{26}(p, \gamma)$; beta decay of $Mg^{27}$ and $Mg^{28}$. The internal agreement is excellent and the resulting correction to $D$ is $+1.71\pm0.05$ MeV, giving for the desired term $D = 7.22\pm0.15$ MeV.

The two lines of argument leading to the $1d_{\frac{3}{2}}-2s_{\frac{1}{2}}$ spacing effective in the (n, p) reaction give the values $7.46\pm0.30$ MeV and $7.22\pm0.15$ MeV. Their weighted mean ($7.30\pm0.20$ MeV) appears in table 2 and in the text.

## References


1) L. Allen, Jr., W. A. Biggers, R. S. Prestwood and K. R. Smith, Phys. Rev. **107** (1957) 1363;
E. B. Paul and R. L. Clarke, Can. J. Phys. **31** (1953) 267
2) A. W. Dalton, S. Hinds and G. Parry, Proc. Soc. **70** (1957) 586
3) B. B. Kinsey, G. A. Bartholomew and W. H. Walker, Phys. Rev. **85** (1952) 1012;
T. H. Braid, Phys. Rev. **102** (1956) 1109
4) H. A. Bethe and S. T. Butler, Phys. Rev. **85** (1952) 1045
5) R. A. Peck, Jr. and H. P. Eubank, Rev. Sci. Instr. **26** (1955) 444
6) J. M. Blatt and V. F. Weisskopf, Theoretical Nuclear Physics (Wiley and Sons, New York, 1952) p. 367;
M. Shapiro, Phys. Rev. **90** (1953) 170
7) J. M. B. Lang and K. J. LeCouteur, Proc. Phys. Soc. A **67** (1954)
8) T. D. Newton, Can. J. Phys. **34** (1956) 804
9) S. T. Butler and O. Hittmair, Nuclear Stripping Reactions (John Wiley and Sons, New York, 1957) Ch. 13
10) S. T. Butler, Phys. Rev. **106** (1957) 272
11) W. Tobocman and M. H. Kalos, Phys. Rev. **97** (1955) 132
12) P. M. Endt and C. M. Braams, Revs. Mod. Phys. **29** (1957) 683
13) P. F. Klinkenberg, Revs. Mod. Phys. **24** (1952) 63
14) D. R. Inglis, Revs. Mod. Phys. **25** (1953) 430
15) M. G. Mayer and J. H. D. Jensen, Elementary Theory of Nuclear Shell Structure (John Wiley and Sons, New York, 1955) pp. 24, 34, 35
16) R. Huby and H. C. Newns, Proc. Phys. Soc. A **68** (1955) 758
17) R. A. Peck, Jr. and J. Lowe, Phys. Rev. (to be published)
18) D. J. Hughes and J. A. Harvey, Neutron Binding Energies, Table 8h-1 in American Institute of Physics Handbook (McGraw-Hill Book Company, New York, 1957)
19) A. E. S. Green, Nuclear Physics (McGraw-Hill Book Company, New York, 1955) p. 287
20) A. A. Ross, H. Mark and R. D. Lawson, Phys. Rev. **102** (1956) 1613;
**103** (1956) 1906

1.D.3 *Nuclear Physics* 9 (1958/59) 287—295; © *North-Holland Publishing Co., Amsterdam*
Not to be reproduced by photoprint or microfilm without written permission from the publisher

# QUASI-LATTICE MODEL OF NUCLEAR MATTER

L. E. H. TRAINOR, A. B. BHATIA and P. C. SOOD
*University of Alberta, Edmonton, Canada*

Received 28 August 1958

**Abstract:** Brueckner and others have applied an extension of the self-consistent method of Hartree-Fock to the determination of the properties of a hypothetical nuclear matter consisting of roughly equal numbers of neutrons and protons, the electrical forces between protons being "turned off". Taking the nucleon-nucleon interaction potentials to be those of Gammel and Thaler, we have applied the well-known Wigner-Seitz method for crystal lattices to a quasi-lattice model of nuclear matter. This method gives the energy of the lowest single particle state as a function of the internucleonic separation. Good agreement is obtained with the experimental values for the nuclear density and the binding energy per nucleon.

## 1. Introduction

Several studies [1–4]) have been made of the properties of a hypothetical nuclear matter which, it is presumed, would exist in bulk form were it not for the electrical repulsion between protons. Nuclear matter defined in this way is approximated to in the interior of heavy nuclei, and its properties would be described in part by the volume term in the Weiszäcker semi empirical mass formula. According to Gomes and coworkers [3]), the equilibrium value of the binding energy per particle determined from experiment in this way is 15 MeV, and the equilibrium value of the nuclear density $\rho_0$ is $2.17\times10^{38}$ particles per cm$^3$, corresponding to an average separation $d_0 = \rho_0^{-\frac{1}{3}}$ of about $1.66\times10^{-13}$ cm between nucleons. These values, which correspond to the situation where equal numbers of neutrons and protons comprise the nuclear matter, are to be regarded as experimental values which a reasonable theory ought to predict.

It appears from the studies mentioned above that reasonable agreement can be obtained from an extended Hartree-Fock self-consistent calculation employing phenomenological two-body potentials. In particular, satisfactory results have been obtained with Gammel-Thaler potentials, i.e. with Yukawa potentials which have been fitted to the deuteron data and to the various two-body scattering data. In the present work, reasonable agreement with experiment has also been obtained but from an entirely different type of calculation. The present calculation starts from the basic assumption that bulk nuclear matter can be characterized in part by a quasi-periodic struc-

ture. The method of Wigner and Seitz [5]), well known in the studies of the binding energy of metals, is then employed to calculate the equilibrium density and the binding energy per nucleon of the bulk nuclear matter.

## 2. Quasi-Periodicity of Nuclear Matter

A possible periodicity of nuclear matter as it occurs in the independent particle model is suggested by the structure of the experimentally fitted two-body potentials of Gammel and Thaler [6]). These potentials are characterized by very large repulsive cores on the one hand, and on the other by ranges which are roughly equal to the average internucleonic spacing. For example, the Yukawa potential corresponding to the singlet interaction in even parity states is given by †

$$V_s = \infty, \quad r \leqq r_c,$$

$$V_s = \frac{V_{0s} \exp(-\mu_{0s} r)}{\mu_{0s} r}, \quad r > r_c, \tag{1}$$

where $r_c = 0.4$, $\mu_{0s} = 1.45$, and $V_{0s} = -434$. The triplet interaction even parity potential $V_t$ is given by a similar expression with $r_c = 0.4$, $\mu_{0t} = 2.09$ and $V_{0t} = -877$. Comparing the core radius of 0.4 in these potentials with the average spacing of 1.66 between nucleons, it is evident that extremely high local concentrations of nuclear matter are not possible. On the other hand, because of the short range nature of the attractive forces, marked variations below the average density are also improbable. Thus, the packing is reasonably close and the nuclear matter presents a granular structure, From the independent particle point of view, in which the nuclear matter is traversed by a single particle making successive scatterings, one would expect to find roughly the same potential in each "nucleon volume" ††. This implies a regularity of the granular structure of nuclear matter. In other words, it seems likely that in the model transformation from the actual nuclear particles to the single particles of the individual particle model, the effective single particle potential corresponding to the ground state of the nucleus would have a periodic or regular structure in order to enhance minimization of the total energy. We have used the term quasi-periodicity of nuclear matter because the distribution of nucleons in nuclear matter is more analogous to that of a liquid than that of a crystal. One might anticipate that when excitation energy is added to nuclear matter fluctuations from quasi-periodicity occur, whereas in the ground state there is little tendency towards clustering among the nucleons. This situation may be related to the

† In this paper, energies are expressed in MeV and distances in units of $10^{-13}$ cm.

†† The term "nucleon volume" is used here for the average volume per nucleon in nuclear matter; this phrase is suggested by the analogy of atomic volume or the volume of the Wigner-Seitz sphere.

phase change in nuclear matter previously proposed [7,8]) to explain anomalies in the variations of nuclear level densities with excitation energy. An investigation of this point is being carried out.

It is interesting to note that the individual particle model which forms the starting point of the considerations of Gomes *et al.*[3]) and Weisskopf [9]) is a special case of the periodic model discussed here. Weisskopf has pointed out that the independent particle model implies that each nucleon moves in a potential which is independent of the detailed positions of all other nucleons and depends only on the coordinates of the particle itself. He states that in infinite nuclear matter, this potential would be constant in space, and that the resulting many-body wave function would be a product of plane waves, appropriately antisymmetrized. This conclusion seems to us too restrictive, for the potential seen by the independent particle could have a periodicity without making any reference to the detailed coordinates of any other nucleon. In fact, Weisskopf's uniform background potential is seen to be a special case in which the periodicity vanishes. The situation is somewhat reminiscent of the Sommerfeld model of a metal in which the periodicity in the potential due to the regular arrangement of the ions is neglected and the periodic potential replaced by a constant negative potential.

Actually, according to Hugenholtz and Van Hove [4]), the concept of a single particle energy in a system of interacting Fermi particles applies only to states which are occupied near the Fermi surface. For this reason it is probably true that the independent particle model is only a very crude approximation, and that it is essential in a proper theory to take correlation effects into account. To the extent, however, that one uses an independent particle model as a first approximation it would seem that the approximation is improved by using a periodic background potential. Refinements to this periodic potential model are under study, but in the present paper we are concerned only with the question whether the model leads to anything like reasonable results.

## 3. Application of the Wigner-Seitz Method

Assuming that nuclear matter can be characterized in part by a basic periodicity, our problem is to derive the nuclear density and the binding energy per nucleon from a reasonable choice of the nucleon two-body potential. We elected to adapt the method of Wigner and Seitz [5]), which has been used with much success in the studies of crystal lattices in solid state theory. In this method one replaces the actual potential surrounding a lattice site by a spherically symmetric potential which approximates to it in a sphere (Wigner-Seitz sphere) whose volume is equal to the nucleon volume (volume per ion in metals); the radius of the sphere thus corresponds roughly

to half the distance between nearest neighbours. The periodicity is guaranteed by the requirement that the wave function (suitably normalized) has a horizontal slope at the boundary of the region thus defined. This requirement is sufficient to determine the energy of the ground state, and one gets a value of this energy for each possible choice of the lattice constant. In this manner one obtains a curve of energy versus lattice constant and the minimum of the curve gives the equilibrium values of both the energy and the lattice constant.

Clearly our situation is not the same as in a crystal lattice where the lattice sites can be regarded as fixed and the particle under consideration is an electron. In the case of nuclear matter, the nucleons are certainly not fixed but they are assumed to space themselves with such regularity that in the independent particle approximation the potential is characteristically periodic. The potential in each nucleon volume is then replaced by a spherically symmetric potential in a sphere of equal volume centered on the lattice site, and the wave function is subjected to the condition of horizontal tangency at the boundary. We shall loosely refer to the sphere as the Wigner-Seitz sphere. In the more usual application this procedure represents an approximation to the actual potential about a lattice site in a metal. In the present application we are already one step removed (model transformation) from the physical situation and it is not as clear what this procedure represents. However, it would appear to be a distinct improvement as a first approximation over a procedure employing an independent particle potential which is constant.

## 4. Choice of Potential in the Wigner-Seitz Sphere

Application of the Wigner-Seitz method to the problem of nuclear matter is complicated by several factors — two types of nucleons are involved, the forces are spin-dependent, and the exclusion principle must be taken into account. In order to simplify the calculations as much as possible without sacrificing the major physical considerations, we have assumed that the inclusion of tensor and spin-orbit forces would not materially affect the sort of averages considered here. We have also assumed a Serber force for the two-body interactions in the same manner as has been done by other authors [1–3]). This force gives zero contribution in states of odd relative angular momentum, which is in substantial agreement with experiment according to the analysis of Gammel and Thaler [6]). Adopting the Serber force, we take the exclusion principle into account in a statistical way by assuming that when a single nucleon traverses nuclear matter, only 3 of every 4 nucleons contribute to the interaction, and of these half contribute through the singlet even parity interaction and half through the triplet even

parity interaction. This is similar to the procedure adopted by Bethe [2]. From this point of view it is just as though the effective density $\rho_{eff}$ of nuclear matter were reduced by a factor $\frac{3}{4}$ from the true value $\rho$.

Adopting an average of the Gammel-Thaler potentials $V_s$ and $V_t$ given in eq. (1), we take as the potential in the Wigner-Seitz sphere

$$\bar{V}(r, a) = \tfrac{1}{2}(V'_s + V'_t), \tag{2}$$

where

$$V'_s = V_s(r) + V_s(2a - r) \tag{3}$$

and

$$V'_t = V_t(r) + V_t(2a - r).$$

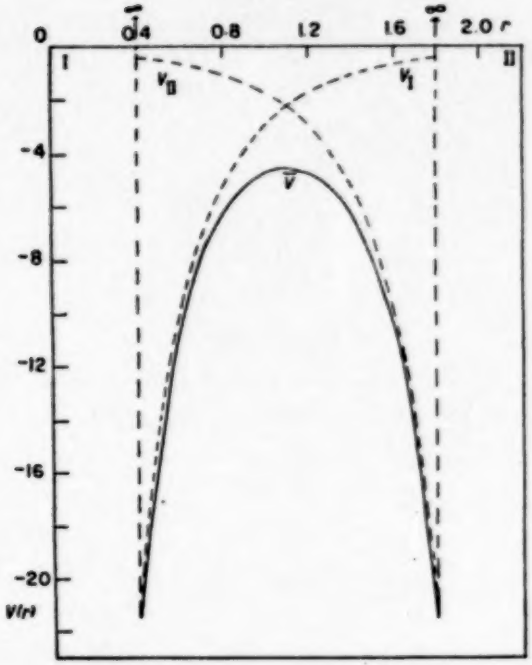


Fig. 1. Potential $\bar{V}$ in units of 20.73 MeV in two neighbouring Wigner-Seitz spheres, each of radius $1.10 \times 10^{-13}$ cm; $V_I$ and $V_{II}$ are separately the average of singlet and triplet even parity Gammel-Thaler potentials.

Here $a$ is the radius of the Wigner-Seitz sphere (not to be confused with the nuclear radius constant) and is related to the internucleonic separation by the requirement that the volume of the sphere be the "effective nucleon volume"

$$\tfrac{4}{3}\pi a^3 = 1/\rho_{eff} = 4/3\rho. \tag{4}$$

In eq. (3), the terms $V_s(2a-r)$ and $V_t(2a-r)$ are assumed to represent the effect of the nucleons which are in the neighbouring Wigner-Seitz spheres. They make only a very small contribution, in keeping with the remark of Gomes *et al.*[3]) that the "healing distance" is much smaller than the average

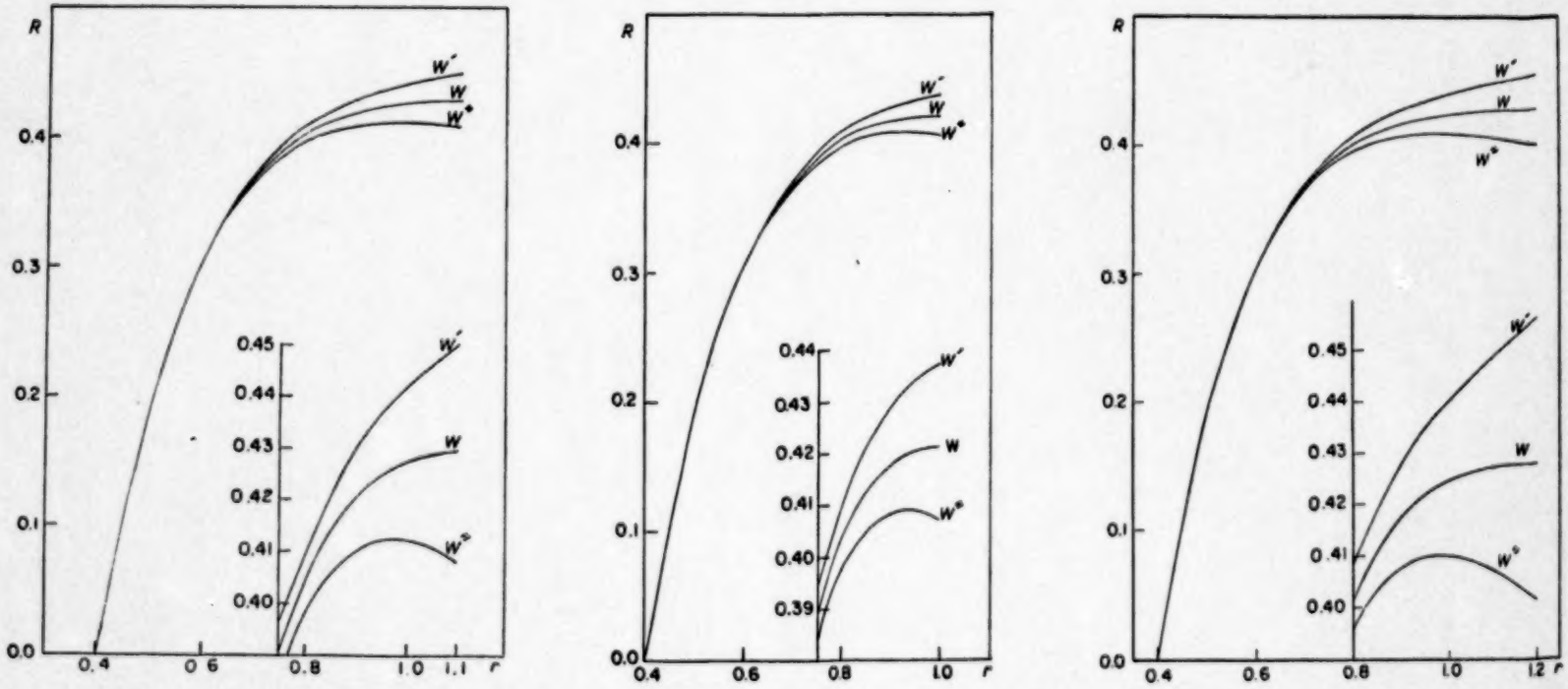


Fig. 2. Sample wave functions for various values of the Wigner-Seitz radius $a$, illustrating the method of choosing the correct energy $W$ by requiring a horizontal tangent at $r = a$. In fig. 2a the correct value of the interaction energy is $W$, corresponding to Wigner-Seitz radius 1.00. In figs. 2b and 2c similar results are shown for radii $a = 1.10$ and 1.20.

spacing between nucleons. The potential $\bar{V}(r, a)$ is plotted in fig. 1 for a value of $a = 1.10$.

The calculation now proceeds as follows. A choice is made for the radius $a$ of the Wigner-Seitz sphere and a whole family of solutions of the Schrödinger equation with the potential of eq. (2) is found by numerical integration, corresponding to various choices of the energy. The requirement of horizontal tangency at $r = a$ then selects the appropriate wave function. In this manner one determines which value $W(a)$ of the energy is appropriate to any particular choice of the Wigner-Seitz radius $a$. This energy is to be regarded in the independent particle model as the interaction energy between one nucleon and the remainder. Since in summing over all nucleons in the system this energy is counted twice, the average interaction energy per nucleon is $\frac{1}{2}W(a)$.

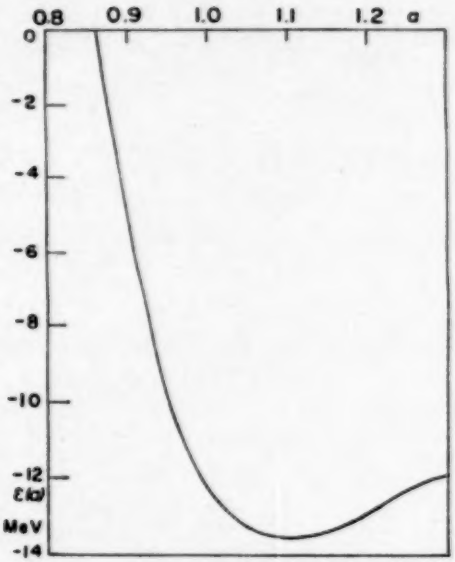


Fig. 3. Total energy per particle as a function of the radius of Wigner-Seitz sphere. The equilibrium value $\varepsilon_0 = -13.6$ MeV corresponds to the minimum of the curve at $a_0 = 1.10$.

The total energy per particle is now obtained by adding the interaction energy per nucleon to the average energy per nucleon in the absence of interaction. Hence, the total energy per nucleon is given by

$$\varepsilon(a) = \tfrac{3}{5}\frac{\hbar^2 k_f^2}{2m} + \tfrac{1}{2}W(a), \tag{5}$$

where the first term on the right is the usual expression for the average energy in a degenerate Fermi distribution. The Fermi momentum is given in terms of $a$ by

$$\hbar k_f = \hbar(\tfrac{3}{2}\pi^2\rho)^{\frac{1}{3}} = (\tfrac{3}{2}\pi)^{\frac{1}{3}}\hbar/a \tag{6}$$

according to eq. (4).

The equilibrium value $\varepsilon_0$ of the total energy per nucleon is obtained by plotting the expression (5) for $\varepsilon(a)$ as a function of Wigner-Seitz radius $a$ and taking the minimum of the curve. The equilibrium density $\rho_0$ is then obtained by substituting the equilibrium value $a = a_0$ into expression (4) for $\rho$.

## 5. Results

Numerical integration of the Schrödinger equation with the potential of eq. (2) was carried out on the University of Alberta electronic digital computer. Three families of wave functions corresponding to values $a = 1.00$, 1.10 and 1.20 of the Wigner-Seitz radius, are shown in figs. 2a, 2b and 2c for illustrative purposes. In each family, the appropriate interaction energy $W(a)$ is determined by selecting that wave function which has a horizontal tangent at the Wigner-Seitz radius.

In fig. 3, the total energy $\varepsilon(a)$ of eq. (5) is plotted against the radius $a$ of the Wigner-Seitz sphere. From the minimum of this curve, we deduce the value $a_0 = 1.10$ for the equilibrium radius and $E_b = 13.6$ MeV for the equilibrium energy per nucleon. According to eq. (4) the equilibrium radius corresponds to an equilibrium value of the nuclear density $\rho_0 = 2.39 \times 10^{38}$ particles/cm$^3$, and to an internucleonic separation of $d_0 = \rho_0^{-\frac{1}{3}} = 1.61$. These values are compared to the experimental values in table 1. It is seen

TABLE 1
Nuclear Matter Data

| | Present work | Experimental values |
|---|---|---|
| Nuclear density in particles/cm$^3$ | $2.39 \times 10^{38}$ | $\approx 2.17 \times 10^{38}$ |
| Average nucleon spacing in $10^{-13}$ cm | 1.61 | $\approx$ 1.66 |
| Average binding energy per particle in MeV | 13.6 | $\approx$ 15 |

that the agreement is excellent. One can also calculate the compressibility coefficient

$$K = a^2\left(\frac{\partial^2 E_b}{\partial a^2}\right)\Bigg]_{a=a_0}$$

from fig. 3. The value obtained in this way is 128 MeV, which is closer to the experimental value obtained from isotope shifts [10]) † than that calculated by Brueckner and Gammel [1]).

The agreement between the present values and experiment appears to be at least as good as has been obtained by other methods. This agreement may

† *Editor's Note:* On this point, see, however, a forthcoming paper by A. R. Bodmer, to be published in this journal.

be in some part fortuitous, but we believe that the method has some substantial basis in fact, namely, that nuclear matter in its degenerate bulk form exhibits a characteristic regularity. The question naturally arises as to precisely what this regularity is and whether it can be detected in some more direct way. These are points which require further study.

The sensitivity of the Wigner-Seitz method to choice of two-body potential is of interest and is under study at the present time. Also under study is the question of two-body correlations and the effects of spin-orbit and tensor forces.

We are indebted to Miss Ursula Bielenstein for carrying out the numerical computations. We are also indebted to the University of Alberta Research Committee, and to the National Research Council of Canada for general financial assistance and for a postdoctorate fellowship for one of us (PCS).

## References

1) K. A. Brueckner and J. L. Gammel, Phys. Rev. **109** (1958) 1023
2) H. A. Bethe, Phys. Rev. **103** (1956) 1353
3) L. C. Gomes, J. D. Walecka and V. F. Weisskopf, Ann. of Phys. **3** (1958) 241
4) N. M. Hugenholtz and L. Van Hove, Physica **24** (1958) 363
5) E. Wigner and F. Seitz, Phys. Rev. **43** (1933) 804; **46** (1934) 509
6) J. Gammel and R. M. Thaler, Phys. Rev. **107** (1957) 291; **107** (1957) 1337
7) V. F. Weisskopf, Proc. Am. Acad. Arts Sci. **82** (1953) 360
8) L. E. H. Trainor and W. R. Dixon, Can. J. Phys. **34** (1956) 229
9) V. F. Weisskopf, Nuclear Physics **3** (1957) 423
10) K. W. Ford and D. L. Hill, Annual Review of Nuclear Science (Annual Reviews Inc., Stanford, 1955) p. 46;
L. Wilets, D. L. Hill and K. W. Ford, Phys. Rev. **91** (1953) 1488

4.D *Nuclear Physics* 9 (1958/59) 296—305; © *North-Holland Publishing Co., Amsterdam*
Not to be reproduced by photoprint or microfilm without written permission from the publisher

# BRANCHING RATIOS OF ELECTRON CAPTURE TO POSITON EMISSION

J. KONIJN, B. VAN NOOIJEN, H. L. HAGEDOORN and A. H. WAPSTRA
*Laboratorium voor Technische Physica der Technische Hogeschool, Delft*

Received 30 August 1958

**Abstract:** Ratios of electron capture to positon emission have been measured by coincidence measurements with proportional counters, scintillation spectrometers and a beta ray spectrometer. Results for allowed transitions ($^{22}$Na, $^{44}$Sc, $^{48}$V, $^{52}$Mn, $^{58}$Co and $^{57}$Ni) agree well with theoretical values as derived from Zweifel's work, and indicate a value of $-(0.007 \pm 0.010)$ for the Fierz term parameter. Results for $2^- \rightarrow 2^+$ first forbidden transitions are about 20 % to 60 % higher than values derived from Zweifel's tables for allowed transitions.

## 1. Introduction

The uncertainties in the experimental values of branching ratios of electron capture to positon emission are mostly of the order of 10 % or larger. Exceptions are the measurements by Sherr and Miller [1]), Drever *et al.*[2]) and Scobie and Lewis [3]) on $^{22}$Na, $^{18}$F and $^{11}$C respectively. These measurements show excellent agreement with theory, when it is assumed that no Fierz term is present. In this paper precise measurements have been extended to cover other nuclei. Comparison of the experimentally obtained material with theory sets limits to the Fierz term.

According to Brysk and Rose [4]) branching ratios of electron capture to positon emission in non-unique first forbidden transitions should not differ much from those in allowed transitions. Below, a description is given of some measurements designed to test this assumption.

## 2. Some Theoretical Remarks

The theory of beta radio-activity based on the use of a linear combination of all five relativistic invariants, has been developed by several authors [5, 6, 7]) and recently been extended by Lee and Yang [8]) in order to include the effects of non-conservation of parity. The formula for the ratio of K capture to positon emission for allowed transitions is found to be

$$\varepsilon_K/\beta^+ = (\varepsilon_K/\beta^+)_0 \times \frac{(1+2bW_K^{-1})}{(1-2b\overline{W^{-1}})}; \qquad (1)$$

$(\varepsilon_K/\beta^+)_0$ depends on the nuclear charge $Z$ of the daughter nucleus and on the maximum positon energy release $W_0$ (in units of $m_0c^2$ including rest mass). $W_K$ is the K shell binding energy including the rest mass; $\overline{W^{-1}}$ is the average value of $W^{-1}$ over the continuous beta spectrum. Evidently the ratio $\varepsilon_K/\beta^+$ is very sensitive to the actual value of the Fierz term parameter $b$.

Values of $(\varepsilon_K/\beta^+)_0$ have been calculated by Zweifel [9]) for certain values of $Z$. The function $(\varepsilon_K/\beta^+)_0\ (W_0-1)^4 Z^{-4}(W_0+1)^{-2}$ shows much less variation in terms of $Z$ and $W_0$ than $(\varepsilon_K/\beta^+)_0$. Therefore, this combination is given as a function of $Z$ in fig. 1. This figure can be used to obtain accurate interpolated values of $(\varepsilon_K/\beta^+)_0$. A rapid estimate of $(\varepsilon_K/\beta^+)_0$ can be obtained from fig. 2, which has been constructed using the interpolation method explained above

The Fierz term parameter $b$ can be derived from experimental values for $\varepsilon_K/\beta^+$ by the following relation which can easily be derived from formula (1):

$$b = \tfrac{1}{2}\frac{\varepsilon_K/\beta^+ - (\varepsilon_K/\beta^+)_0}{(\varepsilon_K/\beta^+)_0 + (\varepsilon_K/\beta^+)\overline{W^{-1}}}. \tag{2}$$

The result of such measurements, described in § 3, showed the Fierz term parameter to be very small.

If parity were conserved in beta decay, the emitted electron would not be longitudinally polarized. Wu *et al.*[10]) discovered, however, that parity is not conserved in beta transitions, and slightly later Frauenfelder *et al.*[11]) observed the longitudinal electron polarization; many other laboratories have later confirmed this result.

The general expression for the beta ray polarization is

$$P_{\beta^\pm} = \mp\frac{v}{c}\frac{\{|C_S^L|^2-|C_S^R|^2-|C_V^L|^2+|C_V^R|^2\}|M_F|^2+\{|C_T^L|^2-|C_T^R|^2-|C_A^L|^2+|C_A^R|^2\}|M_{GT}|^2}{\{|C_S^L|^2+|C_S^R|^2+|C_V^L|^2+|C_V^R|^2\}|M_F|^2+\{|C_T^L|^2+|C_T^R|^2+|C_A^L|^2+|C_A^R|^2\}|M_{GT}|^2}, \tag{3}$$

in which $M_F$ and $M_{GT}$ are the nuclear matrix elements involved in Fermi and Gamow-Teller coupling respectively, the parameters $C_x^y$ (x = S, V, T, A, and y = R, L) being a measure of the relative strength of the forms of the different interactions in which right- and left-handed neutrinos are emitted. The electron polarizations measured so far are almost equal to $\pm v/c$ with an accuracy of about 10 %. Thus, negatons are polarized left-handedly, positons right-handedly. This experimental result is in agreement with the following combination:

$$C_S^L = C_T^L = C_V^R = C_A^R = 0. \tag{4}$$

For the sake of completeness it should be mentioned that the recent experiments by Goldhaber *et al.*[12]) indicate that $C_V^L \approx -C_A^L$, and that all other coefficients are zero.

The Fierz term parameter $b$ has the following form:

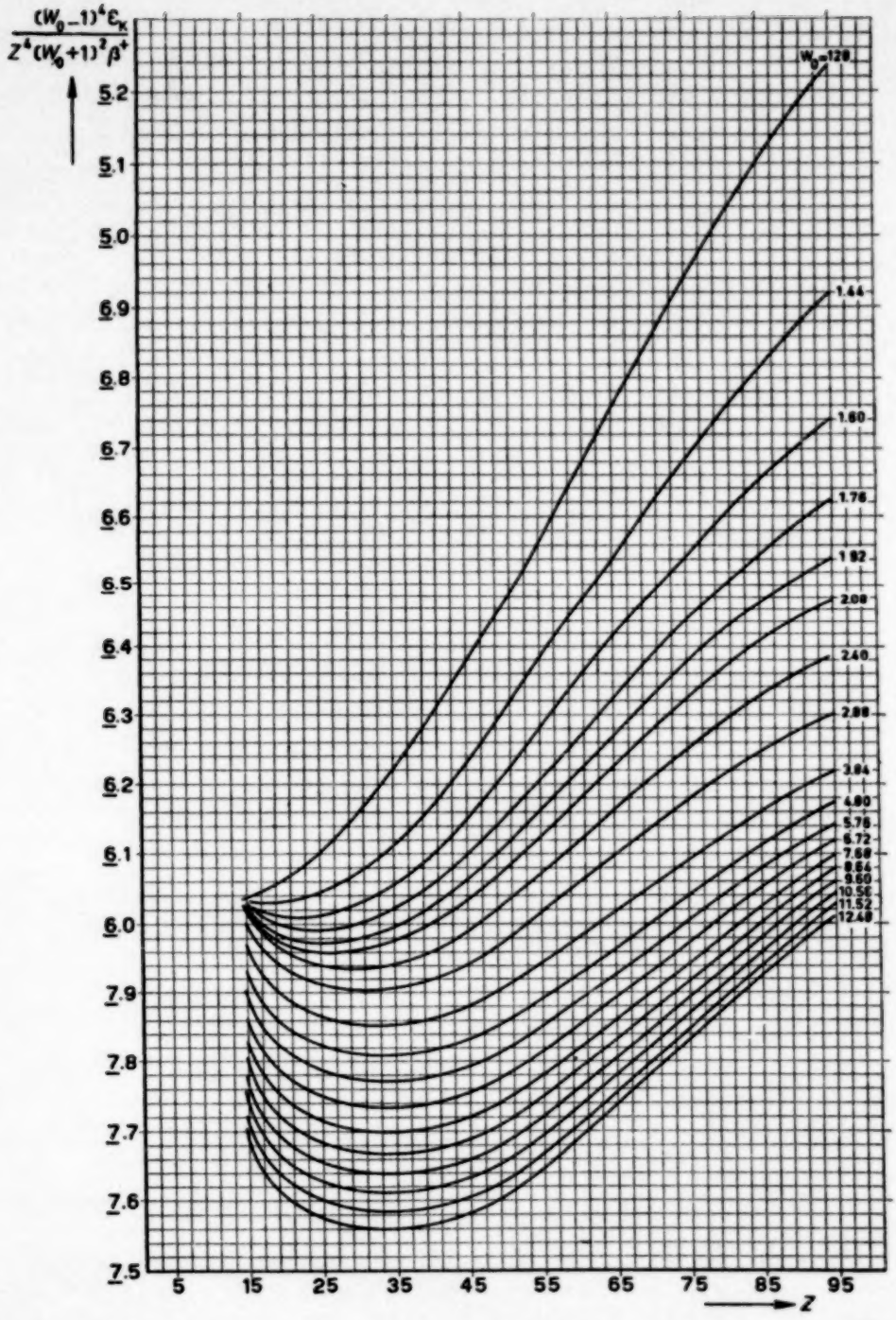


**Fig. 1.** $\{(\varepsilon_K/\beta^+)_0(W_0-1)^4 Z^{-4}(W_0+1)^{-2}\}$ as a function of $Z$ (i.e. the charge of the radio-active daughter nucleus) for the indicated values of $W_0$. The scale of the vertical axis is logarithmic; 6.4 means 0.4—6.

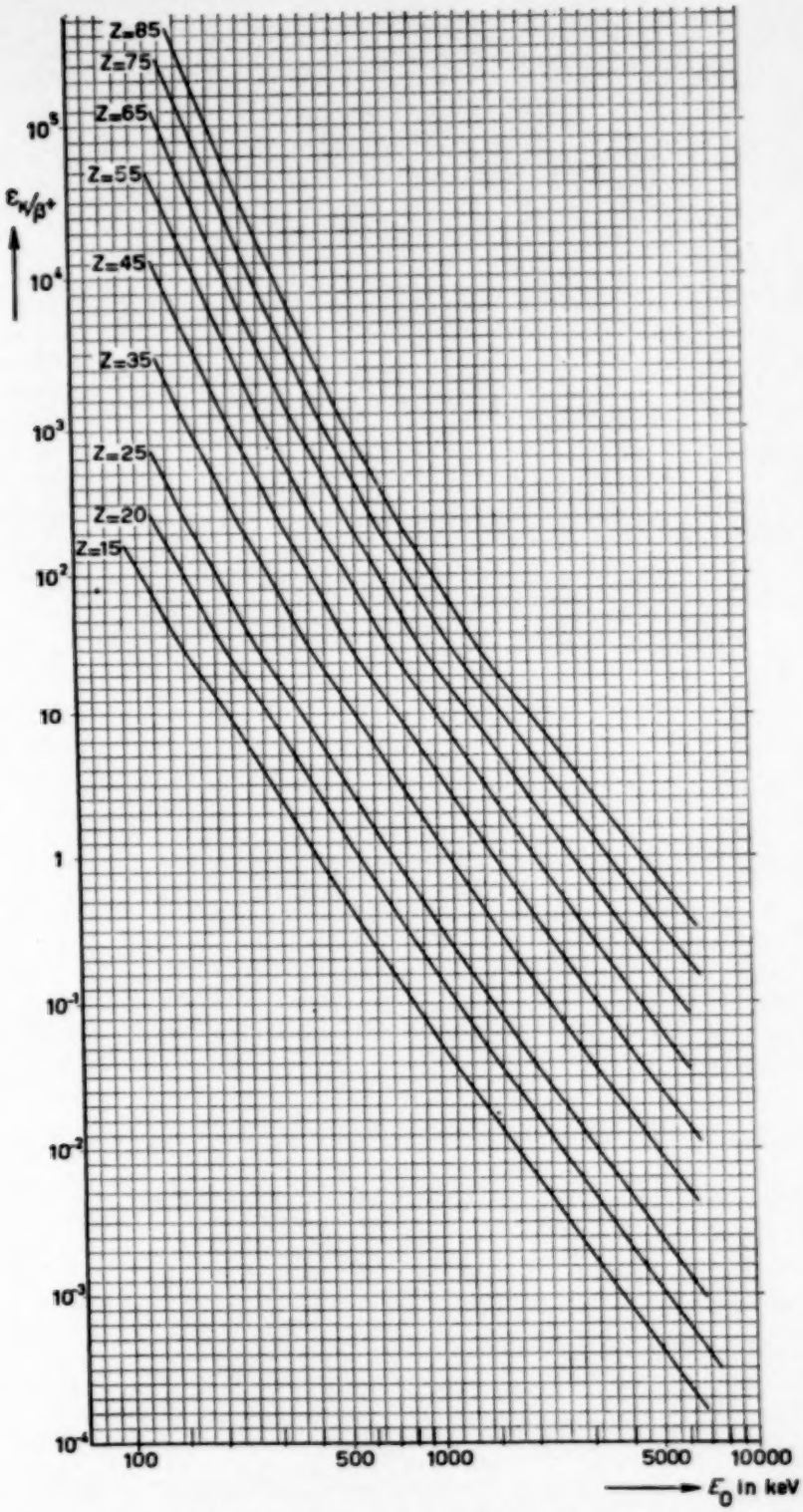


Fig. 2. The $(\varepsilon_K/\beta^+)_\theta$ branching ratios as functions of $W_\theta$, with $Z$ (charge of daughter nucleus) as a parameter. These values are obtained from the plots in fig. 1.

$$b = \gamma \frac{\mathrm{Re}\,\{C_S^{R*} C_V^{R} + C_S^{L*} C_V^{L}\}|M_F|^2 + \mathrm{Re}\,\{C_T^{R*} C_A^{R} + C_T^{L*} C_A^{L}\}|M_{GT}|^2}{\{|C_S^{R}|^2 + |C_S^{L}|^2 + |C_V^{R}|^2 + |C_V^{L}|^2\}|M_F|^2 + \{|C_T^{R}|^2 + |C_T^{L}|^2 + |C_A^{R}|^2 + |C_A^{L}|^2\}|M_{GT}|^2} \quad (5)$$

in which $\gamma = \sqrt{1-(\alpha Z)^2} \approx 1$, $\alpha$ being the fine structure constant.

In fact, the modification (4) automatically cancels any Fierz interference terms, no matter what values $C_S, C_V, C_T, C_A$ are found to have. The accuracy of the polarization experiments, however, still allows considerable errors in the determination of the Fierz term, so that one can only conclude that $b = 0.0 \pm 0.2$. Measurements of the shape of allowed and unique forbidden spectra show that $|b|$ is smaller than 0.15 [13]), and an analysis of reduced half-lives of Fermi transitions give a similar limit [14]).

In principle, the Fierz term parameter for tensor and axial interaction can also be determined by measuring K capture to positon emission ratios in unique first forbidden transitions. A measurement on $^{126}$I (see § 3) again yields a parameter $b$ which is approximately equal to zero. Assuming $|b| = 0$ the electron capture to positon emission ratio for unique first forbidden transitions ($|\Delta \mathbf{J}| = 2$, yes) is

$$\varepsilon_K/\beta^+ = (\varepsilon_K/\beta^+)_0 \times [q_K^2/\overline{(p^2+q^2)}] \approx (\varepsilon_K/\beta^+)_0 \times \frac{2(W_0+1)}{W_0-1}. \quad (6)$$

In first forbidden transitions with spin change of one unit ($|\Delta \mathbf{J}| = 1$) this ratio (in the event that only V and A interactions are present, and $C_V^{R} = C_A^{R} = 0$) becomes approximately

$$\frac{\varepsilon_K/\beta^+}{(\varepsilon_K/\beta^+)_0} = \left[\frac{v_{1a}+v_1+a_1}{v_{1a}+v_1-a_1}\right]^2. \quad (7)$$

The quantities $v$ and $a$ are combinations of interaction constants and matrix elements:

$$v_1 = C_V^{L} \int i\mathbf{r}; \quad a_1 = C_A^{L} \int \boldsymbol{\sigma} \times \mathbf{r}; \quad v_{1a} = \xi^{-1} C_A^{L} \int \alpha,$$

in the notation used by Konopinski [6]); $\xi = \alpha\hbar Z/2m_0cR$, where $Z$ and $R$ are the charge and radius of the daughter nucleus and $\alpha$ is the fine structure constant. These quantities $v$ and $a$ have the same order of magnitude. Theoretically, it is to be expected that $v_{1a}$ and $a_1$ are approximately equal [49]). Then the $K/\beta^+$ ratios for first forbidden transitions will be approximately equal to those for allowed transitions. A small deviation from $v_{1a} = a_1$, however, introduces a large variation in the $K/\beta^+$ ratio.

In first forbidden transitions with spin change $|\Delta \mathbf{J}| = 0$, the electron capture to positon emission ratio becomes equal to the allowed ratio using the same approximations as used in eq. (7). A few measurements of these ratios in first forbidden transitions are discussed in § 4.

## 3. Measurements

The electron capture to positon emission ratios have been measured by means of beta-gamma ray coincidence measurements. The gamma rays were recorded in a NaI(Tl) scintillation spectrometer; the beta rays in either a long lens beta ray spectrometer or a proportional counter. For details of the arrangements is referred to refs.[15, 16, 17]).

Both the beta ray spectrometer and the proportional counter have been calibrated by beta-gamma ray coincidence measurements relating to the decay of $^{198}$Au (see refs.[15, 17])). The ratio of true to accidental coincidences was larger than 4 : 1 for the beta ray spectrometer measurements, and at least 20 : 1 in all measurements using the proportional counter.

The following isotopes have been investigated: $^{22}$Na, $^{44}$Sc, $^{48}$V, $^{52}$Mn, $^{58}$Co, $^{57}$Ni and $^{84}$Rb. Carrier-free sources were used, deposited on formvar films rendered conductive by evaporating aluminium onto the backing. All the sources were prepared in the I.K.O. synchrocyclotron in Amsterdam.

The experimental values of electron capture to positon emission ratios $\varepsilon/\beta^+$ have to be compared with theoretical ratios derived from $(K/\beta^+)_0$ ratios (see ref.[9]) and § 2), $L_I/K$ capture ratios [18]) and ratios of capture in higher shells to that in the L shell [19]). The experimental results of our measurements are discussed in detail in ref.[17]) and have been collected in table 1.

## 4. Discussion and Conclusions

The electron capture to positon emission ratios of all measurements of allowed beta transitions are shown in table 1; earlier precise measurements have also been included. The theoretical branching ratios of electron capture to positon emission are derived, as described above, from the curves in fig. 1 and the data mentioned in § 3.

The experimental values for the allowed transitions are all in close agreement with theoretical predictions. Limits to the Fierz term parameter $b$ are obtained by comparing our results with the theoretical ratios, using formula (2). In the last column of table 1 the Fierz term parameter $b$ has been calculated separately for each of our measurements. The mean value found for $b$ is $-0.007 \pm 0.005$. The error in this result does not include a possible systematic error due to the calibration of the coincidence arrangement. Such a systematic error could be caused by the intensity of the back-scattered electrons being different for isotopes with different maximum positon energies; this error is about 0.005. In order to allow for various other small experimental errors which may occur, inaccuracies in the theoretical values obtained by the interpolation procedure, and the approximations used by Zweifel in computing the latter values, the following value for $b$ is

TABLE 1

Electron capture to positon emission ratios for allowed beta transitions

| Nucleus | End point of the positon spectrum | | Experimental results | | | | | Theoretical value $(\varepsilon/\beta^+)_0$ | Fierz term parameter $b$ (this paper) in $^0/_{00}$ |
|---|---|---|---|---|---|---|---|---|---|
| | | | This paper | | Earlier results | | | | |
| | Average value in keV | Ref. | $P_{\beta+}$ in % | $\varepsilon/\beta^+$ | $P_{\beta+}$ in % | $\varepsilon/\beta^+$ | Ref. | | |
| $^{11}C$ | 968 ± 8 | [38]) | — | — | 99.83 ± 0.03 | 0.0020 ± 0.0003 | [3]) | 0.0021 | — |
| $^{18}F$ | 649 ± 9 | [20]) | — | — | 96.9 ± 0.2 | 0.032 ± 0.002 | [2]) | 0.0310 | — |
| $^{22}Na$ | 541 ± 5 | [21]) | † 90.2 ± 0.6 | 0.109 ± 0.008 | 89.0 ± 1.0 | 0.124 ± 0.012 | [23]) | 0.1135 ± 0.002 | — 12 ± 22 |
| | | [22]) | | | 89.1 ± 0.8 | 0.122 ± 0.010 | [24]) | | |
| | | | | | 90.1 ± 0.5 | 0.110 ± 0.006 | [1]) | | |
| $^{44}Sc$ | 1467 ± 3 | [25]) | † 97.8 ± 1.8 | 0.023 ± 0.019 | 93.2 ± 1.5 | 0.073 ± 0.017 | [26]) | 0.049 ± 0.001 | (—220 ± 160) |
| | | [26]) | | | | | | | |
| $^{48}V$ | 695 ± 3 | [15]) | † 56.0 ± 0.6 | 0.74 ± 0.02 | 56 ± 3 | 0.79 ± 0.10 | [15]) | 0.765 ± 0.014 | — 10 ± 10 |
| | | [27]) | †† 55.6 ± 0.8 | 0.75 ± 0.03 | 58 ± 4 | 0.72 ± 0.11 | [30]) | | — 6 ± 13 |
| | | [28]) | | | 57 ± 3 | 0.76 ± 0.09 | [31]) | | |
| | | [29]) | | | 60 ± 4 | 0.67 ± 0.11 | [32]) | | |
| $^{52}Mn$ | 575 ± 4 | [33]) | † 33.8 ± 0.8 | 1.97 ± 0.07 | 35 ± 2 | 1.86 ± 0.17 | [30]) | 2.03 ± 0.06 | — 9 ± 13 |
| | | | †† 33.0 ± 1.0 | 2.03 ± 0.09 | 33 ± 2 | 2.01 ± 0.22 | [34]) | | 0 ± 16 |
| $^{56}Co$ | 472 ± 6 | [35]) | † 14.77 ± 0.30 | 5.67 ± 0.16 | 14.5 ± 0.4 | 5.8 ± 0.2 | [30]) | 5.56 ± 0.26 | + 11 ± 15 |
| | | | | | 14.5 ± 0.4 | 5.8 ± 0.2 | [36]) | | |
| $^{57}Ni$ | 324 ± 16 | [37]) | † 6 ± 2 | 18 ± 6 | — | — | | 24 ± 6.5 | (— 78 ± 110) |
| | 722 ± 6 | [37]) | † 41.0 ± 1.0 | 1.438 ± 0.059 | — | — | | 1.477 ± 0.040 | — 8 ± 15 |
| | 849 ± 6 | [37]) | †, †† 55.4 ± 1.2 | 0.805 ± 0.040 | — | — | | 0.858 ± 0.020 | — 20 ± 17 |

† proportional counter. †† beta spectrometer.

In calculating the mean value of $b$, the values shown in parentheses are not taken into account.

proposed as a result of our experiments:

$$b = -0.007 \pm 0.010.$$

Most transitions investigated in this work occur without spin change. Nevertheless, there are reasons [39]) for believing that even these transitions are due almost entirely to Gamow-Teller interactions (Fermi transitions being forbidden by isobaric spin selection rules). Our results then suggest that

$$\frac{\mathrm{Re}\,(C_T^{R*}C_A^{R}+C_T^{L*}C_A^{L})}{|C_T^{R}|^2+|C_T^{L}|^2+|C_A^{R}|^2+|C_A^{L}|^2} = -0.007 \pm 0.010. \qquad (8)$$

Unique first forbidden transitions have been measured in the case of three isotopes, viz. $^{84}$Rb, $^{122}$Sb and $^{126}$I. The most accurate results of the measurements of these isotopes are shown in table 2. Our measurements yielding a result $1.12 \pm 0.25$ for the $K/\beta^+$ ratio of the ground state transition in $^{84}$Rb are described elsewhere [17]). Other measurements of the $K/\beta^+$ ratio of the unique first forbidden transition in $^{126}$I have been made by Marty *et al.*[40]) and Perlman and Welker [41]) who found $K/\beta^+$ to be $12.5^{+7}_{-3}$ and $21 \pm 8$, respectively. Glaubman [42]) has reported a measurement yielding a $K/\beta^+$ value of $300 \pm 130$ for the transition in $^{122}$Sb.

TABLE 2

K capture to positon emission ratios in unique first forbidden ($2^- \rightarrow 0^+$) transitions

| Nucleus | End point of the positon spectrum | | $K/\beta^+$ experimental values | | Theoretical values of $K/\beta^+$ ratios for | | Fierz term parameter $b$ in ‰ |
|---|---|---|---|---|---|---|---|
| | | | | | Allowed transitions | Unique first forbidden transitions | |
| | $E_0$ in keV | Ref. | | Ref. | $(K/\beta^+)_0$ | $\frac{2(W_0+1)}{W_0-1}(K/\beta^+)_0$ | |
| $^{84}$Rb | $1667 \pm 11$ | [17]) | $1.12 \pm 0.25$ | [17]) | $0.280 \pm 0.008$ | $0.91 \pm 0.02$ | $98 \pm 100$ |
| $^{122}$Sb | $565 \pm 25$ | [44]) | $300 \pm 50$ | [44]) | 49 | $275\ ^{+70}_{-55}$ | $26 \pm 80$ |
| $^{126}$I | $1110 \pm 20$ | [43]) | $20.2 \pm 2.0$ | [43]) | 5.13 | $19.7 \pm 0.8$ | $8 \pm 35$ |

The experiments and theory agree within the uncertainties. The mean value of the Fierz term parameter $b$, derived from these measurements (see the last column of table 2), is

$$b = 0.02 \pm 0.03.$$

On non-unique first forbidden beta transitions little information is available; accurate measurements are available only for $2^- \rightarrow 2^+$ transitions in $^{74}$As, $^{84}$Rb and $^{126}$I. The observed and calculated K capture to positon emission ratios for these non-unique first forbidden transitions are shown in

table 3. Our measurement yields $5.12 \pm 0.11$ for the $K/\beta^+$ ratio of the transition to the first excited level in $^{84}Kr$ (see ref.[17])). Other investigations into the $K/\beta^+$ ratio in $^{126}I$ have been carried out by Marty *et al.*[40]) and Koerts *et al.*[43]), who found this ratio to be larger than 75 and equal to $95 \pm 10$ respectively. The value in table 3, reported by Harmer and Perlman, is a tentative, hitherto unpublished value, which has been chosen in preference to earlier values, because it is the result of a direct measurement.

TABLE 3

K capture to positon emission ratios in non-unique first forbidden ($2^- \rightarrow 2^+$) transitions

| Nucleus | End point of the positon spectrum | | $K/\beta^+$ experimental values | | Theoretical values of $K/\beta^+$ ratios for | | Ratio of the values from column 3 / column 4 |
|---|---|---|---|---|---|---|---|
| | | | | | Allowed transitions | Unique first forbidden transitions | |
| | $E_0$ in keV | Ref. | | Ref. | $(K/\beta^+)_0$ | $\frac{2(W_0+1)}{W_0-1}(K/\beta^+)_0$ | |
| $^{74}As$ | 920 | [45]) | 1.5<br>1.49 | [45])<br>[48]) | 1.16 | 4.9 | 1.3 |
| $^{84}Rb$ | $787 \pm 12$ | [17]) | $5.12 \pm 0.11$<br>$5.1 \pm 0.4$ | [17])<br>[46]) | $3.23 \pm 0.21$ | $14.8 \pm 2.4$ | $1.58 \pm 0.11$ |
| $^{126}I$ | $460 \pm 15$ | [43]) | 148 | [47]) | $125 \pm 7$ | $810^{+500}_{-260}$ | $1.2 \pm 0.2$ |

The experimental values for $2^- \rightarrow 2^+$ non-unique first forbidden transitions are 20 % to 60 % higher than the theoretical values for allowed transitions (see § 2). Perlman *et al.*[44]) try to explain these differences by assuming that in the part of the transitions in which the spin change $|\Delta \mathbf{J}|$ is 0 or 1, the $K/\beta^+$ ratio is nearly equal to that for allowed transitions, but that, in all three cases in question, an appreciable part occurs with a spin change $|\Delta \mathbf{J}| = 2$. This explanation seems to demand somewhat higher intensities for the ($|\Delta \mathbf{J}| = 2$)-part in these transitions than is compatible with the known reduced half-lives of unique first forbidden ($\Delta|\mathbf{J}| = 2$) transitions. The above results therefore tend to indicate that in non-unique first forbidden transitions small deviations from $v_{1a} = a_1$ occur (see § 2).

*Note added in proof:* The above explanation can only be true if, as assumed in eq. (7) for V-A interactions and as stated explicitly e.g. by Brysk and Rose [4]) for S-T interactions, the signs of the V-A (S-T) cross terms in the transition probability for electron capture are different from those in positon emission. According to Perlman *et al.*[44]), this is, however, not true; their opinion is shared by Bincer [50]). Then, if indeed the admixture of transitions with $|\Delta \mathbf{J}| = 2$ is small, deviations of the ratios of electron capture to positon emission in non-unique first forbidden transitions from the allowed values should be explained by the fact that the coefficients of the matrix elements in the numerator and the denominator of eq. (7) are somewhat different [44]).

We thank Dr. Perlman for an enlightening discussion upon this subject.

## References


1) R. Sherr and R. H. Miller, Phys. Rev. **93** (1954) 1076
2) R. W. P. Drever, A. Moljk and J. Scobie, Phil. Mag. **1** (1956) 942
3) J. Scobie and G. M. Lewis, Phil. Mag. **2** (1957) 1089
4) H. Brysk and M. E. Rose, ORNL 1830 report, Oak Ridge National Laboratory
5) E. J. Konopinski and G. E. Uhlenbeck, Phys. Rev. **60** (1941) 368
6) E. Greuling, Phys. Rev. **61** (1942) 568
7) H. A. Tolhoek and S. R. de Groot, Physica **16** (1950) 456
8) T. D. Lee and C. N. Yang, Phys. Rev. **104** (1956) 254
9) P. F. Zweifel, Phys. Rev. **107** (1957) 329
10) C. S. Wu, E. Ambler, R. Hayward, D. Hoppes and R. Hudson, Phys. Rev. **105** (1957) 1413
11) H. Frauenfelder, R. Bobone, E. Van Goeler, N. Levine, H. R. Lewis, R. N. Peacock, A. Rossi and G. De Pasquali, Phys. Rev. **106** (1957) 386
12) M. Goldhaber, L. Grodzins and A. W. Sunyar, Phys. Rev. **109** (1958) 1015
13) H. M. Mahmoud and E. J. Konopinski, Phys. Rev. **88** (1952) 1266
14) R. Sherr and J. B. Gerhart, Bull. Am. Phys. Soc. **1** (1956) 219
15) B. van Nooijen, J. Konijn, A. Heyligers, J. F. van der Brugge and A. H. Wapstra, Physica **23** (1957) 753
16) H. L. Hagedoorn and J. Konijn, Physica **23** (1957) 1069
17) J. Konijn, Thesis 1958, Technical University of Delft
18) M. E. Rose and J. L. Jackson, Phys. Rev. **76** (1949) 1540
19) A. H. Wapstra, G. J. Nijgh and R. van Lieshout, Nuclear spectroscopy tables (North Holland Publ. Co., Amsterdam, 1959)
20) L. Ruby and J. R. Richardson, Phys. Rev. **83** (1951) 698
21) P. A. Macklin, L. J. Lidofsky and C. S. Wu, Phys. Rev. **78** (1950) 318, C5
22) B. T. Wright, Phys. Rev. **90** (1953) 159
23) W. E. Kreger, Phys. Rev. **96** (1954) 1554
24) R. A. Allen, W. E. Burcham, K. F. Chackett, G. L. Munday and P. Reasbeck, Proc. Phys. Soc. A **68** (1955) 681
25) J. A. Bruner and L. M. Langer, Phys. Rev. **79** (1950) 606
26) J. W. Blue and E. Bleuler, Phys. Rev. **100** (1955) 1324
27) P. L. Roggenkamp, C. H. Pruett and R. G. Wilkinson, Phys. Rev. **88** (1952) 1262
28) L. Marquez, Phys. Rev. **92** (1953) 1511
29) L. E. Killion, Thesis 1955, Washington University
30) W. M. Good, D. Peaslee and M. Deutsch, Phys. Rev. **69** (1946) 313
31) R. Bock, Max Planck Inst. Heidelberg, private communication quoted in Nuclear Level Schemes (Washington, U. S. Atomic Energy Commission June 1955)
32) M. J. Sterk, A. H. Wapstra and R. E. W. Kropveld, Physica **19** (1953) 135
33) J. Konijn, B. van Nooijen and H. L. Hagedoorn, Physica **24** (1958) 377
34) R. Sehr, Z. Phys. **137** (1954) 523
35) L. S. Cheng, J. L. Dick and J. D. Kurbatov, Phys. Rev. **88** (1952) 887
36) C. S. Cook and F. M. Tomnovec, Phys. Rev. **104** (1956) 1407
37) J. Konijn, H. L. Hagedoorn and B. van Nooijen, Physica **24** (1958) 129
38) C. Wong, Phys. Rev. **95** (1954) 765
39) F. Boehm and A. H. Wapstra, Phys. Rev. **109** (1958) 456
40) N. Marty, H. Langevin and M. P. Hubert, J. Phys. Rad. **14** (1953) 663
41) M. L. Perlman and J. P. Welker, Phys. Rev. **95** (1954) 133
42) M. J. Glaubman, Phys. Rev. **98** (1955) 645
43) L. Koerts, P. Macklin, B. Farrelly, R. van Lieshout and C. S. Wu, Phys. Rev. **98** (1955) 1230
44) M. L. Perlman, J. P. Welker and M. Wolfsberg, Phys. Rev. **110** (1958) 381
45) S. Johansson, Y. Cauchois and K. Siegbahn, Phys. Rev. **82** (1951) 275
46) J. P. Welker and M. L. Perlman, Phys. Rev. **100** (1955) 74
47) D. S. Harmer and M. L. Perlman, see ref. [44])
48) J. Scobie, Nuclear Physics **3** (1957) 465
49) R. W. King and D. C. Peaslee, Phys. Rev. **94** (1954) 1284
50) A. M. Bincer, Phys. Rev., to be published

1.C *Nuclear Physics* 9 (1958/59) 306—313; © *North-Holland Publishing Co., Amsterdam*
Not to be reproduced by photoprint or microfilm without written permission from the publisher

# ON A THEOREM CONCERNING THE SINGLE PARTICLE ENERGY OF A FERMI GAS WITH INTERACTIONS

C. VILLI

*Istituto di Fisica dell'Università di Trieste*

and

*Istituto Nazionale di Fisica Nucleare, Sottosezione di Trieste*

Received 24 September 1958

**Abstract:** It is shown that the Hugenholtz and Van Hove theorem is a consequence of another theorem, which involves the existence of a hyperbolic partial differential equation, obeyed by the potential energy of a nucleon in an infinite sea of nuclear matter. The fundamental role played by this nuclear equation in describing the nucleus as a Fermi gas with interactions is discussed.

Recently Hugenholtz and Van Hove [1]) have proved a remarkable theorem concerning the single particle energy of a Fermi gas with interactions, which might provide a test for the internal consistency of the Brueckner theory on the structure of nuclear matter. The theorem states that *at the density minimizing the total energy of the nucleus, the average volume energy per nucleon is equal to the total energy of the most energetic nucleon.*

The aim of this note is to outline a different approach for the derivation of this theorem, and to examine the physical content of its foundations.

In a system of units where $\hbar = c = 1$, let $k$ be the nucleon momentum and $\kappa = (9\pi/8)^{\frac{1}{3}} r_0^{-1}$ the limiting Fermi momentum for a standard nucleus of radius $R = r_0 A^{\frac{1}{3}}$ and volume $\Omega(\kappa) = (3\pi^2/2\kappa^3)A$. Then, calling $\mathscr{E}(k, \kappa)$ the total energy of a nucleon of momentum $k \leqq \kappa$ in the interior of a nucleus whose average total energy $\langle W(\kappa) \rangle$ possesses a minimum at a certain value $k_F$ of the limiting Fermi momentum $\kappa$, the above theorem is simply expressed by the following equality

$$B_v = \frac{\langle W(k_F) \rangle}{A} = \mathscr{E}(k_F, k_F), \tag{1}$$

where, neglecting surface, Coulomb, symmetry and pairing effects, $\langle W(k_F) \rangle$ has been identified with the bulk of the nuclear binding, i.e., with the whole volume energy $B_v A$.

Eq. (1), which has been already discussed by Bethe [2]), Weisskopf [3]) and the writer [4]), is valid provided the potential energy $\mathscr{V}(k, \kappa)$ of a nucleon having momentum $k \leqq \kappa$, inside a nucleus of density $\rho(\kappa) = A/\Omega(\kappa)$,

satisfies certain restrictive conditions to be determined by evaluating the minimum of $\langle W(\kappa)\rangle$ and by taking into account some other peculiar features of the nuclear matter. It is, in fact, easy to show that the condition necessary for the minimum of $\langle W(\kappa)\rangle$ to occur at the density $\rho(k_F)$ is not sufficient for the validity of eq. (1). This condition physically means that there exists a value $k_F$ of the limiting momentum $\kappa$, at which the pressure $P(\kappa)$ is zero, namely

$$P(k_F) = \frac{2k_F^2}{3\pi^2}\left[\frac{\mathrm{d}\langle W(\kappa)\rangle}{\mathrm{d}\kappa}\right]_{\kappa=k_F} = 0. \tag{2}$$

Using the explicit expression for the average total energy of the nucleus

$$\langle W(\kappa)\rangle = \frac{3A}{\kappa^3}\int_0^\kappa [(k^2/2M)+\tfrac{1}{2}\mathscr{V}(k,\kappa)]k^2\mathrm{d}k, \tag{3}$$

eq. (2) yields

$$P(k_F) = \frac{2k_F^2}{3\pi^2}\left[\frac{\langle W(k_F)\rangle}{A} - \mathscr{E}(k_F, k_F) + \frac{Q(k_F)}{2k_F^2}\right] = 0, \tag{4}$$

where the total energy of the nucleon having momentum $k$ has been defined as

$$\mathscr{E}(k,\kappa) = (k^2/2M)+\mathscr{V}(k,\kappa), \tag{5}$$

and $Q(k_F)$ is given by

$$Q(k_F) = k_F^2\mathscr{V}(k_F, k_F) - \int_0^{\kappa_F} k^2\left[\frac{\partial\mathscr{V}(k,\kappa)}{\partial\kappa}\right]_{\kappa=k_F}\mathrm{d}k. \tag{6}$$

From eq. (4) it follows that

$$\frac{\langle W(k_F)\rangle}{A} = \mathscr{E}(k_F, k_F) - \frac{Q(k_F)}{2k_F^2}. \tag{7}$$

This result shows that the validity of eq. (1) is not insured by the equilibrium prescription, expressed in eq. (2), but requires the additional restrictive condition

$$Q(k_F) = 0. \tag{8}$$

Does eq. (8) express some general feature of the nuclear matter? The problem of discovering the physical meaning and the theoretical background which stands behind eq. (8) is essential for a deeper insight into the Hugenholtz and Van Hove theorem.

With this aim in view, it is important to note that, at the limit of zero nuclear density, the nucleon potential energy $\mathscr{V}(k,\kappa)$, which can be thought of as constructed in terms of two-body forces, according to some procedure which we do not need to specify, must also tend to zero, *independently* of the state of motion of the nucleon: i.e., one must have $\mathscr{V}(k, 0) = 0$. This condition follows from the fact that for $\kappa = 0$ the average distance [5])

$\langle d(\kappa)\rangle \simeq (\frac{5}{3})^{\frac{1}{3}}\kappa^{-1}$ between the nearest neighbors of the $A$ particles, uniformly distributed in the interior of the nuclear sphere, tends to infinity and consequently the nucleon-nucleon interaction vanishes. Of course, the preceding condition holds also for $k = 0$:

$$\mathscr{V}(0, 0) = 0. \tag{9}$$

It is fairly easy to realize that condition (9), which is so obvious as to appear trivial on physical grounds, must be included in the general relations which led us to eq. (7), because otherwise the function $\mathscr{V}(k, \kappa)$, used in eq. (3), would have no physical meaning. Since no alternative comes into play, one is inescapably led to suspect that the physically intuitive condition (9) must in some way be related to the awkward mathematical condition (8), and that the validity of the former should imply that of the latter. We shall now prove that this is indeed true by virtue of the following theorem: *if the potential energy of a nucleon in an infinite sea of nuclear matter obeys the hyperbolic partial differential equation*

$$\left(\frac{\partial^2}{\partial k^2}+\frac{2}{k}\frac{\partial}{\partial k}-\frac{\partial^2}{\partial \kappa^2}+\frac{2}{\kappa}\frac{\partial}{\partial \kappa}\right)\mathscr{V}(k, \kappa) = 0, \tag{10}$$

*then the necessary and sufficient condition in order that* $\mathscr{V}(0, 0) = 0$ *is*

$$Q(\kappa) = 0, \tag{11}$$

*where*

$$Q(\kappa) = \kappa^2\mathscr{V}(\kappa, \kappa)-\int_0^\kappa k^2\frac{\partial\mathscr{V}(k, \kappa)}{\partial \kappa}\,dk. \tag{12}$$

The proof of this theorem is straightforward. Let us consider the function $\kappa^{-2}Q(\kappa)$ and evaluate its derivative with respect to $\kappa$. Taking into account that for $k = \kappa$ the following relation holds among the derivatives of $\mathscr{V}(k, \kappa)$:

$$\frac{d\mathscr{V}(\kappa, \kappa)}{d\kappa} = \left[\left(\frac{\partial}{\partial k}+\frac{\partial}{\partial \kappa}\right)\mathscr{V}(k, \kappa)\right]_{k=\kappa}, \tag{13}$$

one obtains

$$\frac{d}{d\kappa}\left[\frac{Q(\kappa)}{\kappa^2}\right] = \left[\frac{\partial\mathscr{V}(k, \kappa)}{\partial k}\right]_{k=\kappa}-\int_0^\kappa\frac{\partial}{\partial \kappa}\left[\left(\frac{k}{\kappa}\right)^2\frac{\partial\mathscr{V}(k, \kappa)}{\partial \kappa}\right]dk. \tag{14}$$

Assuming that $\mathscr{V}(k, \kappa)$ is a solution of eq. (10), which may be written in the more convenient form

$$\frac{\partial}{\partial k}\left[\left(\frac{k}{\kappa}\right)^2\frac{\partial\mathscr{V}(k, \kappa)}{\partial k}\right] = \frac{\partial}{\partial \kappa}\left[\left(\frac{k}{\kappa}\right)^2\frac{\partial\mathscr{V}(k, \kappa)}{\partial \kappa}\right], \tag{15}$$

eq. (14) yields

$$\frac{d}{d\kappa}\left[\frac{Q(\kappa)}{\kappa^2}\right] = \left[\left(\frac{k}{\kappa}\right)^2\frac{\partial\mathscr{V}(k, \kappa)}{\partial k}\right]_{k=0} = 0 \tag{16}$$

because the invariance prescription of the potential under time reflection implies that for small momenta $\partial\mathscr{V}(k, \kappa)/\partial k$ varies linearly with $k$. Finally, from eq. (16) one gets $Q(\kappa) = C\kappa^2$, where $C$ is an arbitrary integration constant. Inserting this relation into eq. (12), where $k$ has been replaced by $\kappa x$, one has

$$\mathscr{V}(\kappa, \kappa) - \kappa \int_0^1 x^2 \frac{\partial \mathscr{V}(\kappa x, \kappa)}{\partial \kappa} \, dx = C, \tag{17}$$

which at the limit $\kappa = 0$ evidently reduces to $\mathscr{V}(0, 0) = C$. Then, eq. (11) is proved to be true because condition (9) is satisfied provided $C = 0$. Eq. (8) is therefore nothing but a special case of the more general condition $Q(\kappa) = 0$ valid at *any* nuclear density and not only at the density $\rho(k_F)$ minimizing the average total energy of the nucleus. Thus, the Hugenholtz and Van Hove theorem, stated in eq. (1), appears to be related to eq. (10), and its validity for a system in equilibrium $[P(k_F) = 0]$ follows from the obvious condition that the potential energy of a nucleon of zero momentum is zero at zero nuclear density $[Q(k_F) = 0]$.

Before going further with the discussion of this theorem, it is worth while to concentrate on eq. (10) and see what it really means. If this equation is not purely accidental and has something to do with the structure of the nuclear matter, one should expect that, among the variety of descriptions potentially contained in it, and each one corresponding to definite boundary conditions imposed on the surface $z = \mathscr{V}(k, \kappa)$, there should also be those obtained by constructing $\mathscr{V}(k, \kappa)$ on the basis of suitable physical assumptions and mathematical approximations. It is indeed gratifying that such an expectation is substantiated by the fact that all theories, treating the nucleus as a Fermi gas with interactions, lead to functions $\mathscr{V}(k, \kappa)$ which are solutions of eq. (10), underlying different and, to a certain extent, preconceived specifications of the associated Cauchy problem. For this reason, although the nuclear equation (10) is apparently only sufficient as far as the proof of eq. (11) is concerned, it may be assumed as the basic equation for treating the nucleus as a many-body system of strongly interacting Fermi particles. A simple example will clear up these remarkable circumstances.

Let us represent the ground state of the nucleus by a totally antisymmetrized wave function $\Phi$, built up in determinantal from from the $A$ individual functions $\Psi_r = \psi_j \omega_\mu$ for single particles, and assume that the nucleons, described by space, spin and isobaric spin coordinates, interact via two-body forces through the potential $v(1, 2) = \mathcal{O}_{12} f(r_{12})$, whose exchange properties and radial behaviour will be left completely unspecified. Then, if the nuclear interaction is treated as a perturbation and the $\frac{1}{4}A$ spatial wave functions $\psi_j(m) = \Omega^{-\frac{1}{2}}(\kappa) \exp[i\mathbf{k}_j \cdot \mathbf{r}_m]$ are associated in turn with all four spin and isobaric spin wave functions $\omega_\mu$, the expectation value of the potential

energy of the nucleus reads

$$\langle V(\kappa)\rangle = \tfrac{1}{2}\sum_{j=1}^{A} \mathscr{V}(k_j, \kappa), \tag{18}$$

where

$$\mathscr{V}(k_j, \kappa) = \sum_{i=1}^{\frac{1}{2}(A-1)} [c_1(ij|f|ij) - c_2(ij|f|ji)], \tag{19}$$

$(ij|f|ij)$ and $(ij|f|ji)$ being the ordinary and exchange matrix elements of $f(r_{12})$, and the two constants $c_1$ and $c_2$ being defined as

$$c_1 = \sum_{\mu,\nu=1}^{4} (\mu\nu|\mathscr{O}_{12}|\mu\nu), \quad c_2 = \sum_{\mu,\nu=1}^{4} (\mu\nu|\mathscr{O}_{12}|\nu\mu). \tag{20}$$

Eq. (19) is easily worked out and finally yields ($\mathbf{k}_j \equiv \mathbf{k}$)

$$\mathscr{V}(k, \kappa) = \kappa^3 \int^{\infty} [c'_1 - c'_2(\kappa r_{12})^{-1} j_0(k r_{12}) j_1(\kappa r_{12})] r_{12}^2 f(r_{12}) \mathrm{d}r_{12}, \tag{21}$$

where $c'_1 = 2(A-1)c_1/3\pi^2 A$, $c'_2 = (A-1)c_2/4\pi A$ and $j_1(x)$ are spherical Bessel functions [6]). A different way to evaluate $\mathscr{V}(k, \kappa)$ is based on a very ingenious modification [7]) of the Hartree-Fock theory, namely in replacing the potential $v$ by the $t$-matrix and then expressing $(ij|t|ij)$ and $(ij|t|ji)$ in terms of the nucleon-nucleon scattering amplitudes. In this case, instead of eq. (21), one has for $k \leqq \kappa$

$$\mathscr{V}(k, \kappa) = -\frac{4}{\pi M}\left\{\int_0^{\frac{1}{2}(\kappa-k)} F(k') k'^2 \mathrm{d}k' + \frac{1}{8k}\int_{\frac{1}{2}(\kappa-k)}^{\frac{1}{2}(\kappa+k)} F(k')[\kappa^2 - (2k'-k)^2] k' \mathrm{d}k'\right\},$$

where $F(k')$ is a complicated function of the nucleon momentum, expressed as a sum of the scattering amplitudes, classified according to spin and isobaric spin substates of the two-nucleon system [7,8,9]). Although eqs. (21) and (22) are widely different, they are nevertheless solutions of eq. (10), corresponding to two distinct Cauchy problems. In particular, this is true for eq. (21) irrespective of the values of the two constants $c'_1$ and $c'_2$, and also of the fact that the lower limit of the radial integral is taken equal to the core radius $r_c$, or equal to zero, according as the repulsive core is assumed to characterize, or not, the behaviour at small distances of the two-nucleon potential $v(1, 2)$. In fact, applying to these functions the differential operator

$$\mathscr{D} = \nabla_k^2 - \frac{\partial^2}{\partial\kappa^2} + \frac{2}{\kappa}\frac{\partial}{\partial\kappa}, \tag{23}$$

where $\nabla_k^2$ is the "radial" part of the Laplacian in the $k$-space, no traces remain of any of their special features related to the two-nucleon potential $v(1, 2)$, or to the nucleon-nucleon phase-shifts, contained in $F(k')$, or to the analytical approximations used in their derivation. Since it can be shown [10]) that this result is more general than it may appear from the preceding examp-

les, one is tempted to conclude that the hyperbolic nature of the nuclear equation $\mathscr{D}\mathscr{V}(k, \kappa) = 0$ and its mathematical structure arises entirely from the common background of eqs. (21) and (22), namely from the exclusion principle.

Although at this stage it would be interesting to investigate whether eq. (10) is somewhere hidden within the Hugenholtz and Van Hove formalism, we shall limit ourselves only to a further remark, namely that the above proof of eq. (1) does not involve only eq. (10), but also the additional assumption, contained in eq. (3), that the average kinetic energy of the whole system be given by

$$\langle T(\kappa)\rangle = -\frac{1}{2M}\int \Phi^* \left(\sum_{j=1}^{A} \nabla_j^2\right)\Phi \, \mathrm{d}\mathbf{r} = \tfrac{3}{5} A \left(\frac{\kappa^2}{2M}\right), \tag{24}$$

where $\Phi$ is the wave function for the nucleus ground state, already used in deriving eq. (21). Thus, in spite of the fact that the preceding considerations have shown that eq. (11) is valid whatever the radial dependence of the nucleon-nucleon interaction may be, the problem arises as to whether the physical assumption of non-interacting point nucleons, underlying eq. (24), does not prevent the Hugenholtz and Van Hove theorem from holding when the nuclear collisions are described by means of a potential containing a repulsive core, and the pairwise correlation of the nucleons in nuclear matter is accounted for by a step-function $\mathscr{U}(r_{12}) = 0$ for $r_{12} \leqq r_c$ and $\mathscr{U}(r_{12}) = 1$ for $r_{12} > r_c$. We shall now prove that the theorem is still valid in this case, provided the single particle energy, given in eq. (4), be properly redefined.

An elementary argument will convince us that eq. (24) underestimates the average kinetic energy of the nucleus when the repulsive core is taken into account. In fact, from a statistical point of view, the existence of the repulsive core gives rise, as global effect, to a sort of nuclear "covolume", which tends to reduce the available coordinate space. Therefore, since the product of the volumes of the coordinate and momentum space is a constant, proportional to the number of particles of the whole system, the effect of the core is to increase the momentum space and, consequently, the average kinetic energy $\langle T_c(\kappa)\rangle$ of the nucleus. Hence, one should expect that $\langle T_c(\kappa)\rangle = \langle T(\kappa)\rangle \xi(\kappa, r_c)$, where the function $\xi(\kappa, r_c) \geqq 1$ must obviously be equal to unity either at the limit $\kappa = 0$ or $r_c = 0$. According to a procedure, developed by Lenz [11]) in studying the problem of non-interacting hard spheres, the function $\xi(\kappa, r_c)$, which accounts for the additional curvature of the nucleon wave function, arising from repulsive core boundary conditions, can be approximately written as $1+\chi(r_c)\kappa$. For instance, if one pictures the nucleons as rigid particles of radius $\frac{1}{2}r_c$ (and not $r_c$!), it is found $\chi(r_c) \approx 0.705 r_c$ at the limit of large interparticle separation with respect to $r_c$. The modified expression

$$\langle T_c(\kappa)\rangle = \langle T(\kappa)\rangle[1+\chi(r_c)\kappa] \tag{25}$$

leads one to the conclusion that the effect of the core repulsion on the average kinetic energy of the nucleus, accounted for by the Lenz correction term, is exactly the same which one would obtain by considering non-interacting point nucleons, each having the individual kinetic energy $k^2/2M$ shifted by the amount

$$\varepsilon(\kappa, \kappa, r_c) = (\tfrac{3}{2}\pi^2)^{\frac{1}{3}}\rho^{\frac{1}{3}}(\kappa)\chi(r_c)\left(\frac{k^2}{2M}\right). \tag{26}$$

In the light of this remark, the single particle energy $\mathscr{E}(k, \kappa)$ and the nucleus average total energy $\langle W(\kappa)\rangle$, defined in eqs. (5) and (3) respectively, become

$$\mathscr{E}_c(k, \kappa) = \mathscr{E}(k, \kappa)+\varepsilon(k, \kappa, r_c), \tag{27}$$

$$\langle W_c(\kappa)\rangle = \langle W(\kappa)\rangle + \frac{9\pi^2 A}{20M}\chi(r_c)\rho(\kappa). \tag{28}$$

By imposing on $\langle W_c(\kappa)\rangle$ to satisfy the two conditions $P(k_F) = Q(k_F) = 0$, one finds

$$B_v = \frac{\langle W_c(k_F)\rangle}{A} = \mathscr{E}_c(k_F, k_F), \tag{29}$$

which shows that the validity of the Hugenholtz and Van Hove theorem is closely related in this case to the redefinition (27) of the single particle energy. Furthermore, since $\varepsilon(k, \kappa, r_c)$ tends to zero at the limit $\kappa = 0$, eq. (1) should be considered as the low density approximation of eq. (29). The definition (27) gives a new content to Brueckner's suggestion concerning the shift of the single particle energy [12]) and circumvents the Hugenholtz and Van Hove criticism [1]) as far as the momentum and density dependence of such a shift is concerned. Using the Brueckner and Gammel values [13]) in eq. (29), the misterious discrepancy of about 13 MeV, brought about by eq. (1), disappears. Finally, it has to be emphasized that the Hugenholtz and Van Hove theorem, either in the form (1) or (29), substantially expresses a peculiar property of the single particle energy valid at the point $k = \kappa = k_F$ lying on the characteristic line $k = \kappa$, along which the solutions of eq. (10) are not uniquely determined. It follows that the saturation of the nuclear binding energy and density provides only a weak test for the reliability of $\mathscr{V}(k, \kappa)$.

The Author is indebted to Prof. L. Rosenfeld, as well as to Prof. P. Budini and to Prof. E. Clementel, for several stimulating discussions.

## References


1) N. M. Hugenholtz and L. Van Hove, Physica **24** (1958) 363
2) H. A. Bethe, Phys. Rev. **103** (1956) 1353
3) V. F. Weisskopf, Nuclear Physics **3** (1957) 423
4) C. Villi, On the momentum dependence of the nuclear potential (Nuovo Cimento, in press)
5) J. M. Blatt and V. F. Weisskopf, Theoretical Nuclear Physics (New York, 1952) p. 129
6) L. Schiff, Quantum Mechanics (New York, 1949) p. 77
7) K. A. Brueckner, C. A. Levinson and H. M. Mahmud, Phys. Rev. **95** (1954) 219
8) K. A. Brueckner, Phys. Rev. **96** (1954) 508
9) N. Fukuda and R. G. Newton, Phys. Rev. **103** (1956) 1558
10) C. Villi, to be published
11) W. Lenz, Zeit. f. Physik **56** (1929) 778; see also S. D. Drell and K. Huang, Phys. Rev. **91** (1953) 1527
12) K. A. Brueckner, Phys. Rev. **110** (1958) 597
13) K. A. Brueckner and J. L. Gammel, Phys. Rev. **105** (1957) 1679; ibid **109** (1958) 1023

8.B *Nuclear Physics* 9 (1958/59) 314—325; © *North-Holland Publishing Co., Amsterdam*
Not to be reproduced by photoprint or microfilm without written permission from the publisher

# $K^-$-ABSORPTION IN NUCLEI, AN ISOBARIC SPIN AND ANGULAR MOMENTUM ANALYSIS

P. K. ROY

*Department of Mathematics, Imperial College, London*

Received 1 September 1958

**Abstract:** The consequences of the conservation of isobaric spin in $K^-$-meson capture on a pair of nucleons are investigated. Certain relations involving production cross-sections and capture and production ratios are derived; the effect of the assumption of the predominance of the final baryonic or meson-nucleon interaction is determined. Similar considerations are applied to the absorption processes in light nuclei like the deuteron and helium, etc. Lastly, an angular momentum analysis of the absorption processes is considered to determine the relative parities of the K and Y particles.

## 1. Introduction

It is well-known in pion physics [1]) and in strong interaction theory of the strange particles [2]) that the assumption of the hypothesis of charge independence (i.e., conservation of isobaric spin) leads to important relations for the various reactions. In the present note we examine the consequences of this hypothesis in dinucleon absorption processes of $K^-$-mesons in nuclear matter. For, recent investigations † into such processes indicate that, besides capture on a single nucleon, it is necessary to consider the absorption process by two nucleons having a rather high relative momentum owing to correlations in the nuclear ground state wave function. A fairly clear group of hyperons appears at such a high energy that they can be taken as evidence for capture by two nucleons.

In section 2 we analyze the processes

$$K+N+N \rightarrow Y+N \qquad (A)$$

and

$$K+N+N \rightarrow Y+N+\pi \qquad (B)$$

in terms of isobaric spin. Quantitative restrictions on the absorption processes, as a consequence of conservation of isobaric spin, are also determined. Some of these relations, involving differential cross-sections and production and capture ratios are singled out for testing the hypothesis. Some relations are derived which are valid if, in the final baryonic or meson-nucleon interaction, a state with a particular value of the isobaric spin predominates.

† The present work was stimulated by the experimental results of ref.[3]).

Similar considerations are applied to the K⁻-interaction with such light nuclei as the deuteron, helium, etc. Lastly, we make an angular momentum analysis to determine the relative parities of the strange particles involved. The relative importance of the two-nucleon process over the single nucleon one is noted.

## 2. Isobaric Spin Analysis

### 2.1. THE PROCESS K+N+N → Y+N

The final baryons are in an isobaric spin state $F = \frac{3}{2}, \frac{1}{2}$. The isobaric spin combination of the initial dinucleon system is $I_1 = 1,0$. Accordingly, there are five possible isobaric spin amplitudes depending upon the nature of the hyperons, the total isobaric spin and the initial isobaric spin state of the two-nucleon system. We denote these various amplitudes by $Y_{2F,I_1}$ (see table 1).

TABLE 1

Possible transitions of K+N+N → Y+N and corresponding amplitudes

| Total isobaric spin | Initial isobaric spin of (NN) | Amplitude † |
|---|---|---|
| $\frac{3}{2}$ | 1 | $\Sigma_{31}$ |
| $\frac{1}{2}$ | 1 | $\Sigma_{11}$ |
| $\frac{1}{2}$ | 1 | $\Lambda_{11}$ |
| $\frac{1}{2}$ | 0 | $\Sigma_{10}$ |
| $\frac{1}{2}$ | 0 | $\Lambda_{10}$ |

† The notation $\Sigma_{31}$, e.g., means that in the final state the hyperon is a $\Sigma$ particle, that the final baryons are in an isobaric spin $\frac{3}{2}$ state, while the initial dinucleon system is in an isobaric spin 1 state.

For the $\Sigma$ particles in the final state there are in all fourteen different processes. This presumes that we consider [4]) differential cross-sections in which one can distinguish between pn and np initial states. However, under charge symmetry, one has

$$p \leftrightarrow n, \quad \Sigma^+ \leftrightarrow \Sigma^-, \quad \Sigma^0 \leftrightarrow \Sigma^0, \quad \overline{K}^0 \leftrightarrow K^-.$$

There are then seven pairs of amplitudes; these are not related by charge symmetry. They can be expressed in terms of three complex amplitudes (or five real parameters: the three absolute values and the two relative phases).

For the $\Lambda$ particle in the final state, however, the three pairs of amplitudes unrelated by charge symmetry are expressed in terms of two complex amplitudes (or three real parameters).

These relations are

$$\begin{aligned}
\langle \Lambda^0 n|K^- pn\rangle &= 6^{-\frac{1}{2}}(\Lambda_{11}+3^{\frac{1}{2}}\Lambda_{10}) = \langle \Lambda^0 p|\overline{K}^0 np\rangle \\
\langle \Lambda^0 n|K^- np\rangle &= 6^{-\frac{1}{2}}(\Lambda_{11}-3^{\frac{1}{2}}\Lambda_{10}) = \langle \Lambda^0 p|\overline{K}^0 pn\rangle \qquad (1) \\
\langle \Lambda^0 p|K^- pp\rangle &= -2^{\frac{1}{2}}\cdot 3^{-\frac{1}{2}}\Lambda_{11} \quad = \langle \Lambda^0 n|\overline{K}^0 nn\rangle
\end{aligned}$$

and

$$\begin{aligned}
\langle\Sigma^+\mathrm{n}|\mathrm{K}^-\mathrm{pp}\rangle &= 3^{-1}(\Sigma_{31}+2\Sigma_{11}) &&= \langle\Sigma^-\mathrm{p}|\overline{\mathrm{K}}^0\mathrm{nn}\rangle\\
\langle\Sigma^0\mathrm{p}|\mathrm{K}^-\mathrm{pp}\rangle &= 2^{\frac{1}{2}}\cdot 3^{-1}(\Sigma_{31}-\Sigma_{11}) &&= \langle\Sigma^0\mathrm{n}|\overline{\mathrm{K}}^0\mathrm{nn}\rangle\\
\langle\Sigma^0\mathrm{n}|\mathrm{K}^-\mathrm{pn}\rangle &= 2^{-\frac{1}{2}}\cdot 3^{-1}[(2\Sigma_{31}+\Sigma_{11})+3^{\frac{1}{2}}\Sigma_{10}] &&= \langle\Sigma^0\mathrm{p}|\overline{\mathrm{K}}^0\mathrm{np}\rangle\\
\langle\Sigma^0\mathrm{n}|\mathrm{K}^-\mathrm{np}\rangle &= 2^{-\frac{1}{2}}\cdot 3^{-1}[(2\Sigma_{31}+\Sigma_{11})-3^{\frac{1}{2}}\Sigma_{10}] &&= \langle\Sigma^0\mathrm{p}|\overline{\mathrm{K}}^0\mathrm{pn}\rangle \qquad (2)\\
\langle\Sigma^-\mathrm{p}|\mathrm{K}^-\mathrm{pn}\rangle &= 3^{-1}[(\Sigma_{31}-\Sigma_{11})-3^{\frac{1}{2}}\Sigma_{10}] &&= \langle\Sigma^+\mathrm{n}|\overline{\mathrm{K}}^0\mathrm{np}\rangle\\
\langle\Sigma^-\mathrm{p}|\mathrm{K}^-\mathrm{np}\rangle &= 3^{-1}[(\Sigma_{31}-\Sigma_{11})+3^{\frac{1}{2}}\Sigma_{10}] &&= \langle\Sigma^+\mathrm{n}|\overline{\mathrm{K}}^0\mathrm{pn}\rangle\\
\langle\Sigma^-\mathrm{n}|\mathrm{K}^-\mathrm{nn}\rangle &= \Sigma_{31} &&= \langle\Sigma^+\mathrm{p}|\overline{\mathrm{K}}^0\mathrm{pp}\rangle.
\end{aligned}$$

The three linear relations (1) between the amplitudes of the three processes give rise to the usual triangular inequalities between the square-roots of the three differential cross-sections, such as

$$\sigma^{\frac{1}{2}}(\mathrm{K}^-\mathrm{pn}\to\Lambda^0\mathrm{n})+\sigma^{\frac{1}{2}}(\mathrm{K}^-\mathrm{np}\to\Lambda^0\mathrm{n})\geqq\sigma^{\frac{1}{2}}(\mathrm{K}^-\mathrm{pp}\to\Lambda^0\mathrm{p}). \qquad (3)$$

The seven equations (2), involving five real parameters, however, imply two relations between the amplitudes and the relative phases. To derive the relation involving the phases we introduce the following:

$$\begin{aligned}
\sigma_1^{\pm} &= \sigma(\mathrm{K}^-\mathrm{pp}\to\Sigma^+\mathrm{n})\pm\sigma(\mathrm{K}^-\mathrm{pp}\to\Sigma^0\mathrm{p})\\
\sigma_2^{\pm} &= \sigma(\mathrm{K}^-\mathrm{pn}\to\Sigma^0\mathrm{n})\pm\sigma(\mathrm{K}^-\mathrm{np}\to\Sigma^0\mathrm{n})\\
\sigma_3^{\pm} &= \sigma(\mathrm{K}^-\mathrm{np}\to\Sigma^-\mathrm{p})\pm\sigma(\mathrm{K}^-\mathrm{pn}\to\Sigma^-\mathrm{p})\\
\sigma_4 &= \sigma(\mathrm{K}^-\mathrm{nn}\to\Sigma^-\mathrm{n}).
\end{aligned} \qquad (4a)$$

Then one obtains

$$\begin{aligned}
&\cos^{-1}\left[\frac{3^{-\frac{1}{2}}(2\sigma_2^-+\sigma_3^-)}{2[2\sigma_4\{(\sigma_2^++\sigma_3^+)-\sigma_1^--\sigma_4\}]^{\frac{1}{2}}}\right]\\
&\qquad+\cos^{-1}\left[\frac{3^{-\frac{1}{2}}(\sigma_2^--\sigma_3^-)}{[2(3\sigma_1^+-\sigma_4)\{2(\sigma_2^++\sigma_3^+)-\sigma_1^--\sigma_4^-\}]^{\frac{1}{2}}}\right] \qquad (4b)\\
&\qquad=\cos^{-1}\left[\frac{3(2\sigma_2^+-\sigma_3^+)-(\sigma_1^++\sigma_1^-)}{4\{\sigma_4(3\sigma_1^+-\sigma_4)\}^{\frac{1}{2}}}\right].
\end{aligned}$$

The relation involving the differential cross-sections is

$$\begin{aligned}
&\sigma(\mathrm{K}^-\mathrm{np}\to\Sigma^-\mathrm{p})+\sigma(\mathrm{K}^-\mathrm{pn}\to\Sigma^-\mathrm{p})+\sigma(\mathrm{K}^-\mathrm{pp}\to\Sigma^+\mathrm{n})+\sigma(\mathrm{K}^-\mathrm{nn}\to\Sigma^-\mathrm{n})\\
&\qquad=2[\sigma(\mathrm{K}^-\mathrm{pn}\to\Sigma^0\mathrm{n})+\sigma(\mathrm{K}^-\mathrm{np}\to\Sigma^0\mathrm{n})+\sigma(\mathrm{K}^-\mathrm{pp}\to\Sigma^0\mathrm{p})]; \qquad (5a)
\end{aligned}$$

in terms of production ratios this becomes

$$\frac{\Sigma^++\Sigma^-}{\Sigma^0}=2 \qquad (5b)$$

with an obvious notation. Eq. (5b) is an analogue in the strong interaction theory of Watson's relation [5]) in pion physics.

The set of eqs. (1) and (2) permits one to estimate the modes of $\mathrm{K}^-$-meson capture and the ratios of the numbers of captures on the various dinucleon

systems. For this we assume that the matrix elements for each of the production channels do not depend upon energy and that there are equal numbers of protons and neutrons in the capture nucleus. Furthermore, we assume that the electromagnetic interaction is negligible. It then follows that for the $\Lambda$ hyperon one obtains

$$\frac{\text{capture on other systems}}{\text{capture on (pp)}} = \frac{1}{2}\,\frac{|A_{11}|^2+3|A_{10}|^2}{|A_{11}|^2} \geqq \frac{1}{2}. \tag{6}$$

For the $\Sigma$ hyperons we have

(a)
$$\frac{\text{capture on (pp)}}{\text{capture on (nn)}} = \frac{1}{3}\,\frac{|\Sigma_{31}|^2+2|\Sigma_{1.}|^2}{|\Sigma_{31}|^2} \geqq \frac{1}{3} \tag{7a}$$

(b)
$$\frac{\text{capture on other systems}}{\text{capture on (nn)}} = \frac{|\Sigma_{31}|^2+|\Sigma_{11}|^2+|\Sigma_{10}|^2}{|\Sigma_{31}|^2} \geqq 1 \tag{7b}$$

(c) the ratio of the number of captures in the isobaric spin $\frac{1}{2}$ state to the number of captures in the $\frac{3}{2}$ state is

$$\frac{N_1}{N_3} = \frac{\Sigma^0\mathrm{p}+\Sigma^0\mathrm{n}+\Sigma^-\mathrm{p}-\Sigma^-\mathrm{n}}{\Sigma^-\mathrm{n}}. \tag{7c}$$

All these various ratios might provide a rough check on the theory; assuming the theory to be acceptable, these ratios give a measure of the relative strengths of the two isobaric spin $\frac{1}{2}$ states and the spin $\frac{3}{2}$ state. Should one of these amplitudes be found to dominate, the ratios would then be determined by the coefficients in eqs. (1) and (2). For example, if the isobaric spin-zero state of the dinucleon system predominates, then (6) implies that the probability for $\Lambda^0$ production by $\mathrm{K}^-$-capture on (pp) will be small.

We shall now state the special properties of these relations in case of predominance of the $F = \frac{3}{2}$ or $\frac{1}{2}$ state. If the contribution due to the $\frac{3}{2}$ state be negligible, then one has $\sigma(\mathrm{K}^-\mathrm{pp} \to \Sigma^+\mathrm{n}) = 2\sigma(\mathrm{K}^-\mathrm{pp} \to \Sigma^0\mathrm{p})$; that is, for $\mathrm{K}^-$-capture on diproton the probability of producing a positively charged $\Sigma$ hyperon is twice that of producing a neutral one. The production ratios become

$$\Sigma^0/\Sigma^+ \geqq \tfrac{3}{4}, \quad \Sigma^-/\Sigma^+ \geqq \tfrac{1}{2}$$

or

$$\Sigma^0/\Sigma^+ \geqq \tfrac{3}{2}, \quad \Sigma^-/\Sigma^+ \geqq 2$$

according as the isobaric spin-zero or one state of the dinucleon predominates.

If, however, the total isobaric spin $\frac{3}{2}$ state predominates, $\Sigma^0/\Sigma^+ = 6$, $\Sigma^-/\Sigma^+ = 11$; that is, there is a very small probability for producing positively charged hyperons. One thus approximately obtains $\Sigma^-/\Sigma^0 = 2$ instead of (5b).

### 2.2 THE PROCESS $K+N+N \to \pi+N+Y$

For three particles in the final state we modify accordingly our notation. This modification is conditioned by the results involving the pion-nucleon interaction where different isobaric spin states dominate in different energy regions. In order to obtain quantitative consequences of these states in hyperon production we expand the final state into subsystems consisting of the pion and the nucleon whose isobaric spin is denoted by $I_f$. We note, however, that since the $\Sigma$ hyperons and the pions are both isobaric spin triplets, it is easy to derive relations involving the hyperon-nucleon subsystem. For this process there are nine possible isobaric spin amplitudes denoted by $Y^{I_i}_{2F,2I_f}$ (see table 2).

TABLE 2

Possible transitions of $K+N+N \to \pi+N+Y$ and corresponding amplitudes

| Total isobaric spin | Initial isobaric spin (NN) | Final isobaric spin ($\pi$N) | Amplitude † |
|---|---|---|---|
| $\frac{3}{2}$ | 1 | $\frac{3}{2}$ | $\Sigma^1_{33}$, $\Lambda^1_{33}$ |
| $\frac{3}{2}$ | 1 | $\frac{1}{2}$ | $\Sigma^1_{31}$ |
| $\frac{1}{2}$ | 1 | $\frac{3}{2}$ | $\Sigma^1_{13}$ |
| $\frac{1}{2}$ | 1 | $\frac{1}{2}$ | $\Sigma^1_{11}$, $\Lambda^1_{11}$ |
| $\frac{1}{2}$ | 0 | $\frac{3}{2}$ | $\Sigma^0_{13}$ |
| $\frac{1}{2}$ | 0 | $\frac{1}{2}$ | $\Sigma^0_{11}$, $\Lambda^0_{11}$ |

† The notation $\Sigma^0_{13}$, e.g., means that in the final state of total isobaric spin $\frac{1}{2}$ the pion-nucleon system is in an isobaric spin $\frac{3}{2}$ state, while the initial nucleonic system is in an isobaric spin 0 state.

For the $\Lambda$ particle in the final state, since it is an isobaric spin singlet while the pion is a triplet, it follows that the amplitudes obey relations similar to (2), with obvious replacements. Accordingly, one concludes that results similar to those in (7) obtain here also. To summarize,

$$\frac{\pi^+ + \pi^-}{\pi^0} = 2, \tag{8a}$$

$$\frac{\text{capture on (pp)}}{\text{capture on (nn)}} \geqq \tfrac{1}{3}, \tag{8b}$$

$$\frac{\text{capture on other systems}}{\text{capture on (nn)}} \geqq 1, \tag{8c}$$

and

$$\frac{N_1}{N_3} = \frac{\pi^0 p + \pi^0 n + \pi^- p - \pi^- n}{\pi^- n}. \tag{8d}$$

For the other hyperon in the final state, there are eighteen pairs of amplitudes unrelated by charge symmetry. These are

$$\langle\pi^+p\Sigma^-|K^-pp\rangle = 3^{-\frac{1}{2}}[2^{\frac{1}{2}}5^{-\frac{1}{2}}\Sigma^1_{33}+\Sigma^1_{13}] = \langle\pi^-n\Sigma^+|\bar{K}^0nn\rangle$$
$$\langle\pi^+n\Sigma^0|K^-pp\rangle = 3^{-\frac{1}{2}}[5^{-\frac{1}{2}}\Sigma^1_{33}+2\Sigma^1_{31}-2^{\frac{1}{2}}\Sigma^1_{13}-2\Sigma^1_{11}] = \langle\pi^-p\Sigma^0|\bar{K}^0nn\rangle$$
$$\langle\pi^-p\Sigma^+|K^-pp\rangle = 3^{-\frac{1}{2}}[2^{\frac{1}{2}}5^{-\frac{1}{2}}\Sigma^1_{33}-2^{\frac{1}{2}}\Sigma^1_{31}+\Sigma^1_{13}-2^{\frac{1}{2}}\Sigma^1_{11}] = \langle\pi^+n\Sigma^-|\bar{K}^0nn\rangle$$
$$\langle\pi^0p\Sigma^0|K^-pp\rangle = 3^{-\frac{1}{2}}[2^{\frac{1}{2}}5^{-\frac{1}{2}}\Sigma^1_{33}-2^{\frac{1}{2}}\Sigma^1_{31}-2\Sigma^1_{13}+2^{\frac{1}{2}}\Sigma^1_{11}] = \langle\pi^0n\Sigma^0|\bar{K}^0nn\rangle$$
$$\langle\pi^0n\Sigma^+|K^-pp\rangle = 3^{-\frac{1}{2}}[-4\cdot5^{-\frac{1}{2}}\Sigma^1_{33}+\Sigma^1_{31}+2^{\frac{1}{2}}\Sigma^1_{13}+2\Sigma^1_{11}] = \langle\pi^0p\Sigma^-|\bar{K}^0nn\rangle$$
$$\langle\pi^-p\Sigma^-|K^-nn\rangle = 2^{\frac{1}{2}}3^{-\frac{1}{2}}[5^{-\frac{1}{2}}\Sigma^1_{33}-\Sigma^1_{31}] = \langle\pi^+n\Sigma^+|\bar{K}^0pp\rangle$$
$$\langle\pi^-n\Sigma^0|K^-nn\rangle = -3^{\frac{1}{2}}5^{-\frac{1}{2}}\Sigma^1_{33} = \langle\pi^+p\Sigma^0|\bar{K}^0pp\rangle$$
$$\langle\pi^0n\Sigma^-|K^-nn\rangle = 3^{-\frac{1}{2}}[2\cdot5^{-\frac{1}{2}}\Sigma^1_{33}+\Sigma^1_{31}] = \langle\pi^0p\Sigma^+|\bar{K}^0pp\rangle$$
$$\langle\pi^+n\Sigma^-|K^-pn\rangle = 3^{-\frac{1}{2}}[2^{\frac{1}{2}}5^{-\frac{1}{2}}\Sigma^1_{33}+2^{\frac{1}{2}}\Sigma^1_{31}+2^{-1}\Sigma^1_{13} - 2^{\frac{1}{2}}\Sigma^1_{11}+2^{-1}3^{\frac{1}{2}}\Sigma^0_{13}-2^{\frac{1}{2}}3^{\frac{1}{2}}\Sigma^0_{11}] = \langle\pi^-p\Sigma^+|\bar{K}^0np\rangle \quad (9)$$
$$\langle\pi^-p\Sigma^0|K^-pn\rangle = 3^{-\frac{1}{2}}[5^{-\frac{1}{2}}\Sigma^1_{33}+2\Sigma^1_{31}+2^{-\frac{1}{2}}\Sigma^1_{13} +\Sigma^1_{11}+3^{\frac{1}{2}}2^{-\frac{1}{2}}\Sigma^0_{13}+3^{\frac{1}{2}}\Sigma^0_{11}] = \langle\pi^+n\Sigma^0|\bar{K}^0np\rangle$$
$$\langle\pi^0n\Sigma^+|K^-pn\rangle = 3^{-\frac{1}{2}}[-2^{\frac{1}{2}}5^{-\frac{1}{2}}\Sigma^1_{33}+2^{-1}\Sigma^1_{13}+3^{\frac{1}{2}}2^{-1}\Sigma^0_{13}] = \langle\pi^+p\Sigma^-|\bar{K}^0np\rangle$$
$$\langle\pi^0p\Sigma^-|K^-pn\rangle = 3^{-\frac{1}{2}}[4\cdot5^{-\frac{1}{2}}\Sigma^1_{33}-\Sigma^1_{31}+2^{-\frac{1}{2}}\Sigma^1_{13} +\Sigma^1_{11}+2^{-\frac{1}{2}}3^{\frac{1}{2}}\Sigma^0_{13}+3^{\frac{1}{2}}\Sigma^0_{11}] = \langle\pi^0n\Sigma^+|\bar{K}^0np\rangle$$
$$\langle\pi^0n\Sigma^0|K^-pn\rangle = 3^{-\frac{1}{2}}[-2^{\frac{1}{2}}5^{-\frac{1}{2}}\Sigma^1_{33}+2^{\frac{1}{2}}\Sigma^1_{31}-\Sigma^1_{13} +2^{-\frac{1}{2}}\Sigma^1_{11}-3^{\frac{1}{2}}\Sigma^0_{13}+2^{-\frac{1}{2}}3^{\frac{1}{2}}\Sigma^0_{11}] = \langle\pi^0p\Sigma^0|\bar{K}^0np\rangle.$$

The remaining five pairs are the same as the last five, except for the fact that, in the initial states, p is replaced by n and n by p and that the signs of the amplitudes $\Sigma^0_{13}$, $\Sigma^0_{11}$ are also changed.

These eighteen processes are described by six complex amplitudes, that is, eleven real parameters. This implies that there are seven relations between the absolute values of the amplitudes and the relative phases. The most important relation involving the cross-sections is an exact analogue of eqs. (1)—(2), (8). That is, in this case also we have

$$\frac{\Sigma^+ + \Sigma^-}{\Sigma^0} = 2 = \frac{\pi^+ + \pi^-}{\pi^0}. \quad (10)$$

We now briefly state the consequences of the assumption of predominance of the isobaric spin $\frac{3}{2}$ or $\frac{1}{2}$ state of the pion-nucleon system.

(i) If one assumes that the former predominates when the total isobaric spin is $\frac{1}{2}$, then for absorption on (pp) one has

$$\Sigma^-/\Sigma^+ = 3,\ \Sigma^0/\Sigma^+ = 2,\ \frac{\Sigma^-\pi^+}{\Sigma^+\pi^-} = 9,\ \pi^-/\pi^+ = \tfrac{1}{11},\ \pi^0/\pi^+ = \tfrac{6}{11};$$

for absorption on (pn)

$$\Sigma^-/\Sigma^+ = \tfrac{1}{3},\ \Sigma^0/\Sigma^+ = \tfrac{2}{3},\ \frac{\Sigma^-\pi^+}{\Sigma^+\pi^-} = \tfrac{1}{3},\ \pi^-/\pi^+ = 11,\ \pi^0/\pi^+ = 6;$$

while the absorption on (nn) becomes negligible. The capture ratio becomes

$$\frac{\text{capture on (pn)}}{\text{capture on (nn)}} = \frac{1}{2}\,\frac{|\Sigma'_{13}|^2+|\Sigma^0_{13}|^2}{|\Sigma'_{13}|^2} \geqq \frac{1}{2}.$$

If, however, the total isobaric spin $\frac{3}{2}$ state predominates, we have some very large production ratios:

$$\Sigma^-/\Sigma^0 = 6, \quad \Sigma^+/\Sigma^0 = 8, \quad \frac{\Sigma^-\pi^+}{\Sigma^+\pi^-} = \frac{9}{4},$$

and

$$\Sigma^-/\Sigma^0 = 8, \quad \Sigma^+/\Sigma^0 = 6, \quad \frac{\Sigma^-\pi^+}{\Sigma^+\pi^-} = \frac{4}{9},$$

for the absorption processes on (pp) and (pn) respectively; besides

$$\frac{\text{capture on (pp)}}{\text{capture on (nn)}} = \frac{1}{3}$$

$$\frac{\text{total capture}}{\text{capture on (nn)}} = 2$$

and

$$\frac{\Sigma^-\pi^+}{\Sigma^+\pi^-} = \frac{17}{22}.$$

(ii) Similarly, if the isobaric spin $\frac{1}{2}$ state of the pion-nucleon system predominates when the total spin is $\frac{1}{2}$, $K^-$-absorption on (nn) becomes negligible. For absorption on (pp) and (nn) we have

$$\Sigma^+/\Sigma^0 = 2, \quad \Sigma^-/\Sigma^0 \approx 0, \quad \frac{\Sigma^-\pi^+}{\Sigma^+\pi^-} \approx 0$$

and

$$\Sigma^+/\Sigma^0 \approx 0, \quad \Sigma^-/\Sigma^0 = 2, \quad \frac{\Sigma^-\pi^+}{\Sigma^+\pi^-} \approx 0$$

respectively; and

$$\frac{\text{capture on (pn)}}{\text{capture on (pp)}} \geqq 1.$$

For the predominance of the total spin $\frac{3}{2}$ state, we have

$$\Sigma^-/\Sigma^+ = \frac{33}{5}, \quad \Sigma^0/\Sigma^+ = 4, \quad \frac{\Sigma^-\pi^+}{\Sigma^+\pi^-} = 1.$$

The capture ratios become

$$\frac{\text{capture on (pp)}}{\text{capture on (nn)}} = \frac{11}{27}$$

$$\frac{\text{capture on (pn)}}{\text{capture on (nn)}} = \frac{1}{3}.$$

An examination of the eqs. (9) shows that should the amplitudes with the initial nucleons in the spin-zero state alone contribute significantly, then the capture processes on diproton and dineutron do not take place. In that case a simple relation like (5b) or (10) does not hold and we have

$$\Sigma^-/\Sigma^+ = \frac{8}{3}\,\frac{\frac{1}{4}|\Sigma^0_{13}|^2+|\Sigma^0_{11}|^2}{|\Sigma^0_{13}|^2} \geqq \frac{2}{3}$$

$$\Sigma^0/\Sigma^+ = \frac{4}{3}\,\frac{|\Sigma^0_{13}|^2+|\Sigma^0_{11}|^2}{|\Sigma^0_{13}|^2} \geqq \frac{4}{3}$$

$$\frac{\Sigma^-\pi^+}{\Sigma^+\pi^-} \geqq \frac{2}{9}.$$

### 2.3. K⁻-INTERACTION WITH LIGHT NUCLEI

We have so far considered hyperon production in K⁻-interaction with nucleons only. Evidently, similar relations exist for nuclei provided they are in a definite isobaric spin state. In this part we shall analyze, in terms of isobaric spin, the interaction of K⁻ with light nuclei. Relations thus obtained are useful for checking the hypothesis of charge independence or for obtaining information on the purity of the isobaric spin in the states of the nuclei and also for obtaining information regarding difficult reactions.

We give below a discussion of interaction with light nuclei of isobaric spin-zero state. The simplest of such nuclei are the deuteron and the normal helium.

For the process $K^-+d \to Y+N$ we have

$$\sigma(K^-+d \to \Sigma^-+p) = 2\sigma(K^-+d \to \Sigma^0+n) \tag{11}$$

Attention has already been drawn to this relation as a possible means of determining the spin of the $\Sigma$ hyperon [6]).

For the three-particle final state process

$$K^-+d \to \pi+N+Y$$

one obtains

$$\begin{aligned}
\langle \pi^+ n\Sigma^-|K^-d\rangle &= 3^{-1}[2^{-\frac{1}{2}}\Sigma_{13}-2\Sigma_{11}] &&= \langle \pi^- p\Sigma^+|\bar{K}^0 d\rangle \\
\langle \pi^- n\Sigma^+|K^-d\rangle &= 2^{-\frac{1}{2}}\Sigma_{13} &&= \langle \pi^+ p\Sigma^-|\bar{K}^0 d\rangle \\
\langle \pi^- p\Sigma^0|K^-d\rangle &= -3^{-1}[\Sigma_{13}+2^{\frac{1}{2}}\Sigma_{11}] &&= \langle \pi^+ n\Sigma^0|\bar{K}^0 d\rangle \\
\langle \pi^0 p\Sigma^-|K^-d\rangle &= 3^{-1}[\Sigma_{13}+2^{\frac{1}{2}}\Sigma_{11}] &&= \langle \pi^0 n\Sigma^+|\bar{K}^0 d\rangle \\
\langle \pi^0 n\Sigma^0|K^-d\rangle &= -3^{-1}[2^{\frac{1}{2}}\Sigma_{13}-\Sigma_{11}] &&= \langle \pi^0 p\Sigma^0|\bar{K}^0 d\rangle \\
\langle \pi^0 n\Lambda^0|K^-d\rangle &= 3^{-\frac{1}{2}}\Lambda_{11} &&= \langle \pi^0 p\Lambda^0|\bar{K}^0 d\rangle \\
\langle \pi^- p\Lambda^0|K^-d\rangle &= -2^{\frac{1}{2}}3^{-\frac{1}{2}}\Lambda_{11} &&= \langle \pi^+ n\Lambda^0|\bar{K}^0 d\rangle.
\end{aligned} \tag{12}$$

It follows that

$$\sigma(K^-d \to \pi^- p\Sigma^0) = \sigma(K^-d \to \pi^0 p\Sigma^-) \tag{13a}$$

and

$$\sigma(K^-d \to \pi^+ n\Sigma^-)+\sigma(K^-d \to \pi^- n\Sigma^+)+\sigma(K^-d \to \pi^0 p\Sigma^-)+\sigma(K^-d \to \pi^- p\Lambda^0)$$
$$= 2[\sigma(K^-d \to \pi^- p\Sigma^0)+\sigma(K^-d \to \pi^0 n\Sigma^0)+\sigma(K^-d \to \pi^0 n\Lambda^0). \tag{13b}$$

In terms of production ratios

$$\frac{\Sigma^+ + \Sigma^-}{\Sigma^0} = \frac{\pi^+ + \pi^-}{\pi^0} = 2 \quad \text{and} \quad \frac{\Lambda^0 \pi^-}{\Lambda^0 \pi^0} = 2;$$

one further obtains

$$\Sigma^-/\Sigma^+ = \frac{2}{3}\left[\frac{\frac{1}{2}|\Sigma_{13}|^2+2|\Sigma_{11}|^2}{|\Sigma_{13}|^2}\right] \geqq \frac{1}{2}$$

and

$$\Sigma^0/\Sigma^+ = \frac{2}{3}\left[\frac{|\Sigma_{13}|^2+|\Sigma_{11}|^2}{|\Sigma_{13}|^2}\right] \geqq \frac{2}{3}.$$

In case of predominance of the isobaric spin $\frac{3}{2}$ state for the pion-nucleon system, i.e., in the energy range where $\Sigma_{11}$ is negligible compared to $\Sigma_{13}$, we get

$$\Sigma^-/\Sigma^+ = \tfrac{1}{3}, \quad \Sigma^0/\Sigma^+ = \tfrac{2}{3}, \quad \frac{\Sigma^-\pi^+}{\Sigma^+\pi^-} = \tfrac{1}{9}.$$

If, however, the other amplitude predominates,

$$\Sigma^-/\Sigma^+ \geqq \tfrac{5}{3}, \quad \Sigma^0/\Sigma^+ \geqq \tfrac{4}{3}, \quad \frac{\Sigma^+\pi^+}{\Sigma^-\pi^-} = \tfrac{8}{9}.$$

For normal helium the following relations are known [6]) to hold:

$$\begin{aligned}
\sigma(K^-He^4 \to He^3\Sigma^-) &= 2\sigma(K^-He^4 \to H^3\Sigma^0) \\
\sigma(K^-He^4 \to He^3\Sigma^-\pi^0) &= 2\sigma(K^-He^4 \to He^3\Sigma^0\pi^-) \\
\sigma(K^-He^4 \to He^3\Lambda^0\pi^-) &= 2\sigma(K^-He^4 \to H^3\Lambda^0\pi^0).
\end{aligned} \tag{14a}$$

With the present knowledge about hyperfragments one can add to these the following:

$$\begin{aligned}
\sigma(K^-He^4 \to {}_\Lambda He^4\pi^-) &= 2\sigma(K^-He^4 \to {}_\Lambda H^4\pi^0) \\
\sigma(K^-He^4 \to {}_\Lambda H^3 p\pi^-) &= 2\sigma(K^-He^4 \to {}_\Lambda H^3 n\pi^0)
\end{aligned} \tag{14b}$$

where we have assumed that the $({}_\Lambda He^4, {}_\Lambda H^4)$ form an isobaric doublet and ${}_\Lambda H^3$ an isobaric singlet [7]).

The relations (13), (14) provide a stringent test for the validity of the hypothesis of charge independence.

For absorption in $C^{12}$ one can show that relations similar to (14) hold between the reactions, provided one adds two α-particles to the final state products.

## 3. Parity and Angular Momentum

A consequence of the strong interaction theory is that only the relative parity of two strange particles is well-defined, and measurable if a comparison can be made of the orbital and intrinsic parities in the initial and final systems in a reaction involving strange particles. As a result of non-conservation of parity in the weak interactions several investigations into possible production processes [8]) have been made for determining the relative parities. The absorption of slow $K^-$-mesons in nuclear matter, however, offers an alternative possibility. Dalitz [2]) has already suggested an experiment on the selection rules in the capture of K mesons by $He^4$.

We first note that the single nucleon reaction $K+N \rightarrow Y+\pi$ fails to provide one with an adequate means of distinguishing the parity of any state: an angular momentum consideration shows that the pion is emitted in high angular momentum states and a given angular momentum state, $j$ say, can be produced by an orbital angular momentum $l = j \pm \frac{1}{2}$ of the pion. (We assume that the hyperon is a spin-half particle.) Besides, information about characteristic properties of the reaction is also lacking. For example, if, as in pion physics, we were given a resonance in the total (K—N) or (Y—$\pi$) cross-section, then it would be possible to ascertain the angular momentum and parity of the resonance state. Whence the relative parity would be determined by the angular distribution of the reaction.

On the other hand, arguments similar to one employed in pion absorption experiments, coupled with the present data on hyperfragments, make all the two-nucleon absorption processes amenable to analysis. We assume that the dinucleon system can only be in an S state and that the N—N force is strong enough to lead to a bound state. Then, at least for a certain fraction of the process of subsection 2.1, a true two-body reaction takes place. For such processes the baryons are highly likely to be produced in higher relative momentum states. It is, however, possible to represent the *three*-particle final state process as a two-body reaction by employing arguments similar to those in ref. [8]). That is, one can assume that the $\Sigma$—N force is strongest in the $^1S_0$ state [9]) and that it is strong enough to lead, as in the Panofsky experiment on absorption of pions, to a bound state.

We give in table 3 the selection rules, summarizing the properties of the process of subsections 2.1 and 2.2. In preparing it the $K^-$-meson has been assumed to be a spinless particle and the intrinsic parities of the baryons have been defined to be identical. These rules may then distinguish, through the energy dependence and angular distribution, between a scalar and a pseudoscalar $K^-$-meson. For example, one infers from table 3 that, for a scalar $K^-$, the angular distribution is a $\sin^2\theta$ term for the (NN) in the $^1S_0$ "bound" state; this term increases as the cube of the relative momentum of

TABLE 3

Angular distribution of the hyperons produced in the reaction $K+(N+N) \rightarrow Y+N$

| Y−K Parity | $l_K$ † | Initial (NN) state | Final Y+N state | Angular distribution †† |
|---|---|---|---|---|
| + | 0 | $^1S_0$ | $^1S_0$ | 1 |
| | 1 | $^1S_0$ | $^3P_1$ | $1-x^2$ |
| | 0 | $^3S_1$ | $^3S_1$, $^3D_1$ | 1, $x^4-4/3x^2+1/9$ |
| | 1 | $^3S_1$ | $^3P_{0,1,1}$ | 1, $1-x^2$, $1/3+x^2$ |
| − | 0 | $^1S_0$ | $^3P_0$ | 1 |
| | 1 | $^1S_0$ | $^3S_1$, $^3D_1$ | 1, $x^4-4/3x^2+1/9$ |
| | 0 | $^3S_1$ | $^3P_1$ | $1-x^2$ |
| | 1 | $^3S_1$ | $^1S_0$, $^3S_1$, $^3D_1$, $^1D_2$, $^3D_2$ | 1, 1, $x^4-4/3x^2+1/9$, $3x^2-1$, $x^2(1-x^2)$ |

† $l_K$ = orbital angular momentum of the captured $K^-$-meson.
†† The number 1 means isotropic distribution; $x = \cos\theta$.

the baryons. For a pseudoscalar $K^-$, there should not be any *pure* $\sin^2\theta$ term. (For reasons stated above any possible interference between S and D waves has been ignored.) Such special features as described here may permit a determination of the $K^-$-meson parity by careful observations on the present experiments. We should, however, note that if the two-nucleon system is in the $^3S_1$ state, as in the absorption experiments on pions, these rules do not allow any definite conclusion to be drawn.

The author wishes to express his best thanks to Dr. P. T. Matthews for suggesting the problem and for very helpful discussions, and to Dr. J. C. Taylor for a helpful criticism.

## References

1) E. Fermi, Nuovo Cimento Suppl. **2** (1955) 17;
L. I. Lapidus, Soviet Physics (JETP) **4** (1957) 740
2) M. Gell-Mann, Nuovo Cimento Suppl. **4** (1956) 848;
R. H. Dalitz in Reports on Progress in Physics **20** (1957) 163;
C. Franzinetti and G. Morpurgo, Nuovo Cimento Suppl. **6** (1957);
G. Feldman and P. T. Matthews, Phys. Rev. **109** (1958) 546 †
3) E. H. S. Burhop, private communication;
Y. Eisenberg *et al.*, Interactions and decays of $K^-$-mesons III (Phys. Inst. der Univ. Bern, preprint);
B. Chadwick *et al.*, Observations of $K^-$-meson interaction in nuclear emulsion (Oxford University, preprint)
4) L. Van Hove, R. Marshak and A. Pais, Phys. Rev. **88** (1952) 1211
5) K. M. Watson, Phys. Rev. **85** (1952) 852

† In this paper the following two misprints should be corrected: In eq. (2.7) $2^{\frac{1}{2}}B_\Sigma$ should be replaced by $2^{-\frac{1}{2}}I_\Sigma B$, while in eq. (2.5) $\frac{1}{2}$ should replace 1/18.

6) T. D. Lee, Phys. Rev. **99** (1955) 337
7) R. H. Dalitz and B. W. Downs, preprint
8) G. Costa and B. T. Feld, Phys. Rev. **109** (1958) 606
9) D. B. Lichtenberg and M. H. Ross, Phys. Rev. **103** (1956) 1131;
N. D. Dallaporta and F. Ferrari, Nuovo Cimento **5** (1957) 111, 749

8.B *Nuclear Physics* 9 (1958/59) 326—328; © *North-Holland Publishing Co., Amsterdam*
Not to be reproduced by photoprint or microfilm without written permission from the publisher

# GLOBAL AND RESTRICTED SYMMETRY TESTS IN ANTIHYPERON PRODUCTION

B. d'ESPAGNAT and J. PRENTKI
CERN, *Geneva*

Received 2 October 1958

**Abstract:** The conditions of "global" and "restricted" symmetry of meson-hyperon interactions are stated and their consequences for hyperon pair creation briefly discussed.

## 1. Definitions of Global and Restricted Symmetry

The purpose of this note is to investigate the consequences for antihyperon ($\bar{\Lambda}$, $\bar{\Sigma}$) production of the following assumptions:

A) Invariance under P, C and I (isospin rotations) and relative smallness of K- (as compared with $\pi$-) interactions.

B) Same parity for $\Lambda$ and $\Sigma$ and either one of the two assumptions

$$B_1) \quad g_{\Lambda\Sigma\pi} = g_{\Sigma\Sigma\pi},$$
$$B_2) \quad g_{NN\pi} = g_{\Lambda\Sigma\pi} = g_{\Sigma\Sigma\pi} = g_{\Xi\Xi\pi}.$$

The hypothesis A+$B_2$ is called "global symmetry" G (Gell-Mann [1])). The wider hypothesis A+$B_1$ is hereafter referred to as "restricted symmetry" R. It was pointed out some years ago (Espagnat, Prentki and Salam [2])) that assumption $B_1$ makes the $\pi$ interactions 4-dimensionally invariant in a Euclidean 4-space where N and $\Xi$ are two 2-components spinors of the same type † (i.e. $\mathcal{D}(\frac{1}{2}, 0)$) while $\pi$ is a self-dual antisymmetric tensor $\mathcal{D}(1, 0)$ and $\Sigma$, $\Lambda$ build up a 4-vector $\mathcal{D}(\frac{1}{2}, \frac{1}{2})$ ††. An extensive use of this property will be made in what follows, as regards both the R and the G hypothesis.

If the group of 4-rotations is taken in the usual way as a direct product of two groups of 3-rotations in two 3-spaces $I_a$ and $I_b$ the above-mentioned property clearly means that the $\pi$ interactions are separately invariant under rotations in these two spaces with the attributions

$$I_a(N) = I_a(\Xi) = I_a(\Lambda, \Sigma) = \tfrac{1}{2}, \quad I_a(\pi) = 1$$
$$I_b(N) = I_b(\Xi) = I_b(\pi) = 0, \quad I_b(\Lambda, \Sigma) = \tfrac{1}{2}.$$

The meaning of $I_a(\Lambda, \Sigma) = \frac{1}{2}$, $I_b(\Lambda, \Sigma) = \frac{1}{2}$ can be made more explicit by

† $\varphi \to s\,\varphi$, $u \to tu$ with $s^\dagger s = t^\dagger t = 1$, Det $s$ = Det $t$ = 1.

$\varphi \leftrightarrow \mathcal{D}(\frac{1}{2}, 0)$, $u \leftrightarrow \mathcal{D}(0, \frac{1}{2})$, $\varphi_\alpha^* u_\beta \leftrightarrow \mathcal{D}(\frac{1}{2}, \frac{1}{2})$ $\varphi_\alpha^* \varphi_\beta \leftrightarrow (\mathcal{D}1,0) + \mathcal{D}(0, 0)$.

†† The K interactions could also be made fully invariant by choosing K as a $\mathcal{D}(0, \frac{1}{2})$, but difficulties then arose concerning the $\Lambda - \Sigma$ mass difference.

writing, in Gell-Mann's notations,

$$\Sigma_1 = \begin{pmatrix} Z \\ \Sigma^- \end{pmatrix}, \quad \Sigma_2 = \begin{pmatrix} \Sigma^+ \\ Y \end{pmatrix}, \quad Y = (\Lambda - \Sigma^0)/\sqrt{2}, \quad Z = (\Lambda + \Sigma^0)/\sqrt{2}:$$

then $\Sigma_1$ and $\Sigma_2$ are spinors in $I_a$ space and $\binom{\Sigma_1}{\Sigma_2}$ is a spinor in $I_b$ space. As regards the usual isobaric spin space it is of course simply the subspace which is orthogonal to the 4th axis.

## 2. Consequences for Hyperon Pair Creation

Let us consider all phenomena where a hyperon-antihyperon pair is created without K particle production. According to A) these phenomena are predominantly due to $\pi$ interactions alone. Therefore the $I_b$ of the pair is necessarily 0 independently of how many non-strange particles are simultaneously created (because all non-strange particles have $I_b = 0$). On the other hand the $I_a$ of the pair can be either 1 or 0.

Let $Q$ be the charge of the pair. What are the consequences of R or G, for different $Q$'s?

a) $Q = \pm 2$: such pairs should be very few because, with $I_b = 0$, $I_a \leqq 1$ and $U = 0$ ($\Lambda$, $\Sigma$ have $U = 0$) the relations

$$Q = I_3 + \tfrac{1}{2}U, \quad I_3 = I_{a3} + I_{b3}$$

give $Q \leqq 1$.

b) $Q = \pm 1$: then $I_a = 1$, $I_b = 0$ for the pair. From this it is easily deduced that ($\bar{\Sigma}$ denoting anti-$\Sigma$)

$$\sigma(\bar{\Sigma}^-, \Sigma^0) \approx \sigma(\bar{\Sigma}^-, \Lambda) \approx \sigma(\bar{\Sigma}^0, \Sigma^+) \approx \sigma(\bar{\Lambda}, \Sigma^+),$$
$$\sigma(\bar{\Sigma}^+, \Sigma^0) \approx \sigma(\bar{\Sigma}^+, \Lambda) \approx \sigma(\bar{\Sigma}^0, \Sigma^-) \approx \sigma(\bar{\Lambda}, \Sigma^-).$$

c) $Q = 0$: the pair is in a superposition of a state S with $I_a = 0$ and $I_b = 0$ and of a state $V_3$ with $I_a = 1, I_b = 0$, with arbitrary coefficients. Elimination of these coefficients leads to

$$\sigma(\bar{\Sigma}^+, \Sigma^+) + \sigma(\bar{\Sigma}^-, \Sigma^-) \approx 2[\sigma(\bar{\Sigma}^0, \Lambda) + \sigma(\bar{\Lambda}, \Lambda)],$$
$$\sigma(\bar{\Sigma}^0, \Sigma^0) \approx \sigma(\bar{\Lambda}, \Lambda),$$
$$\sigma(\bar{\Lambda}, \Sigma^0) = \sigma(\bar{\Sigma}^0 \Lambda);$$

the last relation, however, being just a consequence of charge independence.

It is clear that experimental devices for checking many of these relations can be found [3]). One may e.g. think of using $\pi$, $\bar{p}$ collisions where, when two hyperonic particles appear in the final products, they are presumably a hyperon-antihyperon pair in most cases.

## 3. Special Consequences of Global Symmetry

A particular feature of G, not shared by R, is that everywhere $\Sigma_1$ can be replaced by N. Consequences of this are that $\bar{\Sigma}^+$ should be produced roughly

as often as $\bar{p}$ and also — as is easily shown — that $\bar{\Sigma}^-$ should be produced roughly as often as $\bar{n}$. (This statement should of course be corrected by taking phase space factors into account when necessary). A simple consequence of this and of the relations in section 2 is that the total number of $\bar{\Lambda}$ (i.e. directly produced $\bar{\Lambda}$'s *plus* the $\Lambda$'s arising from $\bar{\Sigma}^0$ decay) should equal the total number of antinucleons.

## References

1) M. Gell-Mann, Phys. Rev. **106** (1957) 1296
2) B. d'Espagnat, J. Prentki and A. Salam, Nuclear Physics **3** (1957) 446
3) B. d'Espagnat et J. Prentki, Rapport CERN 58—26 (Genève, 1958)

4.D:8.B *Nuclear Physics* 9 (1958/59) 329—333; ©*North-Holland Publishing Co., Amsterdam*
Not to be reproduced by photoprint or microfilm without written permission from the publisher

# ANGULAR CORRELATION BETWEEN NEUTRINO AND GAMMA QUANTUM RELEASED BY ELECTRON CAPTURE

K. NAGY
*Institute for Theoretical Physics of the Roland Eötvös University*
and
J. ZIMANYI
*Central Research Institute for Physics, Budapest*

Received 21 July 1958

## 1. Introduction

In the course of investigating parity violating interactions and the nature of neutrino, the phenomenon of electron capture became increasingly interesting. Since only one particle (the neutrino) is emitted in this process, the study of its physical properties is easier than, for instance, in $\beta$-decay. The wave function determining the state of the electron captured in the process is exactly known; consequently, the result of our calculations for suitably chosen problems, will depend essentially only on the type of interaction and on the helicity of the neutrino. Conditions are simplified further by the fact that for capture from a given electron shell, the neutrino is emitted always with the same energy, that is, the recoil energy imparted to the nucleus is always the same. This condition which does not prevail at all in beta decay, facilitates considerably experimental investigations.

Recently, several papers dealt with the angular correlation between the neutrino and gamma quantum resulting from electron capture. These calculations, however, are not sufficiently general, being restricted usually to the allowed K-capture. In the present paper we attempt to extend above calculations to K-captures being forbidden to an arbitrary order, and to mixed gamma transitions. Correlations concerning captures from the L-shell will be considered in a separate paper. With the aid of our results one can extend the experimental investigations of neutrino properties even to forbidden K-captures and besides we obtain results which may serve as a theoretical basis for nuclear spectroscopy studies.

## 2. Angular Correlation Formula

To start with, let us find the angular correlation between the neutrino emitted by electron capture in direction $k_\nu$ with polarization $p_\nu$ and the

gamma quantum flying in direction $k_\gamma$ with polarization $p_\gamma$, resulting from this capture. Let $j_1, m_1; j_2, m_2$; and $j_3, m_3$ represent the angular momentum quantum numbers and the magnetic quantum numbers of the nucleus in the initial, intermediate and final state, respectively, and $m_e$ the magnetic quantum number of the electron. Thus, the following composite process has to be considered: $j_1, m_1, m_e \xrightarrow{\nu} j_2 m_2 \xrightarrow{\gamma} j_3 m_3$. By means of perturbation theory the correlation in question is obtained [1]) as

$$W(\vartheta, p_\nu, p_\gamma) = \sum_{m_2, m'_2} E^{(\nu)}(m_2, m'_2) E^{(\gamma)}(m_2, m'_2), \tag{1}$$

where $E^{(\nu)}(m_2, m'_2)$ and $E^{(\gamma)}(m_2, m'_2)$ are the density matrices of the two processes, which can be constructed using the interaction Hamiltonian, as

$$E^{(\nu)}(m_2, m'_2) = \sum_{m_1, m_e} \langle j_2 m_2; \nu | H^{(\nu)} | j_1 m_1; m_e \rangle^* \langle j_2 m'_2; \nu | H^{(\nu)} | j_1 m_1; m_e \rangle, \tag{2}$$

$$E^{(\gamma)}(m_2, m'_2) = \sum_{m_3} \langle j_3 m_3; \gamma | H^{(\gamma)} | j_2 m_2 \rangle^* \langle j_3 m_3; \gamma | H^{(\gamma)} | j_2 m'_2 \rangle, \tag{3}$$

where $H^{(\nu)}$ and $H^{(\gamma)}$ are Hamiltonian operators for electron capture-neutrino emission and for gamma quantum emission, respectively. Factors irrelevant for correlation have been emitted.

## 3. Density Matrix for Electron Capture

The general Hamiltonian operator according to the two component neutrino theory is given by

$$H^{(\nu)} = f \sum_i C_i (\psi_n^* O_i \psi_p)(\psi_\nu^* \tfrac{1}{2}(1 - p_\nu \gamma_5) O_i \psi_e) + \text{h.c.} \tag{4}$$

Indices $i$ refer to pure interactions S, V, T, A and P. In the lepton matrix element $p_\nu = \pm 1$ depending on the spin of the neutrino being oriented in the direction of motion or in the opposite sense. Although, according to most recent studies [2]), it is highly probable that $p_\nu = -1$, our calculations were carried out for both states of polarization, thus upholding the possibility of deciding about neutrino helicity on the basis of our results.

For the density matrix $E^{(\nu)}(m_2, m'_2)$ we obtain by the usual methods (in a coordinate system with axis $z$ in the direction of motion of the neutrino) an expression of the form

$$E^{(\nu)}(m_2, m'_2) = \sum_{ll'} \sqrt{(2l+1)(2l'+1)} \{ e_1(ll', m_2 m'_2) a(ll', p_\nu)$$
$$+ \sum_{LL'} e_2(lLl'L', m_2 m'_2, p_\nu) b(lLl'L', p_\nu) + \sum_{L'} e_3(ll'L', m_2 m'_2) c(ll'L', p_\nu) \}, \tag{5}$$

where $e_1, e_2, e_3$ are quantities of geometrical type and $a$, $b$ and $e$ represent sums of reduced matrix elements. One finds †

† We use for the Clebsch-Gordan coefficients $c_{jj'}(J, M; m, m')$ the symbol $(jj'mm'|JM)$.

$$e_1(ll', m_2m'_2) = (j_1 l m_2 0|j_2 m_2)(j_1 l' m_2 0|j_2 m_2)\delta(m_2, m'_2),$$

$$e_2(lLl'L', m_2m'_2, \mathfrak{p}_\nu) = \{(l100|L0)(l'100|L'0)(j_1 L m_2 0|j_2 m_2)(j_1 L' m_2 0|j_2 m_2)$$
$$+2p_\nu^{l+l'+L+L'}(l10-1|L-1)(l'10-1|L'-1)(j_1 L m_2+\mathfrak{p}_\nu, -\mathfrak{p}_\nu|j_2 m_2)$$
$$\cdot (j_1 L' m_2+\mathfrak{p}_\nu, -\mathfrak{p}_\nu|j_2 m_2)\}\,\delta(m_2, m'_2),$$

$$e_3(ll'L', m_2m'_2) = (l'100|L'0)(j_1 L' m_2 0|j_2 m_2)(j_1 l m_2 0|j_2 m_2)\delta(m_2, m'_2),$$

$$a(ll', \mathfrak{p}_\nu) = C_S^2 M_S(l)M_S(l')+C_V^2 M_{V_O}(l)M_{V_O}(l')+C_A^2 M_{A_R}(l)M_{A_R}(l')$$
$$+C_P^2 M_P(l)M_P(l')-2C_A C_P M_{A_R}(l)M_P(l')+2\mathfrak{p}_\nu[C_S C_P M_S(l)M_P(l')$$
$$+C_V C_A M_{V_O}(l)M_{A_R}(l')-C_S C_A M_S(l)M_{A_R}(l')-C_V C_P M_{V_O}(l)M_P(l')],$$

$$b(lLl'L', \mathfrak{p}_\nu) = C_V^2 M_{V_R}(lL)M_{V_R}(l'L')+C_T^2 M_{T_O}(lL)M_{T_O}(l'L')$$
$$+C_T^2 M_{T_R}(lL)M_{T_R}(l'L')+C_A^2 M_{A_O}(lL)M_{A_O}(l'L')$$
$$-2C_V C_T M_{V_R}(lL)M_{T_R}(l'L')+2\mathfrak{p}_\nu[-C_T^2 M_{T_O}(lL)M_{T_R}(l'L')$$
$$+C_V C_T M_{V_R}(lL)M_{T_O}(l'L')+C_V C_A M_{V_R}(lL)M_{A_O}(l'L')],$$

$$c(ll'L', \mathfrak{p}_\nu) = 2\{-C_V^2 M_{V_O}(l)M_{V_R}(l'L')-C_A^2 M_{A_R}(l)M_{A_O}(l'L')$$
$$-C_S C_T M_S(l)M_{T_R}(l'L')+C_V C_T M_{V_O}(l)M_{T_R}(l'L')+C_T C_P M_P(l)M_{T_O}(l'L')$$
$$+C_A C_P M_P(l)M_{A_O}(l'L')+\mathfrak{p}_\nu[C_S C_T M_S(l)M_{T_O}(l'L')$$
$$+C_S C_A M_S(l)M_{A_O}(l'L')-C_V C_T M_{V_O}(l)M_{T_O}(l'L')$$
$$-C_V C_A M_{V_O}(l)M_{A_O}(l'L')-C_V C_A M_{A_R}(l)M_{V_R}(l'L')$$
$$+C_V C_P M_P(l)M_{V_R}(l'L')-C_T C_P M_P(l)M_{T_R}(l'L')]\}.$$

Indices O and R refer to the "ordinary" and the "relativistic" matrix elements [3]) of pure interactions. The reduced matrix elements occurring in $a$, $b$ and $c$ are

$$M_S(l) = \langle j_2||l\rho_3||j_1\rangle\Pi(l)(-1)^l,$$

$$M_{V_O}(l) = \langle j_2||l||j_1\rangle\Pi(l)(-1)^l, \qquad M_{V_R}(lL) = \langle j_2||lL\rho_1||j_1\rangle\Pi(l+1)(-1)^l,$$

$$M_{T_O}(lL) = \langle j_2||lL\rho_3||j_1\rangle\Pi(l)(-1)^l, \quad M_{T_R}(lL) = \langle j_2||lLi\rho_2||j_1\rangle\Pi(l+1)(-1)^l,$$

$$M_{A_O}(lL) = \langle j_2||lL||j_1\rangle\Pi(l)(-1)^l, \quad M_{A_R}(l) = \langle j_2||l\rho_1||j_1\rangle\Pi(l+1)(1-)^l,$$

$$M_P(l) = \langle j_2||li\rho_2||j_1\rangle\Pi(l+1)(-1)^l.$$

The parity symbol means that

$$\Pi(l) = \delta[\Pi_f\Pi_1, (-1)^l],$$

where $\Pi_1$ and $\Pi_f$ are parities of the initial and final states, respectively. The reduced matrix elements used here are real. All interference terms are included in $E^{(\nu)}(m_2, m'_2)$ except SV and TA, which do not occur as we know from beta decay experiments. Only some of the interference terms occur in a transition of a given order according to the selection rules.

For a given spin and parity change of the nucleus, however, several types of transition are possible. For instance for $|\mathbf{j}_1-\mathbf{j}_2| = 2$, $\Pi_f = \Pi_1$, the following transitions of minimum order are possible with given pure interactions (the figures in brackets refer to order $l_{\min}$ allowed by the selection rules):

$$\mathrm{S}(2),\ \mathrm{V_O}(2),\ \mathrm{V_R}(1),\ \mathrm{T_O}(2),\ \mathrm{T_R}(1),\ \mathrm{A_O}(2),\ \mathrm{A_R}(3),\ \mathrm{P}(3).$$

Since the relativistic transitions of $l$-th order may be of the same order of magnitude as the ordinary transition of $(l+1)$-th order, contributions made by transitions $S(2)$, $V_O(2)$, $V_R(1)$, $T_O(2)$, $T_R(1)$, $A_O(2)$ are about of the same order of magnitude. Selection rules, of course, may permit also other transitions even of a higher order; their order of magnitude, however, is much lower than that of the above transitions.

In the particular case under consideration, interference terms SV, ST, SA, VT, VA and TA are possible, but some are of so high an order that they can be omitted.

## 4. Density Matrix for $\gamma$-Emission

By means of the usual multipole expansion the interaction Hamiltonian $H^{(\gamma)}$ may be written as follows:

$$H^{(\gamma)} = -\frac{1}{c}\mathbf{j}\cdot\mathbf{A} \approx \sum_{\lambda,\mu}\sqrt{2\lambda+1}D^{\lambda}_{\mu p_\gamma}(\mathbf{k}_\gamma)\{T^{(\mathrm{m})}_{\lambda\mu}-p_\gamma T^{(\mathrm{e})}_{\lambda\mu}\}, \tag{6}$$

where $T^{(\mathrm{m})}_{\lambda\mu}$ and $T^{(\mathrm{e})}_{\lambda\mu}$ are $\lambda$-th order irreducible tensor operators. In the usual way one finds

$$\langle j_3 m_3;\gamma|H^{(\gamma)}|j_2 m_2\rangle \approx \sum_{\lambda,\mu}\sqrt{2\lambda+1}\,D^{\lambda}_{\mu p_\gamma}(\mathbf{k}_\gamma)(j_2\lambda m_2\mu|j_3 m_3)\langle j_3||\lambda||j_2\rangle\Pi(\lambda),$$

where

$$\Pi(\lambda) = \delta(\Pi_{\lambda_e},\Pi_2\Pi_3)-p_\gamma\delta(\Pi_{\lambda_e},\Pi_2\Pi_3).$$

From this one obtains for circularly polarized $\gamma$-quanta

$$\begin{aligned}E^{(\gamma)}&(m_2,m'_2)\\ &= (-1)^{2j_2+j_3+1+m_2}\sum_{k,\lambda,\lambda'}(-1)^{\lambda-\lambda'}\sqrt{(2\lambda+1)(2\lambda'+1)}\,\langle j_3||\lambda||j_2\rangle\langle j_3||\lambda'||j_2\rangle \\ &\cdot p_\gamma{}^k(-1)^k(\lambda\lambda'\,1-1|k0)W(j_2j_2\lambda\lambda';kj_3)(j_2j_2-m_2m'_2|km'_2-m_2)D^k_{m'_2-m_2,0}(\mathbf{k}_\gamma).\end{aligned} \tag{7}$$

## 5. The $\nu$-$\gamma$ Angular Correlation

Introducing the expressions (5) and (7) into the formula (1) and reducing by the usual techniques, one gets

$$W(\vartheta,p_\nu,\dot{p_\gamma}) = \sum_k A_k{}^{(\nu)}A_k{}^{(\gamma)}P_k(\cos\vartheta), \tag{8}$$

with

$$A_k^{(\gamma)} = (-1)^{j_3+j_3+1} \sum_{\lambda,\lambda'} (-1)^{\lambda-\lambda'} \sqrt{(2\lambda+1)(2\lambda'+1)}\, \langle j_3||\lambda||j_2\rangle\langle j_3||\lambda'||j_2\rangle \cdot p_\gamma{}^k(\lambda\lambda' 1-1|k0) W(j_2 j_2 \lambda\lambda'; k j_3), \quad (9)$$

$$A_k^{(\nu)} = (-1)^{j_2-j_1} \sum_{ll'} \sqrt{(2l+1)(2l'+1)} \{\alpha_k(ll') a(ll', p_\nu) + \sum_{LL'} \beta_k(lLl'L', p_\nu) \cdot b(lLl'L', p_\nu) + \sum_{L'} \gamma_k(ll'L') C(ll'L')\}.$$

Here $\alpha_k$, $\beta_k$ and $\gamma_k$ are quantities obtained by multiplying $e_1$, $e_2$ and $e_3$ given above with $(-1)^{j_2-m_2}(j_2, j_2, -m_2, m_2|k0)$ and summing over $m_2 m'_2$:

$$\alpha_l(ll') = (ll'00|k0) W(j_2 j_2 ll'; k j_1),$$

$$\beta_k(lLl'L', p_\nu) = [(l100|L0)(l'100|L'0)(LL'00|k0) - 2p_\nu{}^{l+l'+k}(l10-1|L-1) \cdot (l'10-1|L'-1)(LL'1-1|k0)] W(j_2 j_2 LL'; k j_1), \quad (10)$$

$$\gamma_k(ll'L') = (l'100|L'0)(lL'00|k0) W(j_2 j_2 lL'; k j_1).$$

The factors $A_k^{(\nu)}$ and $A_k^{(\gamma)}$ depend on $p_\nu$ and $p_\gamma$, respectively, only for odd $k$. The product $A_k^{(\nu)} A_k^{(\gamma)}$ is then proportional to $p_\nu p_\gamma$. It is seen that if the polarization of the gamma quantum is not measured, the angular correlation does not depend on neutrino helicity, but by measuring the angular correlation of $\nu-\gamma$ and the circular polarization of the $\gamma$-quantum, the neutrino helicity may be determined. By comparing results obtained in experiments on the polarization of $\beta$-electrons with those of experiments on the helicity of neutrino, the interactions occurring in nature can be determined. The general expression given here makes it possible to evaluate measurements concerning forbidden K-capture.

Without measuring the circular polarization of the $\gamma$-quantum, $\nu-\gamma$ correlation may give valuable information for nuclear spectroscopy studies, e.g. on the order of forbiddenness of K-capture, on the multipole order of $\gamma$-transitions and on the spin values of the levels involved in the transition.

## References

1) L. C. Biedenharn and M. E. Rose, Revs. Mod. Phys. **25** (1953) 729
2) M. Goldhaber *et al.*, Phys. Rev. **109** (1958) 1015
3) F. M. Blatt and V. F. Weisskopf, Theoretical nuclear physics (1952) p. 735

2.A.1 *Nuclear Physics* 9 (1958/59) 334—336; © *North-Holland Publishing Co., Amsterdam*
Not to be reproduced by photoprint or microfilm without written permission from the publisher

# ACTIVATION CROSS-SECTIONS FOR REACTIONS OF CHLORINE AND COPPER WITH 14.8 MeV NEUTRONS

R. S. SCALAN † and R. W. FINK

*Department of Chemistry, University of Arkansas, Fayetteville, Arkansas* ††

Received 29 October 1958

**Abstract:** Absolute neutron activation cross-sections at 14.8 MeV have been measured for chlorine and for the $Cu^{65}$(n, p) reaction, based on comparison with the $Cu^{63}$(n, 2n)$Cu^{62}$ reaction (556 mb) which was used as a standard monitor for the neutron flux. The observed reactions, half-lives, and cross-sections are: $Cl^{37}$(n, p)$S^{37}$, 5.0 min, 25.4±2.1 mb; $Cl^{37}$(n, α)$P^{34}$, 12.5 sec, 43.8±6.9 mb; $Cl^{35}$(n, α)$P^{32}$, 14.5 d, 122±56 mb; $Cl^{35}$(n, 2n)$Cl^{34m}$ (upper state), 32.4 min, 5.6±2.0 mb; $Cl^{35}$(n, 2n)$Cl^{34g}$(ground-state), 1.5 sec, 2.8±0.5 mb; and, from the copper monitor, $Cu^{65}$(n, p)$Ni^{65}$, 2.56 h, 31±13 mb. Comparisons of the chlorine cross-sections with values estimated according to the compound nucleus theory as outlined by Blatt and Weisskopf show the usual deviations. These deviations are attributed to inadequacies in the simple version of the compound nucleus theory.

For the determination of cross-sections of chlorine isotopes, hexachlorobenzene ($C_6Cl_6$) was used as the target for irradiations with 14.8 MeV neutrons from the 400 kV Cockcroft-Walton accelerator at the University of Arkansas. This compound contains 74.75 percent by weight of chlorine, and the only other element present is carbon which gives no interfering background activity. Samples 9.5 and 12.7 mm in diameter were formed in a pellet press to surface densities as low as 85 mg/cm². After irradiation, these samples were counted on a thin-window, methane-flow beta proportional counter.

Samples of 45 mg/cm² copper foil similar in size were irradiated simultaneously as neutron flux monitors, and all cross-sections were measured relative to the $Cu^{63}$(n, 2n)$Cu^{62}$ reaction, the cross-section for which has been measured by Yasumi [1]) to be 556 mb at 14.8 MeV. The counting efficiencies for $Cu^{62}$, $S^{37}$, $Cl^{34m}$, $P^{32}$ and $Ni^{65}$ were assumed to be the same since all of these nucleides emit hard beta-particles and the self-scattering-self-absorption corrections are therefore approximately the same. The bombardments generally were made with fluxes ranging from $10^{10}$ to $10^{11}$ neutrons/cm² · sec.

In addition to 5.0 min $S^{37}$, 32.4 min $Cl^{34m}$, and 14.5 d $P^{32}$, whose yields were determined as described above, two short-lived species were observed in these bombardments, namely, 1.5 sec $Cl^{34g}$ and 12.5 sec $P^{34}$. To facilitate

† Postdoctoral fellow, 1957-58; present address: Chemical Laboratories, Phillips Petroleum Co., Bartlesville, Oklahoma.

†† Supported in part by the U.S. Atomic Energy Commission.

the counting of these activities, the hexachlorobenzene pellets were mounted on polyethylene holders 3.2 mm thick and 38 mm square. The sample holder was held in place at the target of the accelerator, poised over an aluminium channel which allowed the sample to slide into place beneath a shielded detector at the instant of cessation of the bombardment. The sample was released by means of a remotely-actuated solenoid catch. Pulses from the detector were scaled and fed into a Sanborn recorder which registered simultaneously the scaled pulses and a one-second time-base. In some cases, where a plastic scintillation detector was used in place of a GM tube, the pulses were differentially or integrally analyzed prior to being scaled and recorded. The cross-sections for the production of the short-lived nucleides were determined relative to the cross-section for the formation of 5.0 min $S^{37}$, which served as an internal monitor.

TABLE 1

Cross-section measurements and their comparison with previous work and with theoretical values at 14.8 MeV

| Reaction | Product | Observed half-life | No. of runs | Measured cross-section (mb) | | Calculated cross-section (mb) | Ratio $\sigma$ obs./$\sigma$ calc. |
|---|---|---|---|---|---|---|---|
| | | | | Present work | Paul and Clarke | Present work | |
| $Cl^{37}(n, p)$ | $S^{37}$ | 5.0 min | 3 | 25.4± 2.1 | 33.4± 6.7 | 54.0 | 0.47 |
| $Cl^{37}(n, \alpha)$ | $P^{34}$ | 12.5 sec | 7 | 43.8± 6.9 | 52.4±26 | 55.5 | 0.79 |
| $Cl^{35}(n, \alpha)$ | $P^{32}$ | 14.5 d | 4 | 122 ±56 | 199 ±31 | 40.6 | 3.0 |
| $Cl^{35}(n, 2n)$ | $Cl^{34m}$ | 32.4 min | 4 | 5.6± 2.0 | 3.5± 1.6 | 34.6 | 0.164 |
| $Cl^{35}(n, 2n)$ | $Cl^{34g}$ | 1.5 sec | 9 | 2.8± 0.5 | | 34.6 | 0.084 |
| $Cu^{65}(n, p)$ | $Ni^{65}$ | 2.56 h | 5 | 31 ±13 | | | |

The cross-sections are given in table 1, together with the early results of Paul and Clarke [2]) and theoretical values, based on the theory of compound nucleus decay as outlined by Blatt and Weisskopf [3]).

The experimental values for the cross-sections in general agree well with those reported by Paul and Clarke; in most cases, the percentage deviation has been reduced. In the case of the $Cl^{37}(n, \alpha)P^{32}$ reaction, the present cross-section value is considerably smaller than previously reported, but still within the experimental error limits. Our lower value might be due to the lower beta energy of $P^{32}$(1.71 MeV). Since the other nucleides studied have beta energies in excess of 2.5 MeV, the assumption of equal detection efficiencies might fail somewhat in the case of $P^{32}$ and $Ni^{65}$.

The assistance of Mr. J. Wray of the Accelerator Laboratory in making the bombardments is appreciated. Special thanks are due Dr. M. J. Nurmia for helpful discussions and for development of the fast counting system.

The help of Mr. Alex Poularikas in making the theoretical computations is appreciated. One of us (R.S.S.) is indebted to the Phillips Petroleum Company for post-doctoral fellowship support.

## References

1) S. Yasumi, J. Phys. Soc. Japan **12** (1957) 443
2) E. B. Paul and R. L. Clarke, Can. J. Phys. **31** (1953) 267
3) L. M. Blatt and V. F. Weisskopf, Theoretical Nuclear Physics (John Wiley and Sons, New York, 1952)

8.C *Nuclear Physics* 9 (1958/59) 337—346; © *North-Holland Publishing Co., Amsterdam*
Not to be reproduced by photoprint or microfilm without written permission from the publisher

# ON THE SECOND ORDER WAVE EQUATION OF THE FERMIONS

G. MARX
*Institute for Theoretical Physics of the Roland Eötvös University*
*and*
*Central Research Institute for Physics, Budapest*

Received 21 July 1958

**Abstract:** Following the suggestion of Feynman some problems have been considered in connection with the description of fermions by a second order wave equation, e.g. the problem of interactions. The possibility of the description of isodoublet fermions by a four-component spinor field is demonstrated. The latter method eliminates some difficulties in connection with forming the commutation rules. The transformation properties of the second order equation are analogous to those of the new non-linear Heisenberg equation.

## 1. Boson Fields

Feynman and Gell-Mann [1,2]) have recently suggested that all the elementary particles should be described uniformly by means of second order wave equations. Owing to the relativistic relation between the momentum $p_i$ and rest mass $m$,

$$p_i p_i + m^2 c^2 = 0,$$

for a case without interaction the wave equation

$$\Box\varphi - \kappa^2\varphi = 0 \qquad (\kappa = mc/\hbar) \tag{1}$$

has to be valid universally. The different particles are distinguished by the transformation properties of the field quantity $\varphi$ and, as a consequence, by the form of the interactions.

For bosons with spin zero $\varphi$ is a one-component scalar (with respect to the proper Lorentz group). For a neutral boson $\varphi$ is hermitian ($\varphi = \varphi^+$), for a charged boson it is a two-component hermitian or a one-component non-hermitian operator. In the case of electromagnetic interaction eq. (1) is modified:

$$(\partial_i - ia_i)(\partial_i - ia_i)\varphi - \kappa^2\varphi = 0, \tag{2}$$

this being the Klein-Gordon equation with the Lagrangian

$$L = -(\partial_i + ia_i)\varphi^+(\partial_i - ia_i)\varphi - \kappa^2\varphi^+\varphi - \tfrac{1}{4}F_{ik}F_{ik}. \tag{3}$$

Here $A_i$ is the electromagnetic vector potential,

$$F_{ik} = \partial_i A_k - \partial_k A_i, \quad a_i = \frac{e}{\hbar c} A_i, \quad f_{ik} = \frac{e}{\hbar c} F_{ik}. \tag{4}$$

With the combination of the charged and neutral boson fields isomultiplet boson fields may also be formed.

The photon field may also be described by eq. (1), but on the basis of the "principle of minimum number of states" the Lorentz condition is to be postulated as well [3]).

## 2. Fermion Fields

For fermions the spin doubles the number of the degrees of freedom: therefore for such kind of particles $\varphi$ is a two-component spinor in eq. (1). If a fermion possesses charge $e$ and magnetic momentum $e\hbar/2mc$, the electromagnetic interaction is expressed by the Feynman equation

$$[(\partial_i - ia_i)(\partial_i - ia_i) + \mathbf{B}\cdot\boldsymbol{\sigma} - \kappa^2]\varphi = 0. \tag{5a}$$

Here

$$\mathbf{B} = \frac{e}{\hbar c}(\mathbf{H} + i\mathbf{E}) = (f_{23} + f_{41}, \quad f_{31} + f_{42}, \quad f_{12} + f_{43})$$

is a selfdual antisymmetrical tensor. The equation (5) is invariant with respect to the proper Lorentz group: for an infinitesimal rotation of the angle $\alpha_i$ round the axis $x_i$ the spinor $\varphi$ has to be transformed according to

$$\varphi \to (1 + \tfrac{1}{2} i\alpha_i \sigma_i)\varphi$$

and for changing over to a system moving with an infinitesimal velocity $c\beta_i$ in the direction $x_i$ it has to be transformed according to

$$\varphi \to (1 + \tfrac{1}{2}\beta_i \sigma_i)\varphi.$$

It should be noted that without derivation only one Lorentz covariant quantity can be formed out of $\varphi$: the vector $\varphi^+ \sigma_i \varphi (\sigma_4 = -i)$. No scalar can be formed, with the result that no first order Lagrangian of the type (3) can be found for the Feynman equation (5) [4]).

Following Gell-Mann and Feynman it is clearly seen that eq. (5) is equivalent to the Dirac equation. By writing the two-component $\varphi$'s one below the other, let us form a four-component Dirac spinor. Then using the Dirac representation of the $\gamma_i$ matrices one sees that

$$\chi = \gamma_5 \chi, \qquad \chi = \begin{pmatrix} \varphi \\ -\varphi \end{pmatrix}. \tag{6}$$

Taking into account the subsidiary condition (6), eq. (5a) can be written as

$$[(\partial_i - ia_i)(\partial_i - ia_i) + \tfrac{1}{2}\sigma_{ik} f_{ik} - \kappa^2]\chi = 0. \tag{5b}$$

Here

$$\sigma_{ik} = \frac{1}{2i}(\gamma_i\gamma_k - \tilde{\gamma}_k\gamma_i).$$

If

$$\psi = [1-\kappa^{-1}\gamma_i(\partial_i - ia_i)]\chi, \tag{7}$$

the Dirac equation

$$[\gamma_i(\partial_i - ia_i)+\kappa]\psi = 0 \tag{8}$$

is satisfied in virtue of (5b). If, on the other hand, $\psi$ is the solution of the Dirac equation (8), the spinor

$$\chi = \tfrac{1}{2}(1+\gamma_5)\psi \tag{9}$$

formed from it, satisfies the Feynman equation (5).

Thus both descriptions of the fermion field are equivalent. This equivalence accounts for the fact that quantum electrodynamics makes no distinction between (5) and (8). The operator $\chi$ is identical with the "even" part of the operator $\psi$; however, it makes it possible to reconstruct the whole $\psi$ from $\chi$ according to (7), as the Dirac equation (8) connects the "even" and "odd" parts:

$$\psi_{(\pm)} = \tfrac{1}{2}(1+\gamma_5)\psi, \quad \psi = \psi_{(+)}+\psi_{(-)}, \quad \psi_{(\pm)} = -\kappa^{-1}\gamma_i\partial_i\psi_{(\mp)}.$$

This is not so, however, if the mass is zero ($\kappa = 0$). In the usual Dirac theory of the neutrino it is possible to separate the "even" part of $\psi$ and thus one arrives at the two component theory, with only negative helicity neutrinos. But if one postulates — following the suggestion of Feynman and Gell-Mann — the second order wave equation

$$\Box\chi_\nu = 0 \tag{10}$$

with the subsidiary condition (6), the operator defined by

$$\psi_\nu \equiv \tfrac{1}{2}(1+\gamma_5)\psi_\nu = \chi_\nu \tag{11a}$$

will not satisfy the Dirac equation

$$\gamma_i\partial_i\psi_\nu = 0 \tag{12}$$

and thus one will not have any connection between velocity and spin, contrary to the helicity experiments. Another possibility is to retain (10), but instead of (11a) to use the definition

$$\psi_\nu = \gamma_i\partial_i\chi_\nu. \tag{11b}$$

From (10) and (11b) eq. (12) follows, but one arrives at neutrino helicity opposite to that needed in the general theory of weak interactions. One cannot find the inversion of (11b), eq. (9) becoming invalid. Thus the $\chi_\nu$ and $\psi_\nu$ descriptions are not equivalent †. The only possibility is to use some kind of

† Using the definition (11b) the Feynman-Gell-Mann Hamiltonian will not be equivalent to the V$\pm$A coupling of the conventional theory of the $\beta$-decay. I am obliged to Dr. K. Nagy for this remark.

limiting process $\kappa_\nu \to 0$; in this case eqs. (10), (11a) and (12) should remain valid, the "odd" part of $\psi_\nu$ would increase over any limit according to (7), but this divergence would be unobservable. ("Odd" neutrinos with positive helicity are never emitted.)

The space reflection is described in the usual way by the transformation

$$\psi \to p_s \gamma_4 \psi, \quad (p_s^4 = 1)$$

which corresponds to the transformation

$$\chi \to -p_s \gamma_4 \kappa^{-1} \gamma_i (\partial_i - i a_i) \chi$$

of the $\chi$ spinor. On charge conjugation ($a_i \to -a_i$) the $\psi$ spinor is transformed according to

$$\psi \to \psi^c, \tag{13}$$

where $^c$ generally designates the following operation:

$$\omega^c = \gamma_C \bar{\tilde{\omega}},$$

$$\tilde{\gamma}_i = -\gamma_C \gamma_i \gamma_C^{-1}, \quad \gamma_C^+ = \gamma_C^{-1}, \quad \tilde{\gamma}_C = -\gamma_C; \quad \bar{\omega} = \omega^+ \gamma_4.$$

Thus on charge conjugation the $\chi$ spinor has to be transformed according to

$$\chi \to -\kappa^{-1} \gamma_i (\partial_i + i a_i) \chi^c.$$

It is shown by the connection (7), (9) that the momentum eigenstates for the spinors $\chi$ and $\psi$ are the same in the interaction free case. In the Feynman equation the spin matrix $\sigma$ is not coupled directly to the velocity (as contrasted with the Dirac equation), but in the rest system the eigenstates of $\sigma$ coincide in both descriptions.

## 3. Isodoublet Fermion Fields

The two-components spinor description of fermions involves some difficulties. The Feynman equation (5) seems to violate "the principle of minimum electromagnetic interaction" [5]). (Why should just one magneton be the magnetic moment of the bare electron?) In this theory the neutrino cannot have zero rest mass and negative helicity from the beginning, which destroys the chief beauty of the new neutrino theory. According to Kibble and Polkinghorne [4]) the only correct way of deducing commutation rules is to regard $\chi$ in (5b) as a four-component spinor operator and to remove the superfluous degrees of freedom by the condition

$$\tfrac{1}{2}(1-\gamma_5)\chi|\rangle = 0 \tag{14}$$

imposed upon the state vector. Obviously we have good reason to investigate what we get if we apply (7) to a four-component $\chi$ operator, without the conditions (6) or (14) respectively.

Let the interaction free wave equation be

$$\Box\chi-\kappa^2\chi=0. \tag{15}$$

This is invariant with respect to the infinitesimal Lorentz transformation

$$\chi\to(1+\tfrac{1}{4}\varepsilon_{ik}\sigma_{ik})\chi$$

and (contrary to the corresponding two-component equation) it may also be deduced from the first order Lagrangian

$$L=-\partial_i\bar{\chi}\partial_i\chi-\kappa^2\bar{\chi}\chi. \tag{16}$$

Let us now introduce the following spinor:

$$\xi=-\kappa^{-1}\gamma_5\gamma_i\partial_i\chi^c \tag{17}$$

and with its help the following to spinors as well [6]):

$$\psi_p=\tfrac{1}{2}(1+\gamma_5)\chi+\tfrac{1}{2}(1-\gamma_5)\xi^c,\quad \psi_n=i\tfrac{1}{2}(1+\gamma_5)\chi^c-i\tfrac{1}{2}(1-\gamma_5)\xi. \tag{18}$$

From eq. (15) it is clearly seen that the two independent $\psi_p$ and $\psi_n$ fields both satisfy the Dirac equation:

$$(\gamma_i\partial_i+\kappa)\psi_p=0,\quad (\gamma_i\partial_i+\kappa)\psi_n=0. \tag{19}$$

The mass constants of the two fields agree; therefore, eq. (15) describes an isobaric fermion doublet, thus being suitable for the joint description of the proton-neutron field.

## 4. Interactions

### 4.1. ELECTROMAGNETIC INTERACTION

The equation taking into account the unit charge and unit magnetic moment of the bare proton is the following:

$$[(\partial_i-i\tfrac{1}{2}(1+\gamma_5)a_i)(\partial_i-i\tfrac{1}{2}(1+\gamma_5)a_i)+\tfrac{1}{2}\sigma_{ik}\tfrac{1}{2}(1+\gamma_5)f_{ik}-\kappa^2]\chi=0. \tag{20}$$

(Decomposing $\chi=\chi_{(+)}+\chi_{(-)}$ eq. (20) may be split into the Feynman equation (5) of a charged fermion and that of a neutral one.) Putting

$$\xi=-\kappa^{-1}\gamma_5\gamma_i(\partial_i+i\tfrac{1}{2}(1-\gamma_5)a_i)\chi^c \tag{21}$$

we obtain the Gürsey equations [6]) of the nucleon doublet (disregarding a minor modification):

$$\begin{aligned}&\gamma_5\gamma_i(\partial_i-i\tfrac{1}{2}(1+\gamma_5)a_i)\chi-\kappa\xi^c=0,\quad \gamma_5\gamma_i(\partial_i+i\tfrac{1}{2}(1+\gamma_5)a_i)\xi-\kappa\chi^c=0,\\ &\gamma_5\gamma_i(\partial_i+i\tfrac{1}{2}(1-\gamma_5)a_i)\chi^c+\kappa\xi=0,\quad \gamma_5\gamma_i(\partial_i-i\tfrac{1}{2}(1-\gamma_5)a_i)\xi^c+\kappa\chi=0.\end{aligned} \tag{22}$$

On the basis of these, with the help of the Gürsey formulas (18), the Dirac equation of the nucleons can be deduced:

$$\left\{\gamma_i\left[\partial_i - ia_i\begin{pmatrix}1 & 0\\ 0 & 0\end{pmatrix}\right]+\kappa\right\}\begin{pmatrix}\psi_p\\ \psi_n\end{pmatrix}=0. \tag{23}$$

It may be seen from (23) that the charge conjugation $p \longleftrightarrow \tilde{p}$, $n \longleftrightarrow \tilde{n}$ is described by the transformations

$$a_i \to Ca_iC^{-1} = -a_i, \quad \psi \to C\psi C^{-1} = \psi^c$$

and

$$\chi \to C\chi C^{-1} = \xi = -\kappa^{-1}\gamma_5\gamma_i(\partial_i + i\tfrac{1}{2}(1-\gamma_5)a_i)\chi^c.$$

The charge conjugation is identical for (22) with the simple change $\chi \longleftrightarrow \xi$ but for (20) it is a rather complicated gradient transformation.

Taking into account the electromagnetic interaction as well, the *equivalent* Lagrangians of the Dirac, Gürsey and second order equations are the following:

$$L = L_m - \tfrac{1}{4}F_{ik}F_{ik},$$

with

$$\begin{aligned} L_m &= -\hbar c\{\bar{\psi}_p[\gamma_i(\partial_i - ia_i)+\kappa]\psi_p + \bar{\psi}_n[\gamma_i\partial_i+\kappa]\psi_n\} \\ &= -\hbar c\{\bar{\chi}\gamma_i(\partial_i - ia_i\tfrac{1}{2}(1+\gamma_5))\chi + \bar{\xi}^c\gamma_i(\partial_i - ia_i\tfrac{1}{2}(1-\gamma_5))\xi^c - \kappa(\bar{\chi}\gamma_5\xi^c - \bar{\xi}^c\gamma_5\chi)\} \\ &= \frac{\hbar c}{\kappa^2}\bar{\chi}(\overleftarrow{\partial}_i + ia_i\tfrac{1}{2}(1-\gamma_5))\gamma_i\cdot[(\partial_k - ia_k\tfrac{1}{2}(1+\gamma_5))(\partial_k - \tfrac{1}{2}ia_k\tfrac{1}{2}(1+\gamma_5)) + \tfrac{1}{2}\sigma_{ik}f_{ik} - \kappa^2]\chi. \end{aligned} \tag{24}$$

From (24) the following current vector is obtained:

$$j_i = iec\bar{\chi}\gamma_i\tfrac{1}{2}(1+\gamma_5)\chi - C(iec\bar{\chi}\gamma_i\tfrac{1}{2}(1+\gamma_5)\chi)C^{-1} = -Cj_iC^{-1}.$$

The interaction Lagrangian is as follows:

$$L_\gamma = j_iA_i = i\hbar c^2\bar{\chi}\gamma_i a_i\tfrac{1}{2}(1+\gamma_5)\chi + C\ (\text{idem})C^{-1}. \tag{25}$$

It is to be noted that the Dirac Lagrangian (also for the interaction free field) is *not* equivalent to the first order Lagrangian (16), but only to the higher order Lagrangian (24). The use of (16) instead of (24) would give different results for interactions.

### 4.2. WEAK INTERACTIONS

According to the suggestion of Feynman and Gell-Mann [2]) the Dirac equation and the Feynman equation of fermions should be considered as equivalent. The interaction Lagrangian is to be set up in the simple form containing only $\chi$. Using the two-component equation this programme has led simply to the V$\pm$A variant of the $\beta$ interaction, as from two component spinors no other covariant quantity can be formed. This result is in rather good harmony with experiment.

Using the four-component second order wave equation suggested above such kind of restriction does not exist. From $\chi$ scalars, vectors, tensors may equally be formed (without derivation). The use of scalar and tensor in-

variants in the interaction Lagrangian, however, would lead to transitions which would violate the conservation of baryon number:

Fig. 1

Only the vector covariants are invariant with respect to the phase transformation connected with baryon conservation:

$$\bar{\chi}\gamma_i\tfrac{1}{2}(1+\gamma_5)\chi = \bar{\psi}_p\gamma_i\tfrac{1}{2}(1+\gamma_5)\psi_p \qquad (26)$$

$$-\bar{\chi}\gamma_i\tfrac{1}{2}(1-\gamma_5)\chi = \bar{\psi}_n\gamma_i\tfrac{1}{2}(1+\gamma_5)\psi_n \qquad (27)$$

$$\bar{\chi}^c\gamma_5\gamma_i\chi = -2i\bar{\psi}_n\gamma_i\tfrac{1}{2}(1+\gamma_5)\psi_p \qquad (28)$$

$$\bar{\chi}\gamma_5\gamma_i\chi^c = 2i\bar{\psi}_p\gamma_i\tfrac{1}{2}(1+\gamma_5)\psi_n \qquad (29)$$

Type (26) occurs in the electromagnetic interaction. The $\beta$ decay may be described solely by (28) and (29) (only this leads to $p \longleftrightarrow n$ transitions). Thus the four-component theory leads just as well to the unambiguous choice of the coupling type $V \pm A$, as the two-component theory. The expression (29) does not contain derivative terms, but the interaction term of the second order wave equation contains such derivatives, if (29) is added to the Lagrangian (25).

The four-component wave equation (15) proved to be equivalent with the Dirac equation of isobar doublets, therefore the application to nucleons was obvious. For the description of the leptons there are two possibilities: the different leptons are described separately with two-component operators, which has certain difficulties [4]), or doublets (e.g. electron-neutrino) are formed from the leptons, although their masses differ. Let us consider the latter possibility. The Dirac equations of the electron-neutrino doublet are

$$\gamma_i(\partial_i - ia_i)\psi_e + \kappa\psi_e = 0, \quad \gamma_i\partial_i\psi_\nu = 0. \qquad (30)$$

If

$$\mu = \tfrac{1}{2}(1+\gamma_5)\psi_e + i\tfrac{1}{2}(1-\gamma_5)\psi_\nu^c, \quad \omega = \tfrac{1}{2}(1+\gamma_5)\psi_e^c + i\tfrac{1}{2}(1-\gamma_5)\psi_\nu, \qquad (31)$$

then by means of (30) we arrive at the following equations:

$$\begin{aligned} \gamma_i(\partial_i - ia_i\tfrac{1}{2}(1+\gamma_5))\mu + \kappa\tfrac{1}{2}(1-\gamma_5)\omega^c = 0, \\ \gamma_i(\partial_i - ia_i\tfrac{1}{2}(1-\gamma_5))\omega^c + \kappa\tfrac{1}{2}(1+\gamma_5)\mu = 0, \end{aligned} \qquad (32)$$

and eliminating $\omega^c$ we get the second order equation

$$[(\partial_i - ia_i\tfrac{1}{2}(1+\gamma_5))(\partial_i - ia_i\tfrac{1}{2}(1+\gamma_5)) + \tfrac{1}{2}\sigma_{ik}f_{ik} - \kappa^2\tfrac{1}{2}(1+\gamma_5)]\mu = 0. \qquad (33$$

Eq. (33) in itself is not equivalent to (32) and (30). From (33) it is impossible to deduce the Dirac equations. The equivalence can be obtained, if starting

from (33) the spinor

$$\omega^c = -\kappa^{-1}\gamma_i(\partial_i - ia_i\tfrac{1}{2}(1+\gamma_5))\mu \tag{34}$$

is defined and the subsidiary condition

$$\gamma_5\omega^c = -\omega^c \tag{35}$$

is postulated. In this way eqs. (33) and (35) result in the Dirac equation of the electron and in the two-component theory of the neutrino. Thus it becomes obvious that with the four-component spinor $\chi$ two fermions (isobaric doublet) of identical bare mass or two fermions of different mass may be described, provided that in the latter case one of the particles has a vanishing rest mass. The interaction Lagrangian of the $\beta$ decay is the following:

$$L_\beta = -\tfrac{1}{2}if\hbar c(\bar{\mu}^c\gamma_5\gamma_i\mu\cdot\bar{\chi}^c\gamma_5\gamma_i\chi + \text{hermit. conj.}). \tag{36}$$

4.3 STRONG INTERACTIONS

Let us consider the (axial) vector interaction of the nucleon doublet with the $\pi$-meson field:

$$\left[\gamma_i\partial_i+\kappa+\frac{ig}{2Mc^2}\gamma_i\gamma_5\tau\cdot\partial_i\varphi\right]\begin{pmatrix}\psi_p\\ \psi_n\end{pmatrix} = 0; \tag{37}$$

$\tau$ is the isobaric spin matrix. Putting

$$\frac{g}{2Mc^2}\partial_i\varphi_A = b_{iA}, \quad b_{i1}+ib_{i2} = B_i \neq B_i^+, \quad b_{i3} = b_i = b_i^+, \tag{38}$$

we get from the Dirac equation (37) with the substitution (18) the following Gürsey equations:

$$\gamma_5\gamma_i(\partial_i\chi+ib_i\chi-\gamma_5 B_i^+\chi^c)-\kappa\xi^c = 0, \quad \gamma_5\gamma_i(\partial_i\xi+ib_i\xi-\gamma_5 B_i\xi^c)-\kappa\xi^c = 0.$$

Eliminating $\xi$ we arrive at the second order equation

$$\{(\partial_i-ib_i)(\partial_i-ib_i)+B_i^+B_i+\sigma_{ik}[(b_i\partial_k-b_k\partial_i)+\tfrac{1}{2}i(B_i^+B_k-B_k^+B_i)]-\kappa^2\}\chi$$
$$+\{i\sigma_{ik}[B_i^+(\partial_k-ib_k)-B_k^+(\partial_i-ib_i)]-\partial_i B_i^+\}\gamma_5\chi^c = 0. \tag{39}$$

Eq. (37) may be deduced from (39), therefore the two are equivalent. Had we described the N$\pi$ interaction by a pseudoscalar coupling, this equivalence would not have been valid, just as in the case of two fermions with different non-vanishing masses. The Gell-Mann-Feynman programme prefers the vector type to the scalar for the Yukawa interaction as well. A second argument for the preference of the vector interaction is that only (26), (28) are invariant against the baryonic phase transformation and thus account for the conservation of the baryons. The interaction Lagrangian of the N$\pi$ coupling is

$$L_\pi = i\bar{\chi}\gamma_i b_i\chi-\bar{\chi}\gamma_i\gamma_5 B_i^+\chi+i\bar{\chi}^c\gamma_i\gamma_5 B_i\chi+C\ (\text{idem})\ C^{-1}. \tag{40}$$

Broadly speaking the same is true of the NK interaction as well. The Györgyi theory [7]) of the NK interaction leads also to the vector type, starting from an another (phenomenological) point of view. In that theory the baryons are built up from the N and $\tilde{K}$ doublets, so that the isobaric singulet and triplet states become eliminated, which is in harmony with the possibilities of the fermion doublet theory proposed above.

We now see that for all interactions the "principle of universal vector coupling" is found to be satisfied: all the interaction Lagrangians are products of two vectors constructed from the operators of the lighter particles and of those of the heavier ones respectively †.

The equations of the elementary particles are invariant with respect to the phase transformation which ensures baryon conservation:

$$\psi_p \to e^{ic}\psi_p, \quad \psi_n \to e^{ic}\psi_n, \quad \psi_p^c \to e^{-ic}\psi_p^c, \quad \psi_n^c \to e^{-ic}\psi_n^c.$$

We see from (18) that *the baryonic phase transformation of $\psi$ is equivalent to the Touschek transformation* [8]) *of $\chi$*:

$$\chi \to e^{ic\gamma_5}\chi. \tag{41}$$

The second order equations are invariant with respect to the Touschek transformation.

The strong interactions are invariant with respect to the "rotations" round the 1st, 2nd and 3rd "isobaric axis":

$$\psi \to e^{\frac{1}{2}i\alpha\tau_1}\psi, \quad \psi \to e^{\frac{1}{2}i\alpha\tau_2}\psi, \quad \psi \to e^{\frac{1}{2}i\alpha\tau_3}\psi.$$

The $\chi$-transformations connected with these rotations are the following:

$$\begin{gathered}\chi \to \cos\tfrac{1}{2}\alpha\chi - \gamma_5 \sin\tfrac{1}{2}\alpha\chi^c, \quad \chi \to \cos\tfrac{1}{2}\alpha\chi + i\gamma_5 \sin\tfrac{1}{2}\alpha\chi, \\ \chi \to \cos\tfrac{1}{2}\alpha\chi + i \sin\tfrac{1}{2}\alpha\chi.\end{gathered} \tag{42}$$

A general isobaric rotation is made up of the transformations (42):

$$\chi \to a\chi + b\gamma_5\chi^c, \quad |a|^2+|b|^2 = 1. \tag{43}$$

*The isobaric rotation is equivalent to the Pauli transformation* [9]) of $\chi$.

## 4. A "Model" of the new Heisenberg Equation

Heisenberg suggests the following equation for the unified description of the elementary particles:

$$\gamma_i \partial_i \chi + l_0^2 \gamma_5 \gamma_i \chi \cdot (\bar{\chi}\gamma_5\gamma_i\chi) = 0. \tag{44}$$

This is invariant with respect to the transformations (41) and (43). The resulting conservation theorems are explained by Heisenberg and Pauli as conservation rules for the baryonic number and the isobaric spin [10]).

Eq. (15) (and for strong interactions eq. (39)) has entirely similar invariance properties. In view of the equivalence of (39) with the usual

† Had we taken the first order Lagrangian (16), only scalar and tensor couplings would have been allowed for all types of interactions; but this possibility is contradicted by the well-known electromagnetic interaction law.

theory this explains how the invariance properties mentioned can be connected with the two conservation theorems of the strong interactions, and gives also an example of how the nucleon doublet may be described by a single four component spinor. A striking property of eq. (15) is that the isobaric rotation transforms $\chi$ into itself (and partly into $\gamma_5\chi^c$). The physical charge conjugation does not transform $\chi$ into $\chi^c$, but into a gradient expression:

$$C\chi C^{-1} = -\kappa^{-1}\gamma_5\gamma_i(\partial_i + i\tfrac{1}{2}(1-\gamma_5)a_i)\chi^c. \tag{45}$$

We see that the second order character of the wave equation for $\chi$ is an essential requirement for describing also the antiparticles.

The Heisenberg equation (44) is of the first order; therefore neither the transformation (13) nor (45) can describe the charge conjugation. To make the description of the antiparticles possible, Heisenberg considers $\chi$ not as complex but as quaternion operator [10]). To find an analogous procedure let us start from the Gürsey equations (22). In addition to the imaginary unit $i(i^2 = -1)$ let us introduce also the second unit $j(j^2 = -1,\ ij = -ji)$ and define

$$\zeta = (\chi + \xi^c) + j(\chi - \xi^c). \tag{46}$$

Then the equations (22) may be merged into one:

$$\gamma_5\gamma_i(\partial_i\zeta - \tfrac{1}{2}ia_i\zeta - \tfrac{1}{2}ija_i\gamma_5\hat{\zeta}) = j\kappa\zeta$$

and this is equivalent to the Dirac equation (22). The operation $\hat{}$ gives rise to the change in the sign of $j$. The invariance with respect to the transformation

$$\zeta \to \zeta\cos c + ij\gamma_5\,\hat{\zeta}\sin c$$

leads to the baryonic conservation and the invariance with respect to

$$\zeta \to a\zeta + b\gamma_5\,\zeta^c, \quad |a|^2 + |b|^2 = 1$$

to the conservation of the isobaric spin. The common phase transformation

$$\zeta \to e^{ic}\,\zeta$$

indicates the rotation around the 3rd isobaric axis. The charge conjugation is described by the transformation

$$\zeta \to C\zeta C^{-1} = \hat{\zeta}^c.$$

## References

1) R. P. Feynman, Rochester Conf. (April 1957)
2) R. P. Feynman and M. Gell-Mann, Phys. Rev. **109** (1958) 193
3) G. Marx, Nuovo Cimento **6** (1957) 1235
4) T. W. Kibble and J. C. Polkinghorne, Nuovo Cimento **8** (1958) 74
5) M. Gell-Mann, Nuovo Cimento Suppl. **2** (1956) 848
6) F. Gürsey, Nuovo Cimento **7** (1958)
7) B. Györgyi, in preparation
8) B. F. Touschek, Nuovo Cimento **5** (1957) 754
9) W. Pauli, Nuovo Cimento **6** (1957) 204
10) W. Heisenberg and W. Pauli (1958) preprint

7.A

*Nuclear Physics* 9 (1958/59) 347—354; © *North-Holland Publishing Co., Amsterdam*

Not to be reproduced by photoprint or microfilm without written permission from the publisher

# DISPERSION RELATIONS FOR PION-DEUTERON SCATTERING (II)

FRANK KASCHLUHN

*Joint Institute of Nuclear Research, Laboratory of Theoretical Physics, Dubna, USSR*

Received 25 April 1958

**Abstract:** The dispersion relation for elastic spin-flip forward scattering of pions on deuterons is derived and compared with the experimental data by means of Chew's impulse approximation. Unlike the previously treated case of elastic forward scattering without spin-flip the contribution from the non-observable region in the dispersion relation is now large and permits one to determine the pion-nucleon coupling constant. Its value is in accord with that following from the dispersion relations for pion scattering on free nucleons. The investigations indicate the possibility of treating bound states within the framework of the theory of dispersion relations; however, it is necessary to perform explicitly the analytic continuation in the relations because of divergences which appear in the matrix elements of the current in the non-observable region.

## 1. Introduction

In two preceding papers [1, 2]) the dispersion relation for elastic no-spin-flip forward scattering of pions by unpolarized deuterons was derived and compared with the experimental data by means of Chew's impulse approximation. It was shown that the dispersion relation is consistent with the results of the impulse approximation, but a detailed test of the theory was not possible, because the contribution from the non-observable part turned out to be small. It was therefore suggested in ref.[2]) that elastic forward scattering with spin-flip be investigated since in this case the contribution from the non-observable region in the dispersion relation should be large and comparable, as indicated by the corresponding results of the impulse approximation.

In the present work we derive the dispersion relation for elastic spin-flip forward scattering of pions by deuterons under the same assumptions as in ref.[1]). As in the latter paper it will be necessary to perform explicitly the analytic continuation because of divergences which appear in the matrix elements of the current with respect to the deuteron system in the non-observable region. This is done again by means of Bogolubov's method [3]). As in ref.[1]) the whole non-observable region yields a continuous contribution (without pole contributions) which can be calculated to a sufficient approxi-

mation. As in ref.[1]) the dispersion relation is again independent from the pion charge.

Comparison of the dispersion relation with the results of the impulse approximation requires, as in ref.[2]), that the contribution from the non-observable part be equal to that in the dispersion relation for the sum of the spin-flip amplitudes for forward scattering of positive and negative pions on free nucleons; however, it is well known that this contribution is a pure pole one, so that this requirement is not a trivial matter. The contribution from the non-observable part in the dispersion relation for elastic spin-flip forward scattering of pions by deuterons resulting from the analytic continuation does indeed exhibit the required behaviour over the complete energy range. In other words, the dispersion relation for spin-flip scattering of pions by deuterons allows one to determine the pion-nucleon coupling constant by using Chew's impulse approximation. Its value is $g^2/\hbar c = 18$ as found by Davidon and Goldberger [4]) from the dispersion relation for spin-flip scattering of pions by free nucleons, the error of course being a little larger in our case.

The present investigations show that it is practically possible also to treat bound states within the framework of the theory of dispersion relations, it being necessary, however, to carry out explicitly the analytic continuation because of divergences which appear in the matrix elements of the current in the non-observable region.

## 2. Spin-Flip Amplitude

As suggested in section 4 of ref.[2]), we define the spin-flip amplitude for elastic scattering of pions on deuterons by

$$\tilde{T} = \frac{1}{2i|\mathbf{q}' \times \mathbf{q}|} \{\langle \chi_{1,1}|T|\chi_{1,1}\rangle - \langle \chi_{1,-1}|T|\chi_{1,-1}\rangle\}; \tag{1}$$

$T$ is the usual transition amplitude for elastic pion-deuteron scattering, $\mathbf{q}'$ and $\mathbf{q}$ are the final and initial momenta of the pion and $\chi_{1,1}$ and $\chi_{1,-1}$ are the spin functions for the triplet states †. We assume, as in section 4 of ref.[2]), that the deuteron is polarized (contrary to ref.[1])) perpendicular to the scattering plane in the direction of $\mathbf{q}' \times \mathbf{q}$. As usual [3]), we choose that frame in wnich the sum of the initial and final momenta of the deuteron vanishes,

$$\mathbf{p}' + \mathbf{p} = 0. \tag{2}$$

For the dispersion relation derived in the next section we need the anti-hermitian part of the spin-flip amplitude (1) in the non-observable region.

† We remark that eq. (1) corresponds to the second term in the general expression (ref.[3]), eq. (5)) exhibiting the spin structure of the transition matrix.

The antihermitian part of the transition matrix $T$ is generally given by (cf. ref. [3]) and eq. (13) of ref.[1]) for notation)

$$\begin{aligned} A_{\alpha\omega}(E, \mathbf{q}) &= \pi\{\sum_n \langle -\mathbf{p}, s'|j_\rho(0)|\mathbf{p}+\mathbf{q}, n\rangle\langle \mathbf{p}+\mathbf{q}, n|j_\rho(0)|\mathbf{p}, s\rangle \\ &\cdot \delta(E-\sqrt{M_n{}^2+(\mathbf{p}+\mathbf{q}^2)}+\sqrt{M_D{}^2+\mathbf{p}^2})\sum_n \langle -\mathbf{p}^2, s'|j_\rho(0)|-\mathbf{p}-\mathbf{q}, n\rangle \\ &\cdot \langle -\mathbf{p}-\mathbf{q}, n|j_\rho(0)|\mathbf{p}, s\rangle\delta(E+\sqrt{M_n{}^2+(\mathbf{p}+\mathbf{q})^2}-\sqrt{M_D{}^2+\mathbf{p}^2})\} \end{aligned} \tag{3}$$

where we have already used the fact that, according to ref.[1]), the scattering amplitude is diagonal in the isotopic spin indices of the pion. Since for practical reasons we shall restrict ourselves in the following section to forward scattering, we may directly use the results obtained in ref.[1]); it was found in this paper that in the non-observable region only two-nucleon-terms contribute. The required general matrix element of the current is again given by (2) of ref.[1]).

Calculation of the antihermitian part of the spin-flip amplitude (1) with the aid of (3) yields in the non-observable region, after summation over the spin and isobaric spin states of the two-nucleon system, for the special case of forward scattering (compare the corresponding considerations in ref.[1]) leading to formula (27) there),

$$\tilde{A}(E, \mathbf{q}) = \operatorname{Im}\tilde{T} = \tfrac{1}{2}\pi\sum_z\left\{|1-\frac{E_z}{M_D}|[B_-(\mathbf{q}, z)+B_+(\mathbf{q}, z)]\right. \\ \left.[\delta(E+E_z)+\delta(E-E_z)]\right\} \tag{4}$$

with

$$B_\mp(\mathbf{q}, z) = \frac{g^2}{M^2}\left|\int \mathrm{d}^3\mathbf{x}_r\,\chi'^*_{z,\binom{t}{s}}\begin{matrix}\sin\\ \cos\end{matrix}(\tfrac{1}{2}\mathbf{q}\cdot\mathbf{x}_r)\chi_D\right|^2 \tag{5}$$

($0 < E < m$). $E_z$ is defined by (30) in ref.[1]) and investigation of the possible contributions from the individual $\delta$-functions in the non-observable region can be performed in exactly the same way as in section 3 of ref. [1]). We notice, that contrary to the no-spin-flip scattering amplitude (27) [1]) the two $\delta$-functions in (4) have the same sign, a fact which is very important for the following. Furthermore, the wave functions $\chi'_{z,t}$, $\chi'_{z,s}$ of the continuous spectrum of (3) in ref.[1]) will again be replaced by plane waves due to (43) [1]) and calculation of the matrix elements in (5) by using, as in ref.[1]), the Hulthén function (44) [1]) for $\chi_D$ leads to the expressions (45), (46) [1]). The results from section 3 of ref. [1]) (especially those at the end) concerning the divergences in the matrix elements of the current in the non-observable region are valid here without any change and the analytic continuation will be performed in the following section in the same way as in section 4 of ref.[1]) for the case of no-spin-flip scattering.

## 3. Dispersion Relation

The dispersion relation for elastic spin-flip forward scattering of pions by deuterons, which for the present will again be written down for $\tau < 0$, has, unlike (47) in ref.[1]), the form

$$\tilde{D}(E,\tau) = \frac{2}{\pi} E \mathrm{P}\left[\int_{|E_{\min}(\tau)|}^{\infty} \mathrm{d}E' \frac{\tilde{A}(E',\tau)}{E'^2 - E^2} + \int_{|E_{\max}(\tau)|}^{|E_{\min}(\tau)|} \mathrm{d}E' \frac{\tilde{A}(E',\tau)}{E'^2 - E^2}\right]; \quad (6)$$

$\tilde{D}(E,\tau)$ is the hermitian part of the spin-flip amplitude (1). The subtraction needed for convergence with respect to large $E'$ in the case of no-spin-flip scattering is unnecessary here (compare also ref. [4])).

As in (50), (51) of ref.[1]) the contribution of the second term in (6) that yields the non-observable part after the analytic continuation $\tau \to m^2$ can be written in the form (we suppress in the following the P-symbol)

$$-\frac{g^2}{M^2} E \int_0^P \left|1 - \frac{E_z(\tau)}{M_D}\right| \left\{\left|\int \mathrm{d}^3\mathbf{x}_r \frac{\mathrm{e}^{i\mathbf{p}_r\cdot\mathbf{x}_r}}{(2\pi)^{\frac{3}{2}}} \sin\tfrac{1}{2}\mathbf{q}'(\tau)\cdot\mathbf{x}_r \chi_D\right|^2 + \left|\int \mathrm{d}^3\mathbf{x}_r \frac{\mathrm{e}^{i\mathbf{p}_r\cdot\mathbf{x}_r}}{(2\pi)^{\frac{3}{2}}} \cos\tfrac{1}{2}\mathbf{q}'(\tau)\cdot\mathbf{x}_r \chi_D\right|^2\right\} \frac{\mathrm{d}^3\mathbf{p}_r}{E^2 - E_z^2(\tau)} \quad (7)$$

with

$$\mathbf{q}'^2(\tau) = E_z^2(\tau) - \tau > 0 \quad (8)$$

where $P$ is given by (36) in ref.[1]) and $E_z(\tau)$ by (40) in ref.[1]).

The analytic continuation $\tau \to m^2$ can be performed in exactly the same way as in (52–56) of ref.[1]), and (7) becomes similar to (57) in ref.[1]):

$$-\frac{g^2}{M^2} E \frac{4\alpha\beta(\alpha+\beta)}{\pi(\alpha-\beta)^2} \frac{P^{-1}}{m} \int_0^1 \mathrm{d}x Z(x) \quad (9)$$

with

$$Z(x) = (1-\kappa)^2\left(1 - \frac{m}{M_D}\frac{\kappa - x^2}{1-k}\right)\left[\frac{1}{f_1^2+g^2} + \frac{1}{f_2^2+g^2} - \frac{1}{(f_2-f_1)g}\left(\operatorname{arctg}\frac{2f_1 g}{f_1^2-g^2} - \operatorname{arctg}\frac{2f_2 g}{f_2^2-g^2}\right)\right] \frac{x^2}{\left(\frac{E(1-\kappa)}{m}\right)^2 - (\kappa - x^2)^2}. \quad (10)$$

The functions $f_1$, $f_2$ and $g$, as well as the constants $P$ and $\kappa$ are given by (58), (59) in ref.[1]) and $\alpha$ and $\beta$ by (44) in ref.[1]).

The dispersion relation for elastic spin-flip scattering thus assumes the final form

$$\tilde{D}(E) = \frac{2}{\pi} E \int_m^{\infty} \mathrm{d}E' \frac{\tilde{A}(E')}{E'^2 - E^2} - \frac{g^2}{M^2} E \frac{4\alpha\beta(\alpha+\beta)}{\pi(\alpha-\beta)^2} \frac{P^{-1}}{m} \int_0^1 \mathrm{d}x Z(x) \quad (11)$$

where $Z(x)$ is defined by (10).

## 4. Comparison with the Impulse Approximation

For comparison of dispersion relation (11) with the results of the impulse approximation we calculate at first the integral over $Z(x)$ appearing in (11); this is a relatively easy task and can be performed in a sufficiently good approximation. We neglect the small quantity $\varkappa(= 0.023)$ in (10) and replace the second bracket involving the ratio $m/M_D$ by 1. The error resulting from this is smaller than 5 % since — as we shall see immediately — $Z(x)$ is large only for small $x$. We consider the function

$$Z(x) = \left[\frac{1}{f_1^2+g^2} + \frac{1}{f_2^2+g^2} - \frac{1}{(f_2-f_1)g}\left(\operatorname{arctg}\frac{2f_1 g}{f_1^2-g^2} - \operatorname{arctg}\frac{2f_2 g}{f_2^2-g^2}\right)\right] \frac{x^2}{(E/m)^2-x^4}. \tag{12}$$

The function

$$z(x) = Z(x)[(E/m)^2-x^4] \tag{13}$$

is independent of $E$ and is represented in fig. 1.

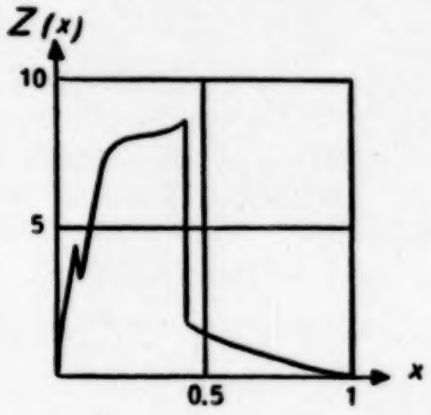


Fig. 1

The two discontinuities at $x = 0.05$ and $x = 0.43$ come from the function arctg $[2f_1 g/(f_1^2-g^2)]$ (compare ref. [1]), especially footnote 15) continued analytically according to ref.[1]), eq. (56).

From fig. 1 we can see that $Z(x)$ contributes to the integral only for such values of $x$ for which it is possible in a sufficient approximation to neglect $x^4$ with respect to $(E/m)^2$ in (12). Furthermore we contend ourselves with the estimate

$$\int_0^1 dx\, z(x) = 3.5 \tag{14}$$

based on fig. 1, so that we finally get

$$\int_0^1 dx Z(x) = 3.5 \frac{m^2}{E^2}. \tag{15}$$

The contribution from the non-observable part in (11) then becomes

$$-\frac{g^2}{M^2}E\frac{4\alpha\beta(\alpha+\beta)}{\pi(\alpha-\beta)^2}\frac{P^{-1}}{m}\int_0^1 \mathrm{d}x Z(x) = -0.91\frac{g^2}{M^2}\frac{1}{E}. \tag{16}$$

Comparison of the dispersion relation (11) with the impulse approximation requires, as in ref.[2]), that the contribution from the non-observable part in (11) be equal to that in the dispersion relation for the sum of the forward spin-flip amplitudes for scattering of positive and negative pions by free nucleons, i.e., equal to

$$\frac{2}{\pi}E\frac{\pi g^2}{2M^2}\frac{1}{\left(\frac{m^2}{2M}\right)^2-E^2} = -\frac{g^2}{M^2}\frac{1}{E} \tag{17}$$

where we have neglected as in ref.[2]) the small quantity $(m^2/2M)^2$ compared to $E^2$.

Indeed, within the required accuracy the quantities (16) and (17) are in accord over the whole energy range, i.e., the dispersion relation (11) is compatible with the results of the impulse approximation.

## 5. Conclusion

It was shown in the last section that dispersion relation (11) for elastic spin-flip forward scattering of pions on deuterons is compatible with the results of the impulse approximation throughout the complete energy range. For the value of the pion-nucleon coupling constant determined in this way we can directly use the result of Davidon and Goldberger [4])

$$g^2/\hbar c = 18 \tag{18}$$

where the error in our case is of course a little larger than that obtained by employing the dispersion relations for scattering of pions by free nucleons.

We emphasize once more that comparison of dispersion relation (11) with the impulse approximation is quite a non-trivial matter, since the contribution from the non-observable part in (11) is a continuous one which is mainly due to the first $\delta$-function in (4) (compare ref.[1])), whereas the contribution from the non-observable part in the dispersion relation from the sum of the spin-flip amplitudes for forward scattering of positive and negative pions by free nucleons is a pure pole contribution which corresponds to the second $\delta$-function in (4). Nevertheless, agreement within the requisite was obtained, since the analytically continued functions in (10) possess such a behaviour, that in accordance with fig. 1, the essential contributions to the integral in (9) are due only to small $x$. We remember, that in the case of no-spin-flip scattering there was necessarily a difference in sign in the two contributions from the non-observable parts which we had to compare in

ref.[2]), since in relation (27) of ref.[1]), which corresponds to (4), the $\delta$-functions have different signs. The contradiction was solved in such a manner that the two aforementioned contributions from the non-observable parts were only small and not testable within the accuracy of the impulse approximation (compare ref.[2]) section 3).

We notice furthermore that very probably the contribution from the non-observable part in dispersion relation (11) is rather insensitive to the special form of the wave function for the deuteron ground state (for which we have chosen for simplicity the Hulthén function (44), ref.[1])) or to the special form of the corresponding two-nucleon potential respectively. This could be anticipated in analogy to the well-known fact that in the low-energy two-nucleon problems only the short range and the great strength of the nuclear forces are important (the modifications arising from the existence of the D-state are certainly unimportant with regard to the accuracy of the whole method).

Concluding we can say that the present investigation shows the practical possibility of including bound states in the theory of dispersion relations; however, it is necessary to carry out explicitly the analytic continuation in these relations because of the divergences which appear in the matrix elements of the current in the non-observable region. Thus the main problem which remains is to give a theoretical basis for the special "renormalization prescription" proposed in ref.[1]) for the matrix elements of the current with respect to the deuteron system.

*Note added in proof*: In order to justify the replacement of the real deuteron wave functions of the continuous spectrum by plane waves, it is necessary to modify the argument given at the end of section 3 in ref.[1]), since the completeness relation cannot be applied directly (this can be seen from (27) in ref.[1]) or from (4) of this work in which the $B$'s are multiplied by factors which depend on $E_s$). However, it can easily be shown that in a good approximation our procedure is correct if one notes that, according to section 3, it is sufficient to put $E_s = 0$ for the calculation of the contribution from the non-observable region (important contributions are due only to small $x$ in (9), and that in the observable region the requisite deuteron wave functions are satisfactorily represented by plane waves (as in this region the energy of the relative motion is larger than 140 MeV). It would be interesting, however, to proceed further and to assume that the matrix elements of the current are sufficiently small in the observable region (which is probably true to a very good approximation) and that it should accordingly be possible to extend the momentum integration in (7) to infinity ($P \to \infty$). Putting again $E_s = 0$ (which is substantiated by an explicit calculation) and using the completeness of the plane wave functions one gets immediately for (7) expression (17) for the contribution from the non-observable region required by Chew's impulse approximation; this expression agrees within 10 % with our explicitly calculated value (16). In such a way it seems to be possible to compute the contribution from the non-observable region in the spin-flip dispersion relation for pion deuteron scattering without a detailed knowledge of the deuteron wave functions.

I should like to thank Prof. Chew for discussions which gave rise to the investigations indicated in this note.

## References

1) F. Kaschluhn, Z. Naturforsch. **13a** (1958) 183
2) F. Kaschluhn, Nuclear Physics **8** (1958) 303
3) N. N. Bogolubov, B. V. Medvedev and M. K. Polivanov, Problems of the Theory of Dispersion Relations, Gostekhizdat, Moscow (in print); abridged German translation in Fortschr. d. Phys. **6** (1958) 169
4) W. C. Davidon and M. L. Goldberger, Phys. Rev. **104** (1956) 119

10.D *Nuclear Physics* **9** (1958/59) 355; © *North-Holland Publishing Co., Amsterdam*

# BOOK REVIEWS

O.E.E.C., *Applications of atomic science in agriculture and food* (European Productivity Agency of the O.E.E.C., Paris, 1958. 113 pages. $ 1.25)

This publication of the O.E.E.C. is the report of an international mission sent by the Organization to the United States. It is a practical hand-book covering the use of radio-isotopes in the most varied aspects of food production, preservation and distribution.

L. R.

*Bevolkingsgroei en energie-verbruik* (Symposium der Universiteit van Amsterdam) (van Gorcum & Co., Assen, 1958. 178 pages. 6.90 fl.)

In the summer of 1957 a symposium was organized by the University of Amsterdam on the theme "Population growth and energy consumption". The neatly produced booklet under review contains, besides an introduction, the texts of the nine reports presented at the symposium. With characteristic Dutch thoroughness the subject is surveyed in all its aspects, starting with a historical study and ending with a discussion of "malthusianism, neo-malthusianism and meta-malthusianism". The reports, most of which have the merit of being short, are written by Dutch specialists of recognized authority in their fields. I would not go so far as to exhort people to learn Dutch in order to read this book (as Maxwell did to read van der Waals' thesis), but it is certainly a useful summary of one of the major problems of our time.

L. R.

*Elementary particle accelerators* (Supplement No. 4 of Atomnaya Energiya) (Consultants Bureau, New York, 1958. 67 pages. $ 15.00, to subscribers of the translated journal $ 10.00)

Papers presented at the Moscow conference of 1956 (this journal **1** (1956) 679); some also at the Geneva conference of the same year (this journal **1** (1956) 682; **4** (1957) 188).

L. R.

*Nuclear reactions in light nuclei* (Supplement No. 5 of Atomnaya Energiya) (Consultants Bureau, New York. 73 pages. $ 15.00, to subscribers of the translated journal $ 10.00)

Collection of papers reporting work done in various laboratories of the U.S.S.R. Academy of Sciences in 1951-55.

L. R.

W. H. SULLIVAN, *Trilinear chart of nuclides*, First revision sheet (U.S. Government Printing Office, Washington 1958)

See this journal **4** (1957) 491.

The first revision sheet was issued on July 1, 1958. It contains 45 hexagons which have to be cut and glued at the appropriate places on the chart. Instructions how to proceed make this operation perfectly fool-proof: a theorist can do it.

A point on which the author deserves the warmest congratulations is his decision to adopt the prefix symbols for units recommended by the SUN Commission of the IUPAP (this journal **1** (1956) 539; **7** (1958) 299). So the SUN is beginning to shine on the other side of the Atlantic; the question is how long it will take the editorial office of the Physical Review to notice it.

L. R.

H. PRIMAKOFF *et al.* (Editors), Proceedings of the Midwest Conference on Theoretical Physics (Washington University, St. Louis, Miss. 1958. 225 stencilled pages).

Prof. Primakoff and his collaborators have done an excellent job of editing the proceedings of the Midwest Conference on Theoretical Physics held at Washington University in March, 1958, under the sponsorship of the National Science Foundation. The subjects covered were: the new methods (using field quantization techniques) in solid state physics, developments in the theory of nuclear structure, the statistical treatment of dense gases and transport phenomena, and (needless to say) weak interactions and dispersion relations. Of special value is the almost complete reporting of the lively discussions. Here and there, a failure of the tape-recorder introduces into the report an unexpected element of suspense, as when Prof. Belinfante's challenging peroration "I would like you to talk, not me" is followed by an Editor's Note: "Unfortunately, a satisfactory recording of the discussion . . . was not obtained." And the mutilated rendering of the discussion remark "One would not be bothered by ghost states at all because . . ." reaches a carrollian effect as powerful as Humpty Dumpty's famous song † itself.

L. R.

† In *Through the looking-glass.*

R. C. GIBBS and K. WAY, *A directory to nuclear data tabulations* (U.S. Government Printing Office, Washington 1958. xiii-185 pages. $ 0.70).

With the unexampled growth of research activity in nuclear physics, the task of keeping a complete and critical record of the accumulating data resulting from it has become a very important as well as an exacting one. It is well known that the conception of the shell-model was decisively catalyzed by the availability of comprehensive data, and it would be easy to name quite a number of other features of our increasing insight into the structure of nuclei which owe their recognition to an analysis of well-tabulated information. The necessity for centralizing and systematizing this new kind of scientific work — which is by no means mere compilation, but critical study demanding the highest competence and judgment — was most clearly recognized in the traditional home of unrestricted individualism, where a Subcommittee on Nuclear Constants is splendidly carrying out the work in the most thorough and comprehensive manner. Much similar work, however, has been done independently, and excellently, by many other people, and tables of nuclear data have grown to such numbers and variety that it has become desirable to take the next step and make a critical survey of *them* so as to guide the bewildered physicist to the source most useful for his particular purposes.

Here again, the Subcommittee on Nuclear Constants has put us deeply in their debt by tackling this job with their usual efficiency. The directory they have produced lists 284 tables, classified in 33 sections; they not only range over all aspects of physics involving nuclei and other particles, but they also cover the theoretical and practical auxiliary requisites, from Coulomb wave functions to energy-range relations in emulsions. Each table is described concisely, but fully, with a perfect sense of the kind of information really needed to decide whether or not the table answers the various requirements which usually arise. The solicitude of the authors goes so far as to quote the price at which the table can be bought, or to indicate from which institution it may be obtained or borrowed. In every respect, this book is in fact so good that one may hope it will discourage similar ventures and thus prevent the need for a catalogue of directories to tables of data.

L. R.